UNIVERSITAT POLITÈCNICA DE CATALUNYA

Doctoral Programme in Natural Resources and Environment

Adsorption of organic and emerging pollutants on carbon materials in aqueous media.

Environmental implications

PhD Thesis

Jordi Lladó Valero

November 2015

UNIVERSITAT POLITÈCNICA DE CATALUNYA

Escola Politècnica Superior d'Enginyeria de Manresa

Department of Mining, Industrial and TIC Engineering

Doctoral programme in Natural Resources and Environment

Instituto Nacional del Carbón (INCAR-CSIC)

Adsorption of organic and emerging pollutants on carbon materials in aqueous media.
Environmental implications

PhD Thesis

Jordi Lladó Valero

Supervised by:

Conxita Lao Luque

Montserrat Solé Sardans

Als meus pares i

a la meva àvia

Agraïments

Ara fa quatre anys i mig que vaig decidir començar el doctorat en l'escola universitària EPSEM on durant 14 anys m'ha vist créixer i he pogut desenvolupar-me i enriquir-me com a persona. Per aquest motiu, i el llarg camí que he viscut amb etapes dures, divertides, intenses però alhora gratificants voldria agrair aquella gent i associacions que de forma especial m'han aportat un ajut i suport com a persona, investigador i alumne.

En primer lloc, voldria expressar el meu agraïment a les meves directores de Tesi, la doctora Conxita Lao Luque i la doctora Solé Sardans per haver confiat en mi a l'hora de realitzar aquest projecte, així com buscar un suport econòmic relacionat al projecte que ha estat difícil degut l'actual context de crisi, i el vincle que van crear amb l'Instituto Nacional del Carbón. També voldria agrair a la Conxita Lao el suport mostrat i correccions en aquesta etapa final d'escriptura de la Tesi.

També voldria agrair la beca que la Universitat Politècnica de Catalunya em va atorgar per a la realització del meu doctorat.

Querría agradecer especialmente al doctor Enrique Fuente Alonso y a la doctora Begoña Ruiz Bobes por su grandísima colaboración y ayuda, estima, aceptación en el INCAR y conocimientos transmitidos, porque sin ellos esta Tesis no hubiera sido posible. Por otro lado quiero agradecer al doctor Roberto Rodriguez Gil y a la doctora Nuria Ferrera Lorenzo por ser mis profesores en la distancia gracias a sus Tesis, así como en la ayuda de la realización de los materiales utilizados.

També en aquest sentit, voldria agrair la doctora Sandra Pérez en doctorand Jaume Aceña per obrir-me les portes al IDAEA, donar-me suport i ajudar-me en els anàlisis per a la meva investigació.

En aquest camí també he compartit molt bones experiències, coneixements i treball amb les persones del laboratori, on des de la primera etapa com a becari en Jordi Portabella i la Xesca Sala m'han ensenyat el funcionament del laboratori, la inquietud pels aparells d'instrumental, la convivència i amistat en el lloc de treball. En aquest sentit, en una etapa més tardana, la Raquel Ibarz em compartit molts moments i experiències en el laboratori que m'han ajudat a aprendre i afrontar la vida real. Voldria agrair molt especialment, al cel sigui, a en Josep Torras, per transmetre'm la il·lusió, inquietud i

saviesa per la ciència, metodologia en el treball i la lluita per la vida. Sempre et recordaré.

També voldria tenir un agraïment aquells professors que m'han aportat una part de la seva saviesa, suport així com l'aprenentatge i la convivència en el dia a dia com una família. En Jordi Bonet per la seva ajuda en el tractament de senyals, en Josep M. Rossell per l'aprenentatge de l'estadística i models, en Josep Freixes pels bons moments conviscuts jugant escacs, a la Roser Gorchs per transmetre que la Universitat també és una família, en Xavier de las Heras per resoldre tots els dubtes analítics i compartir l'ensenyament d'assignatures, a l'Anna Bonfills pel seu interès i preocupació per la meva investigació i la Dolors Grau pels diferents ajuts i beques que m'ha atorgat i m'han permès continuar estudiant, així com la motivació per començar a investigar i la inquietud pel món de les plantes aromàtiques.

Als amics de la Universitat, la Ginesta, l'Olga i en Ramón pels diferent moments conviscuts en les diferent etapes. L'Arianna, en Jordi i en petit Gerard pels moments viscuts durant les carreres i aquest estiu. A la Laia i en Toni per donar-me suport durant l'estiu i poder entrenar amb vosaltres. A la Gabriela per ajudar-me en les correccions. A la Laura Gallardo pels bons moments que vam conviure. A la família de l'Escola Joviat per l'ajut moral, treball i aprenentatge que he adquirit al llarg de tota la meva vida universitària. A les diferents famílies del món dels escacs, sobretot a les famílies Méndez, Escolà, Colom, Masdemont, Pinazo, Clotet, Soultygov,... per donar-me il·lusió en aquest esport. A la colla d'amics i de bàsquet (Laura, Aloma, Edgar, Pipa, Gerard, Buti, Pepe, Ferran, André,....). I aquelles persones que en algun moment m'han aportat el seu granet de sorra.

Per últim voldria agrair la meva família (pares, àvia, germà i família, tiets i cosins) en especial als meus pares i àvia per estar en tot moment en aquest llarg camí universitari.

A tots ells, moltes gràcies

Resum

En les darreres dues dècades s'ha detectat un increment de la presència de substàncies orgàniques com els fàrmacs, els pesticides,... en l'aigua que poden afectar la salut dels éssers vius i del medi ambient. Algun d'aquests contaminants romanen en les aigües després d'haver passat pels tractaments habituals en les plantes depuradores de tractament. Aquest fet fa evident la necessitat de la implantació de tractament terciaris que permetin la seva completa eliminació.

La present Tesi doctoral estudia l'eliminació de diferents compostos orgànics i emergents presents en aigua mitjançant la tecnologia d'adsorció amb nous carbons activats. Concretament, s'han produït i caracteritzat nous materials carbonosos procedents de residus, carbó mineral, materials sintètics, ... que permeten adsorbir diferents compostos orgànics d'ampli us en la nostra societat. S'han estudiat les característiques dels adsorbents (composició química, grups funcionals, porositat) i dels adsorbats (dimensions, hidrofobicitat, pKa, grups funcionals...) que influeixen en el procés d'adsorció.

A més a més, en aquest treball, s'han proposat dos nous models, un d'anàlisi i un altre cinètic. El model analític permet, mitjançant la quimiometria, millorar la quantificació de dos o més compostos orgànics presents en una mescla per espectroscòpia UV-vis. El model cinètic proposat proporciona una millor comprensió i interpretació, així com una millor predicció dels diferents paràmetres del procés d'adsorció.

En aquest sentit, en la següent Tesi es presenten cinc treballs que han permès una millor comprensió del procés d'adsorció mitjançant materials carbonosos de diferents procedències. En el primer treball, *"highly microporous activated carbons from biocollagenic wastes as adsorbents or aromatic pollutants in water originating from industrial activities"*, s'ha estudiat com afecta la textura i la composició química de carbons activats procedents de residus de pells en l'adsorció de compostos aromàtics monosubtituits. A més a més s'estudia com afecten diferents variables com temperatura i agent activant en el procés de fabricació dels carbons activats.

El segon treball, *"Removal of pharmaceutical and Iodinated Contrast Media (ICM) compounds on carbon xerogels and activated carbons. NOM and textural properties influences"*, posa de manifest el rellevant paper que juga la distribució de porus d'un

carbó activat en l'adsorció de diferents fàrmacs (àcid salicílic, paracetamol, diclofenac, ...) i agents de contrast (iohexol, iodixanol, iomeprol,...) de diferent mida. També, s'ha estudiat la influència de la matèria orgànica present en l'aigua en l'adsorció de tots els contaminants.

L'estudi de l'adsorció de paracetamol, fenol i àcid salicílic en diferents carbons activats procedents de carbó mineral es reflexa en el treball *"Removal of pharmaceutical pollutants im water using coal-based activated carbons"*. En aquest treball s'estudia la influència de les característiques químiques de la superfície dels carbons activats en l'adsorció dels diferents compostos orgànics, així com la influència del pH de les aigües. Els resultats van mostrar un augment de l'adsorció de salicilats degut a la presència de sofre en l'adsorbent.

El quart treball, *"Multicomponent adsorption on coal-based activated carbons on aqueous media: new cross-correlation analysis method"*, és una continuació del treball anterior. En aquest cas, es presenta un nova tècnica quimiomètrica que permet analitzar correctament mescles binàries i ternàries per espectroscòpia UV-vis. A més s'estudia l'efecte competitiu entre dues o tres molècules en el procés d'adsorció.

El cinquè i últim treball, *"Role of activated carbon properties in atrazine and paracetamol adsorption equilibrium and kinetics"*, planteja un nou model cinètic per a l'adsorció de paracetamol i atrazina mitjançant carbó activat procedent de fangs de depuradora i dos carbons comercials. El nou model cinètic proposat es basa en balanços de matèria i permet estimar diferent paràmetres com la difusió i l'àrea efectiva que tenen un significat físic respecte altres models empírics.

Abstract

In the last two decades an increasing presence of organic substances such drugs, pesticides, etc has been detected in water which may affect the health of the organisms and the environment. Some of these contaminants remain in the water after the usual treatment in sewage plants. This fact makes evident the need of introduction of the tertiary treatments that allow the complete elimination of these substances .

This Doctoral Thesis researches for the elimination of different organic and emerging compounds present in water by means of the adsorption with new activated carbons. In particular, new carbon materials from different wastes, coal, synthetic materials, which have been produced and characterized, allow the adsorption of the organic compounds widely used in society. Different characteristics of the adsorbents (chemical composition, functional groups, texture, etc) and of adsorbates (dimensions, hydrophobicity, pKa, functional groups, etc) that influence on the adsorption process have been studied.

Moreover, in this work, an analysis and kinetic model have been proposed. The analytic model allow, by chemometrics, enhancing the quantification of two or more organic compounds in solution by spectroscopy UV-vis. The kinetic model proposed provides a better comprehension and interpretation, as a better prediction of the different parameters on the adsorption process.

In this sense, the following Thesis presents five works which have allowed a better comprehension of the adsorption process by means carbon materials from different origin. The first work, "*highly microporous activated carbons from biocollagenic wastes as adsorbents or aromatic pollutants in water originating from industrial activities*", about the texture and chemical composition of activated carbon from biocollagenic wastes which have been studied in order to observe how these parameters affect on the adsorption of aromatic monosubstitued compounds. Moreover, different variables as temperature and activating agent are studied in the process of manufacture activated carbons.

The second work, "*Removal of pharmaceutical and Iodinated Contrast Media (ICM) compounds on carbon xerogels and activated carbons. NOM and textural properties influences*," shows the important role of pore size distribution in activated carbon which

plays on the adsorption of different pharmaceuticals (salicylic acid, paracetamol, diclifenac, etc) and iodinated contrast media (iohexol, iodixanol, iomeprol, etc) of different size. The influence of natural organic matter (NOM) in water is also studied in the adsorption of the all pollutants.

The adsorption of paracetamol, phenol and salicylicacid in different coal-based activated carbon is showed in the contain of the work *"Removal of pharmaceutical pollutants im water using coal-based activated carbons"*. In this work, the chemical characteristics on the surface of activated carbons are studied in order to observe the influence in the adsorption of different organic compounds; and also the influence of the pH water. The results showed an increase of adsorption of salicylates due to the presence of sulphur on the surface of the adsorbent.

The fourth work; *"Multicomponent adsorption on coal-based activated carbons on aqueous media: new cross-correlation analysis method"*, as a continuation of the previous work, shows a new chemometric technique that allows to analysis the binary and ternary solutions correctly by UV-vis spectroscopy. Moreover, the competitive effect between two or three molecules is studied on the adsorption process.

In the last work, *"Role of activated carbon properties in atrazine and paracetamol adsorption equilibrium and kinetics"*, a new kinetic model is proposed for the adsorption of paracetamol and atrazine using activated carbon from sewage sludge and two, commercial, activated carbons. This new kinetic model, based on mass balances, allows estimating different parameters with physical meaning (diffusion and effective area).

Table of contents

Section 4.1.2 Removal of pharmaceuticals and Iodinated Contrast Media (ICM) compounds on carbon xerogels and activated carbons. NOM and textural properties influences 119

Index of Figures

Index of tables

Index of figures and tables Supporting information

Figures

Tables

Chapter 1

Introduction

1. Water, water resources and water treatment

Water is an essential compound for the live of any organism and for the environment. Although the total quantity of fresh water in the world is higher than the total water consumed, the natural resource and the availability of fresh water resources are distributed around the world unevenly [1]. This fact and the bad use of water management have produced a crisis that causes wars and conflicts in different parts of the world.

According the World Health Organization (WHO) [2] millions of people can't access and use clean water. The lack of purification and sanitation water infrastructures cause an increase of the number of persons who can't dispose of water and a lot of children can die. Only with the access to good sanitary water, the risk of death will reduce more than 50% in a child and it will enhance life expectancy. It is expected that the lack of water. Moreover, it is demonstrated that the lack of water has a cost of 485000 millions of Euros a year.

On the other hand, water consumption and availability are closely related to living standard. In USA the total renewable water resources per inhabitant is 9718 m^3/ inhab per year, in Mozambique 8870 m^3/ inhab per year and in Spain 2384 m^3/ inhab per year [1]. As can be seen, Spain is a hot country where precipitations (rain) are irregular and the renewable is limited due environmental problems as reductions of flow water, salinization of aquifers, ... On the other hand, the total withdrawal water per capita (m^3/inhab year) of USA is 1583, in Mozambique 46.05 and in Spain 694. This term shows that extraction water in Spain can be excessive for the conditions of the country while in USA and Mozambique show a relaxed situation. In Spain, an increase of agricultural activities, industrial development and increase of population generate an imbalance between supply and demand of water. Thus scarcity and water stress [3,4] can be one of the main water problems in Spain, because it can contribute the pollution of the water resources and the preoccupation of the people.

Given this situation, new measures should be adopted in the management of water to enhance the health of the environment, the organisms and the humans. In this sense, three main objectives should be achieved. The first one is to reduce the water pollution in the origin namely, minimizes the use of pollutants as pesticides, heavy metals, pick up expired pharmaceuticals,... [5]. The second objective is to improve the waste water

3

treatment plants (WWTP) and related technologies (as membrane filtration, UV disinfection, treatment with activated carbon, ozone, advance oxidation,...) in order to remove more effectively the contaminants. The third objective is to develop new resources that allow to obtain the necessary water. An example can be the construction of reverse osmosis in desalination plants. They allow converting fresh water from sea water, but this process is related to a huge consumption of energy affecting to the global climatic change.

1.1 Water resources in Catalonia

Catalonia is located in the North east of Spain (3º 19' 59,94" E, 0º 9' 41,69" W, 42º 51' 45,97" N, 40º 31' 27,56" S). Catalonia is characterized by a high number of small rivers with irregular flows which most of these rivers flow into the Mediterranean Sea (Fig. 1.1).

Figure 1.1 Hydrographic map of Catalonia from Institut Cartogràfic de Catalunya[6]

The most important rivers in Catalonia are Ebre (source in Fontibre, Cantabria, Spain), Ter (source in Ulldeter, Catalonia, Spain) and Llobregat (Castellar de N'Hug, Serra del Cadí, Catalonia, Spain), both end in the Mediterranean Sea. The Ter basin has an

extension of 2955 Km^2 while the Llobregat basin 4948,3 Km^2 with an average flow of 16.9 m^3 s^{-1}.

Low flows present the Catalan rivers respect the European rivers as Seine, Danube, Rhine, ... This fact and the high crown in some parts of the catalan territory make the necessity of use different WWTP along the river to improve the quality and reuse the water for cities near the river.

A complete treatment of water on a WWTP consists in four parts: Pretreatment, primary, secondary and tertiary (Table 1.1). The tertiary treatment is only applied when water is highly pollutant due to the high cost of the system.

Table 1.1 Process sanitation in a waste water treatment plant.

Process	Technology	Characteristics
Pretreatment	Roughing operation	Separate voluminous wastes
	Weighing up (sieve)	Eliminate some wastes
	Grinding	Decrease volum wastes and eliminate
	Griting (sandfang, desarenat)	Elimination particules > 200 μm
	Fat free	Elimination of fats
Primary treatment	Primary decantation	Sedimentation of solids in suspension, sludge production
	Flocculation	
	Coagulation	
Secondary treatment	Coagulation	
	Activated sludge process	Biologic oxidation Separation liquid-solid
	Nitrification/Denitrification bioreactor	Nutrient removal
Tertiary treatment	UV-disinfection	Disinfection Remove pathogenic organism Remove micropollutants
	Activated Carbon	
	Advanced oxidation	
	Ozone	
	Chlorination	

Along the Llobregat river different WWTP treat the water after their use in the main towns and industrial factories. Nevertheless, recently a variety of organic micropollutants called emerging contaminants such pesticides, pharmaceuticals, surfactants, plasticizers has been detected in the stretch of the Llobregat basin and in

WWTP [7-10]. Banjac et al. [11] estimated 160 different compounds in the river which industrial compounds and pharmaceutical are the dominant. On the other hand, poor elimination efficiencies of emerging pollutants are shown on the secondary and tertiary treatments in the WWTP along the Llobregat basin [12].

As can be seen in Table 1.1 different technology (UV-disinfection, ozone, **activated carbon**, advanced oxidation,...) are applied on the tertiary treatment to enhance the quality of water and later returned and reuse it along the basin. **Activated carbon** is the technology to focus in this study and used to improve the removal of the **emerging pollutants**.

2. Emerging and organic micropollutants

The last three decades, the increase of these organic substances on the environment has been accentuated and they considered the new emerging pollutants. These substances are included in different groups as drugs, pesticides, personal care products, industrial compounds, food additives... (Table 1.2) [13-16].

Table 1.2 Example of different emerging pollutants groups

Pharmaceuticals	Pesticides	PAH	ICM	Food additives	Industrial wastes
Paracetamol	Atrazine	Anthracene	Iodixanol	Acesulfame	EDTA
Ibuprofen	Simazine	Naphthalene	Iopamidol	Saccarine	ETBE
Fenoterol	Diuron	Benzo(a)pirene	Histodenz	Sucralose	Toluene
Caffeine	Isoproturon	Chrysene	Diatrizoate		Diglyme
Lidocaine		Ovalene	Iopromide		Bisphenol A

Most of these organic substances are soluble in water, thus they are easily introduced to the aquatic ecosystem being harmful for most of the organism. These organisms can act as bio-accumulators and they introduce into the food chain affecting the human.

Long periods of contact of these molecules with some organisms affect the growth, the development, genetics and their reproduction. It is demonstrated that some fish species show feminine tendencies due to the presence of disruptor endocrine substances (ethinyl stradiol)[17]. Moreover, bioaccumulation in the tissues organism (molluscs, plants,...) can produce the death in the long term [18].

Different studies show that some drugs as cannabis and cocaine [19,20] and other 80 drugs are present in surface waters and then they are found in the drinking water. It isn't known the concentration threshold of pharmaceutical and mixtures that can be toxic for the human race. It can cause a decrease of the quantity and quality of the sperm and also a decrease of the motility. In addition, it is considered they will cause different disorder in the reproductive system, a decrease of the reproductive aptitude and even cancer [18].

2.1 Origins and fate

The problems caused by emerging pollutants in the environment makes necessary an exhaustive knowledge of their origins, sources, transformation and final fate of these pollutants in order to find where we can introduce measures to minimize their effects on the environment.

Fig. 1.2 shows the different pathways of the emerging pollutants, their origins, their specific consume sources, primary fate and final fate. As can be seen, the pollutants follow different routes, but they all eventually arrived at the same final fate: Water treatment in a WWTP.
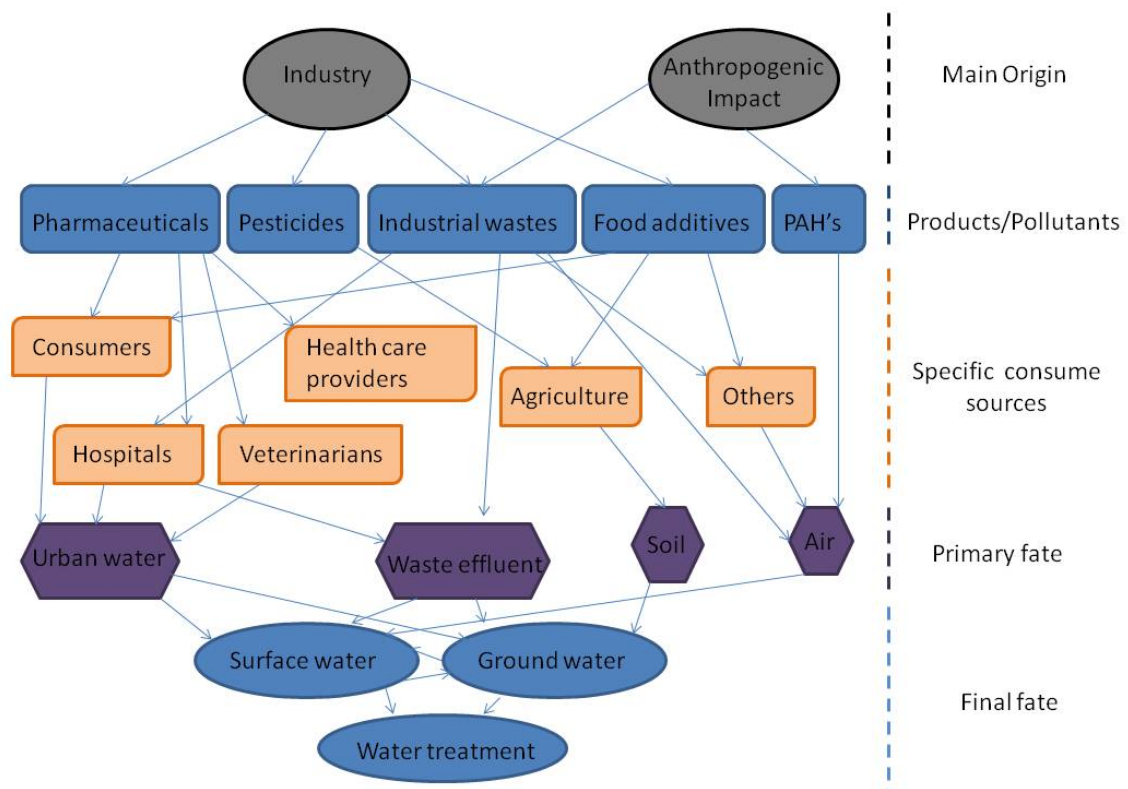
Figure 1.2 Emerging pollutants pathway (adapted from [21])

The main original source of all those contaminants is the industrial activity. Pharmaceutical and cosmetics laboratories, agri-food industries produce these compounds and they can be released to the media trough liquid and gaseous effluents that haven't been properly treated. After that, the specific consume source is pretty different for each group. In the case of pharmaceuticals and drugs (human and veterinarians), they are taken by humans and animals, metabolized in their organism and resealed through excretion, urine, or sweating to the urban wastewater arriving finally at the wastewater treatment plant. The same pathway and fate suffer compounds in the health care providers group (doctors, dentists, hospices or orphanages), where its patients can receive different quantities of drugs and then drugs are eliminated (excreted, urine,...). In the hospitals there is a huge crowd and different drugs throw to the rubbish, the sewer or accumulated on the chemist. The different tracks of pollutants are different but they used to end in the effluent of the hospital. Sometimes hospitals have some water treatment plants to reduce the effect to the environment but not all of them have this infrastructure.

The accumulations of the pesticides, additives spread on the soil and even pharmaceuticals and drugs thrown away in the garbage could reach surface and ground water due to lixiviation into rain or dissolution in the runoff [22].

Others sources of micropollutants are cruisers, cemeteries, humanitarian aid places, clandestine laboratories (also synthesizes pharmaceutical and other substances), ...

As can be seen in Fig. 1.2, the final fate of all those emerging pollutants is the waste water treatment plant (WWTP). During the process in WWTP, some of the compounds, are precipitated, biodegraded or retained on the sewage sludge. However other compounds remain in the water effluent of treatment plant and discharge into the rivers. There they can be bioaccumulate by aquatic organism entering the food chain and eventually affecting human health.

2.2 Legislation

In the European Water Framework Directive (WFD; Directive 2000/60/EV), 33 individual or groups of organic micropollutants are classified as priority or priority hazardous substances (Table 1.3.). Moreover, every four years the directives are revised and in 2012 15 new substances were additional proposed to this list (COM(2011)876

and SEC(2011) 1547) (Table 1.3). This last revision pharmaceutical are proposed for the first time. The proposal does not put into question the medicinal value of these substances, but addresses the potential harmful effects of their presence in the aquatic environment.

Table 1.3 Priority substances polluting surface waters

Priority substances		
Directive 2000/60/EC		COM(2011)876
Alachlor	Hexaclorocyclohexane	Aclonifen
Anthracene	Isoproturon	Bifenox
Atrazine	Lead	Cypermethrin
Benzene	Mercury	Dicofol
Brominated diphenylether	Naphtalene	Heptachlor
Cadmium	Nickel	Quinoxyfen
Chloroalkanes	Nonylphenol	Cybutryne
Chlorfenvinphos	Oxtylphenol	Dichlorvos
Chlorpyrifos	Pentachlorophenol	Terbutryn
1,2-dichloroethane	Pentachlorobenzene	Perfluorooctane sulfonic acid
Dichloromethane	PAH	Hexabromocyclododecane
DEHP	Simazine	Dioxin and Dioxin-Like PCBs
Diuron	Trybutylin	17 α-ethinylestradiol
Endosulfan	Trichlorobenzenes	17 β-ethinylestradiol
Fluoranthene	Trichloromethane	Diclofenac
Hexachlorobenzene	Trifluralin	
Hexachlorobutadiene		

As can be seen, the directive considers a total 48 of prior hazardous substances. But there are other two groups of pollutants to be considered: New pollutants group that is formed by endocrine disruptors and emerging contaminants group (not regulated) which is mainly composed by pharmaceuticals and personal care products. Everyday these groups are taken more importance but there isn't enough data to evaluate the risk that they represent.

3. Activated carbon

Activated carbon is any carbonaceous material that has both high degree of porosity and extended interparticulate surface area available for adsorption or chemical reactions [23-

25]. Carbon materials are mainly composed of the element carbon. Carbon atomic structure allows different bonding possibilities, both with other elements and with itself [26]. So every activated carbon shows different unique characteristics that are defined for its pores structure and its chemical origin or nature.

3.1 Textural and chemical properties

3.1.1 Pore texture

Activated carbons have a porous carbon structure. This structure is a result of an uncertain or random disposition of the porosity and the cross-linking of the macromolecular species, some of them have a pseudo graphitic character, and others are amorphous (Fig. 1.3) [27] (a mixture of graphite-like crystallites and non-organized phase composed of complex aromatic-aliphatic forms).

Figure 1. 3 Activated carbon structure [24]

The porous structure is perhaps the main physical property that characterizes activated carbons. This is formed by pores of different sizes which according to IUPAC can be classified intro there major groups ad one subgroups (Table 1.4).

Table 1.4 Different pore diameters according IUPAC

Main group	Sub group
Micropores Ø < 2 nm	Ultramicropores <0.7 nm
	Supermicropores 0.7-2 nm
Mesopores Ø 2-50 nm	
Macropores Ø > 50 nm	

The micropores constitute a large surface area (in some activated carbons can represent about the 90% of the total surface area) and micropore volume, and they can be considered as slit-shaped pores [24,25]. According to Bansal and Goyal [25] the mesopores contribute about 5% of the total surface area. At present mesopore activated carbons can show more than 25% of the surface area. According to the final application of activated carbon mesopore are very important due to adsorption capacity or due to conduction to micropore. The macropores are important because they facilitate the access to the inner of meso and micropores [28].

Two more characteristic related to pore structure are pore volume and surface area. Pore volume is the space that occupies the different pores and can show values from 0.1 to more than 2 cm^3 g^{-1}. Surface area in activated carbons is mainly determined for the micropores and it ranges from 500 to 2000 m^2 g^{-1}. Although the surface area of the mesopores is relatively low in most activated carbons, some may have a well developed mesoporosity (200 m^2 g^{-1} or even more)[26]. However, values of up 4000 m^2 g^{-1} are found for some super-activated carbons and these are unrealistically high.

3.1.2. Chemical composition and surface chemistry

Activated carbons are made from polycondensated aromatic species where carbon is the major element. Moreover, other element as nitrogen, hydrogen, oxygen, sulphur can be present. Some activated carbons also contain variable amounts of mineral matter (ash content) depending on the nature of the raw material used as precursor.

All these elements functionalize the surfaces of the activated carbon. The most abundant groups are those from oxygen (carbonyl, quinines, lactones, phenolic,...[29,30]) but there also nitrogen functions (nitro, nitroso, pyrrole, nitrile, amine, pyridine, imine, lactam,...[31,32]) and sulphur derivates (sulphide, thiophenol, disulfide, thioquinone, sulfoxide,...[31]), Fig. 1.4.

These groups increase the polarity of the carbon surface and give the ability to set different interactions depending on the functional groups making different every activated carbon [33,34].
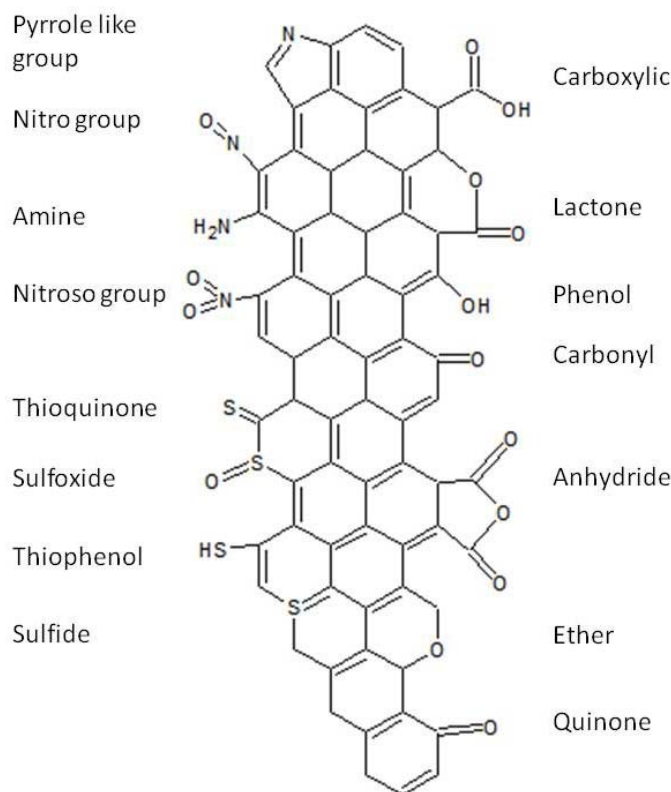
Figure 1. 4 Different functional groups on surface activated carbons

3.1.3. pH, charge and hydrophobicity

Other aspect to be considered is that the activated carbon is an amphoteric material, so the presences of the different functional groups on the surface make the adsorbent acid or basic depending its origin. Moreover, the mineral matter (ashes in the case of activated carbon) can influence to the overall basicity of the adsorbent [32].

When an activated carbon is immersed in an aqueous solution, it develops a surface charge that is produced for the dissociation of the surface groups [35]. This surface charge depends on the solution media and the surface characteristics of the carbon. If the pH of the media is higher than the pH of the activated carbon, acidic functionalities will dissociate, leaving a negative charged surface on the activated carbon (basic medium). On the other hand, in acidic medium (pH medium < pH activated carbon), the surface of the activated carbon is positively charged (Fig. 1.5) [26].

Thus solute adsorption can be influenced depending on charge and electrostatic forces of activated carbons and molecules. Cations will be favoured if the carbon surface is negatively charged, while anions will be adsorbed on positively charged surfaces.
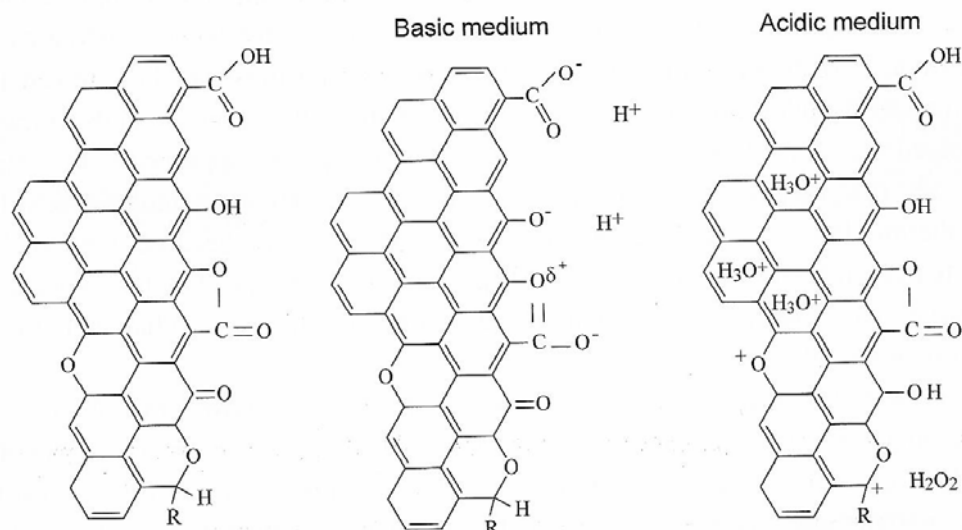
Figure 1.5 Representation of the acidic and basic behaviour of the oxygen-containing surface groups [26]

Activated carbons are, in general, hydrophobic materials. The presence of acidic, basic and neutral functional groups can bind to water molecules through hydrogen bond formation. It causes an increase in hydrophilicity due to the connection of water and oxygen atoms of the carbon surface [36,37]. Water adsorption isotherms can help to explain this fact, oxygen and nitrogen groups (polar groups) can act as nucleation centres at the different stages of cluster formation and pore filling [38]. Clusters and pore filling with water enhance the hydrophilicity of the carbon and reduce the number of available adsorption sites for the solute and block the micropore entrance [39].

3.2. Production of activated carbon

3.2.1 Raw materials

The most used raw material for the activated carbon production is coal with different rank of maturation (anthracite, lignite,...). But with the increasing demand of activated carbon and the generation of different traditional biomass wastes, the market of activated carbon opened to other alternatives as precursors of activated carbon from wood, shells (coconut, almond, walnut, hazelnut,...), fruit stone (pit) as olive, peach, cherry,... [40] Furthermore the global economic crisis of the recent years pushed the market to find other cheaper alternatives for the production of activated carbons from

the generation of different new wastes. These wastes came from sewage sludge [41,42], tyres [43,44], leather industries [45-47], Agar-Agar industries [48,49], oil industries [50],...

In Fig. 1.6 shows the different percentages of the main raw materials for the production of activated carbon.
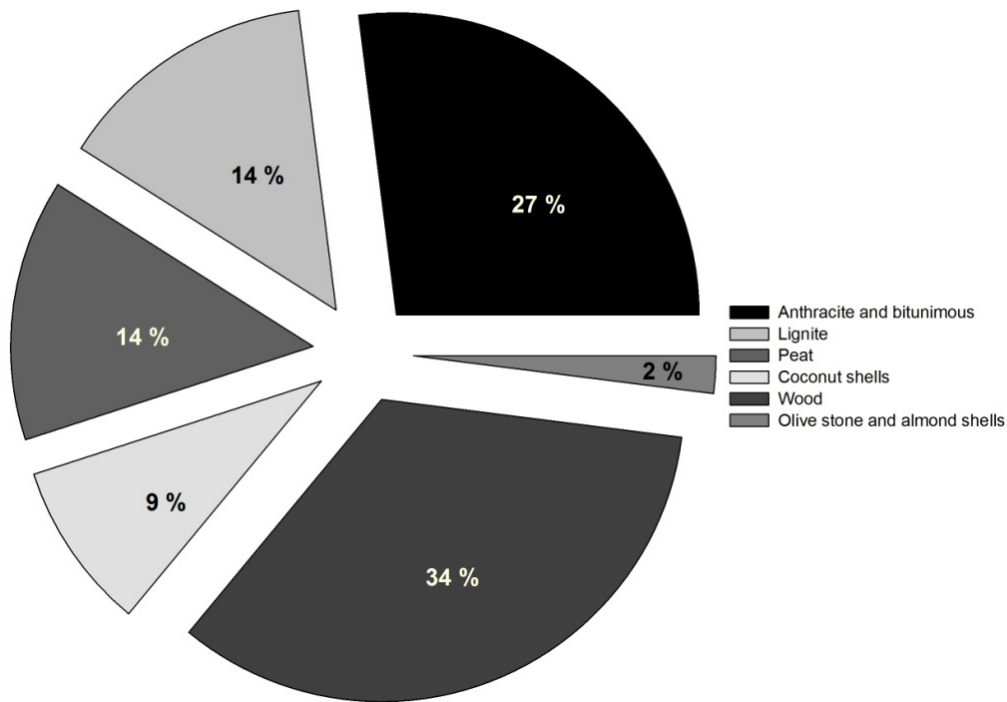
Figure 1.6 Most used raw materials to the production of activated carbon

The selection of the raw material is conditioned or based for different standards:

- The possibility of yielding a good activated carbon in terms of adsorption capacity, high density and hardness
- Cost and availability
- Easy activation
- Low in inorganic matter...

3.2.2 Preparation of activated carbon

Basically, there are two different production processes to prepare activated carbon: Physical activation (or also named thermal activation) and Chemical activation. The main different between both activation process are the kind of activation agent and the

number of steps in the process. Fig. 1.7 shows the general scheme of the production of activated carbons.
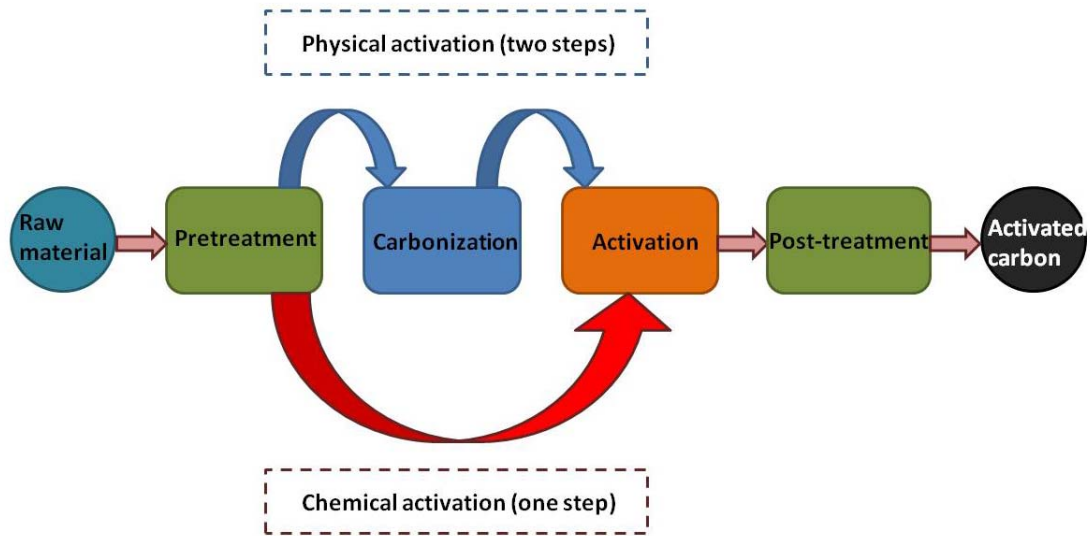
Figure 1.7 General scheme of activated carbon process

Pre-treatment

The raw material is usually crushed, pulverized and sieved to obtain the required particle sized in powder or granular carbons. Sometimes the sample need a first washing step to reduce the mineral matter content, or preoxidation treatment (in coaking coal) to stabilize the coal.

Pyrolysis

The pyrolysis is the thermal decomposition of a material with the absence of oxygen or other different reactive that contains oxygen (air, water and carbon dioxide). In this process the organic substances on the material are volatilized by heating in an inert atmosphere in a furnace. In the process different products can be obtained; the volatiles can be recovered as a gas fraction and a carbonous solid that is called 'char'.

The gas fraction is mainly composed by H_2, CO, CO_2, CH_4, C_2H_2, ... These gases can be used as a combustible or fuel for other process after a properly pre-treatment. They can also be used for electricity generation and production of syn gas [51]. Furthermore part of the gas fraction can be condensed as a liquid fraction. This liquid also can be used as a fuel in different equipment as boilers, engines, turbines, ...[52,53] and as a raw

material for the production different chemical compounds (fungicides, insecticide, combustible additives [54], products for pharmaceutical industries,...

The solid fraction or char is a carbonous material which the decomposition process has allowed a first development of the micropore structure and increase the carbon content. Thus this material can be used as activated carbon. Furthermore this solid can also be used as a combustible in a combustion and/or gasification processes.

Process and reactions in the pyrolysis

The thermal decomposition of a carbonous material takes place in different chemical reactions and heat and mass transfer processes. It can be considered two main steps in the global pyrolysis process: primary pyrolysis and secondary pyrolysis.

- Primary pyrolysis produces the thermal decomposition of the carbonaceous material at lower temperatures than 400 ºC. In this step, different reactions are produced at the same time with simple, multicomponents and intermediate products that give char, liquid and gas products.
- Secondary pyrolysis at higher temperatures than 400 ºC produces secondary decomposition reactions in the carbonaceous solid. These reactions can be classified in homogeneous and heterogeneous, and they include the cracking process, partial oxidation, and condensation and repolimerization.

It can be considered that pyrolysis starts at 250 ºC and it can be completed around the 500 ºC. During the pyrolysis, oxygen and hydrogen present on the material are eliminated as gas by means pyrolytic decomposition. The free carbon is regrouped creating aromatic rings that produce the basic structure units. Moreover, intermediate decomposition products as tar are produced and deposited on the interstitial spaces [51].

Physical activation

The physical or thermal activation is a process that consists in two consecutive steps; the first one is the pyrolysis or carbonization (described before) and the second one is the activation.

In the physical activation, the remaining char from pyrolysis is partially gasified with an oxidizing agent (gas) in direct fired furnaces. Steam is the most common agent used but

carbon dioxide and oxygen or a mixture of the three are also used [55]. The gases react with the carbon atoms and remove some of the mass of the internal surface, creating a well developed microporous material and increasing the specific surface area. The activation is done by means a high temperature of the process (800-1000 ºC).

In the activation process, the general reactions of steam (1), carbon dioxide (4) and molecular oxygen (2,3), as well as producing gaseous reaction products and develop the porosity, also result in the formation of chemisorbed oxygen.

$$C + H_2O \leftrightarrow H_2 + CO \qquad (1)$$

$$C + O_2 \leftrightarrow CO_2 \qquad (2)$$

$$2C + O_2 \leftrightarrow 2CO \qquad (3)$$

$$C + CO_2 \leftrightarrow 2\,CO \qquad (4)$$
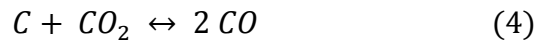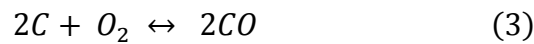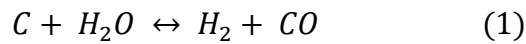
The chemisorbed oxygen (also named surface oxygen complexes) can form different complexes in the surface of the material (descriptive equation (5), no stoichiometry is involved [23])

$$C_f + CO_2 \leftrightarrow CO + C(O) \qquad (5)$$
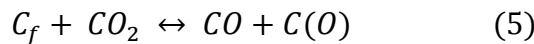
During the course of an activation process, these surface oxygen complexes behave both as reaction intermediates in the gasification of the activated carbon, as well as acting as a retarder to the reaction rate. In the activation with steam, hydrogen can be also chemisorbed on the carbon surface (1, 6)

$$2C + H_2 \leftrightarrow 2C(H) \qquad (6)$$
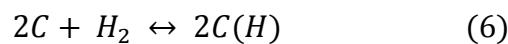
The formation of the different oxygen and hydrogen complexes can retard (inhibit) the reaction rate with the carbon. This effect may not necessarily be negative because it prevents the reaction between carbon and oxygen thus it helps to control the gasification and subsequent porosity development.

Chemical activation

The process consists in mix a chemical compound (named chemical agent) and to put this mesh under thermal treatment (400-700 ºC) [23-25, 56]. It is usually a one step

process that carbonization and activation take place on the same place. The chemical agent reduces the formation of volatile matter and tars and increase the carbon content.

The most common chemical agents are: chlorides (as $ZnCl_2$), acids (H_3PO_4, H_2SO_4, ...), alkaline hydroxides as KOH and NaOH (actually the most used) and different carbonates [57-60]. Most of these chemical agents are dehydrating compounds that influence on the decomposition in the activation process.

In this Thesis the activated agents used are KOH, NaOH and K_2CO_3 and the reactions occurred in the activation process are summarized on the following table 1.5. The effect of the use of hydroxides in the chemical activation is mainly the formation of potassium and sodium, hydrogen and carbonates.

Table 1.5 Reactions produced in the chemical activation with KOH

$6 \ KOH + 2C \rightarrow 2K + 3H_2 + 2 \ K_2CO_3$ (5)	Main reaction with KOH in activation process	
$2 \ KOH \rightarrow K_2O + H_2O$ (360ºC) (6)	(Possible) Simultaneous decomposition secondary reactions with KOH and reduction of carbon	
$C + H_2O \rightarrow H_2 + CO$ (7)		
$CO + H_2O \rightarrow H_2 + CO_2$ (8)		
$K_2O + CO_2 \rightarrow K_2CO_3$ (9)	Reaction (9) is a competitive reaction with (5) which carbonates are formed	
$K_2O + H_2 \rightarrow 2 \ K + H_2O$ (10)		
$K_2O + C \rightarrow 2 \ K + CO$ (11)		
$K_2CO_3 + 2 \ C \rightarrow 2 \ K + 3 \ CO$ (12)		

Sometimes, the use of carbonates can produce CO_2 which can involve a physical activation in this process and over the carbonous material. This physical activation may be produced at 900 ºC approximately due to the decomposition of K_2CO_3 takes place.

Post treatment

After activation process, the obtained materials are not ready to use as adsorbents although porosity have been developed on them. They need a washing step to clean the different unnecessary substances as ashes that block the different pores, and remove the possible agents that excess of activating reagent (mainly in chemical activation). According to the final application of the activated carbon, it will washed with HCl and

water [46] to obtain acid activated carbons or with only water to obtain basic activated carbons. Finally, the adsorbent is dried up.

According to the final application of activated carbon, other process can be made as for example extrusion, pulverize, ...

3.2.4. Types and shapes of activated carbons

Activated carbons can be classified according to the size of its particles in two different groups: pulverized activated carbon (PAC) and granular activated carbon (GAC). PAC adsorbents have a size lower than 100 μm (most usual sizes between 15 and 25 μm), whereas GAC adsorbents show sizes between 1 and 5 mm.

Furthermore, GAC adsorbents can be divided into two different groups: unshaped or broken GAC and shaped GAC of a specific form (cylinder, bead, disks...). Broken GAC are obtained by means of milling, sieving and classifying the different size, whereas shaped GAC can be obtained by means pelletization or extrusion of pulverized carbon mixed with other kind of binder.

There are other activated carbon forms as carbon fibers, carbon fabrics and felts, monolithic structures, carbon films, template derived carbons and carbon nanotubes.

3.2.5. Liquid and gas applications

Activated carbons have been used in wide range of application on liquids and gases treatment and other aspects. The most important applications are:

- Carbon dioxide, hydrogen and methane storage [46,61-64]
- Gold recovery [65]
- Recover sweet odours to increase the quality of products [66]
- Inhalators and masks
- Water, drinking water and waste water treatment plant process [67]
- Elimination of emerging pollutants on hospital waste water [68]
- Discolouration of liquors, vinegars, sugars, honey, juices,...[69]
- Medical adsorbents [70,71]
- Mercury elimination [47,49]
- ...

4. Adsorption in aqueous phase

The mechanism that activated carbons eliminate the emerging pollutants in aqueous phase is the adsorption. Adsorption is a process in which a molecule, atom or ion (all of them considered adsorbates) are retained in the surface of a solid materials (considered as adsorbent). This process is based on the mass transfer phenomenon due to different interactions between molecules and the surface of the adsorbent.

Molecules from gas or liquid phase will be attached in a physical way to a surface of an activated carbon. The adsorption process takes place in three different steps:

- **Macro transport**: the movement of the organic molecules through the macro-pore system of the activated carbon
- **Micro transport**: the movement of the molecules through mainly the mesopore and micropore of high dimensions
- **Sorption**: Physical attachment of the organic molecules in the mesopores and micropores.

To understand the adsorption process and the behaviour of an activated carbon, batch studies (equilibrium adsorption and kinetics) and dynamic studies are required before to design a dynamic reactor.

4.1 Batch studies and equilibrium adsorption

A system which an adsorbate is in contact with a mass of an adsorbent, a mass transfer from the liquid to the solid phase is produced. When the adsorbent is exhausted and no more molecules are adsorbed the system achieve the equilibrium. The equilibrium depends on the solute concentration and water temperature. Different models are proposed to interpret the process of adsorption; the most important are Langmuir and Freunlich. These models represent the experimental isotherms that are the relation between quantities adsorbed at equilibrium (q_e) versus solute concentration (C_e).

Langmuir model

$$q_e = \frac{q_m\, K_L C_e}{1 + K_L C_e} \qquad (13)$$

Where K_L is the equilibrium constant of Langmuir (L mg^{-1} or L mmol^{-1}), q_e is the quantity adsorbed at the equilibrium (mg g^{-1} or mmol g^{-1}), q_m is the maximum adsorption quantity (mg g^{-1} or mmol g^{-1}) and C_e is the equilibrium concentration (mg L^{-1} or mmol L^{-1}).

This model assumes that [72]:

- All the sites of the solid (adsorbent) have the same adsorption activity (surface is homogeneous)
- There is no interaction between adsorbed species
- Every adsorbate-adsorbent link have the same structure and it occurs by the same mechanism
- Every site or pore of the adsorbent only can hold one molecule (the adsorbed layer is a monolayer)

Freundlich model

$$q_e = K_f \, C_e^{\,1/n} \qquad (14)$$

where K_f is the Freundlich adsorption constant ((mg g^{-1}) (L mg^{-1})$^{1/n}$) and n is a constant related to the adsorption intensity. Both constants depend on the interaction solute-adsorbent and the temperature. If the relation 1/n <1 the adsorption if favourable, while if 1/n > 1 the adsorption is not favourable.

This model is considered empirical; it assumes heterogeneity of adsorption sites; It can only be used at lower and intermediate solute concentrations; it lacks of physical meaning (it doesn't include a maximum adsorption capacity) [73].

4.2 Fixed bed adsorption

Adsorption in water treatment is usually taken place on fixed bed adsorbers that contains granular activated carbon. Water passes through the filter by gravity or pressure. The dynamic process in the fixed bed can be divided in three different parts: clean zone where the molecule will be adsorbed, mass transfer zone where the molecule has been adsorbed but the adsorption equilibrium has not been achieved yet and the exhausted zone (saturated) where the maximum adsorption capacity of the activated carbon is achieved and no more molecules can be adsorbed. Fig. 1.8 shows the

evolution of saturation zone progress into the filter. For a constant inlet flow, the exhausted zone is moved through the filter and approaches the end of the bed until the effluent concentration reaches the influent one and no more removal occurs [74]. When the activated carbon is totally exhausted, the filter is emptied and then refilled with new activated carbon. The exhausted activated carbon can be regenerated by means of a thermal process.
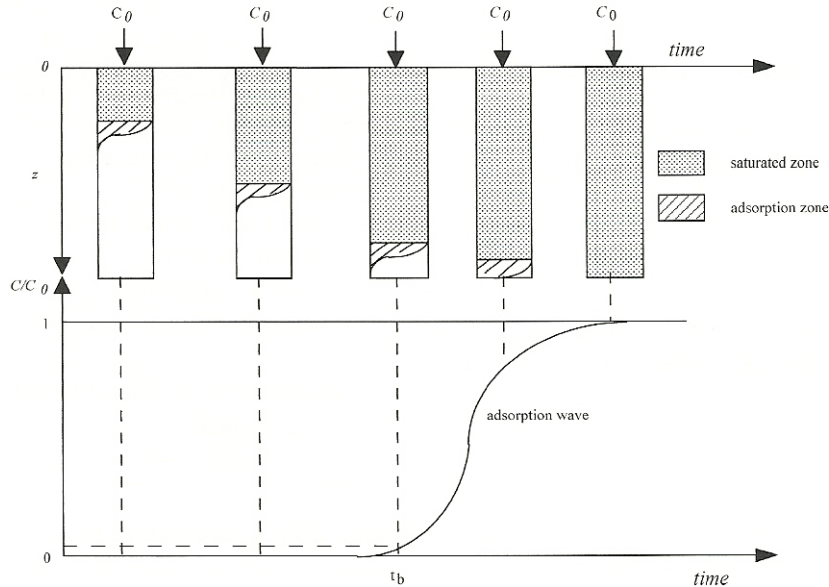
Figure 1.8 Fixed bed adsorber – adsorption zone progression [74]

4.3 Adsorption interactions

Activated carbons have different applications in the treatment of water (drinking and waste). The characteristics of activated carbon (pore size distribution, surface chemistry,...) are very important to the process because they control the different aspects of equilibrium adsorption. On the other hand, the characteristics of waters also are important because they influence the adsorption on the activated carbon, for example the presence on Natural Organic Matter (NOM), pH, temperature, hardness, type of adsorbate,...

In the water adsorption process three general types of interactions control the adsorption of an adsorbate by activated carbon: 1) adsorbate-activated carbon, 2) adsorbate-water and 3) activated carbon water [75].

4.3.1 Adsorbate-activated carbon interactions

Organic pollutants (as emerging compounds) use to be small molecules with a molecular surface area between 1-3 nm^2 [76]. These molecules can access to the micropore of the activated carbon, thus pore size distributions and surface area determine the physical adsorption between adsorbate and adsorbent (activated carbon, AC).

Chemical factors can also be considered, the chemical surface constitution of the activated carbon, the functional groups of the molecules and the solution chemistry can favour or decrease the adsorption. In the case of activated carbons, oxygen is the dominant heteroatom in the functional groups giving to the surface different possibilities to adsorb organic pollutants. The interactions that can occur between them are: π-π dispersion interactions between the aromatic ring of the adsorbate and the basal plane of the activated carbon [77], electrostatic attraction-repulsion interactions, hydrogen bonding between surface functional groups and aromatic molecules [39], electron acceptor-donor complex formation mechanism,....

Furthermore, the presence of Natural Organic Matter (NOM) in surface and waster waters can also interact with water and the organic compounds. NOM are complex molecules that can elucidate the adsorption of organic compounds due to aromatic functionalities [78]. NOM molecules also influence in a net negative charge at the pH range of water treatment, so electrostatic forces (attraction and repulsion) play an important role on the adsorption of the NOM and organic molecules [79,80].

4.3.2 Adsorbate –water interactions

The physical and chemical properties of the adsorbate can influence the interactions between water and the molecules. The hydrophobicity of an organic compound drives force to escape from water solution to the interface surface. In other words, the organic compound tends to be pushed to the surface of activated carbon because activated carbon is usually relatively hydrophobic. This tendency is known as solvent-motivated adsorption [81].

The Lundeliu's rule and Traube's rule explain that the decrease of the solubility of a compound increases the adsorption [75]. Polarity of organic molecules can also play an

important role on the influences with water. Polarity is due to the different electronegativities between the atoms that give an unequal distribution of electron density. Increasing polarity enhances the aqueous solubility of the organic molecule so it is expected that adsorption is reduced.

4.3.3 Activated carbon – water interactions

As it explained in section 3.1., the presence of oxygen, nitrogen and other functional groups on the surface can modify the polarity of the activated carbon. These groups can interact with water molecules, increasing the hyprophilicity of the adsorbent, making cluster and blocking the different pores.

5. References

[1] Food and Agriculture Organization of the United Nations (FAO), AQUASTAT, (2015). http://www.fao.org/nr/water/aquastat/main/index.stm.

[2] World Health Organization (WHO), World Health Organization (WHO), (2015). http://www.who.int/en/.

[3] United nations environment Programme (UNEP), Vital water graphics. An overview of the state of the world's fresh and marine waters, (2008). http://www.unep.org/dewa/vitalwater/article77.html (accessed September 17, 2015).

[4] Food and Agriculture Organization of the United Nations (FAO), Aquamaps global spatial database on water and agriculture, (2012). http://www.fao.org/nr/water/aquamaps/ (accessed September 17, 2015).

[5] D. Barcelo, Aguas continentales, gestión de recursos hídricos, tratamiento y calidad del agua, CSIC, 2008.

[6] Institut Cartogràfic de Catalunya (ICC), Atles Nacional de Catalunya, (n.d.). http://www.atlesnacional.cat/icc/atles-nacional/hidrografia/rius-embassaments-i-estanys/ (accessed September 9, 2015).

[7] R. López-Serna, C. Postigo, J. Blanco, S. Pérez, A. Ginebreda, M.L. de Alda, et al., Assessing the effects of tertiary treated wastewater reuse on the presence emerging contaminants in a Mediterranean river (Llobregat, NE Spain), Environ. Sci. Pollut. Res. 19 (2012) 1000–1012.

[8] A. Masiá, J. Campo, A. Navarro-Ortega, D. Barceló, Y. Picó, Pesticide monitoring in the basin of Llobregat River (Catalonia, Spain) and comparison with historical data., Sci. Total Environ. 503-504 (2015) 58–68.

[9] S. González, R. López-Roldán, J.-L. Cortina, Presence and biological effects of emerging contaminants in Llobregat River basin: a review., Environ. Pollut. 161 (2012) 83–92.

1. Introduction

[10] M. Kuster, M.J. López de Alda, M.D. Hernando, M. Petrovic, J. Martín-Alonso, D. Barceló, Analysis and occurrence of pharmaceuticals, estrogens, progestogens and polar pesticides in sewage treatment plant effluents, river water and drinking water in the Llobregat river basin (Barcelona, Spain), J. Hydrol. 358 (2008) 112–123.

[11] Z. Banjac, A. Ginebreda, M. Kuzmanovic, R. Marcé, M. Nadal, J.M. Riera, et al., Emission factor estimation of ca. 160 emerging organic microcontaminants by inverse modeling in a Mediterranean river basin (Llobregat, NE Spain), Sci. Total Environ. 520 (2015) 241–252.

[12] J. Campo, A. Masiá, C. Blasco, Y. Picó, Occurrence and removal efficiency of pesticides in sewage treatment plants of four Mediterranean River Basins., J. Hazard. Mater. 263 Pt 1 (2013) 146–57.

[13] A. Jurado, E. Vàzquez-Suñé, J. Carrera, M. López de Alda, E. Pujades, D. Barceló, Emerging organic contaminants in groundwater in Spain: a review of sources, recent occurrence and fate in a European context., Sci. Total Environ. 440 (2012) 82–94.

[14] M. Stuart, D. Lapworth, E. Crane, A. Hart, Review of risk from potential emerging contaminants in UK groundwater., Sci. Total Environ. 416 (2012) 1–21.

[15] J. Lladó, Posta a punt del mètode per a la determinació de fàrmacs en aigües residuals. (TFM), Universitat Politècnica de Manresa, Manresa, 2010.

[16] A. Pal, K.Y.-H. Gin, A.Y.-C. Lin, M. Reinhard, Impacts of emerging organic contaminants on freshwater resources: review of recent occurrences, sources, fate and effects., Sci. Total Environ. 408 (2010) 6062–9.

[17] R.H.M.M. Schreurs, J. Legler, E. Artola-Garicano, T.L. Sinnige, P.H. Lanser, W. Seinen, et al., In Vitro and in Vivo Antiestrogenic Effects of Polycyclic Musks in Zebrafish, Environ. Sci. Technol. 38 (2004) 997–1002.

[18] Canada Environment, Pharmaceuticals and Personal Care Products in the Canadian Environment: Research and Policy Directions, (2007) 61. http://www.ec.gc.ca/ (accessed September 8, 2015).

[19] S. Bauer, J. Olson, A. Cockrill, M. van Hattem, L. Miller, M. Tauzer, et al., Impacts of surface water diversions for marijuana cultivation on aquatic habitat in four northwestern California watersheds., PLoS One. 10 (2015)

[20] F. Hernández, M. Ibáñez, A.-M. Botero-Coy, R. Bade, M.C. Bustos-López, J. Rincón, et al., LC-QTOF MS screening of more than 1,000 licit and illicit drugs and their metabolites in wastewater and surface waters from the area of Bogotá, Colombia., Anal. Bioanal. Chem. 407 (2015) 6405–16.

[21] T. Heberer, Occurrence, fate, and removal of pharmaceutical residues in the aquatic environment: a review of recent research data, Toxicol. Lett. 131 (2002) 5–17.

[22] D. C.G., Pharmaceuticals in the environment: sources and their management, in: M. Petrovich, D. Barceló (Eds.), Anal. Fate Remov. Pharm. Water Cycle, Wilson & Wilson's (Elsevier), 2007: pp. 1–58.

[23] H. Marsh, F. Rodríguez-Reinoso, Activated Carbon, Elsevier Science Ltd, 2006.

[24] R.C. Bansal, J.B. Donet, H.F. Stoeckli, Active carbon, New York, 1988.

[25] R.C. Bansal, M. Goyal, Activated carbon adsorption, CRC Press, Taylor and Francis group, Florida, 2005.

[26] J.A. Menendez-Diaz, I. Martín-Gullón, Types of carbon adsorbents and their production, in: T.J. Bandosz (Ed.), Act. Carbon Surfaces Environ. Remediat., first, Elsevier, New York, 2006: pp. 1–47.

[27] N. Ferrera-Lorenzo, Aprovechamiento integral del residuo de macroalga procedente de la obtención industrial de Agar-Agar. Aplicación en el campi de la energía y el medioambiente, Universidad de Oviedo, 2014.

[28] K.S.W. Sing, Reporting physisorption data for gas/solid systems with special reference to the determination of surface area and porosity (Provisional), Pure Appl. Chem. 54 (1982).

[29] E. Fuente, J.A. Menéndez, D. Suárez, M.A. Montes-Morán, Basic Surface Oxides on Carbon Materials: A Global View, Langmuir. 19 (2003) 3505–3511.

1. Introduction

[30] M.A. Montes-Morán, D. Suárez, J.A. Menéndez, E. Fuente, On the nature of basic sites on carbon surfaces: an overview, Carbon N. Y. 42 (2004) 1219–1225.

[31] T.J. Bandosz, C.O. Ania, Surface chemistry of activated carbons and its characterization, in: T.J. Bandosz (Ed.), Act. Carbon Surfaces Environ. Remediat., Elsevier, New York, 2006: pp. 159–229.

[32] M.A. Montes-Morán, D. Suárez, J. Angel Menéndez, E. Fuente, The Basicity of Carbons, in: J.M.. Tascón (Ed.), Nov. Carbon Adsorbents, Elsevier, 2012: pp. 173–203.

[33] J.L. Figueiredo, M.F.R. Pereira, M.M.A. Freitas, J.J.M. Orfao, Modification of the surface chemistry of activated carbons, Carbon N. Y. 37 (1999) 1379–1389.

[34] F. Rodriguez-Reinoso, M. Molina-Sabio, Textural and chemical characterization of microporous carbons, Adv. Colloid Interface Sci. 76 (1998).

[35] C. Moreno-Castilla, Adsorption of organic molecules from aqueous solutions on carbon materials, Carbon N. Y. 42 (2004) 83–94.

[36] R.S. Vartenetyan, A.M. Voloshchuk, M.M. Dubinin, O.E. Babkin, Adsorption of water-vapor and microporous structures of carbonaceous adsorbents. 10. The effect of preliminary preparation conditions and the modification of activated charcoals on their adsorption properties, Bull. Acad. Sci. USSR Div. Chem. Sci. (1986) 1763–1768.

[37] J. Alcañiz-Monge, A. Linares-Solano, B. Rand, Mechanism of Adsorption of Water in Carbon Micropores As Revealed by a Study of Activated Carbon Fibers, J. Phys. Chem. B. 106 (2002) 3209–3216.

[38] A. Tóth, K. László, Water Adsorption by Carbons. Hydrophobicity and Hydrophilicity, in: J.M.. Tascón (Ed.), Nov. Carbon Adsorbents, first, Oxford, 2012: pp. 147–171.

[39] M. Franz, H. a. Arafat, N.G. Pinto, Effect of chemical surface heterogeneity on the adsorption mechanism of dissolved aromatics on activated carbon, Carbon N. Y. 38 (2000) 1807–1819.

[40] S.J.T. Pollard, G.D. Fowler, C.J. Sollars, R. Perry, Low-cost adsorbents for waste and wastewater treatment: a review, Sci. Total Environ. 116 (1992) 31–52.

[41] K.M. Smith, G.D. Fowler, S. Pullket, N.J.D. Graham, Sewage sludge-based adsorbents: A review of their production, properties and use in water treatment applications, Water Res. 43 (2009) 2569–2594.

[42] K.M. Smith, G.D. Fowler, S. Pullket, N.J.D. Graham, Production of activated carbon from sludge, in: A. Fabregat, C. Bengoa, J. Font, F. Stueber (Eds.), Reduction, Modif. Valoris. Sludge, IWA publishing, London, 2011.

[43] V.K. Gupta, B. Gupta, A. Rastogi, S. Agarwal, A. Nayak, A comparative investigation on adsorption performances of mesoporous activated carbon prepared from waste rubber tire and activated carbon for a hazardous azo dye-Acid Blue 113, J. Hazard. Mater. 186 (2011) 891-901.

[44] B. Acevedo, R.P. Rocha, M.F.R. Pereira, J.L. Figueiredo, C. Barriocanal, Adsorption of dyes by ACs prepared from waste tyre reinforcing fibre. Effect of texture, surface chemistry and pH., J. Colloid Interface Sci. 459 (2015) 189–198.

[45] R.R. Gil, B. Ruiz, M.S. Lozano, M.J. Martín, E. Fuente, VOCs removal by adsorption onto activated carbons from biocollagenic wastes of vegetable tanning, Chem. Eng. J. 245 (2014) 80–88.

[46] R.R. Gil, B. Ruiz, M.S. Lozano, E. Fuente, Influence of the pyrolysis step and the tanning process on KOH-activated carbons from biocollagenic wastes. Prospects as adsorbent for CO2 capture, J. Anal. Appl. Pyrolysis. 110 (2014) 194–204.

[47] M.A. Lopez-Anton, R.R. Gil, E. Fuente, M. Díaz-Somoano, M.R. Martínez-Tarazona, B. Ruiz, Activated carbons from biocollagenic wastes of the leather industry for mercury capture in oxy-combustion, Fuel. 142 (2015) 227–234.

[48] N. Ferrera-Lorenzo, E. Fuente, J.M. Bermúdez, I. Suárez-Ruiz, B. Ruiz, Conventional and microwave pyrolysis of a macroalgae waste from the Agar–Agar industry. Prospects for bio-fuel production, Bioresour. Technol. 151 (2014) 199–206.

[49] M.A. Lopez-Anton, N. Ferrera-Lorenzo, E. Fuente, M. Díaz-Somoano, I. Suarez-Ruíz, M.R. Martínez-Tarazona, et al., Impact of oxy-fuel combustion gases on mercury retention in activated carbons from a macroalgae waste: Effect of water, Chemosphere. 125 (2015) 191–197.

[50] I.L. Gee, C.J. Sollars, G. Fowler, S.K. Ouki, R. Perry, Use of a liquid chemical waste to produce a clay-carbon adsorbent, J. Chem. Technol. Biotechnol. 72 (1998) 329–338.

[51] R. Rodriguez Gil, Aprovechamiento integral de residuos sólidos de curtición. Implicaciones ambientales, Universidad de Oviedo/CSIC, 2014.

[52] S. Murugan, M.C. Ramaswamy, G. Nagarajan, A comparative study on the performance, emission and combustion studies of a DI diesel engine using distilled tyre pyrolysis oil–diesel blends, Fuel. 87 (2008) 2111–2121.

[53] I. Gökalp, E. Lebas, Alternative fuels for industrial gas turbines (AFTUR), Appl. Therm. Eng. 24 (2004) 1655–1663.

[54] A. Keskin, M. Gürü, D. Altıparmak, Biodiesel production from tall oil with synthesized Mn and Ni based additives: Effects of the additives on fuel consumption and emissions, Fuel. 86 (2007) 1139–1143.

[55] B. Serrano-Talavera, M.J. Muñoz-Guillena, A. Linares-Solano, C. Salinas-Martínez de Lecea, Activated Carbons from Spanish Coals. 3. Preoxidation Effect on Anthracite Activation, Energy & Fuels. 11 (1997) 785–791.

[56] M.J. Illán-Gómez, A. García-García, C. Salinas-Martínez de Lecea, A. Linares-Solano, Activated Carbons from Spanish Coals. 2. Chemical Activation, Energy & Fuels. 10 (1996) 1108–1114.

[57] M. Angeles Lillo-Rodenas, A. Ros, E. Fuente, M.A. Montes-Moran, M.J. Martin, A. Linares-Solano, Further insights into the activation process of sewage sludge-based precursors by alkaline hydroxides, Chem. Eng. J. 142 (2008) 168–174.

[58] D. Lozano-Castelló, M.A. Lillo-Ródenas, D. Cazorla-Amorós, A. Linares-Solano, Preparation of activated carbons from Spanish anthracite, Carbon N. Y. 39 (2001) 741–749.

[59] M.A. Lillo-Rodenas, D. Cazorla-Amoros, A. Linares-Solano, Understanding chemical reactions between carbons and NaOH and KOH - An insight into the chemical activation mechanism, Carbon N. Y. 41 (2003).

[60] M.. Lillo-Ródenas, D. Lozano-Castelló, D. Cazorla-Amorós, A. Linares-Solano, Preparation of activated carbons from Spanish anthracite, Carbon N. Y. 39 (2001) 751–759.

[61] Y.-K. Choi, S.-J. Park, Preparation and characterization of sucrose-based microporous carbons for increasing hydrogen storage, J. Ind. Eng. Chem. 28 (2015) 32–36.

[62] W. Sangchoom, R. Mokaya, Valorization of Lignin Waste: Carbons from Hydrothermal Carbonization of Renewable Lignin as Superior Sorbents for CO 2 and Hydrogen Storage, ACS Sustain. Chem. Eng. 3 (2015) 1658–1667.

[63] N. Bimbo, A.J. Physick, A. Noguera-Díaz, A. Pugsley, L.T. Holyfield, V.P. Ting, et al., High volumetric and energy densities of methane stored in nanoporous materials at ambient temperatures and moderate pressures, Chem. Eng. J. 272 (2015) 38–47.

[64] N. Ferrera-Lorenzo, E. Fuente, I. Suárez-Ruiz, B. Ruiz, Sustainable activated carbons of macroalgae waste from the Agar–Agar industry. Prospects as adsorbent for gas storage at high pressures, Chem. Eng. J. 250 (2014) 128–136.

[65] E.A. Oraby, J.J. Eksteen, The leaching of gold, silver and their alloys in alkaline glycine–peroxide solutions and their adsorption on carbon, Hydrometallurgy. 152 (2015) 199–203.

[66] D.R. Zuim, D. Carpiné, G.A.R. Distler, A. de Paula Scheer, L. Igarashi-Mafra, M.R. Mafra, Adsorption of two coffee aromas from synthetic aqueous solution onto

granular activated carbon derived from coconut husks, J. Food Eng. 104 (2011) 284–292.

[67] Y. Luo, W. Guo, H.H. Ngo, L.D. Nghiem, F.I. Hai, J. Zhang, et al., A review on the occurrence of micropollutants in the aquatic environment and their fate and removal during wastewater treatment., Sci. Total Environ. 473-474 (2014) 619–41.

[68] L. Kovalova, H. Siegrist, U. von Gunten, J. Eugster, M. Hagenbuch, A. Wittmer, et al., Elimination of Micropollutants during Post-Treatment of Hospital Wastewater with Powdered Activated Carbon, Ozone, and UV, Environ. Sci. Technol. 47 (2013) 7899–7908.

[69] V. Caqueret, B. Cagnon, S. Bostyn, H. Fauduet, Removal of dark coloured and polyphenolic compounds of sugar beet vinasse by adsorption onto activated carbons: Application to a crosscurrent adsorption process, Can. J. Chem. Eng. 90 (2012) 403–411.

[70] P.A. Chyka, D. Seger, E.P. Krenzelok, J.A. Vale, Position paper: Single-dose activated charcoal., Clin. Toxicol. 43 (2005) 61–83.

[71] P.A. Chyka, Position statement: single-dose activated charcoal., J. Toxicol. Clin. Toxicol. 35 (1997) 721–741.

[72] K.K.H. Choy, J.F. Porter, G. McKay, Langmuir Isotherm Models Applied to the Multicomponent Sorption of Acid Dyes from Effluent onto Activated Carbon, J. Chem. Eng. Data. 45 (2000) 575–584.

[73] I. Pikaar, A.A. Koelmans, P.C.M. van Noort, Sorption of organic compounds to activated carbons. Evaluation of isotherm models, Chemosphere. 65 (2006) 2343–2351.

[74] P. Le Cloirec, C. Faur, Adsorption of organic compounds onto activated carbon - applications in water and air treatments, in: T.J. Bandosz (Ed.), Act. Carbon Surfaces Environ. Remediat., First, Elsevier, New York, 2006: pp. 375–419.

[75] T. Karanfil, Activated carbon adsorption in drinking water treatment, in: T. Bandosz (Ed.), Act. Carbon Surfaces Environ. Remediat., First, Elsevier, New York, 2006: pp. 345–373.

[76] S. Okouchi, H. Saugusa, O. Nojima, Prediction of environmental parameters by adsorbability index - water solubilites of hydrophobic organic pollutants, Environ. Int. 18 (1992) 249–261.

[77] M. Keiluweit, M. Kleber, Molecular-Level Interactions in Soils and Sediments: The Role of Aromatic pi-Systems, Environ. Sci. Technol. 43 (2009) 3421–3429.

[78] D.J. de Ridder, A.R.D. Verliefde, S.G.J. Heijman, J.Q.J.C. Verberk, L.C. Rietveld, L.T.J. van der Aa, et al., Influence of natural organic matter on equilibrium adsorption of neutral and charged pharmaceuticals onto activated carbon, Water Sci. Technol. 63 (2011) 416–423.

[79] M. Bjelopavlic, G. Newcombe, R. Hayes, Adsorption of NOM onto Activated Carbon: Effect of Surface Charge, Ionic Strength, and Pore Volume Distribution, J. Colloid Interface Sci. 210 (1999) 271–280.

[80] G. Newcombe, M. Drikas, Adsorption of NOM onto activated carbon: Electrostatic and non-electrostatic effects, Carbon N. Y. 35 (1997) 1239–1250.

[81] W.J. Weber, F.A. DiGiano, Process dynamics in environmental systems, John Wiley & Sons, Ltd., New York, 1996.

Chapter 2

Objectives

1. Objectives

The main objective of this Thesis is the removal of organic and emerging pollutants in the aqueous media by means new and selected carbon adsorbents; trying to understand the mechanism that govern the adsorption process according to the particular characteristics of the studied carbons and contaminants.

To achieve this objective new activated carbons from diverse low cost materials (leather wastes, sewage sludge) and mineral coal and from new interesting synthetic adsorbents (Xerogels) were selected in the collaboration framework with the "Instituto Nacional del Carbón" (INCAR-CSIC). Moreover, different company (Xerolutions, Eurocarb, Kureha, Cabot-Norit, Chemviron and Desotec) supplied different carbon materials from different raw materials. On the other hand, the targeted adsorbates have been carefully selected according to their physical and chemical characteristics in order to a better understanding of the adsorption phenomena.

From the main objective derives other specific objectives that are developed in the different sections of the chapter 4 (Fig. 2.1). Moreover, early results from secondary works derived from chapter 4 and new proposed work are introduced in chapter 6 (future work).
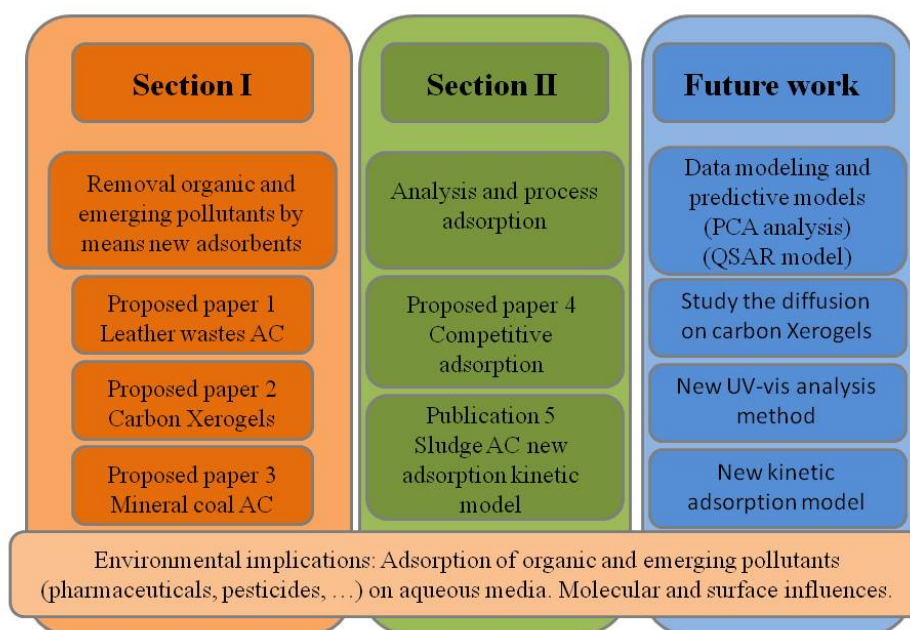
Figure 2.1 General scheme of sections results and future work

Section 4.1 Removal organic and emerging pollutants by means new adsorbents. It describes different specific objectives depending on the material used:

Section 4.1.1 proposed paper: "*Highly microporous activated carbons derived from biocollagenic wastes as adsorbents of aromatic organic pollutants in water originating from industrial activities.*" Objectives:

- Selection of new adsorbents (activated carbons) from leather wastes and the pirolized leather wastes and apply them on the adsorption or different organic pollutants
- Characterization of the new different adsorbents
- Study how influences the temperature and activation agent on different precursor materials (pyrolysed and non-pyrolysed) on the activation process.
- Study which variables or characteristics influence of the adsorbents and molecules on the adsorption of mono substituted aromatic organic pollutants (acetanilide, aniline, benzaldehyde, benzoic acid, methyl benzoate and phenol) on the new biocollagenic adsorbents
- Evaluation the adsorption capacity of the adsorbents

Section 4.1.2 proposed paper: "*Removal of pharmaceuticals and Iodinated Contrast Media (ICM) compounds on carbon xerogels and activated carbons. NOM and textural properties influences.*" Objectives:

- Selection of different carbon Xerogels with a different mesopore diameter
- Characterization of the different carbon Xerogels and compared with different activated carbons
- Evaluate the adsorption capacity of emerging pollutants (pharmaceuticals: phenol, salicylic acid, paracetamol, caffeine, levodopa and diclofenac sodium and ICM: diatrizoic acid, iohexol, iomeprol, iopamidol, iopromide and iodixanol)
- Evaluate how the micropores and mesopores influences on the adsorption of the different molecules
- Evaluate the influences on the adsorption of pharmaceutical and ICM with the presence of Natural Organic Matter (NOM)

Section 4.1.3 proposed paper: *"Removal of pollutants in water using a coal-based activated carbons."* Objectives:

- Selection of new activated carbon from a lignite from Mequinenza rich in sulphur (Mequinenza lignite)
- Selection of mesopore activated carbon from an anthracite (from Coto de Narcea)
- Characterize the chemical and textural properties of the new developed adsorbents
- Evaluate the adsorption capacity for paracetamol, phenol and salicylic acid on the new adsorbents
- Establish possible relationship between the chemical and textural influences and the adsorption of the pollutants and compare the results of the new activated carbons with commercial activated carbons

Section 4.2 Analysis and process adsorption. The main objectives in this section are the development of new analysis technique and a new kinetic adsorption model.

Section 4.2.1 proposed paper: *"Multicomponent adsorption on coal based activated carbons on aqueous media: new cross-correlation analysis method"*. Objectives

- Development of a new analytical method for analyses a multi solution component on the UV-vis
- Study the adsorption competition in binary and ternary solutions on the adsorption of phenol, paracetamol and salicylic acid onto the activated carbons used in section 4.1.3

Section 4.2.2 published paper: *"Role of activated carbon properties in atrazine and paracetamol adsorption equilibrium and kinetics."* Objectives

- Development of a new kinetic model with only two parameters with physical meaning based on mass balances to observe the diffusion coefficient and the effective area
- Characterize the sludge activated carbon with a physical activation with steam

- Evaluate the adsorption capacity for adsorption of paracetamol and atrazine on the sludge activated carbon and compare with commercial activated carbons

2. Memory structure

The structure of the memory of this Thesis has been organized in five different chapters as follow:

Chapter 1: Introduction. In this chapter the problematic with emerging pollutants that are found in the water is summarized. On the other hand, it is exposed the way to produce activated carbon from different raw materials as alternative to eliminate the emerging pollutants. Finally, the adsorption process of organic pollutants in aqueous media and the different interactions between adsorbate, adsorbent and water are explained.

Chapter 2: Objectives and proposal of memory. It is described the different objectives to be achieved in this investigation and the general structure of this Doctoral Thesis.

Chapter 3: Materials and Methods. Here it is exposed the different experimental techniques and materials used in the investigation of this Thesis.

Chapter 4: Results. As it explained before this chapter is composed by three different sections with different topics:

- Section 1 is related to selection and characterization of new adsorbents (activated carbon) for water treatment. In concrete for the adsorption of emerging pollutants (pharmaceuticals)
- Section 2 proposes a new spectrophotographic UV-vis method of analysis of phenol, paracetamol and salicylic acid in binary and ternary solutions and a new kinetic model based on mass balances, using different activated carbons

Chapter 5: Conclusions. In this chapter is summarized the general conclusions of the investigation of this Thesis.

Chapter 6: Future work. In this chapter is presented different ideas for new work related on the adsorption of different emerging molecules, characterize new adsorbents, propose new analysis methods, ... Moreover, the early results of principal component analysis are shown to compare the influence of textural and chemical characteristics of 26 adsorbent on the adsorption of five different molecules (phenol, salycilic acid, paracetamol, diclofenac and iodixanol). In this results different multivariable linear regression model are presented to determinate the maximum adsorption capacity for new adsorbent materials.

Chapter 3

Materials and methods

Theory background

1. Precursor materials

1.1 Lignite from Mequinenza

In the later Oligocene period, in Mequinenza Zone (Ebro basin SE, NE, Spain), a wide and little deep lacustrine zone was developed, that evolved under a subtropical and hot climate and was affected by different wet-arid cycles. The inner lacustrine zone was dominated by carbonates (where coal layers could be found). Different periods of this geologic period, the fresh water changed to saline water (water with 0.5 to 5 parts per mil). At that moment, in the inner lacustrine zone, different sulphur and non sulphur organic compounds were formed due to the contributions of huge aquatic and terrestrial plants, bacterias (cianobacterias) and algae [1].

A later maturation over many years of this coal layers caused the formation of lignite and subbituminous coal with a high sulphur organic content (in contrast a low piritic sulphur) [2,3].

Coal extractions were started in the miner basin of Ebro 150 years ago by "Carbonífera del Ebro" company and the major activity was developed between the two world-wars, and over of 269000 Tm were produced in the year 1949.

Nowadays, Mequinenza coal mine is closed due to their coals have high sulphur content. When this coal is burned produce a negative effect on the environment due to the emission of sulphur dioxide and a possible later acid rain.

1.2 Anthracite from Coto de Narcea

The anthracite comes from Cangas de Narcea (occidental part of Asturias, north-western of Spain). It was developed in the "Estefaniense" period (300 millions of years ago). The basin had mountainous origin and was in the middle of a continental deposit and was rich in swampy zones and peat bogs where vegetation grew were propitious for the formation of this high evolved coal.

This anthracite has a high carbon content and high calorific power; making it a propitious for combustion and the production of energy. The company "Coto Minero del Narcea, S.A." is the responsible of the its commercialisation as well as to find new applications for different technologies.

1.3 Biocollagenic wastes

The solid wastes of the tanning process that were used in this Thesis, were supplied for the company Miquel Farrés Rojas S.A., and they were used in the Thesis "Aprovechamiento integral de residues sólidos de la curtición. Implicaciones ambientales" of the Doctor Roberto Rodríguez Gil. [4]

These wastes came from some stages of the tanning process made with vegetable tannins[4].

- Shaving process: the leather bulk is reduced in order to equalise the thickness on the leather. In this part of the process the wastes generated are shavings
- "Cut out" process: in this stage trimmings are produced, they are the eliminated parts from the leather (wrinkled and imperfectly parts) with the objective to give a better appearance.
- Polish process: The objective of this stage is dissimulated the defects of the flower, polishing the leather and producing buffing dust as waste.

The generation of these wastes are very different depending on the stage they come. In general terms, the generation of shavings represents the 84.19% of the total weight of the wastes; the trimmings represent the 15.15% and finally the buffing dust only the 0.66%.

With the objective to improve the management of the three different wastes, the shavings and the trimmings were grinded (crushed). The same percentage of wastes generation is maintained for a subsequent grinding (grind) and homogenization of the final sample.

2. Sample preparation and pyrolysis in a conventional electric furnace

In accord with the collaboration framework and the experimental methodology developed by the research group "*Biocarbon & Sustainability*" from the Instituto Nacional del Carbon (INCAR-CSIC), the different samples were treated before being used for obtaining activated carbons. Moreover the pyrolysis process of the biocollagenic wastes of this Thesis is only briefly explained because extensive details are available in the Thesis of Dr. Roberto Rodriguez Gil [4].

2.1 Sampling

Once the sample are picked up (lignite from Mequinenza, anthracite from coto Narcea or biocollagenic wastes), it is mixed, homogenized and divided by means different techniques of "quartered" and division with a divisor of parallel channels (also named "rifle"). In general terms, the technique of quartered process consists in prepare a cone with the sample that is want to divide, the top area of the cone is squashed and then the sample is divided in four equal parts. Finally, it is taken one of the four parts and the other three are dismissed. The selected sample is continued divided until a representative sample is obtained for the process of activating carbon.

2.2 Pyrolisis

Previous the chemical activation of biocollagenic wastes, a treated sample weighted in a "ship support" from Alúmina Alsin and it is introduced in a tubular furnace (Carbolite 12/65/550). Then, the reaction chamber (central ceramic pipe) is hermetically seal with metallic closures to guarantee the optimal conditions of the system. Finally a nitrogen flow is connected to create an inert atmosphere in the furnace and control the gases flows. The process is taken at high temperatures with absence of oxygen (air) to eliminate volatile substances, to prevent the combustion of the sample and to obtain a good carbonaceous material (char) that it will be chemical activated [4].

Based on the works of Gil et al. and Ferrera-Lorenzo et al. [5,6], Table 3.1 summarizes optimal experimental conditions for the pyrolysis for the biocollagenic wastes.

Table 3.1 Experimental conditions used on the pyrolysis of biocollagenic wastes

Process variables	
Nitrogen flow	150 mL min^{-1}
Pyrolysis temperature	750 ºC
Overcook time	60 min
Heating slope	5 ºC min^{-1}

3. Preparation of activated carbons by means chemical activation in a conventional furnace

In accord with the collaboration framework and the experimental methodology developed by the research group "*Biocarbon & Sustainability*" from the Instituto

Nacional del Carbon (INCAR-CSIC), the different activated carbon were obtained by means of chemical activation that is described below.

3.1. General process

From a properly treated precursor material (either lignite from Mequinenza, or anthracite from Coto de Narcea or tinning wastes (pyrolysed and non-pyrolysed) is mixed with the correctly proportions of chemical agent (NaOH, KOH or K_2CO_3). The chemical agent is selected according the used precursor material, and their conditions and ratios of use are detailed in subsequent sections. It has been taken care with the experimental process, because the use of pulverized samples mixed with hydroxides (High hygroscopic agents) can be hydrated and carbonated quickly. Once the mixture is obtained, it is introduced in a ceramic container (Alúmina Alsin) that it resists to the corrosion and the alkaline fusions. Then it is introduced into the furnace and the specific work conditions are applied depending on the material selected.

After the chemical process, high porous materials are obtained but their pores can be blocked due the presence of different products from the activation (used inorganic agents and other produced (ashes)). Thus, the different materials need a washing step with acid or water or both depending on the final application of the adsorbent.

3.2. Washing process

A diluted acid solution (HCl 5 M) was used in the washing process. The different steps of the process are following detailed:

- **Step 1:** part of the sample is introduced on a centrifuge tube with 30 mL of diluted acid (HCl 5M)
- **Step 2:** The solution is mixed during 10 minutes in a rotatory agitator (Stuart Sb3)
- **Step 3:** The solution is centrifuged during 15 minutes at 3500 rpm (centrifuge Thermo Electron Corporation (Heraueus Labofuge 400)), separating the solid and liquid parts
- **Step 4:** The same process is repeated different times using 30 mL of deionised water (volumetric dispenser (Opus Hirschmann), until it is achieved the final optimal conditions and taking care the pH of the washing waters.

When the washing process is finished, the solid is separated in the same centrifuge tube, and then the material is dried in a heater at 105ºC during 12 hours. A second dry step of 8 hours is done in a vacuum unit (vacuum heater) at 65 ºC. When it is finished the material can be used as adsorbent.

3.3. Detailed chemical activation conditions for the different raw materials

3.3.1 Activation of lignite from Mequinenza

The lignite from Mequinenza was mixed with KOH as activated agent in solid state with a ratio 1:1. The use of potassium hydroxide as chemical agent allows simplifying with one step the process of preparation of activated carbons from different origin [7-9]. The activation conditions are summarized in table 3.2.

Table 3.2 Experimental conditions used on the activation of the lignite from Mequineza

Activation conditions	
Nitrogen flow	150 ml min^{-1}
Final heating temperature	750 ºC
Heat up (overcook) time	60 min
Heat up slope	5 ºC min^{-1}
Ration weight chemical agent: precursor	1:1

3.3.2 Activation of anthracite from Coto de Narcea

In this case, the anthracite from Coto de Narcea is an evolved material with a high carbon content. For this reason the applied conditions for its activation were very drastic and severe. In the works of Perrin et al [10,11], sodium hydroxide was used as a chemical agent and the ratio conditions (R) were changed. The parameter R was very important to control and develop the porosity on anthracites. For this reason the activation conditions are detailed in table 3.3.

Table 3.3 Experimental conditions used on the activation of the anthracite from Narcea

Activation conditions	
Nitrogen flow	400 ml min^{-1}
Final heating temperature	830 ºC
Heat up (overcook) time	60 min
Heat up slope	5 ºC min^{-1}
Ration weight chemical agent: precursor	3:1

3.3.3 Activation of the biocollagenic wastes

The activation of the tinning wastes were made by means for two different process; with one step (direct activation) and two steps (pyrolysis step and activation step). Two different activated agents were used (KOH and K_2CO_3) and two final heating temperatures (750 ºC and 900 ºC) obtaining a total of eight activated carbons. It should be emphasized that the process with one step the ratio weight chemical agent – precursor was 0.33:1, while the two step process the ratio was 1:1.

In table 3.4 is summarized the different activation conditions used to have a general vision of the produced materials.

Table 3.4 Experimental conditions used on the activation of biocollagenic wastes

Activated carbons	Bioprecursor	Chemical agent	Activating ratio (Agent/precursor)	Activating temperature (ºC)	References
A	BCT	KOH	0.33:1	750	[8,12]
B	BCT	KOH	0.33:1	900	
C	BCTP	KOH	1:1	750	[8,12]
D	BCTP	KOH	1:1	900	
E	BCT	K_2CO_3	0.33:1	750	
F	BCT	K_2CO_3	0.33:1	900	
G	BCTP	K_2CO_3	1:1	750	
H	BCTP	K_2CO_3	1:1	900	

*BCT: Biocollagenic wastes/ BCTP: Pyrolysed Biocollagenic wastes

4. Sewage sludge activated carbon prepared by physical activation

4.1 Preparation of the activated carbon from sewage sludge (Imperial College)

This subsection is referred to the adsorbent from sewage sludge produced and given up for the Imperial College of London.

Previous carbonization of the sludge, they were sterilized, dried at 105-110 ºC to achieve a constant weight and then they were grinded for under 10 mm. 210 grams of sample were introduced in a quartz reactor which were in a rotatory furnace Carbolite (model HTR11/150). The sample was heated up at 5 or 10 ºC min^{-1} in a nitrogen atmosphere at 500 mL min^{-1}. Once a temperature of 1000 ºC was achieved, the furnace

gets cool to obtain the carbonous materials. Steam activation was applied, the equivalent of 0.7 g min^{-1} of steam was mixed with the flow nitrogen (as a carrier gas), and the temperature was maintain during the prescript period. The process is more detailed in the works of Mohamed et al, Lbigue et al. and Smith et al. [13-15].

5 Production of carbon xerogels by means microwave and later carbonization

In accord with the collaboration framework and the experimental methodology developed by the research group "*Microwaves and carbon for technologic applications*" from the Instituto Nacional del Carbon (INCAR-CSIC), the carbon xerogels were obtained by means of the following process.

Organic aqueous xerogels were synthesized by means of policondesation of resorcinol (R) and formaldehyde (F) using deionised water as a solvent and sodium hydroxide (1 M) as a basic agent. The precursor solution was prepared with the follow conditions: first, resorcinol (VWR international, 99%) was diluted with deionised water (using a magnetic agitator). Then the formaldehyde (Aldrich, 37% in water weight, stabilized 10% in weight of methanol) was introduced in the mixture. In all the cases, the molar ratio resorcinol/formaldehyde (R/F) and the dilution ratio were fixed at 0.5 and 5.7 respectively. Three different precursor solutions were prepared with initial pH in based previous works (5<pH<7) [16,17]. Every precursor solution was introduced in a microwave furnace at 85ºC during 3 hours that allows the gelation and maturity of the material was completed. To change the polymeric structure, the water excess was eliminated by means of continuous heat in the microwave furnace until the lost weight was the 50%. The drying step lasted between 1 and 2 hours depending on the final structure of the materials. After the drying step, the xerogel was carbonized at 700 ºC in a horizontal furnace with a 500 mL min^{-1} nitrogen flow [18]. The resident time was two hours and the heating slope was 50ºC min^{-1}.

6. Commercial materials

With the objective to compare the different results obtained with the hand made materials, 12 commercial activated carbons (activated with steam) were acquired. The origin of them is different, as well as the initial shape. Table 3.5 summarizes the

commercial characteristics, company, precedence, raw material, activation and shape of them.

Table 3.5 Commercial activated carbons used in this Thesis

Acronym	Name/simple	Company	Procendence	Raw material	Activation	Shape
BAC	Bead AC	Kureha Corporation	Japan	Petroleum pitch	Steam	Bead
CYCLO	Cyclocarb 401	Chemviron carbon	USA	Coal	Steam	GAC
F400	Filtrasorb 400	Chemviron carbon	USA	Bituminous	Steam	GAC
HYDC		Cabot (Norit)	USA	Lignite	Steam	PAC
HYDRO3000	Hydrodarco 3000 M-1976	Cabot (Norit)	USA	Coal	Steam	GAC
NPK	Norit PK 1-3	Cabot (Norit)	USA	Peat	Steam	GAC
ORGA10	Organosorb 10	Desotec	Belgium	Bituminous	Steam	GAC
ORGAAA	Organosorb 10-AA	Desotec	Belgium	Bituminous	Steam	GAC
ROW	Row 0.8 supra	Norit	Holland	Extruded coal	Steam	Pellet
SAE	SAE Super	Norit	Holland	Coal	Steam	PAC
WAC	Wac AC1108-004 2855	Eurocarb	England	Wood	Steam	PAC
YAO	Yao M325 2855	Eurocarb	England	Coconut	Steam	PAC

7. Characterization techniques of adsorbents

7.1. Proximate and ultimate analysis

Proximate analysis is a normalized technique that allows to know the relative quantities of moisture, volatile matter and ashes.

Ultimate analysis quantify the total content of the different main chemical elements that are in the studied materials (Carbon, Hydrogen, Nitrogen and total Sulphur) according to UNE specifications

The ash content of the activated carbons is determined heating the carbonous sample at 815 ºC in a muffle furnace during 1 hour with presence of oxygen (ISO 1171, UNE 32004). The obtained ashes are the wastes incineration of the material; they are composed of inorganic compounds presence in the initial carbonous material and in the associated mineral matter. The moisture is determined from the lost weigh on the

sample in a furnace at 105 ºC during 1 hour (ISO 11722. UNE 32002). The volatile matter is determined using the standard UNE 32019.

The elemental determination of the different adsorbents (carbon, hydrogen and nitrogen content) is carried out in an automated equipment (LECO CHN -2000). This equipment has a furnace where the sample burns in oxygen atmosphere at 950 ºC. A part of the combustion gases (CO_2, H_2O and NO_x) are carried with Helium. Then the gas goes through in an IR detector that it only detects water molecules. Then the gas sample goes through in another IR that detects CO_2 and finally the gas is analyzed in a thermal detector that is able to detect nitrogen previous reduction of NO_x to N_2.

The sulphur content is determined in automated equipment (LECO Sulphur Determination (S-144-DR) at a maximum work temperature of 1500 ºC. The combustion of the sample is at 1350 ºC with a oxygen flow. This high temperature is necessary because the different forms of sulphur are completed burned (as example the decomposition of some species as sulphates). The gases of the combustion are carried out with oxygen and they go through in a IR selective detector that quantifies the SO_2 content.

7.2 Fourier transform infrared spectroscopy (FTIR)

The different functional groups on the surface of some adsorbents materials are determined by means of a Fourier transform infrared spectroscopy (FTIR) equipment. Infrared spectroscopy is a branch of the electromagnetic absorption. The wavelength range of the infrared spectra is between 400 cm^{-1} to 5000 cm^{-1}, and it excites the transitions between different energy of the molecules [19]. The different functional groups rotate and spin (or twirl) at different frequencies giving different spectra for any molecule or material. The spectra of the different sample are compressed between 4000 and 400 cm^{-1} (medium infrared region) where analytical applications are done for the detection of functional groups in activated carbons.

In the method developed by Schiedt [20], the sample (in this case coal) is grinded in presence of potassium bromide and then the sample is compressed a high pressures making a transparent tablet. A general treatment of the sample is detailed on the studies [21,22], 1 mg of adsorbent is mixed in 500 mg KBr, the sample is compressed at 5

tonnes cm^{-2} during 5 minutes and then at 9 tonnes cm^{-2} during 5 minutes more. Finally the sample is analyzed in a FTIR equipment (in this Thesis a Spectrum 65FTIR Perkin Elmer)

Table 3.6 is shown some different superficial functional groups that can be present on a analysis of a coal [19] and activated carbons [23,24].

Table 3.6 Possible functional groups observed on coals and activated carbons with FTIR

Coal [19]		Activated carbon [23]		Activated carbon [24]	
wavelength (cm^{-1})	Possible functional groups	wavelength (cm^{-1})	Possible functional groups	wavelength (cm^{-1})	Possible functional groups
3330	OH bond and water	-1820	(C=O) 5 membered ring lactone	1880-1740	anhydrides
3000	CH aromatic	-1790		1790-1675	Lactones
2900	CH aliphatic	1810-1780	(C=O, antisymmetric) (C=O, symmetric) anhydride	1760-1665	carboxylic acids
1720	C=O free	1760-1740		1680-1550	Quinones
1660	C=C aisled	1750-1740	C=O carboxyl	1600-1585	aromatic C=C stretching
1600	Aromatic ring, may combined with OH or groups C=O	1700-1650	(C=O) cyclic ketones		
1520	Aromatic ring	1600-1550	(C rings) cyclic ketones		
1460	Aliphatic CH$_2$ y CH$_3$	1620-1580	(C rings) cyclic ethers		
1370	CH$_3$, CH$_2$ cyclic	-1590	(C rings) zigzag phenol gr.		
1250	C-O- y C-O-C-	1480-1420	C-O-H ad C=C deformation zigzag phenol groups		
1170		1700-1660	(C=O) pyrones		
1030	Si-O- (ashes)	1640-1450	(C rings) pyrones		

7.3 Scanning Electron Microscope (SEM)

Scanning Electron Microscope is based on the electronic microscopy which a beam of light is replaced by an electron beam to create an image.

A barrel emit electron that collide against the sample. Different magnetic lens create magnetic field that conduct and focus the electron beam, creating an enlarged image. On the other hand, the vacuum system is an important part of the electronic microscope. The electron can be deviated by some air molecules, for this reason a vacuum system is necessary inner the microscope.

This microscope has a high depth camp so it allows focusing large part of the sample at the same time. The surface of the solid is scanned by means of an electron beam of high energy. It is possible to obtain images of 3-5 nm of maximum resolution. For the preparation of the samples, it is needed that the materials are conductors. In the case that they are not, the sample is recovered with a thin metallic layer to increase the electric conductivity [25].

7.4. Pore characterization: physical adsorption of gases: nitrogen and steam

The physical adsorption of gases (nitrogen, CO_2 and other gases) is a technique extended for the determination of superficial area and pore size distribution of adsorbent materials [26]. Physical adsorption is a general phenomenon that happens when a gas contacts with a solid. It can be distinguished two different concepts on the physical adsorption; the adsorbed material is named adsorbate while the porous solid is the adsorbent. The suitable physical adsorption characteristics for the determination of surface area, different volumes and pore size distribution are [27]:

- Physisorption is an spontaneous process ($\Delta G < 0$), but it don't occur at high temperatures
- Heats of adsorption are low due the weak interaction between adsorbate-adsorbent (the same order of condensation energy of the adsorbate)
- Physical adsorption can be produced by multilayer (relative high pressures). Pore filling is produced, allowing the calculus of the volume.
- No specific interactions between adsorbate and adsorbent are established; molecules are not restricted to be adsorbed in concrete sites of the surface, being available to cover all the surface of the solid
- In general, it doesn't exist activation energy that produces the adsorption, so the process is thermodynamic controlled and the equilibrium is achieved quickly
- Physical adsorption is reversible ($\Delta G \approx 0$), thus adsorption – desorption studies can be carried out

On the other hand, adsorptive gas must be chemical inert, to have a relative high saturation pressure at the work temperature and to have the more spherical shape as

possible minimizing the uncertainty to calculate the cross section of the molecules. For this reason, nitrogen at -196 ºC is used to calculate the porosity in this Thesis.

Porosity is a characteristic of the adsorbents materials. IUPAC classifies pores in three different groups in base the size of the pore and the process that it take place (table 1.4 chapter 1).

Physical adsorption is carried out by means gravimetric and volumetric techniques. The first ones quantify porosity, determining at every relative pressure, the increase of weight for the adsorbent as a consequence of the adsorption process. In the volumetric techniques, a quantity of gas is introduced at a determined pressure and measuring the lost of pressure, it is determined the adsorbed quantity [28].

The experimental determination of the adsorption isotherms consist in measure the quantity of adsorbed at the gas equilibrium pressure, constant temperature and a different partial pressure of the adsorbate. The number of gas moles adsorbed follows the equation:

$$n = f\,(P/P_0)_{T,gas} \qquad\qquad (1)$$

where n is the quantity of gas adsorbed, P_0 is the saturation pressure at a measured saturation temperature, P is the gas pressure, (P/P_0 is the partial pressure) and T is the temperature. This equation represents the expression of the adsorption isptherm.

7.4.1. Adsorption isotherms

The different adsorption isotherms can be classified according its forms by the IUPAC [28] (Fig. 3.1). As can be seen in Fig. 3.1, there are six different adsorption isotherms that are described below:

- **Isotherm type I**: It is characterized of materials with only contain micropores, the maximum adsorption of the isotherm is achieved without inflections. The gradient of the initial part of the isotherm (values p/p^0 from 0 to 0.05, low relative pressures), is indicative of the dimensions of the microporosity. The higher the gradient, the narrower the micropore.

- **Isotherm type II**: It shows an inflexion in the region $p/p^0 > 0.1$, and $p/p^0 > 0,9$, where the adsorption increase reach quickly. These isotherms are characteristic of the adsorption in open surfaces with multilayer formation

(macorpore solids or without porosity, as black carbons). Moreover describes mixed situations as example micropores materials with open surfaces.

- **Isotherm type III**: it is a convex isotherm, characteristic in low potential sites of adsorption (low interaction adsorbate-adsorbant). An example is the adsorption in surfaces on polymeric organic systems.

- **Isotherm type IV**: it is seemed to type II. In addition adsorption in mesoporous is produced. Moreover it presents a hysteresis cycle. It presents an important increase of the quantity adsorbed at intermediate pressures, and it occurs by means of filling pore in multilayer.

- **Isotherm type V**: it is seemed to type III, but they show a homogeneous surface with mesoporosity.

- **Isotherm type VI**: It is an unusual isotherm, it is characteristic of highly homogeneous surfaces. For example, argon adsorption onto graphitic carbon,...
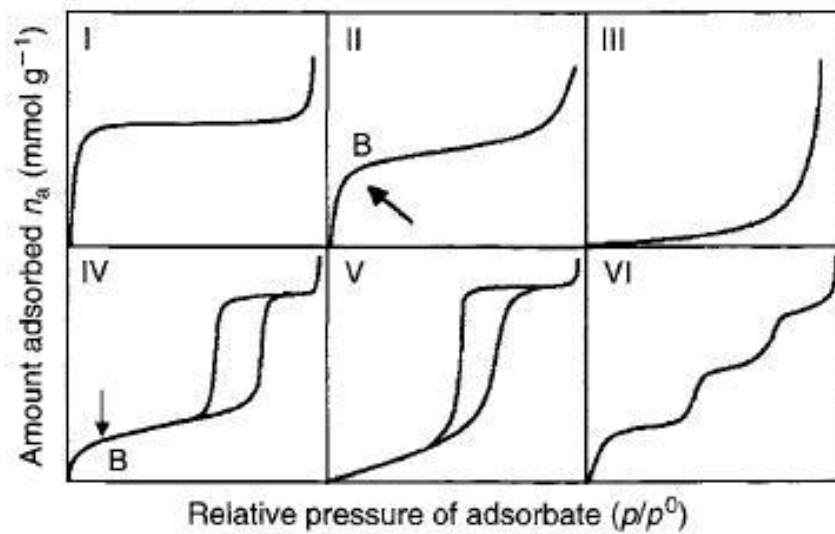
Figure 3.1 Isotherm adsorption classification by IUPAC [29]

7.4.2. Hysteresis cycles on the adsorption isotherms

Isotherms type IV and V are differentiated from the others because they have a hysteresis cycle. This hysteresis cycle is displayed with the multilayer adsorption, and it can be associated to the capillary condensation on mesopore structures [29]. According to IUPAC, there are four types of hysteresis cycles Fig. 3:2
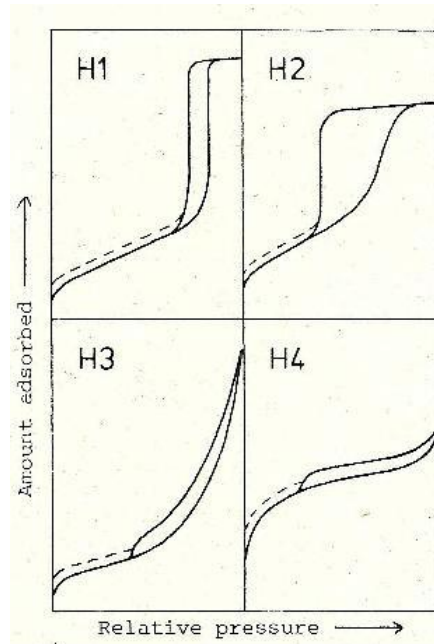
Figure 3.2 Types of hysteresis cycles [29]

The shape of the hysteresis cycle can usually be related to specific pore structure:

-**Type H1**: it is referred to conglomerates or compacted spheres that show narrow pore distributions.

-**Type H2**: The pore distribution and the shape is not well defined. In the past, it was attributed to 'ink bottle' pores but now it is attributed to the effects of the pores net interconnection.

-**Type H3**: These cycles don't exhibit a maximum adsorption and they are associated to slit-shaped pores in aggregates.

-**Type H4**: In this case, the cycle is also associated to slit-shaped pores. In some cases the isotherm is similar to Type I (or hybrid I-IV) and they are indicative of mesopore of small diameter or related to the microporosity.

7.4.3. Specific surface area BET determination

BET theory is based on a kinetic model of the adsorption process proposed by Langmuir in 1916, which a surface of a material is considered as a distribution of equal adsorption sites. Nevertheless, Langmuir isotherm ignores the possibility of the multilayer physiadsorption, which it is arrived a high surface saturation pressures.

Adopting the Langmuir mechanism, but introducing a different series of premises that simplifies it, Brunauer, Memett and Teller (1938) developed the well-known BET equation. They admitted the possibility of multilayer adsorption, allowing the indefinite growth until the gas condensation. The main condition of the BET model is that the different strengths in the gas condensation are responsible of the bond energy in the multymolecular adsorption [30]. This condition is divided in three different parts:

- When $P = P^0$, the adsorbed gas is condensed in a liquid over the surface of the material. It means that the number of layers can be infinite (P^0: vapour saturation pressure)

- All the adsorption sites on the surface are equivalent. The adsorption capacity one site does not depend of the occupation grade of the other sites.

- In every site can be adsorbed different molecular layers, being the adsorption heat equivalent for all of them except the first. All the layers (except the first) show the same evaporation and condensation conditions.

To develop the BET model, it was postulated an equilibrium situation which the molecules' speed that the molecules arrive from the gas phase and are condensed in the available sites is equal to the molecules speed that are evaporated in the occupied sites. At the moment that equilibrium between molecules' condensation speed of the adsorbed gas layer and the evaporation of this layer (and considering a infinite number of layers) is obtained the following expression, known as BET equation:

$$\frac{P/_{P0}}{V^a(1 - P/_{P0})} = \frac{1}{V_m^a C} + \frac{C-1}{V_m^a C} P/_{P0} \qquad (2)$$

Where P/P^0 is the relative pressure, V^a_m is the adsorbed gas volume when it is formed a monomolecular layer of adsorbate onto the solid, V^a is the adsorbed gas volume at pressure P and C is a constant, a parameter related to the heat adsorption of the first layer adsorbed.

$$C = e^{\left(\frac{E_1 - E_L}{RT}\right)} \qquad (3)$$

Where E_1 is the average adsorption enthalpy of the first layer, E_L in the liquefaction enthalpy of the adsorbate, R is the gas constant (8.314 J mol^{-1} K^{-1}) and T is the temperature (K).

To obtain the surface area BET is made a graphic representation of $\dfrac{P/_{P^0}}{V^a\left(1-P/_{P^0}\right)}$ versus

P/P^0, obtaining a line where graphically it can calculate the slope value in the origin and deduce the values V^a_m and C.

The application of BET equation can present some problems as show in Miyamoto et al. work [31]. Different Bet values are obtained depending on the pressure ranges are used. Even so it is the method used to determine the surface area. The linearity of this equation only include a part of the isotherm (between relative pressure from 0.05 and 0.3), and in some cases it must be chosen the appropriate interval that allow to obtain a straight line.

Known the value V^a_m, it can be known the occupied surface of adsorbed molecule, for determine the superficial area of the solid. The superficial area of the solid is determined by the following equation:

$$As = n^a_m N_A a_m \qquad (4)$$

where As is the superficial area of the solid, n^a_m is the capacity of the monolayer, necessary quantity of adsorbate to cover the surface of the solid with one complete layer of molecules, N_A is the Avogadro constant and a_m is the compact packaging area of nitrogen [a_m (N_2) = 0.162 nm^2 at 77 K]. If the expression is referred to a mass unit, it is obtained the superficial specific area of the solid, a_s also named specific area or specific surface.

$$a_s = {A_S/m} \qquad (5)$$

where m is the mass of solid.

7.4.4. Experimental determination of adsorption isotherms

For the analysis of the nitrogen isotherms, as well as water isotherms, it picked up 0.2 grams approximately of sample. The sample was degasified to vacuum at 120 ºC during 18 hours, extracting the moisture and the physiadsorbed gases. Once the sample is degasified, the adsorption desorption nitrogen isotherm at -196 ºC is carried out in a Micromeritics ASAP 2420 equipment. Then with the obtained data, the superficial

specific BET (S$_{BET}$), total pore volume (V$_{TOT}$) at relative pressure 0.95 or 0.99 (ISO 9277-2010, UNE-ISO 9277-2009) were calculated.

7.4.5. Pore size distribution determination (DFT method)

Density functional theory is one of the computational methods developed to describe the pore size distribution inside a material. It exists different applications of this method for determination of pores in zeolites, silica, activated carbons,... [32]. This method allow to calculate the equilibrium density profile of a fluid in the surface and the walls of the pores.

7.4.6. Water adsorption isotherms

Water adsorption isotherms ware used to characterize the chemical surface of some samples. In the case of activated carbons, the vapour adsorption at low relative pressures is strongly influenced by the chemical surface [33,34].

Vapour isotherms were obtained at 25 ºC with water activity (a$_w$) from 0 to 1. The water activity was evaluated by means Hydrosorb HS-12-HT (Quantum Instruments) equipment.

7.5. Mercury intrusion porosimetry

Mercury porosimetry was taken for different samples with high development of mesoporosity as example Xerogels.

Mercury porosimetry allows to know the volume and pore distribution (macropore and mesopore) of a material by means of the determination of the mercury volume introduced under pressure in a porous material. This pressure can be related with the pore size and obtain the distribution of the pore in the interval of macro and mesopores by means the Washburn equation

$$r = \frac{-2\gamma cos\theta}{P} \qquad (6)$$

where r is the pore radius, γ is the superficial mercury tension in the pore, θ is the mercury contact angle with the wall pore and P is the total pressure applied to the

mercury. The tension value is usually 485 dynes cm^{-1}, and the contact angle varies between 112º and 142º (commonly used 140º).

The degasified samples were analyzed in a Micrometrics AutoPore IV 9500 equipment that it can achieve a maximum work pressure of 228 MPa. The contact angle was 130º and a superficial tension of 485 dynes cm^{-1}. The equipment allow to process the data and it can measure the pore diameter higher than 5.5 nm.

8. Maximum adsorption capacity determination in aqueous phase

The maximum adsorption capacity of the activated carbon can be calculated by means of a mass balance of experimental data.

It is considered a solution volume with the presence of a molecule (A) that is in contact with an adsorbent. The system is continuously stirred during a determined time. It is assumed that there is no chemical and biological reaction, but only it is produced a transfer of mass between the aqueous phase to the solid phase. The mass balance can be written as [35]:

$$m(q_t - q_0) = V (C_0 - C_t) \qquad (7)$$

where m is the mass of the adsorbent (g), q_t is the solute concentration in the solid phase at time t (mg g^{-1} or mmol g^{-1}), q_0 is the initial concentration on the solid (mg g^{-1} or mmol g^{-1}), V is the solution volume (L), C_0 is the solution concentration (mg L^{-1} or mmol L^{-1}) and C_t is the solution concentration at time t (mg L^{-1} or mmol L^{-1}). In some cases and considering that in initial conditions the adsorbent is virgin (q_0 = 0), the balance can be rewrite as:

$$q_t = \frac{V (C_0 - C_t)}{m} \qquad (8)$$

8.1 Langmuir Model

The Langmuir theory assumed that the adsorption is a equilibrium reaction between (A) and the surface (σ) [35]

$$A + \sigma \leftrightarrow A\sigma \qquad (9)$$
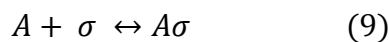
Langmuir proposed a relation to model the evolution of the adsorbed quantity:

$$\frac{dq}{dt} = k_1\, C_t\, (q_m - q_t) - k_2\, q_t \qquad (10)$$

Where k_1 (L mg^{-1} h^{-1}) and k_2 (h^{-1}) are the kinetic coefficients of adsorption and desorption respectively and q_m is the maximum adsorption capacity (mg g^{-1}).

When the kinetic curve is considered t→ ∞, then dq/dt = 0, C_t→C_e y q_t→q_e, the system achieves the equilibrium and the equation remains as

$$k_1 C_e (q_m - q_e) = k_2\, q_e \qquad (11)$$

If isolate q_e:

$$q_e = \frac{q_m\, K_L C_e}{1 + K_L C_e} \qquad (12)$$

Equation (12) is known as Langmuir model as it is shown and described in section 4.1, chapter 1.

8.2. Kinetic models

Different kinetic models describe the adsorption behaviour. The considered models in this Thesis are the pseudo second order (13) and the intraparticle diffusion model (14)

$$\frac{\partial q_t}{\partial t} = k_2 (q_e - q_t)^2 \qquad (13)$$

$$q_t = k_p t^{0.5} + A \qquad (14)$$

Where k_2 (L (mg min)$^{-1}$) and k_p (mg (L min$^{0.5}$)$^{-1}$) are the rate constants for the pseudo second order and intraparticle diffusion respectively, and A is the intercept (mg L^{-1}). The different materials studied achieve the equilibrium before 24 hours at neutral pH.

9. Ultraviolet visible (UV-vis) analysis

The different emerging and aromatic compounds present on water are determined by means ultraviolet visible (UV-vis) equipment. Molecular spectroscopy based upon ultraviolet-visible is widely used for the identification and determination of organic species. The wavelength of the ultraviolet-visible is between 200-400 nm for ultatrviolet and 400-800 nm for visible, and the absorption radiation of the molecules generally

occurs in one or more electronic absorption bands (Table 3.7); each of which is made up of numerous closely packed but discrete lines. Each line arises from the transition of an electron from the ground state to one of the many vibrational and rotational energy states associated with each excited electronic energy state [36].

In the absorption of organic compounds, two types of electrons are responsible for the absorption of ultraviolet and visible radiation: 1) shared electrons (associated with more than one atom); 2) unshared outer electrons (localized in halogens, oxygen, sulphur and nitrogen.

Organic compounds with aromatic ring like benzene, aniline, benzaldehyde (table 3.7), emerging compounds (paracetamol, atrazine, iodixanol, diclofenac,...) contain doble bonds which exhibit useful absorption peaks in the ultraviolet spectra region due to the electrons in unsaturated bonds (that are easily excited).

Table 3.7 Maximum wavelength and absorption coefficient of different organic compounds [37]

Compound	$\pi \rightarrow \pi^*$ (Band E)		$\pi \rightarrow \pi^*$ (Band B)		$\pi \rightarrow \pi^*$ (Band K)		$n \rightarrow \pi^*$ (Band R)	
	λ max	E	λ max	E	λ max	E	λ max	E
Phenol	211	6200	270	1450				
Aniline	230	8600	280	1430				
Benzaldehyde			280	1400	242	14000	330	60
Benzoic Acid	202	8000	270	800	230	10000		
Toluene	208	7900	262	230				

9.1. Lambert-Beer Law

Absorbance is the parameter that is used to quantify the UV-vis spectra and the different concentration of the molecules in solutions. The absorbance (A) is defined by:

$$A = -log_{10} T = \log \frac{P_0}{P} \qquad (15)$$

where T is the transmittance, and P, P_0 are the energy radiation (ergs)

The functional relationship between the quantity measured un an absorption method (A) and the quantity sought (the analyte concentration *c*) in known as Beer's

$$A = \log\frac{P_0}{P} = \varepsilon\, b\, c \qquad (16)$$

where ε is the molar absortivity (L cm^{-1} mol^{-1}), b is the path length of radiation through the absorbing medium (cm) and c is the concentration (mol L^{-1}) [36].

9.2 Analysis of mixtures

The total absorbance of a solution is equal to the sum of the absorbances of the individual components in the solution (Eq. 16)

$$A_{tot} = A_1 + A_2 + \dots + A_n = \varepsilon_1 bc_1 + \varepsilon_2 bc_2 + \dots + \varepsilon_n bc_n \qquad (16)$$

This relationship makes it possible, in principle, to determine the concentrations of the individual components of a mixture even if their spectra overlap.

10. Ultra Performance Liquid Cromatrography - High resolution Mass Spectrometry (UPLC-HRMS) analysis

In accord with to the collaboration framework and the experimental methodology developed by the "*Water and Soil quality research group*" from the Instituto de Diagnóstico Ambiental y Estudios del Agua (IDAEA-CSIC), the different multi compound solutions were analysed using a UPLC-HRMS (Waters ACQUITY UPLC system coupled to a Orbitrap Q Exactive (Thermo Fisher Scientific, San Jose, CA, USA).

The method used followed the specifications on the work of Mendoza et al. [38]: injection volume was 10 μl, analytes were separated on a Waters ACQUITY BEH C18 column (100 × 2.1 mm, 1.7 mm particle size) equipped with a guard column (5 × 2.1 mm) of the same packing material. A simple binary gradient consisting of a) 0.1% HCOOHor 20 mM of NH4OAc for acid and neutral conditions, respectively, and b) acetonitrile was employed for chromatographic separation. Exact mass measurements of the compounds were carried out in full-scan and product ion scan mode by HR mass spectrometer using heated electrospray ionization. The different compounds were analyzed in positive ion (PI) mode or in negative ion (NI) mode. Quantification of the compounds in the sample extracts was performed by internal standard method based on

the peak areas obtained for each analyte and its deuterated analogue, using Thermo Xcalibur 2.2 software.

11. Principal Component Analysis (PCA)

Principal Component Analysis (PCA) is a general method which uses underlying mathematical principles to transforms a number of possibly correlated variables into a smaller number of variables called principal components. PCA is one of the most important applied methods in the linear algebra and perhaps its most common use is as the first step in trying to analyse large data sets.

In general terms, PCA uses a vector space transform to reduce the dimensionality of large data sets. Using mathematical projection, the original data set, which may have involved many variables, can often be interpreted in just a few variables (the principal components). It is therefore often the case that an examination of the reduced dimension data set will allow the user to spot trends, patterns and outliers in the data, far more easily than would have been possible without performing the principal component analysis [39].

The method uses different lineal combinations of the observable variables. The graphic representation of the scores and loadings in the space of the components allow to interpret the relation between the different variables and the different samples.

The methodology applied in this Thesis is described in the work of Polo C. [40].

11. 1 Number of principal component required

As a practical rules to decide how many principal components are required and how are excluded with the object to reduce the quantity of data, it should be considered:

- To include the principal components that explain the 90% of the total variance
- To exclude all the components which their associated eigenvalues are lower than 1.5)
- To choose the required principal component so that all the variables are properly represented (the sum of the square of the correlation coefficients of each variable, explain at least a high percentage of its variance (around 1)

12. References

[1] L. Cabrera, M. Cabrera, R. Gorchs, F.X.C. de las Heras, Lacustrine basin dynamics and organosulphur compound origin in a carbonate-rich lacustrine system (Late Oligocene Mequinenza Formation, SE Ebro Basin, NE Spain), Sediment. Geol. 148 (2002).

[2] M. a. Olivella, J.M. Palacios, a. Vairavamurthy, J.C. del Río, F.X.C. de las Heras, A study of sulfur functionalities in fossil fuels using destructive- (ASTM and Py–GC–MS) and non-destructive- (SEM–EDX, XANES and XPS) techniques, Fuel. 81 (2002) 405–411.

[3] C.M. White, L.W. Collins, G.A. Veloski, G.A. Irdi, K.S. Rothenberger, R.J. Gray, et al., A study of Mequinenza lignite, Energy & Fuels. 8 (1994) 155–171.

[4] R. Rodriguez Gil, Aprovechamiento integral de residuos sólidos de curtición. Implicaciones ambientales, Universidad de Oviedo/CSIC, 2014.

[5] N. Ferrera-Lorenzo, E. Fuente, I. Suárez-Ruiz, R.R. Gil, B. Ruiz, Pyrolysis characteristics of a macroalgae solid waste generated by the industrial production of Agar–Agar, J. Anal. Appl. Pyrolysis. 105 (2014) 209–216.

[6] R.R. Gil, R.P. Girón, M.S. Lozano, B. Ruiz, E. Fuente, Pyrolysis of biocollagenic wastes of vegetable tanning. Optimization and kinetic study, J. Anal. Appl. Pyrolysis. 98 (2012) 129–136.

[7] N. Ferrera-Lorenzo, E. Fuente, I. Suárez-Ruiz, B. Ruiz, KOH activated carbon from conventional and microwave heating system of a macroalgae waste from the Agar–Agar industry, Fuel Process. Technol. 121 (2014) 25–31.

[8] R.R. Gil, B. Ruiz, M.S. Lozano, E. Fuente, Influence of the pyrolysis step and the tanning process on KOH-activated carbons from biocollagenic wastes. Prospects as adsorbent for CO2 capture, J. Anal. Appl. Pyrolysis. 110 (2014) 194–204.

[9] D. Lozano-Castelló, M.A. Lillo-Ródenas, D. Cazorla-Amorós, A. Linares-Solano, Preparation of activated carbons from Spanish anthracite, Carbon N. Y. 39 (2001) 741–749.

[10] A. Perrin, A. Celzard, A. Albiniak, J. Kaczmarczyk, J.F. Marêché, G. Furdin, NaOH activation of anthracites: effect of temperature on pore textures and methane storage ability, Carbon N. Y. 42 (2004) 2855–2866.

[11] A. Perrin, A. Celzard, A. Albiniak, M. Jasienko-Halat, J.F. Marêché, G. Furdin, NaOH activation of anthracites: effect of hydroxide content on pore textures and methane storage ability, Microporous Mesoporous Mater. 81 (2005) 31–40.

[12] R.R. Gil, B. Ruiz, M.S. Lozano, M.J. Martín, E. Fuente, VOCs removal by adsorption onto activated carbons from biocollagenic wastes of vegetable tanning, Chem. Eng. J. 245 (2014) 80–88.

[13] E.F. Mohamed, C. Andriantsiferana, A.M. Wilhelm, H. Delmas, Competitive adsorption of phenolic compounds from aqueous solution using sludge-based activated carbon, Environ. Technol. 32 (2011) 1325–1336.

[14] C. Julcour Lebigue, C. Andriantsiferana, K. N'Guessan, C. Ayral, E. Mohamed, A.-M. Wilhelm, et al., Application of sludge-based carbonaceous materials in a hybrid water treatment process based on adsorption and catalytic wet air oxidation, J. Environ. Manage. 91 (2010) 2432–2439.

[15] K.M. Smith, G.D. Fowler, S. Pullket, N.J.D. Graham, Production of activated carbon from sludge, in: A. Fabregat, C. Bengoa, J. Font, F. Stueber (Eds.), Reduction, Modif. Valoris. Sludge, IWA publishing, London, 2011.

[16] N. Rey-Raap, J. Angel Menéndez, A. Arenillas, Simultaneous adjustment of the main chemical variables to fine-tune the porosity of carbon xerogels, Carbon N. Y. 78 (2014) 490–499.

[17] N. Rey-Raap, J. Angel Menéndez, A. Arenillas, RF xerogels with tailored porosity over the entire nanoscale, Microporous Mesoporous Mater. 195 (2014) 266–275.

[18] A.H. Moreno, A. Arenillas, E.G. Calvo, J.M. Bermúdez, J.A. Menéndez, Carbonisation of resorcinol–formaldehyde organic xerogels: Effect of temperature, particle size and heating rate on the porosity of carbon xerogels, J. Anal. Appl. Pyrolysis. 100 (2013) 111–116.

[19] D.W. Van Krevelen, COAL: Typology-physics-chemistry-constitution, Third, Elsevier Science Publishers, Amsterdam, 1993.

[20] U. Schiedt, Zur infrarot-spektroskopie von aminosauren. 1. Eine neue praparationstechnik zur infrarot-spectroskopie von aminosauren und anderen polaren verbindungen, Zeitschrift Für Naturforschung. B, A J. Chem. Sci. 7 (1952) 270–277.

[21] V. GomezSerrano, J. PastorVillegas, C.J. DuranValle, C. ValenzuelaCalahorro, Heat treatment of rockrose char in air. Effect on surface chemistry and porous texture, Carbon N. Y. 34 (1996) 533–538.

[22] V. GomezSerrano, J. PastorVillegas, A. PerezFlorindo, C. DuranValle, FT-IR study of rockrose and of char and activated carbon, J. Anal. Appl. Pyrolysis. 36 (1996) 71–80.

[23] E. Fuente, J.A. Menéndez, M.A. Díez, D. Suárez, M.A. Montes-Morán, Infrared Spectroscopy of Carbon Materials: A Quantum Chemical Study of Model Compounds, J. Phys. Chem. B. 107 (2003) 6350–6359.

[24] P.E. Fanning, M.A. Vannice, A DRIFTS study of the formation of surface groups on carbon by oxidation, Carbon N. Y. 31 (1993) 721–730.

[25] P. Echlin, Handbook of sample preparation of scanning electron microscopyand X-Ray microanalysis., Springer, United Kingdom, 2009.

[26] F. Rouquerol, J. Rouquerol, K. Sing, Adsorption by active carbons, in: Adsorpt. by Powders Porous Solids, Elsevier, 1999: pp. 237–285.

[27] N. Ferrera-Lorenzo, Aprovechamiento integral del residuo de macroalga procedente de la obtención industrial de Agar-Agar. Aplicación en el campi de la energía y el medioambiente, Universidad de Oviedo, 2014.

[28] H. Marsh, F. Rodríguez-Reinoso, Characterization of activated carbon, in: Act. Carbon, Elsevier, 2006: pp. 143–242.

[29] K.S.W. Sing, Reporting physisorption data for gas/solid systems with special reference to the determination of surface area and porosity (Provisional), Pure Appl. Chem. 54 (1982).

[30] CEDEX, La fisisorción de nitrógeno. Fundamentos físicos, normativa, descripción del equipo y procedimiento experimental, n.d.

[31] . Miyamoto, H. Kanoh, K. Kaneko, The addition of mesoporosity to activated carbon fibers by a simple reactivation process, Carbon N. Y. 43 (2005) 855–857.

[32] J. Landers, G.Y. Gor, A. V. Neimark, Density functional theory methods for characterization of porous materials, Colloids Surfaces A Physicochem. Eng. Asp. 437 (2013) 3–32.

[33] R.S. Vartenetyan, A.M. Voloshchuk, M.M. Dubinin, O.E. Babkin, Adsorption of water-vapor and microporous structures of carbonaceous adsorbents. 10. The effect of preliminary preparation conditions and the modification of activated charcoals on their adsorption properties, Bull. Acad. Sci. USSR Div. Chem. Sci. (1986) 1763–1768.

[34] J. Alcañiz-Monge, A. Linares-Solano, B. Rand, Mechanism of Adsorption of Water in Carbon Micropores As Revealed by a Study of Activated Carbon Fibers, J. Phys. Chem. B. 106 (2002) 3209–3216.

[35] P. Le Cloirec, C. Faur, Adsorption of organic compounds onto activated carbon - applications in water and air treatments, in: T.J. Bandosz (Ed.), Act. Carbon Surfaces Environ. Remediat., First, Elsevier, New York, 2006: pp. 375–419.

[36] A. Skoog, M. West, F.J. Holler, Fundamentals of Analytical Chemistry, 6 th, Saunders HBJ, Orlando, 1992.

[37] E. Pretsch, T. Clerc, J. Seibl, W. Simon, Tables of Spectral Data for Structure Determination of Organic Compounds., 4 th, Springer-Verlag, Zurich, 1980.

[38] A. Mendoza, J. Aceña, S. Pérez, M. López de Alda, D. Barceló, A. Gil, et al., Pharmaceuticals and iodinated contrast media in a hospital wastewater: A case study to analyse their presence and characterise their environmental risk and hazard., Environ. Res. 140 (2015) 225–41.

[39] M. Richardson, Principal component analysis assay, 2009.

[40] C. Polo, Estadística multivariable, fourth, Edicions UPC, Terrassa, 2001.

Chapter 4

Results

Section I

Removal organic and emerging pollutants by means new adsorbents

Section 4.1.1

"Highly microporous activated carbons derived from biocollagenic wastes as adsorbents of aromatic organic pollutants in water originating from industrial activities."

Highly microporous activated carbons derived from biocollagenic wastes as adsorbents of aromatic organic pollutants in water originating from industrial activities

J. Lladó[1], R.R. Gil[2], C. Lao-Luque[1], M. Solé[1] E. Fuente[2*], B. Ruiz[2]

[1]*Department of Mining, Industrial and TIC Engineering (EMIT).* Universitat Politécnica de Catalunya. Bases de Manresa 61-73, 08242 Manresa, Spain.

[2]*"Biocarbon & Sustainability".* Instituto Nacional del Carbón (CSIC), Francisco Pintado Fe, 26, 33011 Oviedo, Spain.

*Corresponding author/Email: enriquef@incar.csic.es

Graphical abstract
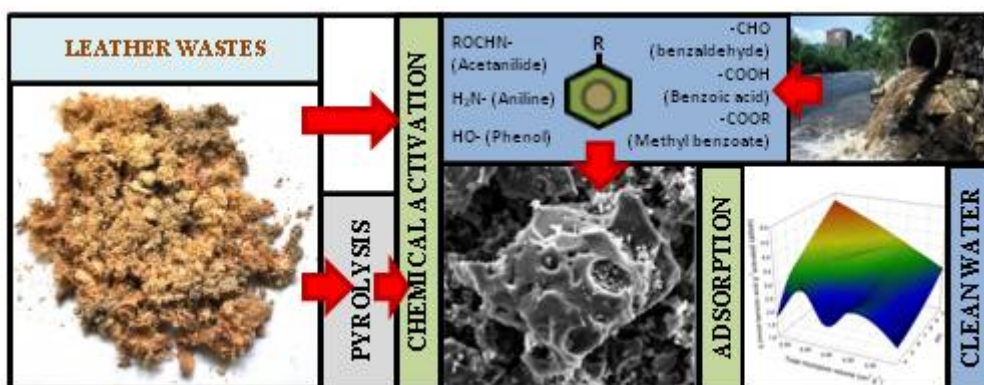
Highlights

- Valorisation of biocollagenic wastes from tanning industry
- Biocollagenic wastes-based ACs are obtained by chemical activation by using KOH and K_2CO_3
- The activated carbons present specific surface area (S_{BET}) of up to 1664 m^2 g^{-1}
- The adsorbents obtained are mainly microporous with micropore volumes up to 0.536 cm^3 g^{-1}
- Superior performance for adsorption of benzaldehyde (q_{max}: 3.77 mmol g^{-1}adsorbent)
- Biocollagenic waste-based ACs for adsorption of organic pollutants in water
- Acetanilide, aniline and benzoic acid were affected by nitrogen content on AC

Abstract

The presence of aromatic organic pollutants produced by different industries (pharmaceutical, food, perfume,...) is increasing in surface and groundwater and this is seriously affecting the environment. Moreover, leather industries generate large amounts of biocollagenic wastes that need to be processed. The purpose of this study is to use biocollagenic wastes (shavings, trimmings and buffing dust) and their pyrolyzed products as bioprecursors of activated carbons for future waste water applications. Activated carbons were prepared by KOH and K_2CO_3 chemical activation at different temperatures. The characteristics of the precursors and the influence of the activating temperature and activating agent on the process were studied and discussed. The manufactured materials and two commercial activated carbons (WAC and YAO) were used as adsorbents to remove the following aromatic organic pollutants from the water: acetanilide, aniline, benzaldehyde, benzoic acid, methyl benzoate and phenol. The results obtained show that an increase in the activating temperature led to a higher textural development in the adsorbents. The best activated carbons were obtained by means of KOH chemical activation resulting in S_{BET} and V_{TOT} values of up to 1664 m^2g^{-1} and 0.735 cm^3g^{-1} respectively. All the adsorbents were predominantly microporous with a certain degree of mesoporosity and a significant amount of nitrogen (up to 3%). The main adsorption mechanism proposed for the different organic pollutants was dispersive interaction influenced by a hydrogen mechanism. Moreover, an increase in the nitrogen content of the adsorbents decreased the adsorption capacity of acetanilide, benzoic acid and aniline, whereas electrostatic influences reduced the adsorption capacity of benzoic acid.

Keywords: Activated-carbon, biocollagenic-materials, organic-pollutants, waste-water, adsorption

1. Introduction

One of the most important industries in Spain is the production of textiles, leather goods and shoes, representing about 4.7% of the total economic production of Spain. The leather production process is divided into different steps in which the raw material is treated (skinning, curing, beamhouse operations, tanning, drying,...). In the tanning

process the putrescent skins of animals are treated so that they are converted into non-biodegradable leather by means vegetable or mineral methods. The leather-making process generates substantial quantities of solid and liquid wastes (hides and skins, fats, shavings and trimmings, buffing dust, process effluents, sludge,...). The most common way to manage most of the solid wastes is by disposing of them on landfill sites or by incineration. For this reason a comprehensive and more rational utilization of this waste would lead to considerable economic and environmental benefits.

One of the ways of taking advantage of these wastes could be the production of activated carbons (ACs), due to the high demand for these adsorbents and the possible introduction of stricter environmental regulations. The main raw materials used to prepare activated carbons are peat and coals of different rank. The price of activated carbons varies from 0.8 to 10 € kg^{-1} depending on the type of activation and the process used [1]. In order to reduce the total cost, efforts are being made to produce low-cost alternatives from waste precursors (sewage sludge [2], macroalgue wastes [3], tyres [4], ...). Similary, the use of leather wastes could result in a decrease in total cost production of activated carbon (considered as a high value-added product) and contribute to an improvement of the environment.

There is little information available in the literature about the use of leather wastes as bioprecursors of activated carbon. Most of them are subjected to physical activation with carbon dioxide or steam [5-8]. Kong et al. [7,9] carried out chemical activation with $H_2P_2O_7$ in a microwave furnace and obtained activated carbons with a specific surface area (S_{BET}) of between 200 and 500 m^2 g^{-1}. The activating agents most frequently used are $ZnCl_2$, H_3PO_4, KOH and NaOH, that result in a narrow pore distribution and a well developed porosity [10]. Chemical activation has been shown to be an efficient method to obtain carbons. Gil et al. [11-13] introduced a previous pyrolysis step in the alkaline activation of biocollagenic wastes and obtained highly microporous activated carbons.

A lot of companies use aromatic compounds (phenol, aniline, benzoic acid, acetanilide,...) in their synthesis process (pharmaceutical, pesticides, food, beverage,...). Sometimes, these compounds are emitted via water effluents which can represent a serious problem for the environment. Sometimes, due their pleasant odour properties,

these compounds can be recovered to improve the quality of the final product (as in the case of benzaldehyde in coffee production) [14]. An effective way to eliminate these aromatic compounds (organic pollutants) or to recover them from effluents could be to introduce an adsorption step with activated carbon during the cleaning process of water or in the production process.

The adsorption capacity of an activated carbon depends on its physical and chemical characteristics (surface area, pore size, functional groups, ...) and the characteristics of the adsorbate (size, hydrophobicity, polarity, ...) [15]. The presence of functional groups on the surface of the activated carbon can affect the dispersion interactions between the aromatic rings of the graphene layers of activated carbons and the aromatic rings of the molecules. Moreover, the presence of water can enhance or decrease the adsorption of organic molecules due to hydrogen bonding[16-18]. The acidity or basicity of the activated carbon and the pH of the solution can also influence the interactions between aromatic compounds with surface of activated carbons [19,20].

The aim of the present study is to obtain activated carbons from biocollagenic wastes and a char able to efficiently remove aromatic organic pollutants from water. The activated carbons are prepared by chemical activation using two chemical agents (KOH and K_2CO_3) at different activating temperatures. Variables such as activation temperature, activating agent and type of precursor are studied and discussed in order to determine their influence on the activation process. The eight activated carbons obtained are used in environmental applications in liquid (aqueous) phase. In addition, two commercial activated carbons, WAC and YAO, are selected for comparison purposes. The different activated carbons are characterized on the basis of elemental composition and textural analysis for the purpose of establishing the factors involved in the adsorption of the six selected aromatic compounds: acetanilide, aniline, benzaldehyde, benzoic acid, methyl benzoate and phenol.

2. Materials and methods

2.1 Materials

This study was aimed at the valorisation of leather solid wastes (shavings, trimmings and buffing dust) from the vegetable tanning of bovine skin [21,22] for environmental applications in aqueous media.

A mixture of biocollagenic wastes (shavings, trimmings and buffing dust) labelled BCT was used as biomaterial to obtain the activated carbons. The proportions of this mixture were generated and homogenized as in the leather industry (84% shavings, 15% trimmings and 1% buffing dust). The sampling and the treatment of the samples has been discussed in a recent work [21].

The mixture of biocollagenic wastes, BCT, was subjected to a pyrolysis process and the resulting char, named BCTP, was also used as bioprecursor of the activated carbons. The pyrolysis conditions for BCT were selected on the basis of a previous work on pyrolysis [21] in which the potential energy of the fractions generated (char, condensable and gas fraction) was studied.

The activated carbons were obtained by means of conventional chemical activation in a horitzontal electrical furnace (Carbolite CTF 12/65/550). The bioprecursors, BCT and BCTP, were activated at activating agent/precursor weight ratios of 0.33:1 and 1:1, respectively, with KOH and K_2CO_3. Moreover, all the activations were carried out at two different temperatures (750 and 900 ºC) as a result of which eight different activated carbons were obtained as shown in Table 4.1.1.

Table 4.1.1 Activation process characteristics and simplified annotation of the activated carbons

Activated carbon	Bioprecursor	Chemical agent	Activating ratio (Agent/precursor)	Activating temperature (ºC)
A	BCT	KOH	0.33:1	750
B	BCT	KOH	0.33:1	900
C	BCTP	KOH	1:1	750
D	BCTP	KOH	1:1	900
E	BCT	K_2CO_3	0.33:1	750
F	BCT	K_2CO_3	0.33:1	900
G	BCTP	K_2CO_3	1:1	750
H	BCTP	K_2CO_3	1:1	900

After chemical activation the samples were washed in order to remove the activating agent residues, inorganic matter and reaction products blocking the porosity. The samples were washed with hydrochloric (5 mol dm^{-3}) and then rinsed with deionised water (milli-Q).

Two commercial activated carbons, YAO and WAC supplied by Eurocarb, were chosen for their organic origin (coconut and wood, respectively) for comparison purposes. Both powdered activated carbons activated with steam and are known to be good products for the adsorption of aromatic organic pollutants on water.

2.2 Chemical and textural characterization

The activated carbons obtained were characterized from their proximate and ultimate analysis. The ash content and humidity were determined according to methods described in norms ISO 1171 and ISO 11722. The ultimate analysis was carried out on a LECO CHN-2000 and a LECO Sulphur Determination S-144-DR. The oxygen content was calculated by difference.

The texture of the different activated carbons was characterized from N_2 adsorption isotherms at -196 ºC, in a conventional volumetric apparatus (ASAP 2420 from Micrometics). Before each experiment, the samples were outgassed under vacuum at 120 ºC for overnight to remove any adsorbed moisture and/or gases. The isotherms were used to calculate the specific surface area (S_{BET}) and total pore volume, (V_{TOT}), at a relative pressure of 0.95 in addition to the pore size distribution. The pore size distribution (PSD) was evaluated using the density functional theory (DFT), assuming slit-shape pore geometry. The surface morphology of the different activated carbons was examined using a scanning electron microscope (FEI, Quanta FEG 650 Model) equipped with an Energy-Dispersive X-ray analyzing system (Ametek-EDAX, Apollo X detector).

2.3 Adsorbates

The six evaluated organic pollutants were acetanilide (CAS 183-44-4, Spain), aniline (CAS 62-53-2, 99%, Scharlau, Spain), benzaldehyde (CAS 100-52-7, 99%, Panreac, Spain), benzoic acid (CAS 65-85-0, 99%, Scharlau, Spain), methyl benzoate (CAS 93-58-3, 98%, Panreac, Spain) and phenol (CAS 108-95-2, 98.5%, Panreac, Spain). The physico-chemical properties of these compounds (pKa, solubility, molecular weight, hydrophobicity, molecular size,…) [23] are shown in Table 4.1.2. The molecule dimensions (the closest fitting "box" around the molecule), surface areas (grid and approximate) and volume were calculated using Hyperchem 8.0 software [24]. The

molar volume was obtained from Basic PhysiChem Properties (Advanced Chemistry Development, Inc. (ACD/Labs).

Table 4.1.2 Physico-chemical properties of the selected organic pollutants

Compound	Acetanilide	Aniline	Benzaldehyde	Benzoic Acid	Methyl Benzoate	Phenol
Molecular formula	C_8H_9NO	C_6H_7N	C_7H_6O	$C_7H_6O_2$	$C_8H_8O_2$	C_6H_6O
Molecular weight (g mol^{-1})	135.16	93.13	106.12	122.12	136.15	94.11
log K_{ow}	1.16	0.90	1.48	1.87	2.12	1.46
pKa	13.4	4.60	14.9	4.29	7.00	9.99
Solubility (mg L^{-1})	6930	36000	6950	3400	157	82000
Dimensions (Å	4.875	4.325	4.566	4.241	4.185	4.383
Å	1.575	0.00067	1.628	2.056	3.037	0.00031
Å)	7.302	5.820	6.042	6.072	6.631	5.767
Surface area grid (Å^2)	311.38	258.49	273.02	281.75	307.36	258.65
Surface area approx. (Å^2)	286.04	211.16	246.29	245.66	278.96	227.95
Volume (Å^3)	464.54	368.39	387.45	407.84	459.48	363.77
Molar volume (cm^3 mol^{-1})	122.5 ± 3	91.7 ± 3	101.0 ± 3	101.9 ± 3	127.3 ± 3	87.8 ± 3
Wave number (λ)	239.2	230.0	249.7	228.0	230.0	269.9

Different stock solutions of each compound (100 mg L^{-1}) were prepared with ultra-pure water obtained from Milli-Q purification systems (Millipore academics). From these solutions, samples for calibration and sorption experiments were obtained by dilution with ultra-pure water (Milli-Q).

2.4 Adsorption assays

For the equilibrium adsorption studies, 10 mg of adsorbent was added to 50 mL of different organic compound solutions with various concentrations (5-100 mg L^{-1}). The mixtures were stirred at 25ºC on a multipoint agitation plate. After 24 hours, samples were taken and filtered through a cellulose acetate filter (0.45 µm diameter pore) and the remaining concentrations of adsorbates were analyzed in a UV/Vis-visible spectrophotometer (Lambda 25 PerkingElmer) at the corresponding wavelength of each compound (Table 4.2). The pollutant uptake, q, was determined using the formula:

$$q = \frac{(C_0 - C_f)\,V}{W} \qquad (1)$$

where q is the amount (mmol g^{-1}) of organic compounds adsorbed, C_0 and C_f are the initial and final concentration (mg L^{-1}), respectively, V is the volume (L) of the adsorbate solution and W is the weight (g) of the activated carbon used.

2.5 Adsorption modelling

The experimental results were fitted to two parameter isotherm models: Langmuir (Eq. 2) and Freundlich (Eq. 3)

$$q_e = \frac{q_{max}K_L C_e}{1 + K_L C_e} \qquad (2)$$

$$q_e = K_f C_e^{1/n} \qquad (3)$$

where q_e (mmol g^{-1}) is the amount of compound adsorbed per mass of unit carbon, C_e (mmol L^{-1}) is the organic compound concentration at equilibrium, q_{max} (mmol g^{-1}) is the maximum adsorption capacity, K_L (L mmol^{-1}) is a constant related to the affinity between the pollutant and the adsorbent, K_f ((mmol g^{-1}) (L mmol^{-1})$^{1/n}$) is the Freundlich sorption constant and n is a constant related to the intensity of the adsorption.

The parameter estimation of the different isotherms was solved using MATLAB software and minimizing the objective function (OF) given in equation (4) [25].

$$OF = \sqrt{\sum_{i=1}^{N} [q(P_1, P_2) - q^*]^2} \qquad (4)$$

where N is the number of measurements performed, q* is the experimental solute uptake, q (P_1, P_2) is the uptake predicted by the model, P_1 and P_2 are the different estimated parameters. In the case of the Langmuir model, the parameters are q_{max} and K_L and for Freundlich K_f and n.

3 Results and discussion

3.1 Chemical analysis of the activated carbons

Different experimental variables play a role in the activation process. The type of precursor, the activating agent and the temperature were selected to study the activation

process to try and determine the influence that these experimental variables have on the physicochemical properties of the adsorbent.

The chemical composition of the bioprecursors, BCT and BCTP, was studied in previous work [21]. Their high carbon and low ash content make these biomaterials a very suitable bioprecursor for obtaining activated carbons. Table 4.1.3 shows the results of the proximate and ultimate analyses for the different activated carbons obtained.

Table 4.1.3 Chemical characterization of the activated carbons

Material	Moisture (%)	Ash (%)*	C (%)*	H (%)*	N (%)*	S (%)*	O (%)**	pH
KOH ACs								
A	4.04	1.68	87.44	-	2.52	2.00	6.36	3.60
B	4.99	5.50	82.43	0.38	2.13	1.78	7.78	3.70
C	4.87	0.78	90.61	0.38	2.60	0.80	4.83	4.10
D	1.27	1.29	93.93	0.28	1.38	0.52	2.60	5.60
K$_2$CO$_3$ ACs								
E	7.54	1.62	83.30	0.81	2.33	1.27	10.67	3.60
F	6.83	3.07	85.43	0.35	1.52	1.81	7.82	3.60
G	1.66	3.21	83.45	1.02	2.93	1.07	8.32	4.00
H	1.35	2.40	92.71	0.33	1.39	0.62	2.55	6.30
Commercial AC								
YAO	4.25	4.87	90.92	0.56	0.78	0.13	2.74	10.40
WAC	13.39	8.36	86.84	0.70	0.52	0.09	3.49	10.60

*Dry base/**Determined by difference

Overall, the activated carbons obtained after chemical activation of the bioprecursors (BCT and BCTP) have a high carbon content, between 82-94 %, and a low ash content, between 0.8-5.5%. These values are similar to, or better than, those of the commercial activated carbons (carbon content: 86-91 %; ash content: 4.9-8.4 %), Table 4.1.3.

There are slight differences in the chemical compositions of the activated carbons based on the bioprecursor type; and so, the ACs derived from BCT are characterized by a carbon content of approx. 82-87% an oxygen content of 6 to 10% and an acid pH (3.6). In contrast ACs from BCTP have a higher carbon content (more than 90%), a medium range oxygen content (between 2-4%) and acid neutral pH (4-6), except in the case of the G sample. The commercial activated carbons, WAC and YAO, activated with steam,

showed a basic pH of approx. 10.5. According to Montes-Morán et al. [20], the presence of ashes is one of the factors leading to the basicity of the activated carbons.

An important experimental variable that has a significant influence on the chemical properties of the activated carbons obtained is the activation temperature. As can be seen in Table 4.1.3, the activated carbon B (from BCT, KOH at 900ºC) presents a lower carbon and higher oxygen content than the adsorbent material obtained at 750 ºC (A sample). This result is in disagreement with the other materials of this study where an increase in the activation temperature entails an increase in carbon content and a decrease in oxygen content. It can also be seen noticed that an increase in activation temperature leads to a much higher ash content in sample B (5.5 %) than A (1.68%). Although, in general, an increase in the activation temperature entails an increase in the ash content, when KOH is used as activating agent, and BCT as bioprecursor, the increase in the ash content is much higher. It seems that a high activation temperature with KOH reduces the elemental composition of the carbon structure against the increase of the quantity of ashes. Ferrera-Lorenzo et al. [3] studied the effect of some of the experimental variables of KOH activation on the chemical and textural properties of macroalgae waste-based ACs and observed that the most suitable temperature without any pyrolyzed wastes was 750 ºC. The activated carbons from BTCP show an increase of up to 20% in the carbon content with the increase in the activation temperature while nitrogen content decreases more than 52% (Table 4.1.3). Thus the chemical evolution of these materials is similar to that observed by Tsai et al. [26] in their work on the activation of agricultural wastes using KOH and K_2CO_3.

3.2 Textural analyses of activated carbons

The nitrogen adsorption isotherms at -196 ºC of the activated carbons obtained from BCT and BCTP with KOH and K_2CO_3 agents is shown in Fig. 4.1.1a) and 1b), respectively. In addition, Table 4.1.4 shows the data corresponding to the equivalent specific surface area, S_{BET}, total pore volume at $p/p^0 = 0,95$, V_{TOT}, and the distribution of porosity (ultramicropore: <0.7 nm; supermicropore: 0.7-2 nm; mesopore: 2-50 nm) obtained by applying the density functional theory (DFT) model to the N_2 adsorption data.

The activated carbons in Fig. 4.1.1 show hybrid adsorption isotherms of type I-IV according to the BDDT classification [27]. Moreover, the N_2 isotherms of these activated carbons display a wide hysteresis loop of type H4 [28], indicating the presence of mesopores of small diameter.

Table 4.1.4 Textural properties of the different activated carbons

Material	S_{BET} $(m^2 g^{-1})$	Vtot at p/p^0=0.95 $(cm^3 g^{-1})$	Vumi $(cm^3 g^{-1})$*	Vsmi $(cm^3 g^{-1})$*	Vtot mi $(cm^3 g^{-1})$*	Vme $(cm^3 g^{-1})$*
KOH ACs						
A	1602	0.695	0.249	0.264	0.513	0.021
B	1421	0.675	0.176	0.260	0.436	0.088
C	1163	0.506	0.249	0.126	0.375	0.040
D	1664	0.735	0.243	0.293	0.536	0.022
K$_2$CO$_3$ ACs						
E	1221	0.539	0.233	0.156	0.389	0.035
F	1433	0.663	0.193	0.262	0.455	0.054
G	838	0.390	0.214	0.046	0.260	0.042
H	1465	0.667	0.241	0.219	0.460	0.044
Commercial ACs						
YAO	1092	0.480	0.194	0.162	0.357	0.020
WAC	893	0.540	0.137	0.111	0.248	0.285

*determined by DFT
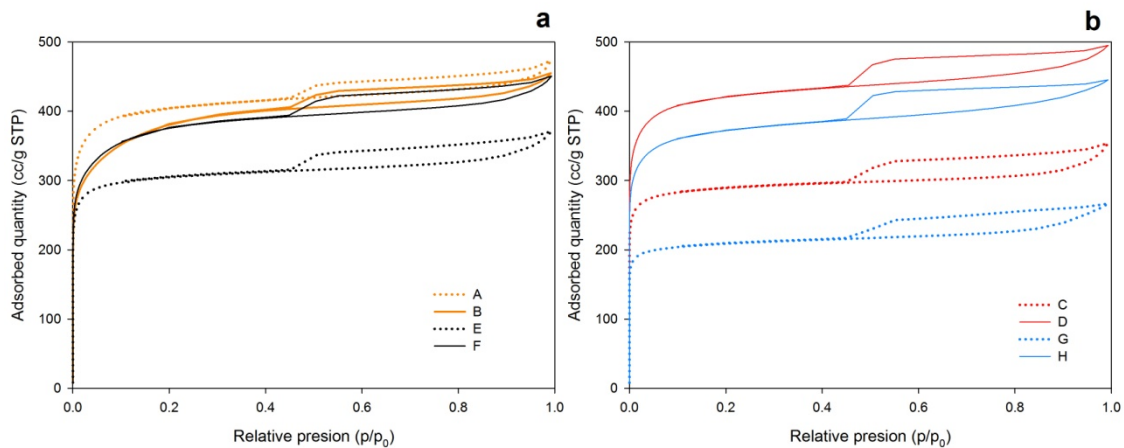
Figure 4.1.1 Nitrogen isotherm of the different leather wastes activated carbons: 1a) Activated carbons from BCT; 1b) Activated carbons from BCTP

Compared to the commercial activated carbons, the N_2 isotherm of YAO (Supporting Information (SI), Fig. SI 1a) is mainly of type I with a narrow knee at low relative

pressures (p/p^0 <0.1), indicating a micropore structure. In the case of WAC (Fig. SI 1. 1b), the nitrogen isotherm is of type I-IV and it is distinguished from that of the biocollagenic activated carbons by its steep slope at a relative pressure of from 0.1 to 1, suggesting a high degree of mesoporosity.

Generally speaking the activated carbons obtained are highly microporous adsorbents with a BET surface area between 838-1664 m^2 g^{-1} and a total pore volume of between 0.390-0.735 cm^3 g^{-1}. These results are similar to, or better than, those of the commercial activated carbons, Table 4.1.4

An important factor to be taken into account is the effect of the activating agent upon the textural properties of activated carbons. In general, the adsorbent materials obtained with KOH (A, B, C and D) present a higher adsorption capacity, BET surface area and total pore volume at p/p^0=0.95 than the corresponding ACs obtained with K_2CO_3 (E,F,G and H), with the exception of sample B (KOH activated carbon from BCT at 900 ºC) that presents the same level of adsorption as sample F (K_2CO_3 activated carbon from BCT at 900 ºC), Fig. 4.1.1 and Table 4.1.4.

The adsorbent materials with the highest textural development are A (KOH activated carbon from BCT at 750 ºC) and D (KOH activated carbon from BCTP at 900 ºC). These samples have a S_{BET} of 1602 and 1664 m^2 g^{-1}, respectively. This work has revealed significant differences in the textural development of the activated carbons. A difference of more than 11.5% of S_{BET} was achieved using KOH with respect to K_2CO_3 (the exception being between the B and F activated carbons). This difference is more remarkable at low temperature of activation (22-27%).

The activating agent used in the chemical activation process is one of the variables that most affects the textural properties of the adsorbents obtained so it is very important to know what reactions occur during the process. Various authors [10,29,30] have studied the different reactions that take place between alkaline hydroxides (KOH) and the carbonaceous material (Table 4.1.5, R1). At lower activation temperatures with KOH (<750 ºC), various secondary reactions (Table 4.1.5, R2, R3 and R4) may occur, that favour the formation of carbon dioxide (CO_2). According to Marsh et al. [31] the formation of CO_2 may lead to physical activation on the carbonaceous structure. In this case these reactions would enhance the development of porosity. On the other hand,

when the activation temperature increases to over 891 ºC the potassium oxide formed in the presence of CO_2 generates more potassium carbonate that reacts with the carbonaceous structure, Table 4.1.5. These reactions cause an increase in the formation of metallic potassium which is introduced into the carbonaceous material. As a result the carbon particles disintegrate into powders [31], reducing the ultramicroporosity, as in sample B (Table 4.1.4).

In the case of activation with K_2CO_3, moderate activation temperatures (<891ºC) give rise to low reactions with the carbonaceous structure (Table 4.1.5, R8). When the activation temperature exceeds 891ºC (R5), the potassium carbonate may decompose to produce CO_2 (Table 4.1.5, R5). This may enhance the chemical-physical activation of the carbonaceous material, increasing the amount of micropores.

Table 4.1.5 Possible reactions produced during the activation with KOH or K_2CO_3

$6\,KOH + 2C \rightarrow 2K + 3H_2 + 2\,K_2CO_3$	R1	Main reaction	$K_2CO_3 + 2\,C \rightarrow 2\,K + 3\,CO$	R8
$2\,KOH \rightarrow K_2O + H_2O\ (360ºC)$	R2	Secondary reactions	$K_2CO_3 \leftrightarrow K_2O + CO_2\ (891\ ºC)$	R5
$C + H_2O \rightarrow H_2 + CO$	R3		$CO + C(O)_m \rightarrow C_f + CO_2$	R9[31]
$CO + H_2O \rightarrow H_2 + CO_2$	R4			
$K_2CO_3 \leftrightarrow K_2O + CO_2\ (891\ ºC)$	R5			
$K_2O + H_2 \rightarrow 2\,K + H_2O$	R6			
$K_2O + C \rightarrow 2\,K + CO$	R7			
$K_2CO_3 + 2\,C \rightarrow 2\,K + 3\,CO$	R8			

Another effect that must be taken into account is that of the activating temperature. As has been seen in the chemical analysis, the activation temperature has a significant influence on the textural properties of the activated carbons. The adsorbent materials A and B, also show the contrary behaviour to that of the others samples since an increase in the activation temperature causes a slight decrease in the adsorption capacity of the material obtained at higher temperatures (sample B). In contrast, the rest of the activated carbon families (C-D, E-F and G-H), exhibit an increase in the adsorption capacity with the increase in activation temperature, Fig. 4.1.1 The isotherms of the adsorbents materials at 750 ºC (A, C, E and G) display a narrow knee at low relative pressures (p/p^0 <0.1) while in the case of the materials obtained at 900 ºC (B, D, F and H) the knee is

broader (p/p^0 <0.2), especially in the adsorbents materials derived from BCT (B and F), suggesting the presence of wide micropores in these materials, Fig. 4.1.1.

Furthermore, an increase in the activation temperature leads to an increase in the S$_{BET}$ which is especially high in the case of the bioprecursor BCTP. In this case, the adsorbents obtained at 900 ºC have a S$_{BET}$ of 1664 and 1465 m^2 g^{-1} (in D and H respectively) which represents an increase greater than 500 m^2 g^{-1} with respect to the materials obtained at 750 ºC, Table 4.1.4. In the activated carbons obtained from BCT the same trend can be observed as in adsorbents E and F, although in this case the variation in S$_{BET}$ is moderate (an increase of only 200 m^2 g^{-1} approx.). Sample B remains an exception to this behaviour. Sample B obtained at 900 ºC has an S$_{BET}$ of 1421 m^2 g^{-1} which is lower than that of sample A obtained at 750 ºC. The total pore volume at p/p^0= 0.95 follows a similar behaviour to that of the BET specific surface area, Table 4.1.4.

On the other hand, the adsorbents with the best textural development are obtained when BCT is used as bioprecursor except when KOH is used as activating agent at high temperature (900 ºC).

Table 4.1.4 and Fig. SI 1.2 show the pore-size distributions by DFT for the adsorbent materials obtained (ultramicropore, umi, <0.7 nm; supermicropore, smi, 0.7-2 nm; mesopore, me, 2-50 nm) while Fig. 4.1.3 shows the proportions (in terms of percentages) of micro-mesoporosity volume distribution in each adsorbent material. From the results it can be observed that all of the adsorbents are microporous materials with a low contribution of mesoporosity.

In Fig. SI 1.2 it can be seen that the pore diameter becomes wider with increasing activation temperature. This is particularly noticeable in materials obtained from BCT (from approx. 1.5 nm to 3 nm in the case of A and B). Furthermore with the increase in temperature from 750ºC to 900ºC, the ultramicroporosity decreases drastically when the activation temperature is high. This is especially remarkable in B (Table 4.1.4). This behaviour at high activation temperatures has been reported in several works on activation with different biomass wastes [3,32,33]. It seems that severe temperature conditions with KOH as activating agent can destroy ultramicroporosity in favour of the development of wider pores (supermicropores and mesopores). There is only one

exception to this behaviour and it occurs when BCTP is used as bioprecursor and K_2CO_3 as activating agent. In this case, an increase in activation temperature entails an increase in the ultramicropore volume (G and H, 0.214 and 0.241 cm^3 g^{-1}, respectively). On the other hand, in agreement with other authors [3,32,33], there is an enhancement in the development of supermicroporosity with the increase in activation temperature due to the development of pores in the 0.7-2 nm size range, which is especially noteworthy in sample H (0.219 cm^3 g^{-1}) when compared to sample G (0.046 cm^3 g^{-1}).

As regards the commercial activated carbons, YAO has a higher S_{BET} than WAC (1092 and 893 m^2 g^{-1} respectively) and also a higher of microporosity volume (Vtot mi= 0.357 cm^3 g^{-1} versus to 0.248 cm^3 g^{-1}), whereas WAC presents a higher mesoporosity (WAC Vme=0.285 cm^3 g^{-1} v.s. YAO Vme=0.020 cm^3 g^{-1}), Table 4.4 and Fig. SI 1.2.

Fig. 4.1.2 shows the percentages of the different kind of pores in the activated carbons obtained. In this study, all the ACs show a well developed of the microporosity and a low contribution of mesoporosity; the ACs from BCT show a well developed microporosity emphasising the high percentage of supermicropore structure while the adsorbents obtained from BCTP is noteworthy the high percentage of ultramicropores.
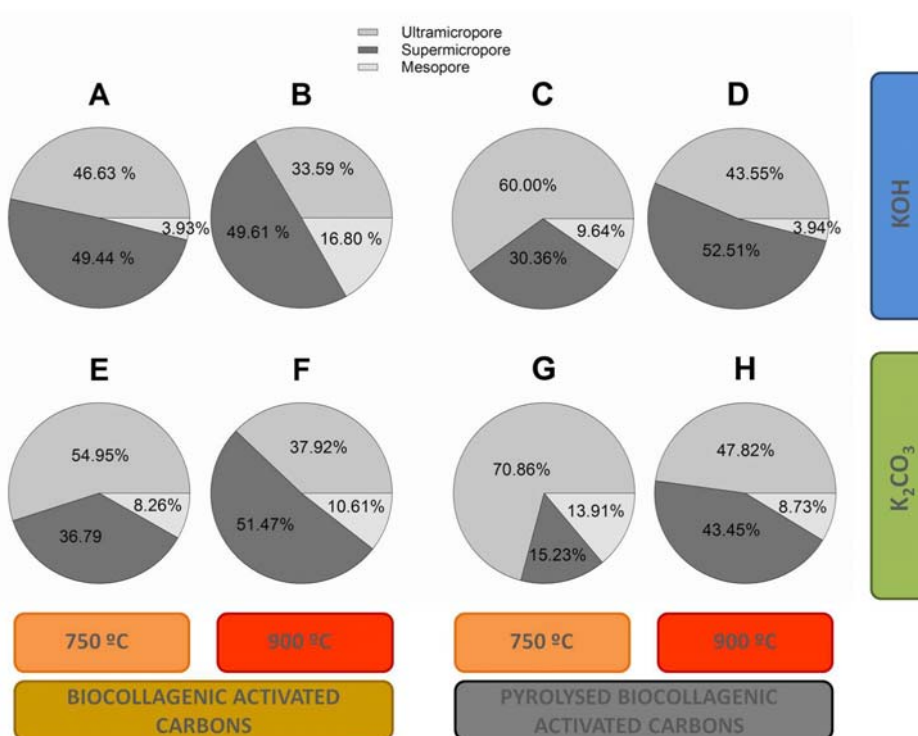
Figure 4.1.2 Pore percentages of the leather wastes activated carbons

3.3 SEM

Fig. 4.1.3 and Fig. 4.1.4 show SEM photographs of the activated carbons obtained at several magnifications.
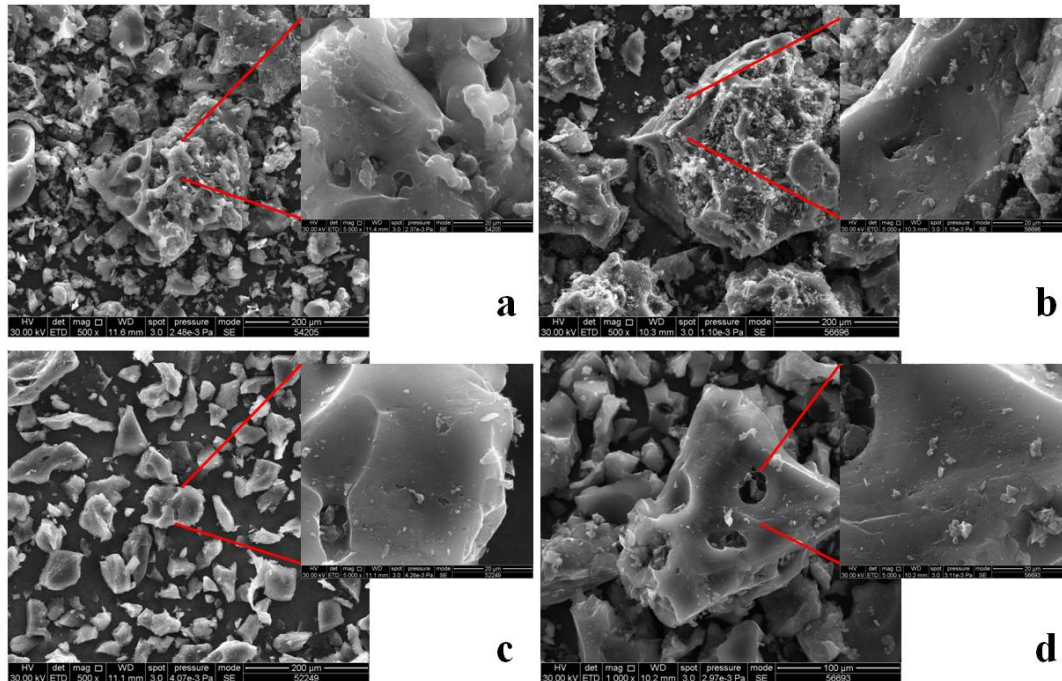
Figure 4.1.3 Scanning electron microscopic images of the activated carbon obtained by means KOH a) A, b) B, c) C and d) D

The initial collagen structure of the original skin not exposed to any previous pyrolysis [21] was destroyed during the activation by KOH or K_2CO_3 (Fig. 4.1.3 and Fig. 4.1.4). In contrast, some of the macropore structure of the original pyrolysed bioprecursor was maintained after chemical activation, as shown in Fig. 4.1.4d.

The ACs from BCT obtained with KOH (Fig 4.1.3a and Fig. 4.1.3b) show a rough surface with some smooth and fine parts. When activation was carried out at 900 ºC (Fig 4.1.3b), the aggressive conditions intensified the rough surface. In the case of pyrolysed materials activated with KOH (Fig 4.1.3c and Fig. 4.1.3d), the resulting surface was completely smooth and more macroporosity developed compared to the activated carbons that had not been previously pyrolysed (Fig. 4.1.3a and Fig. 4.1.3b).

Activated carbons chemically activated with K_2CO_3 showed a higher development of macroporosity at the different temperatures possibly due to the chemical and physical activation originating from the degradation of carbonates to carbon dioxide at 900 ºC

(Fig 4.1.4). The four activated carbons show a fine surface, and the collagenous structure of the raw material [21] having been destroyed at both temperatures (750 and 900 ºC).
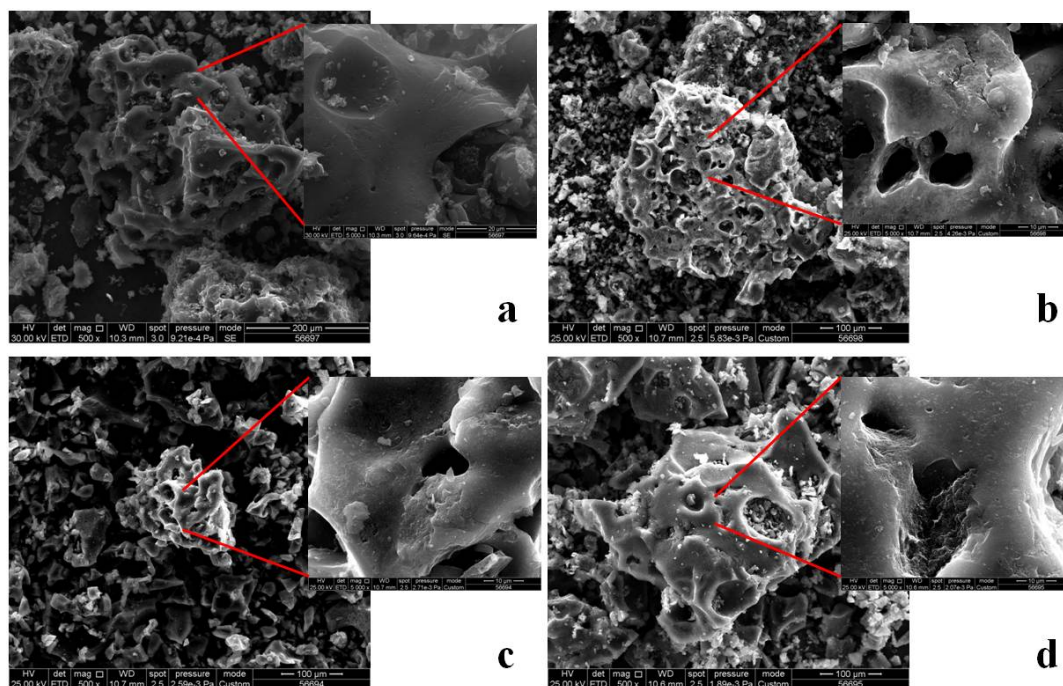
Figure 4.1.4 Scanning electron microscopic images of the activated carbon obtained by means K_2CO_3 a) E, b) F, c) G and d) H

3.4 Adsorption studies

The activated carbons were evaluated for their capacity to remove aromatic compounds from water. Six aromatic compounds with different functional groups (acetanilide, aniline, benzaldehyde, benzoic acid, methyl benzoate and phenol) were selected in order to establish the relationship between the characteristics of these compounds, the characteristics of the activated carbons and their adsorption capacity.

Adsorption isotherms corresponding to the six aromatic compounds studied in the different activated carbons are shown in Fig. 4.1.5, Fig. 4.1.6 and Fig. 4.1.7.

According to Giles' classification [34,35], the methyl benzoate isotherms corresponding to biocollagenic waste activated carbons can be classified as being of type H, which means that all of these adsorbents have a strong affinity for this ester. The isotherms

corresponding to benzaldehyde, acid benzoic, acetanilide, aniline and phenol are of type L (group 2) for most of the activated carbons indicating a weaker affinity of the adsorbents for these compounds. In the case of the adsorption of benzaldehyde onto the activated carbons A, E and F, the isotherm may be of type L, group 3. This group is characterized by a plateau (an initial monolayer) and then a rise that may represent the start of a second layer.
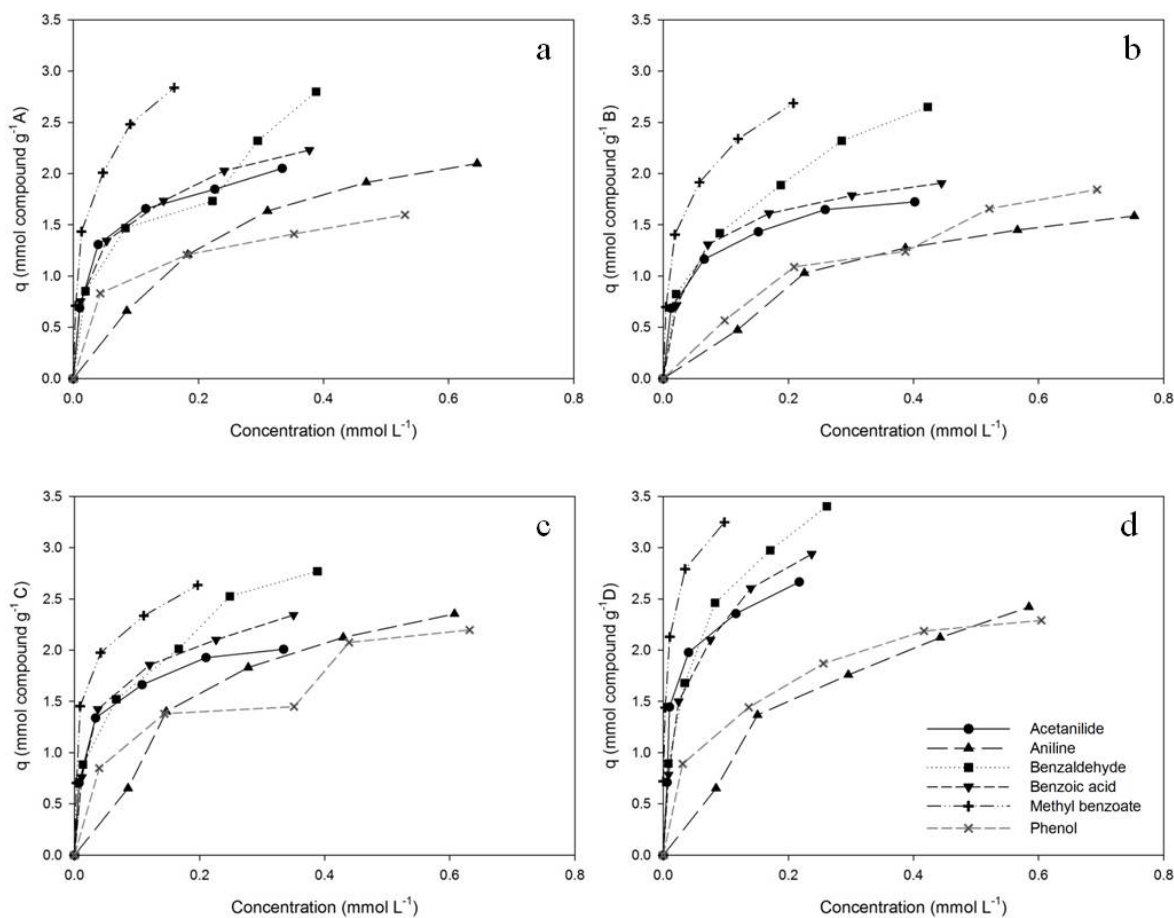
Figure 4.1.5 Adsorption isotherms corresponding to the different aromatic compounds in the KOH activated carbons a) A, b) B, c) C, d) D

The adsorption isotherm of phenol on activated carbon C is of type L, group 4 where a second layer has already formed. WAC shows an isotherm of type S group 2 for benzoic acid (Fig 4.1.7a). It can be seen that on the S curve the slope at first increases with the concentration, because in cooperative adsorption, the number of sites capable of retaining a solute increases [34]. The S curve suggests strong competition between the water molecules and, in this case, benzoic acid when present in low concentrations.
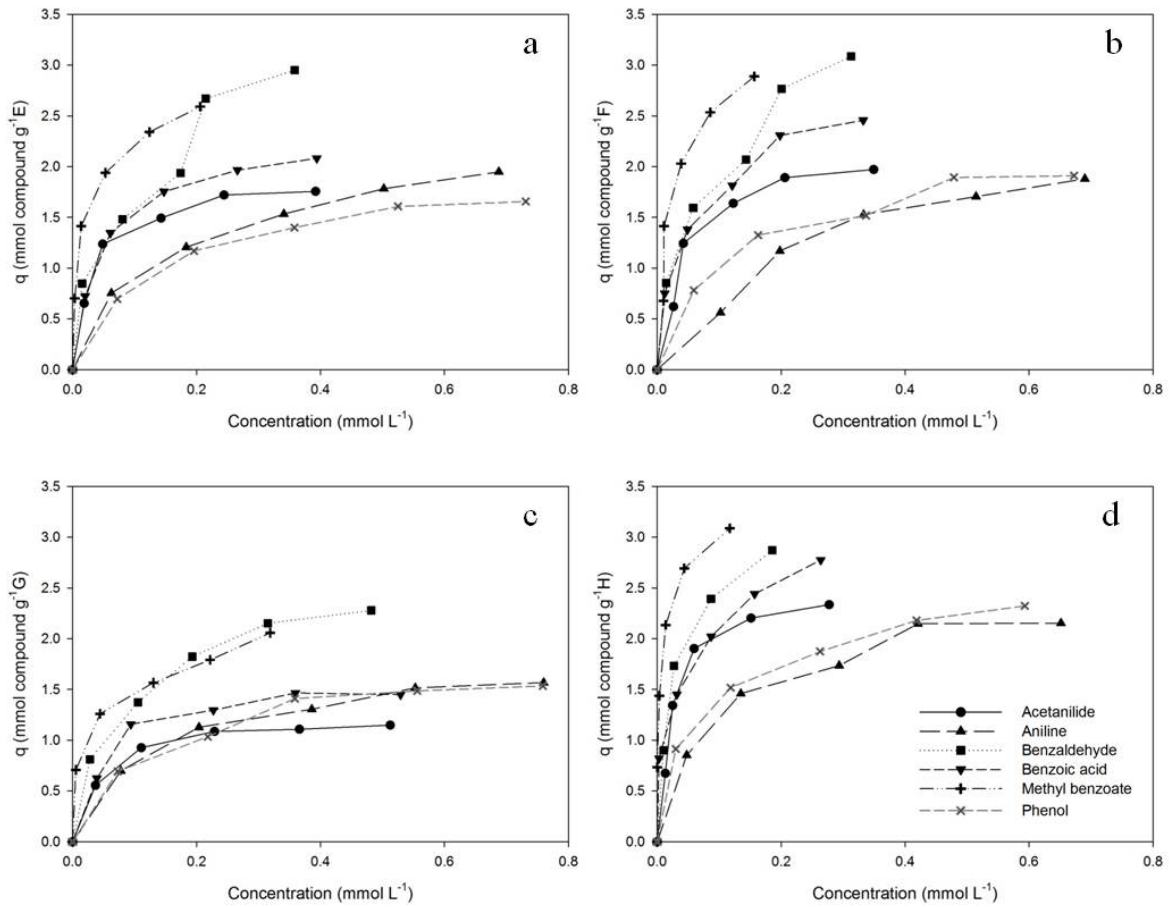
Figure 4.1.6 Adsorption isotherms corresponding to the different aromatic compounds in the K$_2$CO$_3$ activated carbons a) E, b) F, c) G, d) H.
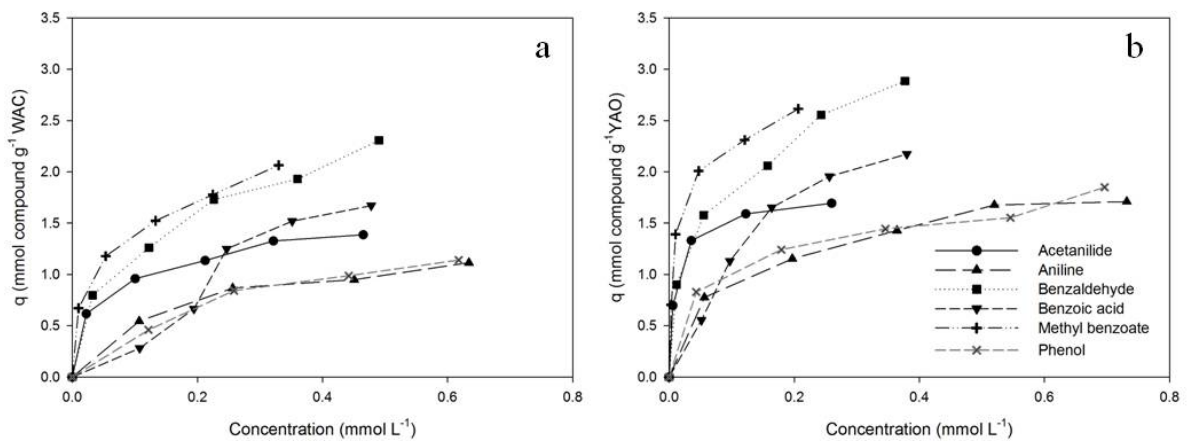
Figure 4.1.7 Adsorption isotherms corresponding to the different aromatic compounds in the commercial activated carbons a) E, b) F, c) G, d) H.

95

3.4.1 Effect of the chemical composition of the activated carbons

A dendrogram (Fig. SI 1.3) shows the textural similarities (taking into account S_{BET} and the different kinds of porosity) of all the activated carbons, in order to determine the possible chemical influences of organic compounds on the adsorption process. Four groups of activated carbons can be established on the basis of their textural similarity: group A_D (where there is a similarity between A and D activated carbon of textural properties higher than 90%), group B_F_H (similarity > 90%), group C_E_YAO (a similarity > 80%) and group G_WAC (a similarity > 90%).

It should be noted that the activated carbon D (S_{BET} = 1664 m^2 g^{-1}) shows the greatest adsorption capacity of all the organic compounds. This cannot be attributed exclusively to its large S_{BET} since activated carbon A, which has a similar surface area ($S_{BET} \approx 1600$ m^2 g^{-1}), exhibits significantly less adsorption capacity than D. It can be the chemical composition of the activated carbon that can influence on the adsorption process by reducing the quantity of each compound adsorbed (e.g. benzaldehyde adsorbed 2.8 mmol g^{-1} in A, approx. 3.5 mmol g^{-1} in D Fig. 4.1.5a and Fig. 4.1.5d, respectively). The activated carbon A has a higher nitrogen and oxygen content than D. The presence of oxygen and nitrogen groups on the activated carbons can enhance or decrease the adsorption of organic pollutants through of hydrogen bonding. Franz et al. [16] studied the adsorption of phenol in water and cyclohexane media. In their study, they concluded that water molecules compete with organic molecules for the same adsorption sites and the presence of oxygen functionalities enhanced the adsorption of water by means of a hydrogen bonding mechanism producing water clusters and reducing the adsorption of organic molecules (as it can occurred in the activated carbon A).

The same effect was observed in the activated carbons B, F and H. These three activated carbons have almost the same surface area. H however exhibited the greatest adsorption capacity of all the adsorbates studied (Fig. 4.1.5b, Fig. 4.1.6b and Fig. 4.1.6d). A difference in adsorption capacity is also observed between activated carbons F and B.

It can be seen that the adsorption of aniline is lower in carbon B (approx. 1.5 mmol g^{-1} Fig 4.1.5b) compared to that of activated carbon F (approx. 1.8 mmol g^{-1} Fig. 4.1.6b). This fact may be due to the difference in the quantity of ashes and/or the difference in the quantity on nitrogen with respect to oxygen. As can be seen in Table 4.1.3, the

quantity of ashes in B is 5.5 % and F 3.07%. The ashes (or mineral matter) might have a negative effect on the adsorption process because, firstly they are hydrophilic and adsorb water, secondly they are able to block the pores of the carbon matrix [15]. In the case of nitrogen content, Tóth and László [36] explained that N groups in carbons give rise to a high polarity on the surface and a strong affinity for water. The adsorption of aniline may be affected by the competition aniline with water molecules for the same sites resulting in a reduction of aniline adsorbed. Franz et al. [16] also observed a decrease in aniline adsorption with an increase in the amount of nitrogen functional groups in aqueous media.

In the activated carbons C_E_YAO and G_WAC, two factors must be considered: the different pH of the activated carbon and the effect of oxygen and nitrogen groups. YAO and WAC are basic activated carbons (Table 4.1.3). When they are in neutral solution, the pH_{sol} is lower than pH_{AC} so the basic sites on the surface of the activated carbons combine with protons from the medium, resulting in a positively charged surface. On the other hand, C and G are acid activated carbons (ph ≈ 4). In a neutral medium where $pH_{sol} > pH_{AC,}$ acid sites on the carbon surface will dissociate, making the surface of the carbon negative. According to Menendez et al. [37] the adsorption of anions will be enhanced on a positively charged surface, whereas in acidic carbons the adsorption of basic compounds will be favoured. In this study, the adsorption of phenol (pKa= 9.9) was favoured on G while that of benzoic acid (pKa= 4.29) was enhanced on WAC.

Other aspect to be considered is the different electron donor-acceptor interactions that may occur between the activated carbon and the adsorbate. The aromatic rings on the activated carbons can be considered as electron donating, and the presence of nitrogen and/or oxygen groups can enhance or reduce the electronic density of the graphitic planes [38]. Thus, both the aromatic rings of the compounds (π-electron acceptors) and those of the activated carbons (π-electron donators) may interact, resulting in an increase in adsorption by means of a donor-acceptor mechanism (referred to as π-π EDA interactions) [39]. On the other hand, adsorption can be reduced by the presence of π-electron donating compounds and electronic repulsion effects.

3.4.2 Effect of the nature of the adsorbate

The experimental results plotted in Fig. 4.1.5, Fig. 4.1.6 and Fig. 4.1.7 show that adsorption selectivity of the aromatic organic compounds on the activated carbons follows the order: methyl benzoate> benzaldehyde> benzoic acid> acetanilide (except in the case of activated carbons G,YAO and WAC)> aniline≈phenol. This order is compared with the physical-chemical properties of the compounds (Table 4.1.2) in order to establish which properties would have the greatest influence on adsorption. It is clear from the results that molecular weight and size do not play a dominant role in the adsorption of these organic molecules. For example, benzaldehyde (smaller dimensions, weight and volume) is more early adsorbed than acetanilide and benzoic acid.

Solubility and the coefficient log K_{ow} of the organic compounds may have an influence on adsorption due to the fact that some activated carbons can show a hydrophobic character and thereby influence adsorption. It is thought that water tends to push the organic compound to the surface of the adsorbent, thereby increasing the amount adsorbed due to a low solubility [40]. In this case, benzaldehyde can be expected to be more readily adsorbed than acetanilide and acid benzoic. On the other hand, it is well known that highly hydrophobic compounds (high coefficient log K_{ow}) are more readily adsorbed on nonpolar surfaces of activated carbons. De Ridder et al. [41] observed in their predictive model, that this parameter seems to be dominant in the adsorption of organic compounds with values higher than 3.7. In the case of compounds with relatively low log K_{ow} values, H-bonds may form, enhancing the amount adsorbed. In our study the adsorption of acetanilide was favoured with respect to that of phenol (log K_{ow} phenol > log K_{ow} acetanilide), and also the adsorption of benzaldehyde with respect to that of benzoic acid. In this way hydrogen bonds can be expected to form which excludes solubility and hydrophobicity as the main factors in the adsorption of these organic compounds.

When the pH of the solution is lower than the pKa, acetanilide, benzaldehyde, methyl benzoate, aniline and phenol are in a non-ionized form and electrostatic interactions do not play an important role in adsorption. On the other hand benzoic acid has a low pKa (pKa = 4.29) and in a neutral solution the molecule is in an anionic form. Due to the charge being negative repulsion on acidic surfaces (biocollagenic activated carbons), and attraction on basic surfaces of activated carbons (WAC and YAO) may occur.

The mechanism of dispersive/repulsive interactions deserves serious considerations. According to our results, the chemical substituent in the aromatic molecule seems to play an important role in adsorption. The -OH, -NH$_2$ and –NHCOR groups act as electron donating while –COOH, -CHO and –COOR groups act as electron withdrawing (acceptor) to the aromatic ring. Donator groups which have unshared pairs of electrons, activate the aromatic ring because the resonance effect is stronger than the inductive effect, moving the electron towards to the ring. On the other hand, withdrawing groups deactivate the ring due to an inductive effect in the presence of an electronegative atom that withdraws the electrons from the ring. In the present work compounds with withdrawing groups (benzoic acid, methyl benzoate and benzaldehyde) are more readily adsorbed than those with donating groups (phenol, aniline and acetanilide) on all the activated carbons except on the activated carbon G. This behaviour suggest the dispersion effects due to the electron donating and withdrawing groups are the main interaction between the organic molecules and the activated carbons, although other properties may also play a secondary role.

3.4.3 Maximum adsorption capacities and adsorption mechanism

The experimental isotherms were fitted to the Langmuir and Freundlich models to determine the maximum adsorption capacities of the activated carbons. Table 4.1.6 shows the maximum adsorption capacities of Langmuir and all the simulated parameters and objective function values (OF) are presented in the Supporting Information (Table SI 1.1 – SI 1.6).

In the case of the minimum OF values, the Langmuir equation provides a better description of acetanilide, aniline and benzoic acid in most of the activated carbons, indicating the formation of a monolayer, whereas the Freundlich model explains the adsorption of benzaldehyde and methyl benzoate better. Which of the two models best describes phenol depends on the activated carbon used.

The highest maximum adsorption (q_{max}) (Table 4.1.6) and the best adsorption equilibrium constant (K_L) for the different organic compounds (except for benzoic acid and phenol) is provided by the activated carbon D. The high K_L value of methyl benzoate reflects its high affinity for all the activated carbons used in this work. The

Freundlich parameter n, indicates that adsorption is favourable for all the activated carbons and six organic compounds because this value is between 1 and 10 [42].

Table 4.1.6 Maximum adsorption capacities of Langmuir for the different compounds on the activated carbons

	q_{max} (mmol g^{-1})					
	Acetanilide	**Aniline**	**Benzaldehyde**	**Benzoic acid**	**Methyl benzoate**	**Phenol**
A	2.0794	3.0630	2.9860	2.2891	2.9021	2.0488
B	1.7543	2.3551	3.0858	2.0427	2.7382	2.8145
C	2.0332	3.3797	3.0099	2.4019	2.5752	2.4958
D	2.6990	3.6499	3.7481	3.1715	3.2710	2.5177
E	1.9028	2.3270	3.7695	2.2989	2.5840	1.9729
F	2.2951	2.7369	3.6702	2.7198	3.2693	2.2279
G	1.2599	1.8248	2.6406	1.6337	1.9048	1.8177
H	2.5699	2.4879	3.1870	2.8597	3.0706	2.5136
YAO	1.8727	1.9186	2.9934	3.4207	2.5685	1.8140
WAC	1.4248	1.4181	2.6547	3.1671	2.0906	1.7065

To assess the influence of pore size distribution on the adsorption of organic compounds, the maximum adsorption capacities (q_{max}) for each compound were correlated with the ultramicropore, total micropore and pH values of the activated carbons (Table SI 1.7). Moreover, q_{max} values were normalized with respect to the pore volumes (ultramicropore and total micropore) to observe the influence of the oxygen and nitrogen contents of the biocollagenic activated carbons (Table SI 1.8 and Table SI 1.9).

The maximum adsorption capacities show a good linear correlation with the total micropore volume values for acetanilide, aniline, benzaldehyde, methyl benzoate and phenol (r > 0.6365). It suggests that the adsorption of these compounds occurs predominantly in pores smaller than 2 nm. There is no correlation between the maximum adsorption capacities of benzoic acid with the total micropore volume (r=0.1355) but a good correlation was observed with the pH (r = 0.7703), suggesting that electrostatic interactions of the benzoates play a higher interactive role than dispersive interactions on the activated carbons. Fig. 4.1.8 shows an increasing trend in the adsorption of benzoic acid with the increase in pH and the micropore volumes.

Furthermore, it seems that an increase in the nitrogen content produces a decrease in the adsorption of benzoic acid on the biocollagenic activated carbons (r= -0.9255, Table SI 1.8). It suggests that the nitrogen content of the biocollagenic activated carbons has a slightly acidic nature that increases the negative charge or the polarity of the activated carbons.
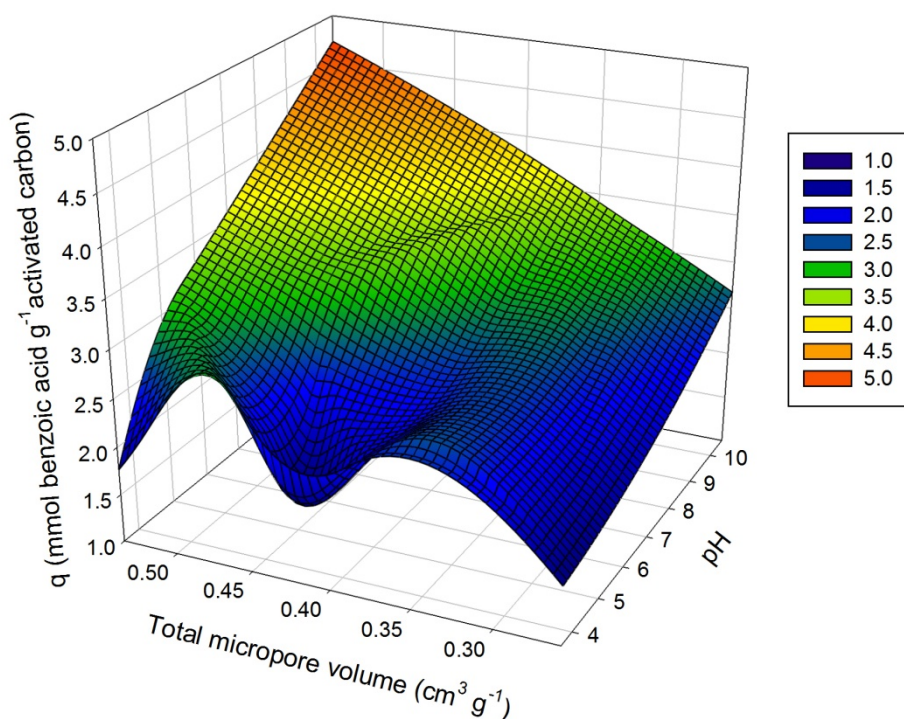
Figure 4.1.8 Trend of the benzoic acid adsorption versus total micropore volume and the pH of the activated carbons

As regards the adsorption of benzaldehyde, this may be affected by the presence of oxygen on the activated carbon. According to the results of this study, the greater the oxygen content of the activated carbon, the greater the adsorption of benzaldehyde (moderate correlation r = 0.6155). These results agree with those of Duman and Ayranci [43] who studied the adsorption of benzaldehyde in an activated carbon cloth from a phenolic polymer fibre with an oxygen content of approx. 4.5%. Their study concluded that benzaldehyde adsorption involved mainly hydrogen bonding and dispersion interactions but no repulsion. In accordance with that, methyl benzoate may also be governed by dispersion interactions (due to its withdrawing group) and by hydrogen

bonding. Furthermore, methyl benzoate shows the highest linear correlation between the maximum adsorption capacity and the total micropore volume (r=0.9276, Table SI 1.7) and a very low correlation with oxygen and nitrogen at total micropore volume (Table SI 1.9), suggesting that physical adsorption might also be playing a role. The physical adsorption mechanism consists of pore filling and a stronger binding of the adsorbate [44].

As can be seen from the high correlation (r= -0.9385) in Fig. 4.1.9, the adsorption of acetanilide is negatively influenced by the nitrogen content in the biocollagenic activated carbons. According to Terzyk [17,18], the adsorption of acetanilide takes place in the smallest micropores. It can be influenced by the surface polarity of the activating carbon because water competes with acetanilide for the same active sites; Physical adsorption may also take place via micropore filling. In this study, the increase in nitrogen content may favour the adsorption of water.
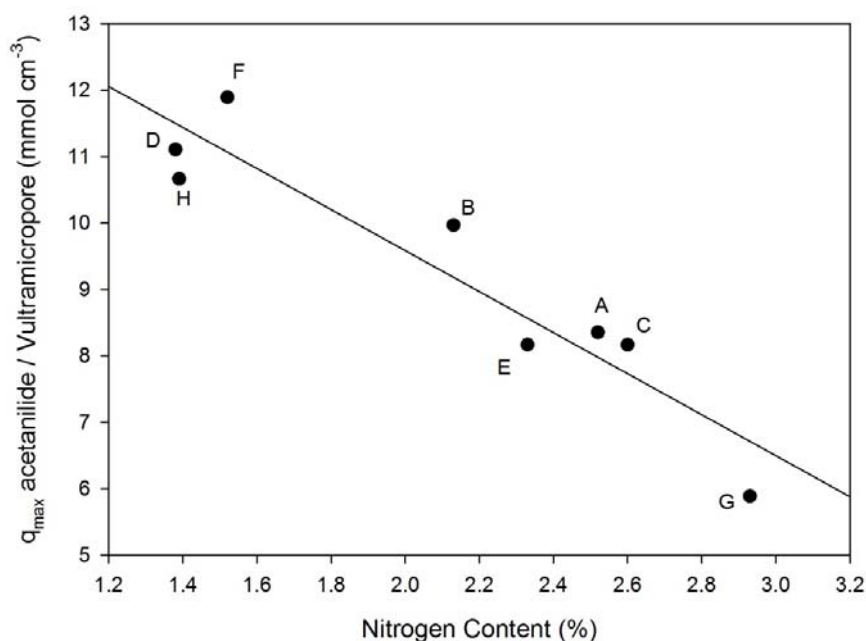
Figure 4.1.9 Relation between the q_{max} of acetanilide/ Volume of ultramicropororosity with respect to the nitrogen content of the activated carbons

In the case of aniline and phenol, the adsorption of both compounds is lower than that of the deactivating group molecules. Moreover, there is lower correlation between the adsorption capacity and the oxygen or/and nitrogen contents of the biocollagenic

activated carbons (r < 0.5). This suggests that the high heterogeneity (i.e. oxygen and nitrogen content) on the biocollagenic activated carbons does not show such a clear tendency in the adsorption of aniline and phenol. Several authors [16,45,46] have studied the adsorption of one or both compounds on aqueous media. According to Faira et al. [45], the adsorption of aniline occurred mainly through dispersive interactions and the presence of oxygen groups (at high pH) enhanced the electronic density and adsorption on activated carbons. Franz et al. [16] observed that aniline and phenol adsorption was influenced by dispersive/repulsive interactions with the aromatic ring and hydrogen bonding. In the case of aniline, the presence of oxygen groups increased adsorption while in the presence of nitrogen groups adsorption was lower. On the other hand, the adsorption of phenol the opposite effects were observed. These difference findings were due to the effect of water adsorption and the hydrogen bonding mechanism. Lorenc-Grabowska et al. [46] discussed three different adsorption mechanisms (π-π dispersion interaction, electron donor-acceptor and hydrogen bonding) for the adsorption of phenol on nitrogen-enriched activated carbons. They concluded that π-π dispersion interaction took place via the filling of small micropores, with the electron donor-acceptor exchange taking place between the nitrogen electron donor groups (pyridinic) and phenol acting as acceptor in the micropores and mesopores, and no hydrogen bonding occurring between phenol and nitrogen groups.

On the basis of the results of the present work and the above discussion, it can be concluded that the main mechanism influencing the adsorption of the organic molecules is that of dispersive/repulsion interaction between the aromatic rings of molecules and aromatic rings in the activated carbons. Nevertheless, other features may affect the main mechanism, such as electrostatic interaction (as in the case of benzoic acid), and the hydrogen bonding mechanism that enhances the adsorption of water, thereby affecting the adsorption of the organic molecules due to the presence of oxygen or/and nitrogen on the activated carbon.

4. Conclusions

Activated carbons were obtained from biocollagenic wastes by means of chemical activation with alkaline agents (KOH and K_2CO_3). The effect of the activation

temperature, chemical agent and type of bioprecursor (pyrolysed and non pyrolysed) was analysed and the main conclusions were:

- Good textural properties were obtained in most of the activated carbons (S_{BET} from 838 m^2 g^{-1} up to 1664 m^2 g^{-1}).

- The adsorbents prepared from non-pyrolysed biocollagenic materials were characterized by a supermicroporous structure and a low degree of mesoporosity. On the other hand, ultramicroporosity was more developed in pyrolysed activated carbons.

- Activation at 900 ºC with KOH reduced the performance of the activated carbons due to the formation of a greater quantity of ashes but their textural properties were similar to those activated at 750 ºC.

- Activated carbons from biocollagenic wastes contained a large quantity of nitrogen (1.4 to 2.5% approx.) and oxygen (2.55 to 10.7% approx) due to their animal origin.

- Activated carbon D (BCTP, agent KOH at 900 ºC) showed higher adsorption capacities (q_{max}) for acetanilide, aniline, benzaldehyde and methyl benzoate, while phenol was more readily adsorbed onto activated carbon B. Commercial activated carbons showed a high adsorption capacity for benzoic acid.

- Dispersion/repulsive interactions between aromatic molecule rings and those on the surface of the activated carbons were found to be the main factor controlling the adsorption process of the aromatic pollutants. However, hydrogen bonding might also have influenced the adsorption of the organic compounds

-The increase in nitrogen content had a negative influence on the adsorption of acetanilide, aniline and benzoic acid and favoured the adsorption of phenol. On the other hand, the presence of oxygen decreased the adsorption of phenol and favoured the adsorption of benzaldehyde.

- Electrostatic interactions acted against the adsorption of benzoic acid onto the acidic biocollagenic waste activated carbons, and favoured its adsorption on basic commercial activated carbons.

- Activated carbons from biocollagenic wastes were observed to be good adsorbents for organic pollutants except for acid or anionic compounds.

Acknowledgements

References

[1] G.G. Stavropoulos, A.A. Zabaniotou, Minimizing activated carbons production cost, Fuel Process. Technol. 90 (2009) 952–957.

[2] K.M. Smith, G.D. Fowler, S. Pullket, N.J.D. Graham, Production of activated carbon from sludge, in: A. Fabregat, C. Bengoa, J. Font, F. Stueber (Eds.), Reduction, Modif. Valoris. Sludge, IWA publishing, London, 2011.

[3] N. Ferrera-Lorenzo, E. Fuente, I. Suárez-Ruiz, B. Ruiz, KOH activated carbon from conventional and microwave heating system of a macroalgae waste from the Agar–Agar industry, Fuel Process. Technol. 121 (2014) 25–31.

[4] J.F. González, J.M. Encinar, C.M. González-García, E. Sabio, A. Ramiro, J.L. Canito, et al., Preparation of activated carbons from used tyres by gasification with steam and carbon dioxide, Appl. Surf. Sci. 252 (2006) 5999–6004.

[5] I.C. Kantarli, J. Yanik, Activated carbon from leather shaving wastes and its application in removal of toxic materials., J. Hazard. Mater. 179 (2010) 348–56.

[6] O. Yılmaz, I. Cem Kantarli, M. Yuksel, M. Saglam, J. Yanik, Conversion of leather wastes to useful products, Resour. Conserv. Recycl. 49 (2007) 436–448.

[7] J. Kong, Q. Yue, B. Wang, L. Huang, B. Gao, Y. Wang, et al., Preparation and characterization of activated carbon from leather waste microwave-induced pyrophosphoric acid activation, J. Anal. Appl. Pyrolysis. 104 (2013) 710–713.

[8] L.C.A. Oliveira, C.V.Z. Coura, I.R. Guimarães, M. Gonçalves, Removal of organic dyes using Cr-containing activated carbon prepared from leather waste., J. Hazard. Mater. 192 (2011) 1094–9.

[9] J. Kong, Q. Yue, L. Huang, Y. Gao, Y. Sun, B. Gao, et al., Preparation, characterization and evaluation of adsorptive properties of leather waste based activated carbon via physical and chemical activation, Chem. Eng. J. 221 (2013) 62–71.

[10] M.A. Lillo-Ródenas, J. Juan-Juan, D. Cazorla-Amorós, A. Linares-Solano, About reactions occurring during chemical activation with hydroxides, Carbon N. Y. 42 (2004) 1371–1375.

[11] R.R. Gil, B. Ruiz, M.S. Lozano, E. Fuente, Influence of the pyrolysis step and the tanning process on KOH-activated carbons from biocollagenic wastes. Prospects as adsorbent for CO2 capture, J. Anal. Appl. Pyrolysis. 110 (2014) 194–204.

[12] M.A. Lopez-Anton, R.R. Gil, E. Fuente, M. Díaz-Somoano, M.R. Martínez-Tarazona, B. Ruiz, Activated carbons from biocollagenic wastes of the leather industry for mercury capture in oxy-combustion, Fuel. 142 (2015) 227–234.

[13] R.R. Gil, B. Ruiz, M.S. Lozano, M.J. Martín, E. Fuente, VOCs removal by adsorption onto activated carbons from biocollagenic wastes of vegetable tanning, Chem. Eng. J. 245 (2014) 80–88.

[14] D.R. Zuim, D. Carpiné, G.A.R. Distler, A. de Paula Scheer, L. Igarashi-Mafra, M.R. Mafra, Adsorption of two coffee aromas from synthetic aqueous solution onto granular activated carbon derived from coconut husks, J. Food Eng. 104 (2011) 284–292.

[15] C. Moreno-Castilla, Adsorption of organic molecules from aqueous solutions on carbon materials, Carbon N. Y. 42 (2004) 83–94.

[16] M. Franz, H.A. Arafat, N.G. Pinto, Effect of chemical surface heterogeneity on the adsorption mechanism of dissolved aromatics on activated carbon, Carbon N. Y. 38 (2000) 1807–1819.

[17] A.P. Terzyk, Molecular properties and intermolecular forces--factors balancing the effect of carbon surface chemistry in adsorption of organics from dilute aqueous solutions., J. Colloid Interface Sci. 275 (2004) 9–29.

[18] A.P. Terzyk, Adsorption of Biologically Active Compounds from Aqueous Solutions on to Commercial Unmodified Activated Carbons. Part VI. The Mechanism of the Physical and Chemical Adsorption of Acetanilide, Adsorpt. Sci. Technol. 22 (2004) 353–376.

[19] F. Villacañas, M.F.R. Pereira, J.J.M. Orfão, J.L. Figueiredo, Adsorption of simple aromatic compounds on activated carbons., J. Colloid Interface Sci. 293 (2006) 128–36.

Section 4.1.1

[20] M.A. Montes-Morán, D. Suárez, J. Angel Menéndez, E. Fuente, The Basicity of Carbons, in: J.M.. Tascón (Ed.), Novel Carbon Adsorbents, Elsevier, 2012: pp. 173–203.

[21] R.R. Gil, R.P. Girón, M.S. Lozano, B. Ruiz, E. Fuente, Pyrolysis of biocollagenic wastes of vegetable tanning. Optimization and kinetic study, J. Anal. Appl. Pyrolysis. 98 (2012) 129–136.

[22] R.R. Gil, B. Ruiz, M.S. Lozano, E. Fuente, The role of crosslinking treatment on the pore structure and water transmission of biocollagenic materials, J. Appl. Polym. Sci. 130 (2013) 1812–1822.

[23] B.S. Bolton E, Wang Y, Thiessen PA, PubChem: Integrated Platform of Small Molecules and Biological Activities, in: American Chemical Society (Ed.), Annu. Reports Comput. Chem. V4, Elsevier B.V., Washington, DC, 2008.

[24] D.J. de Ridder, J.Q.J.C. Verberk, S.G.J. Heijman, G.L. Amy, J.C. van Dijk, Zeolites for nitrosamine and pharmaceutical removal from demineralised and surface water: Mechanisms and efficacy, Sep. Purif. Technol. 89 (2012) 71–77.

[25] J. Lladó, C. Lao-Luque, B. Ruiz, E. Fuente, M. Solé-Sardans, A.D. Dorado, Role of activated carbon properties in atrazine and paracetamol adsorption equilibrium and kinetics, Process Saf. Environ. Prot. (2015).

[26] W. Tsai, C. Chang, S. Wang, C. Chang, S. Chien, H. Sun, Cleaner production of carbon adsorbents by utilizing agricultural waste corn cob, Resour. Conserv. Recycl. 32 (2001) 43–53.

[27] S. Brunauer, L.S. Deming, W.E. Deming, E. Teller, On a theory of the vander Waals adsorption of gases, J. Am. Chem. Soc. 62 (1940) 1723–1732.

[28] K.S.W. Sing, Reporting physisorption data for gas/solid systems with special reference to the determination of surface area and porosity (Provisional), Pure Appl. Chem. 54 (1982).

[29] L. Chunlan, X. Shaoping, G. Yixiong, L. Shuqin, L. Changhou, Effect of pre-carbonization of petroleum cokes on chemical activation process with KOH, Carbon N. Y. 43 (2005) 2295–2301.

[30] T. Tay, S. Ucar, S. Karagöz, Preparation and characterization of activated carbon from waste biomass., J. Hazard. Mater. 165 (2009) 481–5.

[31] H. Marsh, F. Rodríguez-Reinoso, Activation processes (chemical), in: Act. Carbon, Elsevier, 2006: pp. 322–365.

[32] M.J. Pintor, C. Jean-Marius, V. Jeanne-Rose, P.-L. Taberna, P. Simon, J. Gamby, et al., Preparation of activated carbon from Turbinaria turbinata seaweeds and its use as supercapacitor electrode materials, Comptes Rendus Chim. 16 (2013) 73–79.

[33] Y. Ji, T. Li, L. Zhu, X. Wang, Q. Lin, Preparation of activated carbons by microwave heating KOH activation, Appl. Surf. Sci. 254 (2007) 506–512.

[34] C.H. Giles, D. Smith, A. Huitson, General treatment and classification of solute adsorption-isotherm 1. Theoretical, J. Colloid Interface Sci. 47 (1974) 755–765.

[35] C.H. Giles,A. P. Dsilva, I. A. Easton, General treatment and classification of solute adsorption-isotherm 2. Experimental interpretation, J Colloid Interface Sci. 47 (1974) 766–778.

[36] A. Tóth, K. László, Water Adsorption by Carbons. Hydrophobicity and Hydrophilicity, in: J.M.. Tascón (Ed.), Novel Carbon Adsorbents, first ed., Oxford, 2012: pp. 147–171.

[37] J.A. Menendez-Diaz, I. Martín-Gullón, Types of carbon adsorbents and their production, in: T.J. Bandosz (Ed.), Act. Carbon Surfaces Environ. Remediat., first, Elsevier, New York, 2006: pp. 1–47.

[38] R.C. Bansal, J.B. Donet, H.F. Stoeckli, Active carbon, New York, 1988.

[39] M. Keiluweit, M. Kleber, Molecular-Level Interactions in Soils and Sediments: The Role of Aromatic pi-Systems, Environ. Sci. Technol. 43 (2009) 3421–3429.

[40] Q. Lu, G. a Sorial, The effect of functional groups on oligomerization of phenolics on activated carbon., J. Hazard. Mater. 148 (2007) 436–45.

[41] D.J. de Ridder, L. Villacorte, a R.D. Verliefde, J.Q.J.C. Verberk, S.G.J. Heijman, G.L. Amy, et al., Modeling equilibrium adsorption of organic micropollutants onto activated carbon., Water Res. 44 (2010) 3077–86.

[42] C. Namasivayam, S. Senthilkumar, Removal of Arsenic(V) from Aqueous Solution Using Industrial Solid Waste: Adsorption Rates and Equilibrium Studies, Ind. Eng. Chem. Res. 37 (1998) 4816–4822.

[43] O. Duman, E. Ayranci, Adsorption Characteristics of Benzaldehyde, Sulphanilic acid, and p-Phenolsulfonate from Water, Acid, or Base Solutions onto Activated Carbon Cloth, Sep. Sci. Technol. 41 (2007) 3673–3692.

[44] C. Pelekani, V.L. Snoeyink, Competitive adsorption between atrazine and methylene blue on activated carbon: the importance of pore size distribution, Carbon N. Y. 38 (2000) 1423–1436.

[45] P.C.C. Faria, J.J.M. Órfão, J.L. Figueiredo, M.F.R. Pereira, Adsorption of aromatic compounds from the biodegradation of azo dyes on activated carbon, Appl. Surf. Sci. 254 (2008) 3497–3503.

[46] E. Lorenc-Grabowska, G. Gryglewicz, M.A. Diez, Kinetics and equilibrium study of phenol adsorption on nitrogen-enriched activated carbons, Fuel. 114 (2013) 235–243.

Supporting Information

Highly microporous activated carbons derived from biocollagenic wastes as adsorbents of aromatic organic pollutants in water originating from industrial activities

J. Lladó[1], R.R. Gil[2], C. Lao-Luque[1], M. Solé[1] E. Fuente[2*], B. Ruiz[2]

[1]*Department of Mining, Industrial and TIC Engineering (EMIT).* Universitat Politécnica de Catalunya. Bases de Manresa 61-73, 08242 Manresa, Spain.

[2]*"Biocarbon & Sustainability".* Instituto Nacional del Carbón (CSIC), Francisco Pintado Fe, 26, 33011 Oviedo, Spain.

*Corresponding author/Email: enriquef@incar.csic.es
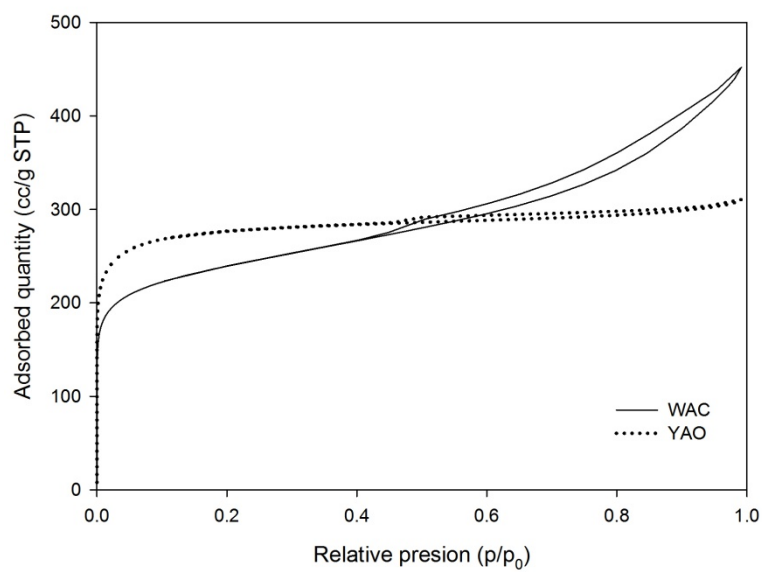
Figure SI 1.1 Nitrogen isotherms of the commercial activated carbon (WAC and YAO)
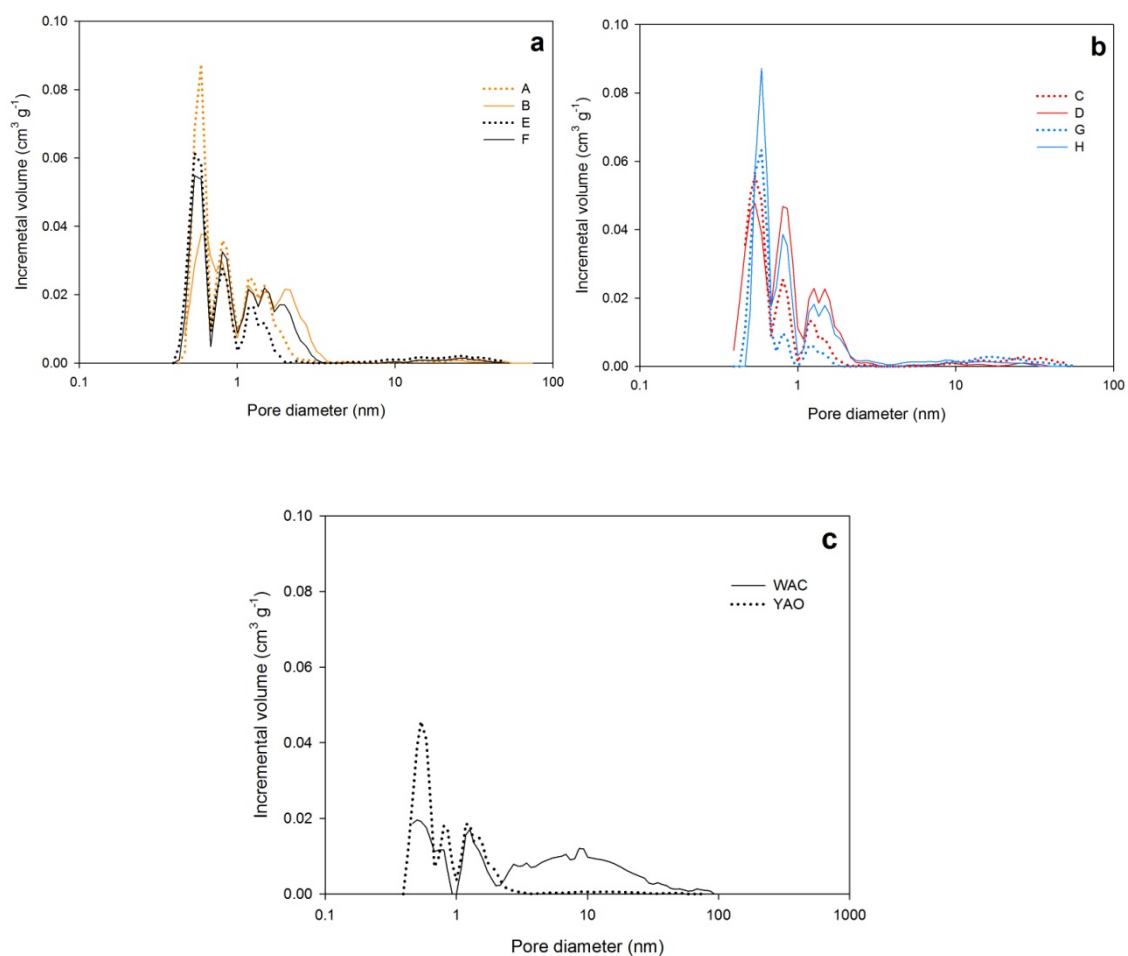
Figure SI 1.2 Pore size distribution of the different activated carbon a) KOH activated carbon, b) K_2CO_3 activated carbon, c) commercial activated carbon
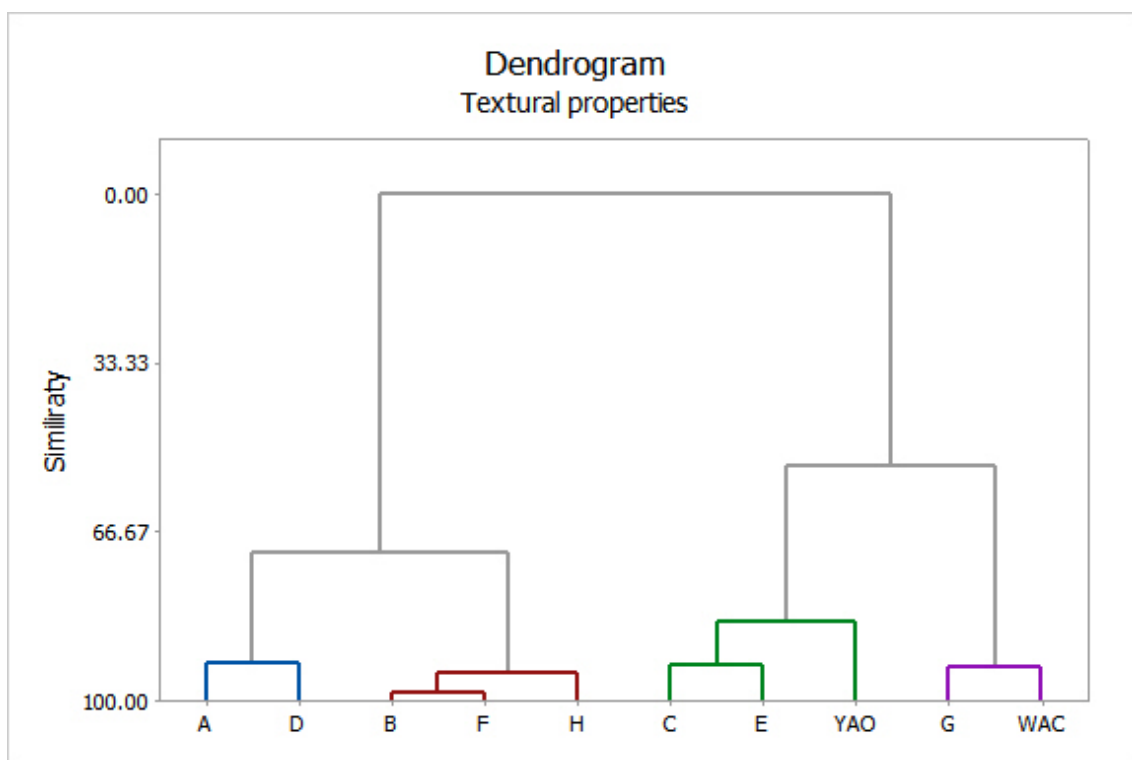
Figure SI 1.3 Similarity of the different textural properties in the activated carbons studied

Table SI 1.1 Isotherm parameters for acetanilide onto the different activated carbons

	AC	Langmuir			Freundlich		
		q_{max}*	K_L*	OF	Kf*	n	OF
Acetanilide	A	2.0794	44.0089	0.1486	2.7897	3.7912	0.2048
	B	1.7543	40.4857	0.1916	2.2523	3.9631	0.1082
	C	2.0332	62.7044	0.1579	2.7217	4.2319	0.2187
	D	2.699	82.0045	0.3489	4.108	3.8309	0.4850
	E	1.9028	31.9099	0.1246	2.3834	3.837	0.2832
	F	2.2951	20.6729	0.2616	2.9733	3.0941	0.4097
	G	1.2599	22.9945	0.0462	1.4162	4.268	0.1638
	H	2.5699	38.6212	0.2451	4.2492	3.9529	0.5892
	YAO	1.8727	83.2845	0.2917	2.4881	4.5397	0.2488
	WAC	1.4248	27.4862	0.1628	1.7355	3.772	0.0579

Table SI 1.2 Isotherm parameters for aniline onto the different activated carbons

	AC	Langmuir			Freundlich		
		q_{max}*	K_L*	OF	Kf*	n	OF
Aniline	A	3.063	3.5131	0.0671	2.7296	1.9974	0.2116
	B	2.3551	2.8840	0.1677	1.9163	1.9767	0.2473
	C	3.3797	3.9873	0.2668	3.1561	2.0312	0.3895
	D	3.6499	3.2751	0.2192	3.3056	1.8437	0.289
	E	2.327	6.4269	0.1315	2.2934	2.5885	0.0595
	F	2.7369	3.3580	0.1814	2.3653	2.0232	0.2899
	G	1.8248	7.7506	0.0742	1.7813	3.0423	0.1263
	H	2.4879	10.3833	0.1871	2.6265	3.067	0.2615
	YAO	1.9186	9.7192	0.1798	1.9591	3.1576	0.1093
	WAC	1.4181	5.6663	0.0835	1.2976	2.8089	0.0852

Table SI 1.3 Isotherm parameters for benzaldehyde onto the different activated carbons

	AC	Langmuir			Freundlich		
		q_{max}*	K_L*	OF	Kf*	n	OF
Benzaldehyde	A	2.986	11.9865	0.6275	3.8365	2.4362	0.4114
	B	3.0858	10.6013	0.3535	3.7462	2.5135	0.0676
	C	3.0099	17.807	0.4285	3.9089	2.8736	0.1505
	D	3.7481	25.8033	0.3227	5.5845	2.8152	0.2023
	E	3.7695	8.8334	0.5767	4.6591	2.301	0.3912
	F	3.6702	13.2508	0.4583	5.0822	2.3874	0.2589
	G	2.6406	12.3391	0.1928	3.0831	2.8535	0.186
	H	3.1870	40.9906	0.1264	5.1880	3.0002	0.3069
	YAO	2.9934	22.5996	0.4484	3.9916	3.0118	0.1262
	WAC	2.6547	8.9107	0.2992	3.0075	2.5233	0.1192

Table SI 1.4 Isotherm parameters for benzoic acid onto the different activated carbons

	AC	q$_{max}$ *	K$_L$*	OF	Kf*	n	OF
			Langmuir			**Freundlich**	
Benzoic acid	A	2.2891	30.9747	0.2503	3.0255	3.4284	0.1072
	B	2.0427	24.6462	0.0551	2.4793	3.6366	0.2140
	C	2.4019	37.3784	0.1673	3.2070	3.5941	0.2383
	D	3.1715	34.133	0.2388	4.9653	2.9165	0.2469
	E	2.2989	22.7935	0.0247	2.8914	3.3295	0.2586
	F	2.7198	22.614	0.2691	3.7248	2.9609	0.2103
	G	1.6337	19.3205	0.1451	1.8279	3.8994	0.2677
	H	2.8597	38.3244	0.6095	4.0613	3.5199	0.1009
	YAO	3.4207	5.0017	0.2009	3.9075	1.8393	0.3396
	WAC	3.1671	2.4967	0.1741	2.8240	1.5725	0.2437

Table SI 1.5 Isotherm parameters for methyl benzoate onto the different activated carbons

	AC	q$_{max}$ *	K$_L$*	OF	Kf*	n	OF
			Langmuir			**Freundlich**	
Methyl Benzoate	A	2.9021	71.0729	0.314	5.1713	3.1725	0.2273
	B	2.7382	56.9786	0.2994	4.4301	3.2819	0.1892
	C	2.5752	121.9669	0.2666	4.0414	4.0485	0.3615
	D	3.271	215.7375	0.7603	5.5339	4.5965	0.7528
	E	2.584	86.0668	0.2552	4.0782	3.7164	0.2529
	F	3.2693	43.5915	0.4828	5.8508	2.7992	0.5796
	G	1.9048	71.0862	0.3851	2.6865	3.9543	0.0835
	H	3.0706	213.8411	0.7753	4.8925	4.9356	0.7601
	YAO	2.5685	107.6916	0.2266	3.9983	3.9513	0.3309
	WAC	2.0906	29.2163	0.3163	2.8936	3.1811	0.0473

Table SI 1.6 Isotherm parameters for phenol onto the different activated carbons

	AC	q$_{max}$ *	K$_L$*	OF	Kf*	n	OF
			Langmuir			**Freundlich**	
Phenol	A	2.0488	10.5034	0.4922	2.2132	2.8728	0.3407
	B	2.8145	2.5862	0.2041	2.2746	1.8246	0.1937
	C	2.4958	10.5759	0.1729	2.6426	2.9453	0.1059
	D	2.5177	12.951	0.2635	2.7878	3.1407	0.1392
	E	1.9729	7.4366	0.0531	1.9364	2.9111	0.1523
	F	2.2279	8.695	0.176	2.2842	2.9242	0.2023
	G	1.8177	7.6559	0.1358	1.7699	3.0413	0.1815
	H	2.5136	15.8067	0.1690	2.7758	3.3332	0.1018
	YAO	1.814	15.7218	0.2589	1.9511	3.6398	0.1343
	WAC	1.7065	3.3249	0.0696	1.4125	2.188	0.1196

*q$_{max}$ (mmol g^{-1}); K$_L$ (L mg^{-1}); Kf (mmol g^{-1})(L mmol^{-1})$^{1/n}$

Table SI 1.7 Linear correlation coefficients r (qmax vs type pore)

	V ultra	V super	Total micro	pH
Acetanilide	0.57093	0.76145	0.86229	-0.18024
Aniline	0.74056	0.60777	0.79751	-0.53585
Benzaldehide	0.37165	0.61001	0.65743	-0.38185
Benzoic acid	-0.2175	0.25829	0.13551	0.77037
Methyl benzoate	0.41084	0.9123	0.92766	-0.29378
Phenol	0.31649	0.61125	0.63652	-0.46918

Table SI 1.8 Linear correlation coefficients r (qmax/ultramicopore vs oxygen or/and nitrogen content)

	O (%)	N (%)	O + N (%)
Acetanilide	-0.4304	-0.9385	-0.5568
Aniline	-0.3836	-0.4793	-0.4298
Benzaldehide	0.3490	-0.5230	0.2126
Benzoic acid	-0.3479	-0.9225	-0.4806
Methyl benzoate	-0.0658	-0.7170	-0.1919
Phenol	-0.0364	-0.339	-0.0955

Table SI 1.9 Linear correlation coefficients r (qmax/ total micropore vs oxygen or/and nitrogen content

	O (%)	N (%)	O + N (%)
Acetanilide	-0.4471	-0.35003	-0.46212
Aniline	-0.18197	0.43017	-0.08153
Benzaldehide	0.61553	0.43666	0.62779
Benzoic acid	-0.19225	-0.11233	-0.1916
Methyl benzoate	0.28369	0.13005	0.27609
Phenol	0.13751	0.46158	0.20798

Section 4.1.2

"Removal of pharmaceuticals and Iodinated Contrast Media (ICM) compounds on carbon xerogels and activated carbons. NOM and textural properties influences."

Removal of pharmaceuticals and Iodinated Contrast Media (ICM) compounds on carbon xerogels and activated carbons. NOM and textural properties influences.

J. Lladó[1*], B. Ruiz[2],J. Aceña[3], C. Lao-Luque[1], M.Solé-Sardans[1], S. Pérez[3], D. Barceló[3], E. Fuente[2]

[1]*Department of Mining, Industrial and TIC Engineering (EMIT).* Universitat Politécnica de Catalunya. Bases de Manresa 61-73, 08242 Manresa, Spain.

[2]*"Biocarbon & Sustainability".* Instituto Nacional del Carbón (ICAR-CSIC), Francisco Pintado Fe, 26, 33011 Oviedo, Spain.

[3]*Department of Environmental Chemistry.* Instituto de Diagnóstico Ambiental y Estudios del Agua (IDAEA-CSIC), Barcelona, Spain

*Corresponding author/Email: jordi.llado@emrn.upc.edu

Highlights

- Mesopore volume on carbon xerogels was included between 0.5 and 1.09 cm^{3}g^{-1} with similar microporosity
- Adsorption of ICM was produced on the mesopore and pharmaceutical on the micropore
- An increase of hydrophobicity decrease the intensity value of adsorption
- NOM in surface water compete directly with ICM for the mesopore
- Electrostatic interactions were produced of acid compounds due to the presence of NOM

Abstract

The presence of pollutants such as pharmaceuticals and Iodinated Contrast Media (ICM) on the aqueous media is an emerging problem to the environment. These compounds need to be eliminated or degraded due their toxicity and persistence in the water. A common way to remove these pollutants is using adsorbent materials. In this work, the adsorption of six widespread pharmaceutical and six ICM onto seven carbonaceous materials was investigated. Adsorbents were selected to study the

chemical and textural properties (micro-mesopores) influence on the adsorption of the pharmaceuticals and ICM pollutants in water: three different carbon xerogels (CX8, CX19 and CX45) with different mesopore diameter and four micro-mesopore commercial activated carbons. Results showed that according to molecular dimensions, mesopore influence on the adsorption of ICM and micropore on the pharmaceuticals. Moreover, different behaviors were observed between carbon xerogels and activated carbons depending on the hydrophobicity or hydrophilicity of the pharmaceuticals and ICM compounds.

Natural organic matter (NOM) on water can affect the adsorption of ICM and pharmaceuticals onto carbon xerogels and activated carbons. The increase of mesopore volume on carbon xerogels allowed the adsorption of NOM and reduces the adsorption of ICM (more than 20%). Moreover, acid compounds (as salicylic acid and diatrizoic acid) were less adsorbed than other pharmaceuticals and ICM compounds with the presence of NOM due to the electrostatic interactions.

Keywords: ICM, pharmaceuticals-pollutants, surface-water, carbon-xerogel, NOM, micro-mesopores

1. Introduction

In the last decades, the presence of emerging pollutants (pharmaceuticals, pesticides, personal care products) is increasing on the Llobregat basin waters [1-3]. These pharmaceutical products enter to the aqueous media by different ways such as treated or untreated domestical and hospital wastes, discharge of controlled industrial manufacturing waste streams, direct release to open water via washing, bathing,… These pollutants are found in quite high concentration in effluent from wastewater treatment plants (WWTP) due to their resistant biological degradation or due that WWTPs are not really design to treat this type of substances.

Iodinated Contrast Media (ICM) compounds are used to enhance the contrast between organs and the surrounding tissues and enable the visualization of organ details. The most common used ICM are diatrizoate (DTZ), iopamidol (IPM), iomeprol (IMPRL), iohexol (IOX), iopromide (IPRD) and iodixanol (IDXL). In 2000, the consumption of ICM in the world was approximately 3500 tons per year [4]. The ICM are applied by intravenous injection and are rapid eliminated via urine or faeces. Due to the high

hydrophilicity of the substituted benzene derivates (logkow < -2, except on DTZ) and higher dimensions, ICM pass in the WWTPs without removal. Moreover, during the aqueous chloramination the formation of iodinated trihalomentanes have been detected in the presence of natural organic matter (NOM) [5,6].

The presence of NOM can influence the mechanism adsorption of micropollutants onto granular activated carbon [7]. NOM adsorption tend to be attributable to different factors as pore volume, pore structure, electrostatic attractive and repulsive forces, specific interactions between NOM and the surface of activated carbons and access to the positive adsorption sites [8]. In the adsorption competition between NOM and micropollutants, NOM molecules block the access but do not penetrate into the ultramicropores and allow the adsorption of micropollutants on these sites. Howeverm, NOM and micropollutants show a direct site competition mechanism in the supermicropore and mesopore [9,10].

In the WWTPs, the secondary treatment only removes pharmaceuticals and ICM in a limited way. For this reason, the introduction of a tertiary step is necessary to improve the treatment. The tertiary treatment may involve in different technologies as activated carbon adsorption, ozone oxidation, UV degradation,…. In this sense, adsorption onto activated carbons can be an efficient alternative for the pharmaceutical removal but less effective with ICM [11]. Commercial activated carbons, showing a microporous character, have tend to need high operation times to remove these compounds [12].

Carbon xerogels are polymeric synthetic materials which have different applications as catalysts support, electric energy storage, hydrogen storage, waste water treatment, …[13,14]. The latest development in the synthesis of carbon xerogels by means microwave treatment provides a final product with a wide versatility since they can be synthesized with different texture (micro, meso and macropores), chemical properties and final shape [15].

To the best of our knowledge, there are not many studies focused on the elimination of emerging contaminants and ICM by synthesized materials with different range of mesoporosity. Alvarez et al. [12] demonstrated some chemical influences on adsorption of caffeine and diclofenac onto modified carbon xerogels. Carabineiro et al. [16,17] compared the adsorption of ciprofloxacin onto different adsorbents (activated carbon,

carbon xerogel and carbon nanotubes) and studied the adsorption with modified surface carbon xerogels.

This study aimed to investigate the influence of pore size of carbon xerogels and commercial activated carbons on the removal of different emerging organic pollutants. For this purpose, a set of six ICM and six pharmaceuticals were selected according their different molecular size, acid dissociation constant (pKa), solubility and molecular weight. Moreover, the different adsorbents were chemical and textural characterized in order to establish how pore size influences on the adsorption of the pollutants. The second objective was to compare the adsorption of a set ICM and pharmaceutical solution on ultrapure water and surface water in order to observe the influence of NOM.

2. Material and Methods

2.1 Adsorbents

Three different carbon xerogels were selected according the average mesopore size and total mesopore volume. These adsorbents were supplied by Xerolutions and were synthesized using the methodology of the *Microwave and carbon technologic applications* group in INCAR described in the works of Rey-Raap et al and Moreno et al. [18-20].

Four commercial activated carbons were selected according to their origin, shape and texture for comparing purposes. Bead-shaped Activated Carbon (BAC, lot n. 1X253) was supplied by Kureha Corporation (Japan) and obtained from raw petroleum pitch. Hydrodarco C, powder (HYD C, lot M-1847) was produced from a lignit coal by Norit Americas Inc (USA). Row 0.8 Supra, extruded (ROW, lot 630207) was produced by Norit the Netherlands. YAO a coconut powder activated carbon (YAO, lot M325 2855) was supplied by Eurocarb Products Ltd (United Kingdom).

2.2 Adsorbates

Six pharmaceuticals pollutants (phenol, salicylic acid, paracetamol, caffeine, levodopa and diclofenac sodium) and six iodinated contrast agents (ICM; DTZ, IPM, IPRL, IPRD, IOX and IDXL) were selected according their pKa, solubility, molecular weight, hydrophobicity and molecular size (Table 4.2.1) [21]. Molar volume was obtained from Basic PhysiChem Properties (Advanced Chemistry Development, Inc. (ACD/Labs).

Moreover, the molecule's Stokes diameter and the diffusion coefficient were calculated as proposed de Ridder [23]:

$$D_{Stokes} = \frac{2\,k_B T}{6\,\pi\eta D_L} \qquad (1)$$

$$D_L = \frac{13.26 * 10^{-5}}{\mu^{1.14} V^{0.589}} \qquad (2)$$

where k_B ($1.38*10^{-23}$ J/K) is the Boltzmann constant, T (K) is the temperature, η (m^2/s) is the kinematic viscosity of water, D_L (cm^2/s) is the diffusion coefficient, μ (centipoises (= 0.001 N s/m^2)) is the dynamic viscosity of water and V (cm^3/mol is the molar volume of the solute.

Table 4.2.1 Physico-chemical properties of ICM and pharmaceutical compounds

	MW (g mol^{-1})	pKa	log Kow	Solubility (mg L^{-1})	Molar volume (cm^3 mol^{-1})	Stokes diameter (Å)	Dimensions (Å)	λ (nm)
Phenol	94.11	9.99	1.46	82000	87,8 ± 3	1.71	4.383*0.00031*5.767	269.9
Salicylic acid	138.12	2.97	2.26	2240	100,3 ± 3	1.85	5.391*2.426*6.077	295.0
Paracetamol	151.16	9.38	0.46	14000	120,9 ± 3	2.06	4.767*1.582*8.762	242.0
Caffeine	194.19	10.4	-0.07	21600	133,3 ± 7	2.19	6.453*1.595*7.309	273.1
Levodopa	197.19	2.32	-2.39	5000	134,2 ± 3	2.20	4.887*2.807*9.551	280.0
Diclofenac sodium	318.13	4.4 ± 0.4	3.91 [22]	2430	206,8 ± 3	2.83	7.424*1.809*10.251	276.2
DTZ	613.91	1.4±0.8*	1.37	50000	234,3 ± 3	3.05	7.002*1.587*11.423	238.1
IPM	777.08	10.7	-2.42	120000	340,6 ± 3	3.80	11.974*3.520*13.521	242.8
IMPRL	777.09	10.7	-2.42	120000	342,2 ± 3	3.81	8.228*0.929*15.908	244.0
IPRD	791.10	10.6 ± 1.1	-2.05	23.80	364,0 ± 3	3.95	8.545*3.110*17.025	242.4
IOX	821.13	11.8 ± 0.7	-3.05	107	373,1 ± 3	4.01	11.924*2.967*15.186	245.5
IDXL	1550.18	7.2-7.6	-3.37	0.00184*	675,3 ± 3	5.69	10.162*2.912*26.995	246.0

*pKa Basic PhysiChem Properties (Advanced Chemistry Development, Inc. (ACD/Labs)

2.3 Textural and chemical characterization methods

Texture of the carbon xerogels and activated carbons were characterized by N_2 adsorption isotherm at -196 ºC, in a conventional volumetric apparatus (ASAP 2420 from Micrometics). Before each experiment, the samples were outgassed under vacuum at 120ºC for overnight to remove any adsorbed moisture and/or gases. The N_2 isotherms

were used to calculate the specific surface area (S_{BET}), total pore volume, (V_{TOT}), at a relative pressure of 0.99, and pore size distribution. The pore size distribution (PSD) was evaluated using the density functional theory (DFT), assuming slit-shape pore geometry. Pore volume measurements by nitrogen adsorption are not precise enough for samples with large mesoporos. For this reason, mercury porosimetry was used as a complementary technique to determine the volume of mesoporos and macropores and the percentage of porosity. Mercury porosimetry was carried out on a Micrometrics AutoPore IV 9500 Series apparatus, which provided a maximum operating pressure of 228 MPa, for carbon xerogels samples. Analysis of mercury porosimetry was based on Washburn's intrusion theory (contact angle = 130º and superficial tension = 485 dina cm^{-1}).

The carbon xerogels and activated carbons were characterized for their elemental analysis using a LECO CHN-2000 and a LECO Sulphur Determination S-144-DR. The ash content and humidity were determined according to the methods described in ISO 1171 and ISO 5068. Slurry pH was determined by preparing a 10% aqueous suspension of samples. Suspensions were agitated for 30 minutes, let stand 24 h and then the pH was measured with a pH-meter.

2.4 Single adsorption assays

Equilibrium adsorption studies were carried out at 25ºC with batch experiments. 20 mg of adsorbent was added to 100 ml of pharmaceutical compounds varying the concentration (10 – 100 ppm). Single isotherms were conducted with ultra-pure water. After 24 hours stirring in a multipoint agitation plate, samples were taken and filtered through a cellulose acetate filter (0.2 μm diameter pore). The remaining concentrations were analyzed in a UV/Vis spectrophotometer (Lambda 25 PerkinElmer) at the corresponding wavelength of each compound (Table 4.2.1). The organic compound uptake (q_t) was calculated by:

$$q_e = \frac{(C_0 - C_e)\,V}{W} \qquad (3)$$

Where q_e is the amount (mmol/g) of pharmaceutical adsorbed at the equilibrium, C_0 is the initial concentration (mmol/L), C_e is the concentration at equilibrium t (mmol/L), V is the volume (L) of the adsorbate solution and W is the weight (g) of carbon used.

Isotherms experimental data were fitted to two-parameters isotherms models: Langmuir and Freundlich [24].

2.5 Multi adsorption assays

Experiments were conducted in ultra pure water (Mil·li Q) and surface water from Cardener River (Barcelona, Spain). Surface water had a TOC content of 3.75 mg C/L and a DOC content of 3.23 mg C/L (analyzed in TOC Multi N/C 3100, Analytical Jena).

Solutions of the six pharmaceuticals and the six ICM mixed in three different concentrations (0.1 µmol L^{-1}, 10 µmol L^{-1} and 100 µmol L^{-1}) were prepared in both ultra pure water and surface water. The multi adsorption process was conducted in the same way than single adsorption assays (20 mg adsorbent, 100 ml sample, 24 h stirring and filtered at 0.2 µm). The remaining concentration of the 12 compounds after the adsorption assays was analysed using a UPLC-HRMS (Waters ACQUITY UPLC system coupled to a Orbitrap Q Exactive (Thermo Fisher Scientific, San Jose, CA, USA).

The method used followed the specifications on the work of Mendoza et al. [25]: injection volume was 10 µl, analytes were separated on a Waters ACQUITY BEH C18 column (100 × 2.1 mm, 1.7 mm particle size) equipped with a guard column (5 × 2.1 mm) of the same packing material. A simple binary gradient consisting of a) 0.1% HCOOHor 20 mM of NH4OAc for acid and neutral conditions, respectively, and b) acetonitrile was employed for chromatographic separation. Exact mass measurements of the compounds were carried out in full-scan and product ion scan mode by HR mass spectrometer using heated electrospray ionization. Eight compounds were analyzed in positive ion (PI) mode and three in negative ion (NI) mode, diclofenac sodium was analyzed with both modes. Quantification of the compounds in the sample extracts was performed by internal standard method based on the peak areas obtained for each analyte and its deuterated analogue, using Thermo Xcalibur 2.2 software.

3. Results and discussion

3.1 Carbon xerogels and activated carbons characterization

Chemical composition of the carbon xerogels shows a high carbon content and low nitrogen and oxygen content (Table 4.2.2). The quantity of ash and humidity were null due the synthetic origin and polymeric materials.

Regarding the commercial activated carbons, BAC and ROW show the highest values of carbon content but differ in the ash content (0.26 and 4.35% respectively). YAO is characterized by its high oxygen content (aprox. 2.75%) and HYDC shows the highest ash content. Ash content is a common feature of low rank coal activated carbons due to the mineral matter of the precursor material. The presence of (basic) inorganic matter will be the strongest contributor to the basicity of carbons, especially in aqueous solutions [26].

Table 4.2.2 Chemical properties of the different adsorbents

	Humity	Ash	C(%)	H(%)	N(%)	S(%)	O(%)	pH
CX8	0.00	0.00	97.20	1.00	0.80	0.00	1.00	9.23
CX19	0.00	0.00	96.30	1.40	0.60	0.00	1.70	9.79
CX45	0.00	0.00	96.50	1.00	1.30	0.00	1.20	9.88
BAC	1.31	0.26	98.00	0.63	0.67	0.02	0.42	9.28
HYDC	3.62	26.27	70.82	0.62	0.77	0.89	0.63	11.63
ROW	2.47	4.35	93.99	0.25	0.75	0.58	0.08	10.17
YAO	4.25	4.87	90.92	0.56	0.78	0.13	2.74	10.42

All adsorbent used have a basic pH (between 9.3 and 11.6), indicating a low level of acidic surface groups. Depending on the pH of the medium and the pH of activated carbon, the surface can be positively or negatively charged. According to Menendez et al. [27], in neutral aqueous solution, the pH < $pH_{adsorbents,}$ basic sites combine with protons from the medium to leave a positively charged surface.

The textural properties of the different carbon xerogels and commercial activated carbons were characterized by means nitrogen adsorption-desorption isotherms (Fig SI 2.1). As can be seen, the three carbon xerogels show a hybrid adsorption isotherm type I-IV according to the BDDT classification [28] and also they exhibit the same adsorption capacity at low relative pressure (p/p^0 < 0.1). The carbon xerogels isotherms differed on the hysteresis loop (fig SI 1a), which CX 8 show a type H2, CX 19 type H1

and CX 45 can be H3 which does not exhibit any limiting adsorption at high p/p^0 [29]. Pore size distribution is shown in Fig. 4.2.1 to try to understand the differences between the carbon xerogels. All three show practically the same microporosity (pore diameter from 0.9 to 1.7 nm approx.). Furthermore the mesoporosity developed on each carbon xerogel is different. So, in the case of CX8, the hysteresis loop type H2 can be interpret as regular pore structure that a mechanism of condensation and evaporation occurs in the narrow mesopores. CX 19 hysteresis loop (H1), the pore structure is also regular but is wider than CX 8. In CX 45, adsorption with nitrogen is difficult to interpret due to the limits of this technique. This pore size distribution can suggest that the pores have a shape as a funnel due to the two differentiated kind of pores and the lack of pores between 1.7 and 2 nm.
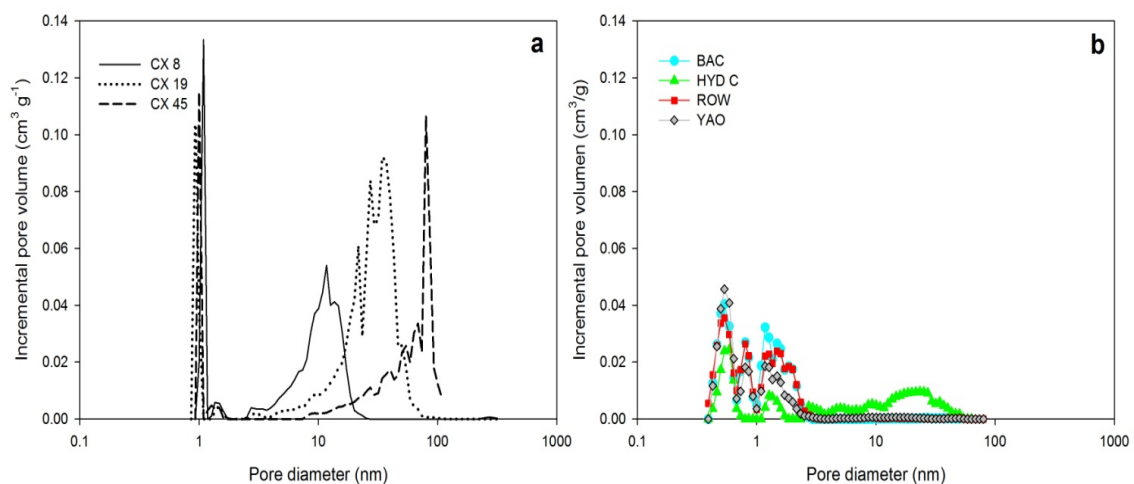
Figure 4.2.1 Pore size distribution obtained by application of the DFT model to the N_2 adsorption data at -196 ºC, a) Carbon xerogels, b) Commercial activated carbons

Regarding the commercial activated carbons, BAC, ROW and YAO exhibit a nitrogen adsorption-desorption isotherm type I (Fig. SI 2.1b) suggesting the high development of microporosity without mesoporos. On the other hand, HYDC shows a type I-IV nitrogen isotherm with a low grade of microporosity but a different mesopore range (2 - 50 nm, Fig. 4.2.1b).

The different textural properties of the carbon xerogels and commercial activated carbons obtained are shown in Table 4.2.3. As can be seen, the three carbon xerogels have a similar micropore structure lower than 23% of the total porosity. On the other

hand, BAC, ROW and YAO are distinctly microporous with greater than 75% of pore volume composed of pore less than 20 Å in width. HYDC shows a high volume of mesopores (0.198 cm^3 g^{-1}) that represents more than 32% of the total porosity. The high value of total volume of HYDC can indicate a development of higher mesoporosity and also macroporosity.

Table 4.2.3 Textural properties of Carbon Xerogels and commercial activated carbons (adsorption-desorption nitrogen isotherms in different groups)

	Nitrogen adsorption-desorption isotherms at 77 K (p/p^0=0.99)						
	S_{BET} $(m^2 g^{-1})$	V_{u-mic} $(cm^3 g^{-1})$	V_{m-mic} $(cm^3 g^{-1})$	V_{micro} $(cm^3 g^{-1})$	V_{meso} $(cm^3 g^{-1})$	V_{macro} $(cm^3 g^{-1})$	V_{total} $(cm^3 g^{-1})$
CX8	657	-	0.169	0.169	0.520	0.002	0.743
CX19	616	-	0.159	0.159	0.990	0.039	1.252
CX45	612	-	0.164	0.164	0.190	0.344	0.909
BAC	1362	0.177	0.276	0.453	0.020	0.005	0.570
HYDC	551	0.097	0.032	0.129	0.198	0.013	0.614
ROW	1306	0.179	0.248	0.426	0.030	0.005	0.575
YAO	1092	0.194	0.162	0.357	0.020	0.001	0.480

Mercury porosimetry (Fig. 4.2.2 and Table SI2.1) revealed the real mesopore volume on CX 45. In this case, the average pore diameter was 45.6 nm and it was characterized for a high volume of macropores (V_{macro} = 0.63 cm^3 g^{-1}, Table 4.2.3). On the other hand, CX8 and CX19 showed a low grade of macroporosity and their average pore diameter were 8.8 and 19.3 nm respectively.
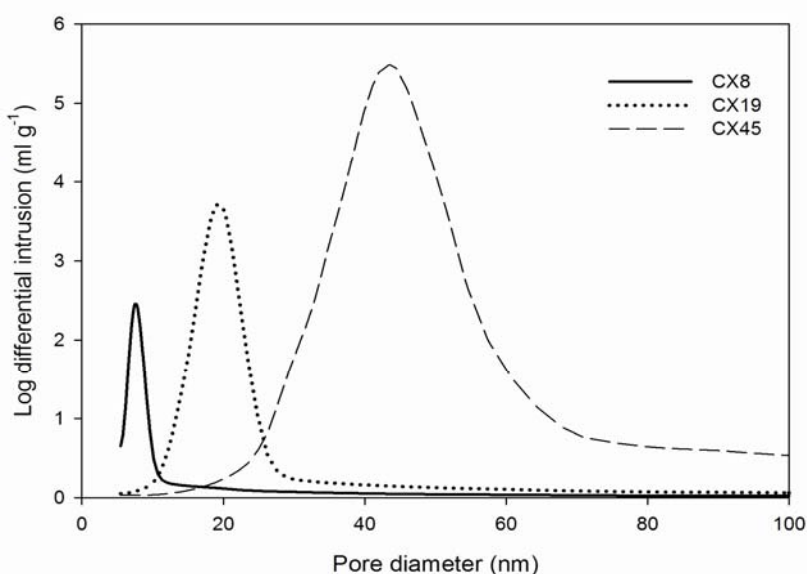
Figure 4.2.2 Mercury intrusion onto carbon xerogels

3.2 Efficiencies of pharmaceutical and ICM adsorption onto the different adsorbents

A first test to compare the different materials was a screening assay to see the maximum adsorption efficiencies of the different pollutants at 100 ppm after 24 h of time. Fig SI 2.3 and Fig SI 2.4 show the maximum adsorption efficiencies for pharmaceutical and ICM onto carbon xerogels and commercial activated carbons. As can be seen, similar adsorption efficiencies are obtained on carbon xerogels for phenol, salycilic acid and paracetamol. Furthermore, considering the molecular molar volume (Table 4.2.1), adsorption of these three pharmaceutical takes up the same volume (approx. 0.105 $cm^3 g^{-1}$) on each carbon xerogel. It can suggest that the adsorption of these three molecules can take place on the total micropore because carbon xerogels have similar micropore volume (approx 0.165 cm^3 g^{-1}). A higher efficiency is observed onto CX8 respect than CX19 and CX45 on the adsorption of caffeine, levodopa and diclofenac sodium. In this case, mesopores can influence the adsorption of these compounds due to the no presence of wider micropore (as example from 1.6 to 2.3 nm in the case of CX8). In the case of ICM efficiencies, the same trend is also observed.

Respect to the commercial activated carbons, they exhibit higher efficiencies are for the adsorption of pharmaceuticals than carbon xerogels. But, lower efficiencies are achieved on the adsorption of ICM respect carbon xerogels.

3.3 Relation of pore size distribution with maximum adsorption capacity

Adsorption isotherms for the different pharmaceuticals and ICM are shown in Fig. SI 2.5 and Fig SI 2.6 (Supporting information). The experimental data are fitted to two isotherm models (Langmuir and Freundlich) and the different parameters values obtained from the models, as well as, the objective function (OF) values are listed in tables SI 2.1. As can be seen, most of the isotherms are better fitted to Freundlich model. The parameter n (Freundlich) is related to the adsorption intensity and values between 1 to 10 means a favourable adsorption [30]. In this case, pharmaceutical and ICM adsorption was favourable onto most of adsorbents. Furthermore the low values from OF in Langmuir also indicates a good fit.

In order to observe in which kind of pores the adsorption of pharmaceuticals can take place, the maximum adsorption capacities (q_{max}) were correlated with the different pore volumes (ultramicropore, supermicropore, total micropore and mesopore (Table 4.2.3))

As can be seen in the Table 4.2.4, phenol, salicylic acid, paracetamol and caffeine qmax's were highly correlated to the total micropore and the ultramicropore ($r^2 > 0.7715$). On the other hand, for the rest of compounds the correlation was low or null for these two types of pores. In the case of higher voluminous ICM, as IPRD and IDXL, different correlation tend was observed, suggesting that an increase of the mesopore could increase the adsorption of these ICM.

Table 4.2.4 Correlation coefficient between the different molecules with different kind of pores

	Ultra micro		Super micropore		Micropore (total)		Mesopore	
Phenol	+	0.717	+	0.709	+	0.772	-	0.558
Salicylic acid	+	0.944	+	0.706	+	0.845	-	0.397
Paracetamol	+	0.786	+	0.705	+	0.792	-	0.644
Caffeine	+	0.827	+	0.744	+	0.835	-	0.670
Levodopa	+	0.748	+	0.377	+	0.520	-	0.729
Diclofenac sodium		0.148		0.030		0.000		0.094
DTZ	+	0.724	+	0.293	+	0.412	-	0.588
IPML		0.035		0.162		0.053		0.107
IMPRL		0.067		0.116		0.026		0.078
IPRD	-	0.282	-	0.666	-	0.548	+	0.384
IOX		0.093		0.062		0.007	-	0.332
IDXL	-	0.352	-	0.501	-	0.491	+	0.645

Mui et al [31] assumed that the pore width should be approximately 1.7 times the adsorbate molecule width. It seems that all pharmaceuticals should be adsorbed on the micropores; besides the pore dimension, chemical interactions of the adsorbents can affect the adsorption process of the different molecules.

3.4 Relationship between physic-chemical properties of pharmaceutical and the maximum adsorption capacities

According to Moreno-Castilla [32] the molecular size, solubility, pKa and the nature of the substituent on the aromatic ring are the most influential characteristics on the adsorption process. In order to determine the importance of different molecular properties (Dstokes, pka, solubility and the highest size of the compound) on the

adsorption process, these properties were correlated to q_{max} obtained from Langmuir equation.

A decreasing trend in q_{max} is observed with an increasing of the size of the molecule (highest molecule dimension) or the D stokes on the adsorption of pharmaceuticals onto the seven adsorbents (Table 4.2.5 and Fig. 4.2.3); in most of the cases the coefficient correlation was higher than 0.75, except in HYDC and YAO. In both activated carbons, it is suspected that different chemical interactions can take place in both activated carbons.

Table 4.2.5 Coefficient of determination (r^2) for linear regression between q_{max} and different physic-chemical characteristics of pharmaceuticals

	Coefficient correlation (r^2) with q_{max}											
	Dstokes		Highest dimension		pKa		Log Kow		Log Kow (with out diclofenac)		Solubility	
CX8	-	0.788	-	0.827		0.047	+	0.475	+	0.815	+	0.299
CX19	-	0.783	-	0.764		0.060	+	0.476	+	0.802	+	0.311
CX45	-	0.689	-	0.703		0.031	+	0.559	+	0.828	+	0.222
BAC	-	0.913	-	0.765		0.078		0.169	+	0.929		0.136
HYDC	-	0.672	-	0.404	+	0.272		0.095		0.197	+	0.698
ROW	-	0.861	-	0.886		0.104	+	0.376	+	0.955		0.222
YAO	-	0.593	-	0.609		0.021	+	0.342	+	0.598		0.012

Hydrophobicity (log Kow) also plays an important role on the adsorption. At first glance, considering all the pharmaceuticals (in this study), there is a low correlation between Logkow and all the adsorbents used ($r^2 < 0.55$). De Ridder et al [33] discuss this characteristic by means a own developed adsorption equilibrium model which they concluded that logkow was the dominant removal mechanism for solutes with logKow > 3.7. Nam et al. [22] classified into three different groups the molecules according their hydrophobicities as low (log Kow< 2), moderate ($2<$ log Kow<3.5) and high ($3.5 <$ logKow). They concluded that high hydrophobic compounds were best fitted to Freundlich model and low hydrophobic and hydrophilic compounds were correlated to the linear isotherm model. Taking into account these considerations, diclofenac sodium is considered as a high hydrophobic compound; and observing the different adsorptions results, its high dimensions can also affect its adsorption. In this sense, the correlations

of hydrophilic low-moderate pharmaceuticals increase without considering diclofenac onto the different adsorbent in the calculations (except HYDC and YAO) ($r^2 > 0.8023$).

Moreover, Table 4.2.5 shows a low correlation on pKa and solubility suggesting that these properties are not important in the adsorption of the different pharmaceuticals onto the different adsorbents.

Figure 4.2.3 Trend of adsorption capacity (q_{max}) of the different pharmaceuticals vs third compound dimension and logkow of pharmaceuticals onto the different adsorbents (Experimental adsorption isotherms and obtained parameters are in the supporting information, Table SI 2.1 and Fig. SI 2.5).

3.4.1 Adsorption of phenol and salicylic acid

It would be expected that phenol, due to its smaller size compared with the salicylic acid, could be more adsorbed than the acid onto ultramicropore and in the total micropore. But the uptake of salicylic is higher onto the all the adsorbents used except HYDC. A possible explanation for this could be related with the pKa of each compound.At neutral pH solutions, phenol is in its molecular form while salicylic acid molecule is dissociated. On the other hand, the carbons surface has a net positive charge due to the basic character at neutral aqueous. That's why the electrostatic interactions between the positive surface and the salicylates bring on a major adsorption of these compounds. This fact is in agreement with different authors [34,35] that obtained similar results on the adsorption onto different adsorbents. Moreover, salicylic acid presents a withdrawing group while phenol has a donor group. So attraction/dispersive interactions that occurs between the ring of these two aromatic compounds and those on the activated carbons could be pretty different. According to Lonrenc-Grawobska [36] the adsorption of phenol may occur in the small micropores by π-π interactions.

In addition, it is known that phenol adsorption can take place via hydrogen bonding [37]. Thus it is possible that phenol competes with water for the same adsorption sites, and this aromatic compound adsorption is decreased in favor to the adsorption of water. The presence of oxygen on the carbon surface can enhance the adsorption of water as it could happen on YAO (oxygen 2.74%), while on ROW, the low oxygen quantity allow increase the adsorption of phenol.

In the case of HYDC, the high content of ashes can affect the adsorption of phenol and salicylic acid. According some authors[32,38], The effect of mineral matter or ashes in case of activated carbon decrease the adsorption capacity of the adsorbent for some pollutants [38]. According to Moreno-Castilla [32] reported that the mineral matter is able to block the pores of the carbon matrix adsorbing water due to its hydrophilic character. It seems that the hydrophilic character of HYDC affects negatively the salicylic acid molecules which show a low solubility and high low Kow.

3.4.2 Adsorption of paracetamol

Adsorption of paracetamol is similar on the three carbon xerogels studied. The similar

micropore dimensions of carbon xerogels (from 0.9 to 1.7 nm approx.) allow paracetamol be adsorbed without mesopore influence. Galhetas et al. [39,40] proposed that paracetamol can form a dimmer of dimensions 1.58 nm (length) x 1.19 nm (width) x 0.66 nm (thickness) which thickness is the critic dimension; and the monomer and dimmer can be adsorbed on the wider micropores and some on the ultramicropore. Other authors [41-43] also considered that paracetamol can be adsorbed and influenced by π-π interactions, hydrogen bonding and hydrophobic effect.

3.4.3 Adsorption of caffeine and levodopa

Caffeine and levodopa have similar molecular size, that's why it would be expected that the adsorption of these two compounds took place on the same size pore (micropore). It can be thought that hydrophobicity can play an important role on the adsorption of both compounds due to caffeine can be considered low hydrophobic character while levodopa hydrophilic. According to Mohammed et al. [44] hydrophobic compounds tend to be pushed to the adsorbent surface and hence they are more adsorbed than hydrophilic compounds due to the strong affinity with hydrophobic activated carbons and with a limited solubility in water. Caffeine is more adsorbed onto the different adsorbents than levodopa except on HYDC and YAO. As can be seen before, HYDC can show a hydrophilic character due to the presence of high quantity of ashes. In this sense, it seems that HYDC can have a high affinity for the hydrophilic compounds as levodopa (log Kow = -2.39).

On the other hand, according to the work of Quesada-Peñate et al. [45], the apparent zwitterion character of levodopa did not seem to have any effect on the adsorption of the different activated carbon they studied. It was concluded that adsorption of levodopa appears to be enhance by the large amount of basic groups by means a donor-acceptor mechanism; moreover, water adsorption penalized the adsorption of levodopa due to the presence of acidic groups on the activated carbon. In this study, HYDC and YAO show the highest value of pH suggesting more presence of basic groups on the surface, thus it is expected a higher levodopa uptake than the rest of adsorbents.

The lower adsorption of caffeine respect to levodopa observed on HYDC and YAO are in agreement with Torrellas et al. [46]. It was showed that the adsorption of caffeine decreased on oxidized carbon (carboxylic groups on the surface) which showed a higher hydrophilic character due to the possible adsorption of water. On the contrary, the

presence of oxygen on carbon xerogels (1-1.7%) does not seem influence the adsorption of caffeine.

3.4.4 Adsorption of diclofenac

Diclofenac is the larger compound of all pharmaceutical studied. The adsorption of diclofenac on HYDC is higher than on BAC and ROW, which both are mainly micropore adsorbents. Thus, it is expected that the adsorption of diclofenac can partly take place on the mesopore. In addition, Sotelo et al. [47] suggested that the adsorption of diclofenac could be in parallel to the carbon surface due to the aromatic rings of the molecule; and there was no major competition between diclofenac and water molecules for the active adsorption sites.

In the case of carbon xerogels, the presence of mesopores diameters seems to have a relevant influence on the adsorption (CX8 adsorbed diclofenac more than 17% and 35% respect CX19 and CX45 respectively). According to Chang et al. [48] the limiting factor for adsorption of diclofenac was the access to the micropores. Alvarez et al. [12] studied the modification of carbon xerogels with different impregnations for diclofenac and caffeine removing in different studies. They concluded that the rapid adsorption of diclofenac was due to the presence of different functional groups on the surface and the mesopore. In the carbon xerogel CX45, although it has a high mesoporosity and macroporosity it seems that the molecule can flow in but it is not retained into the mesopore of wide diameter; suggesting the mesopore pore of small size is more appropriated to the adsorption of diclofenac.

3.5 Relation between physic-chemical properties of ICM and maximum adsorption capacities

The physic-chemical properties of the different ICM compounds were correlated to q_{max} obtained from Langmuir equation. As can be seen in Table 4.2.6 and Fig. 4.2.4, the adsorption of the different ICM onto carbon xerogels showed different behavior than onto activated carbons. In carbon xerogels were observed an increase tend on the adsorption of ICM with the increase of the size of molecule (highest dimensions) or the Dstokes. The presence of a well macropore and mesopore structure can allow the high molecules throw intro the small diameter mesopore and to be adsorbed on these pores.

On the contrary, the low development of macroporosity and mesoporosity on the activated carbons results in a low adsorption of ICM. This fact is more accentuated on shaped materials, BAC and ROW, which maximum adsorption capacities of voluminous molecules are very low or practically null (Fig. 4.2.4).
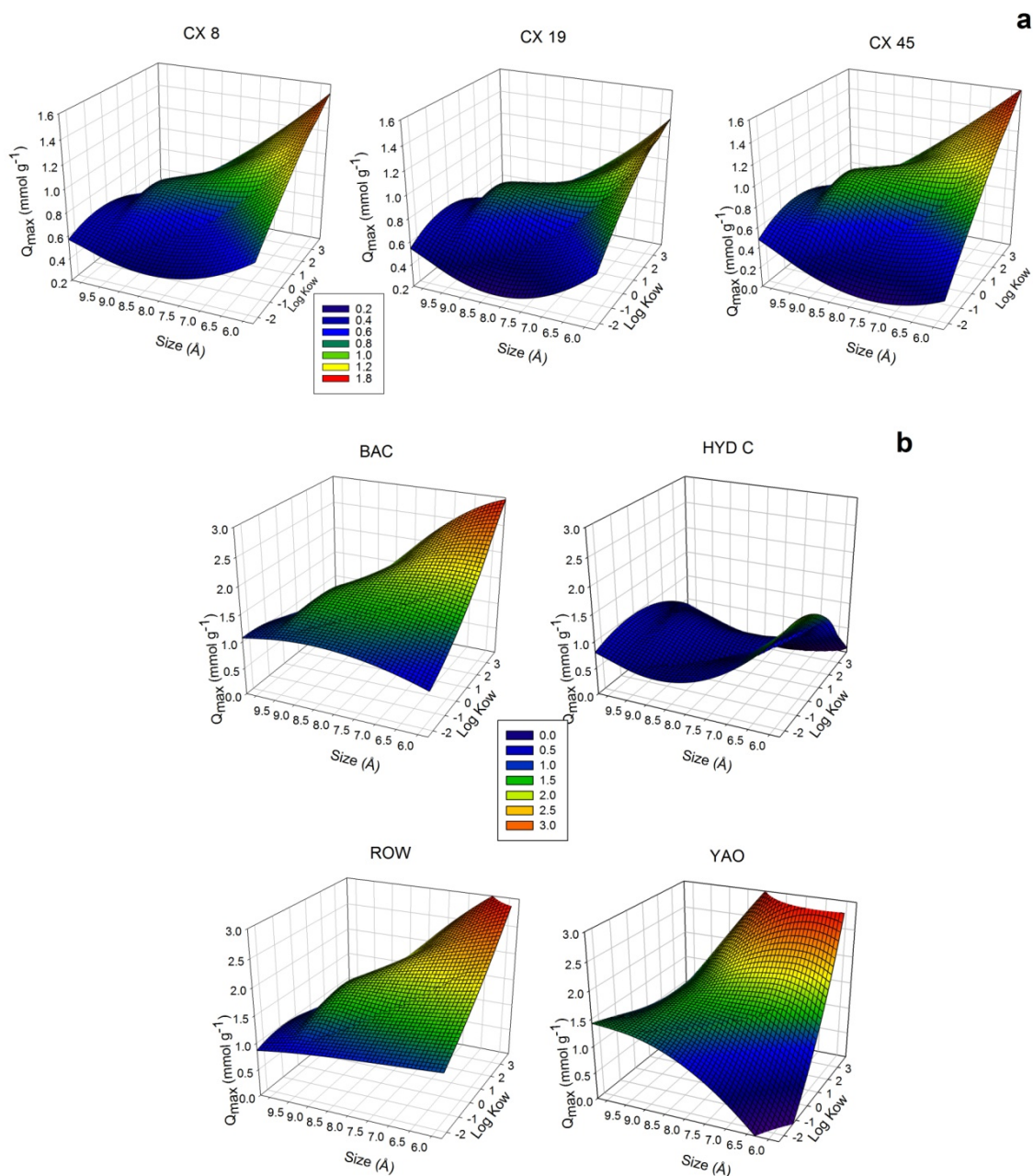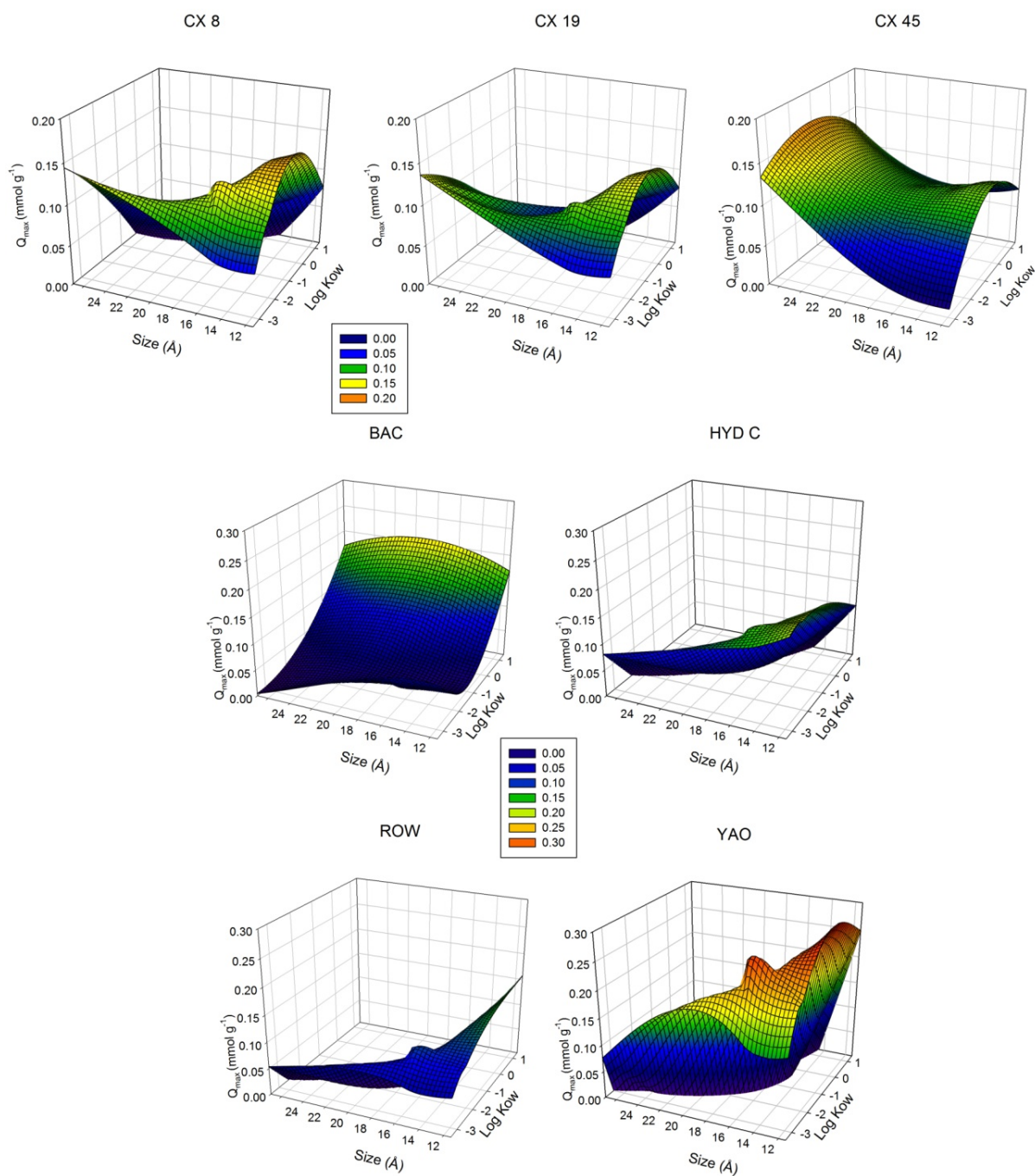

Figure 4.2.4 Trend of adsorption capacity (q_{max}) of the different ICM vs third compound dimension and logkow of pharmaceuticals onto the different adsorbents (Experimental adsorption isotherms and obtained parameters are in the supporting information, Table SI 2.1 and Figure SI 2.6).

Table 4.2.6 Coefficient correlation of q_{max} between different chemical and phisycal molecular characteristics of ICM onto the different adsorbents

	Coefficient correlation (r^2) with q_{max}									
		Dstokes		Highest dimension		pKa		Log Kow		Solubility
CX8	+	0.463	+	0.414		0.006	-	0.548		0.106
CX19	+	0.625	+	0.603		0.101	-	0.386		0.034
CX45	+	0.546	+	0.671	-	0.470		0.060		0.028
BAC	-	0.573	-	0.510		0.036	+	0.830		0.002
HYDC		0.142	-	0.279	+	0.471		0.046	+	0.445
ROW	-	0.552	-	0.549		0.012	+	0.568	+	0.321
YAO	-	0.525	-	0.608		0.102		0.154	+	0.594

The coefficient correlation between q_{max} and hydrophobicity (logkow) was low on the different adsorbent materials, except on BAC. But different tend was observed between carbon xerogels and activated carbons. In carbon xerogels an increase of the lowkog decrease the amount adsorbed, while on activated carbons increase the amount adsorbed. This result suggests that carbon xerogels can have affinity for hydrophobic and hydrophilic compounds due to the different pore size.

Finally, very low correlation coefficients were obtained between q_{max} and solubility. This indicates that these characteristics have no influence on the adsorption of ICM in all the activated carbons studied.

3.5.1 Adsorption of DTZ

The smallest iodinated compound of the ICM series, DTZ, is hydrophobic and present a strong acidic character (pka =1.4±0.8) compared with the rest of ICM (hydrophilic and neutral-basic character). As can be seen in Fig. SI 2.6a, the adsorption of DTZ is higher than adsorption of diclofenac (Fig. SI 2.5f) onto BAC; the dimensions of DZT are similar than diclofenac, so, it can be suggested that adsorption of DZT is influenced by electrostatic interactions onto BAC.

3.5.2 Adsorption of IOX, IMPRL, IPM and IPRD

These four iodinated compounds have similar dimensions and physic-chemical characteristics. In this study, the adsorption of these four compounds onto ROW and

BAC is lower than the rest of the adsorbent in most of the cases. ROW and BAC show the highest supermicropore volumes ($\approx$0.248 and 0.276 cm^3 g^{-1}, respectively), so it can be suggested that the adsorption of them can be produced onto on other pore diameters. This fact can be corroborated by the low or null correlations found on the adsorption of IPM, IMPRL, IPRD and IOX on Table 4.2.4. So, it can be suggested that the total macropore and mesopore structure and the shape of the adsorbent have an important role on the adsorption of these high four ICM (as can be happen on BAC and ROW).

There is no much information about the adsorption of these four pollutants on activated carbons (except IPM). According to Mestre et al [49,50] the adsorption of IPM takes place on the wider micropores (supermicropores) and the mesopores. Moreover, the formation of dimmer (aggregates) can be possible when concentrations of IPM are higher or 100 mg L^{-1} and sometimes can form two-step isotherms.

Carbon xerogels, HYDC and YAO were selected in order to determine where the adsorption of these ICM can take place on (BAC and ROW were discarded due its shaped form). In this sense, different pore volume sections on the mesopore were made from the pore size distribution (table SI 2.2); and then the different q$_{max}$ of the four ICM were correlated with these pore volume (Table 4.2.7). As can be seen in Table 4.2.7 an increase of adsorption of IMPRL, IPM and IOX is observed with an increase of the pore diameter 1.3 to 5 nm (r^2>0.70) (Fig. 4.2.5). On the other hand, IPRD show a low correlation with the different pore volume studied suggesting that some chemical interaction could be occurred.

Table 4.2.7 Correlation coefficient between IOX, IPRD, IMPRL, IPM and IDXL with different pore diameters

	Coefficient correlation r^2			
	1.3-5 (nm)	Meso 2-5 (nm)	meso 5-10 (nm)	meso 2-10 (nm)
IOX	0.7503	0.0164	0.0472	0.0256
IPRD	0.1457	0.0244	0.0028	0.0053
IMPRL	0.7022	0.0013	0.0488	0.0373
IPML	0.7553	0.0037	0.0460	0.0289
IDXL	0.3121	0.0117	0.3118	0.2408
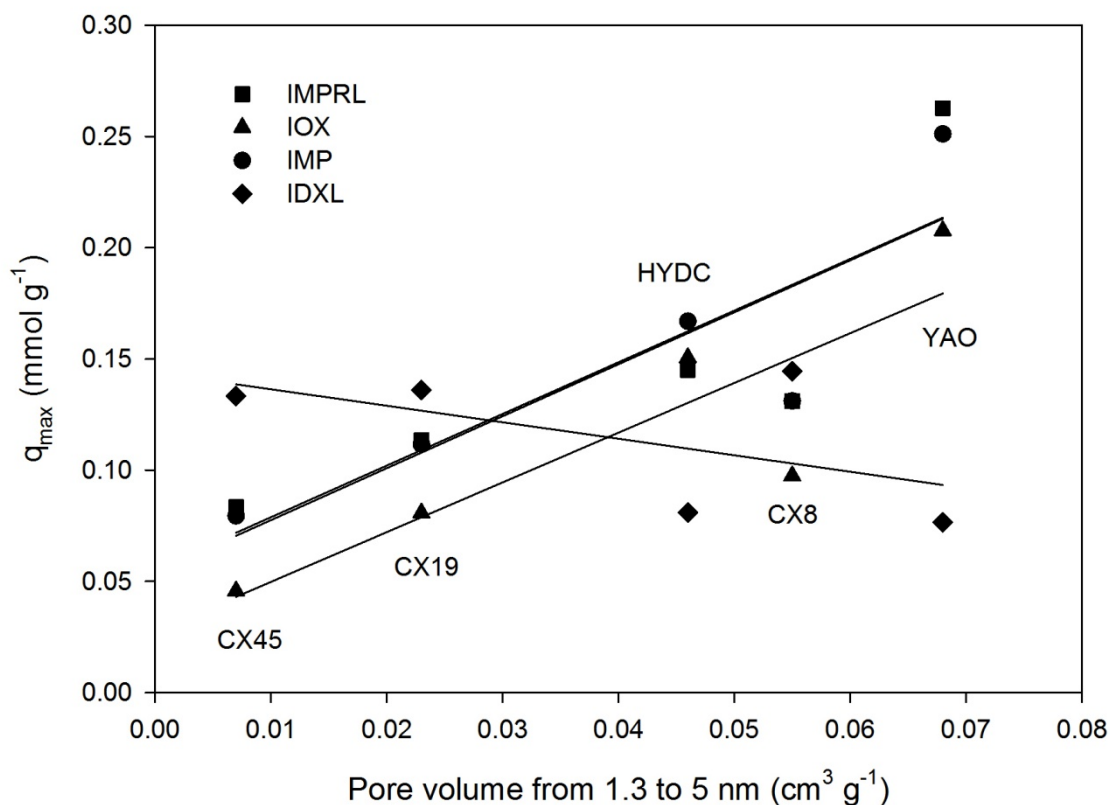
Figure 4.2.5 q_{max} of IMPRL, IOX, IMPL and IDXL vs pore volume from 1.3 to 5 nm (cm^3 g^{-1}) onto carbon xerogels and HYDC and YAO

3.5.3 Adsorption of IDXL

As can be seen in Fig. 4.2.5 and Table 4.2.7, there is a different tend on the adsorption of IDXL depending on the pore 1.3-5 nm. HYDC and YAO adsorbed less IDXL than the expected on this pores. It can suggest that the adsorption of IDXL can be produced in other pore diameters higher than 1.3 nm.

In order to observe where the adsorption of IDXL can take place on carbon xerogels, a new correlation was made between q_{max} of IDXL and the mesopore diameters (2 to 5 nm, 5 to 10 nm and 2 to 10 nm). The coefficient correlations obtained in these new cases were higher than 0.99 in the three different cases. It can suggest that adsorption of IDXL can take place on the pore between 2-10 nm

However, further work is required to confirm the hypothesis of the adsorption of IDXL and the rest of ICM are adsorbed on the pore from 1.3-5 for IOX, IPM, IMPRL and IPRD and 2-10 for IDXL.

3.6 Relation between hydrophobic properties of pharmaceuticals and ICM compounds with intensity of the Freundlich model

As Freundlich model is important on the adsorption of organic pollutants, we studied how hydrophobicity and hydrophilicity can affect on the different materials by means of the adsorption intensity (n). In this sense, the logkow of the different compounds were separated into three groups: hydrophilic or low hydrophobic (logkow<-0.5), moderate hydrophobic (-0.5<logkow<3.5) and highly hydrophobic (logkow>3.5). These hydrophobic groups were correlated with the 'n' values obtained from Freundlich model (Table SI 2.1). The results showed a high correlation between moderate hydrophobic compounds and n for all the adsorbents (Fig. 4.2.6). The n value decreased with the increase of the hydrophobocity; suggesting that the adsorption was more favorable with hydrophobic compounds.

In the case of hydrophilic compounds different trends are showed on carbon xerogels and on activated carbons. On the three carbon xerogels, a decrease of the hidrophilicity decreased the intensity value; suggesting that physical adsorption can be possible onto the mesopores. Moreover, the intensity values onto CX45 were lower than on carbon xerogels CX8 and CX19; it can suggest that higher mesopore can allow the access better and adsorb the voluminous onto mesopore of small diameter easily.

On the other hand, a decrease of hydrophilicity increased the intensity onto the different activated carbon. The intensity of IPRD, IPM and IMPRL increased suggesting that the adsorption was less favorable onto the micropores. In the case of IDXL, the intensity adsorption is lower onto the different commercial activated carbons as well as the quantity adsorbed respect of the other ICM, suggesting that adsorption take place more favorable in other pore diameters than micropore as the mesopore.
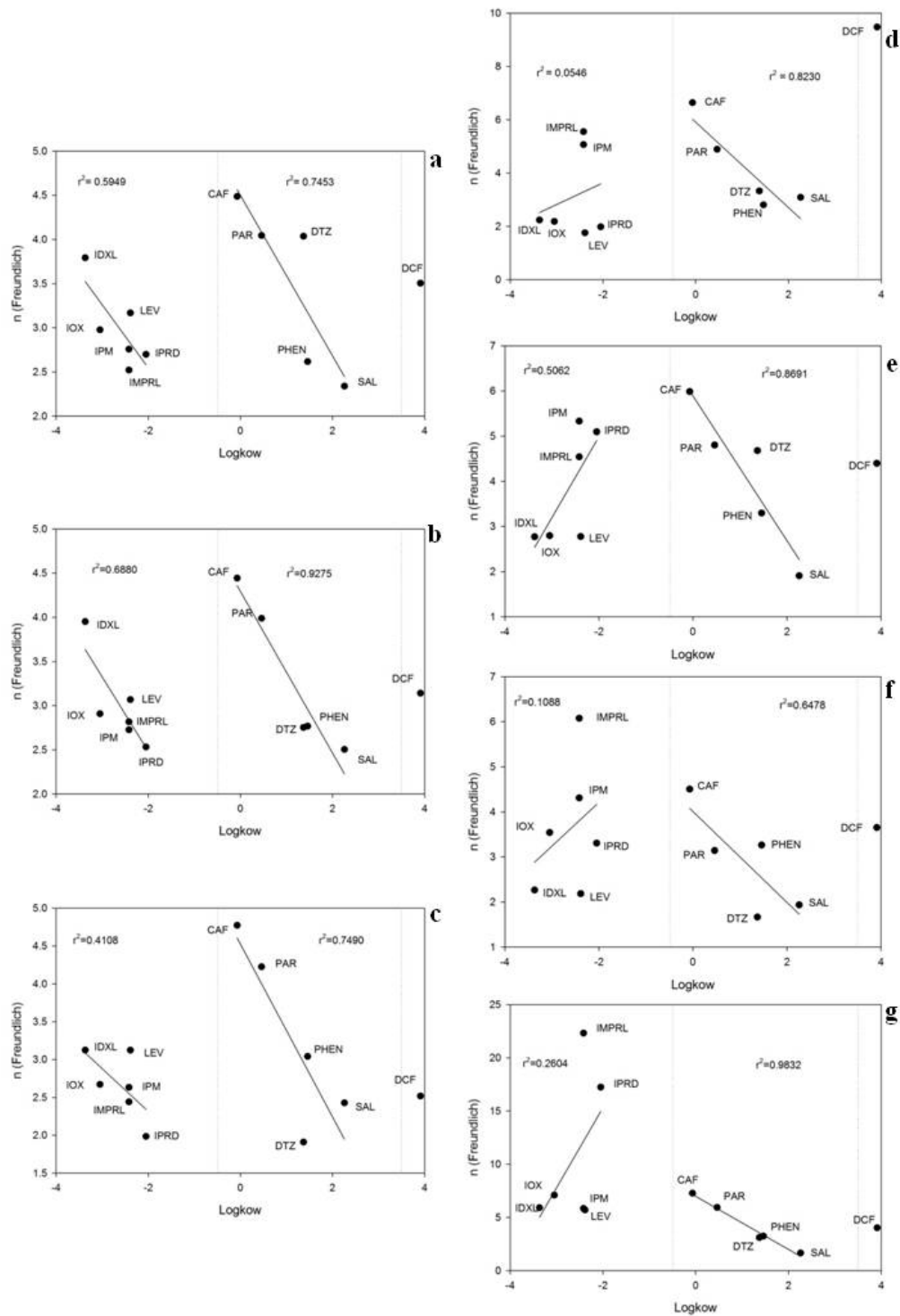
Figure 4.2.6 Correlation between n Freundlich and logkow on a)CX8, b)CX19, c) CX45, d)BAC, e)HYDC, f) ROW, g)YAO

3.7 Multiadsorption and influence of NOM

In order to investigate the effect of organic matter present in water on the adsorption process, competitive adsorption studies were carried out in ultrapure water (Mil·li Q

water) and water from Llobregat river (surface water). Both experiments were performed with solutions containing all the contaminants studied in this work

Table 4.2.8 shows the initial and final concentration (after adsorption experiment) as well as the % removal of all the contaminants in Mil·liQ water experiments. As can be seen, removal is always nearly 90% at low concentrations for all the pharmaceuticals and all the adsorbents. Moreover, at low concentrations, the adsorption of ICM were approximately 100% except on activated carbons BAC and ROW ($\approx$ 70%). It seems that the shape of BAC and ROW can complicate the entrance and the flow in of the ICM onto both activated carbons.

Table 4.2.8 Initial and final concentration and % removal of pharmaceutical and ICM compounds onto the different adsorbents in ultrapure water

		Ultrapure water						
		CX8	**CX19**	**CX45**	**BAC**	**HYDC**	**ROW**	**YAO**
Pharmaceuticals without ICM	Initial concentration (ng L^{-1})	142.1	142.1	142.1	142.1	142.1	142.1	142.1
	Final concentration (ng L^{-1})	3.8	17.1	14.2	13.5	15.6	10.9	10.2
	% removal	97.3	87.9	90.0	90.5	89.0	92.3	92.8
ICM	Initial concentration (ng L^{-1})	397.3	397.3	397.3	397.3	397.3	397.3	397.3
	Final concentration (ng L^{-1})	3.7	4.4	3.9	118.2	0.0	106.1	0.0
	% removal	99.1	98.9	99.0	70.3	100.0	73.3	100.0
Pharmaceuticals without ICM	Initial concentration (ng L^{-1})	1428.8	1428.8	1428.8	1428.8	1428.8	1428.8	1428.8
	Final concentration (ng L^{-1})	3.2	5.3	3.9	285.8	14.5	42.6	8.1
	% removal	99.8	99.6	99.7	80.0	99.0	97.0	99.4
ICM	Initial concentration (ng L^{-1})	4399.2	4399.2	4399.2	4399.2	4399.2	4399.2	4399.2
	Final concentration (ng L^{-1})	308.1	468.3	966.4	3297.2	7.8	1236.1	3.8
	% removal	93.0	89.4	78.0	25.0	99.8	71.9	99.9
Pharmaceuticals without ICM	Initial concentration (ng L^{-1})	13499.4	13499.4	13499.4	13499.4	13499.4	13499.4	13499.4
	Final concentration (ng L^{-1})	844.8	955.4	1095.9	6577.19	977.1	3911.1	71.1
	% removal	93.7	92.9	91.9	51.3	92.8	71.0	99.5
ICM	Initial concentration (ng L^{-1})	41505.1	41505.1	41505.1	41505.1	41505.1	41505.1	41505.1
	Final concentration (ng L^{-1})	29084.2	29907.5	31701.6	37658.2	25618.4	32494.0	29609.8
	% removal	29.9	27.9	23.6	9.3	38.3	21.7	28.7

At middle concentration, the adsorption of pharmaceuticals on carbon xerogels was practically completed while adsorption of ICM showed differences according the total

mesopore volume or pore diameter (93% for CX8, 89.4% for CX19 and 78% for CX45). It can suggest that ICM compete for the small mesopore due its high dimensions while pharmaceuticals can access to the micropore due to low dimensions respect ICM.

At higher concentrations the total pharmaceutical removed is reduced in a similar way on the three carbon xerogels, indicating that the total micropore can be saturated. While the amount of ICM adsorbed was reduced drastically according to the total mesopore or pore diameter. Respect YAO, the amount of pharmaceuticals adsorbed was practically completed while on HYDC was similar to the carbon xerogels ($\approx$ 93%) corroborating that total micropore can be saturated because HYDC and carbon xerogels show similar total micropore volume (Table 4.2.2). In the case of ICM, YAO shows a lower adsorption than HYDC, indicating that mesopore have an important role on the adsorption of these compounds.

As can be seen in Table SI 2.3, the presence of natural organic matter (NOM) reduces significantly the adsorption of the different compounds on practically all the adsorbents studied.

Fig. 4.2.7 shows the difference adsorbed between mil·liQ and surface water of DTZ, IMPRL, IPRD, IOX and IPM at middle concentrations in relation to the total mesopore volumes of carbon xerogels. High correlation coefficient values were obtained indicating that NOM compete directly with these four ICM for adsorption in the mesopore. Moreover, size, pKa and hidrophylic molecular properties can increase or decrease the adsorption on surface water. According to de Ridder et al. [7], NOM competes for available adsorption surface area and is influenced by charge interactions. NOM is negatively charged at neutral pH, and electrostatic repulsion can occur between NOM, activated carbon and organic compounds [8,51]. In this case, adsorption of DTZ was highly affected by the presence of negatively charged NOM. It could be due of the low pKa which at neutral pH solution DTZ is negatively charged. Thus electrostatic repulsion between adsorbed NOM and DTZ can be occurred. The rest of these ICM competed directly for active small mesopore site. Moreover, at this concentration, pharmaceuticals were practically removed on carbon xerogels. Thus the presence of NOM, not affected directly the adsorption on micropores.
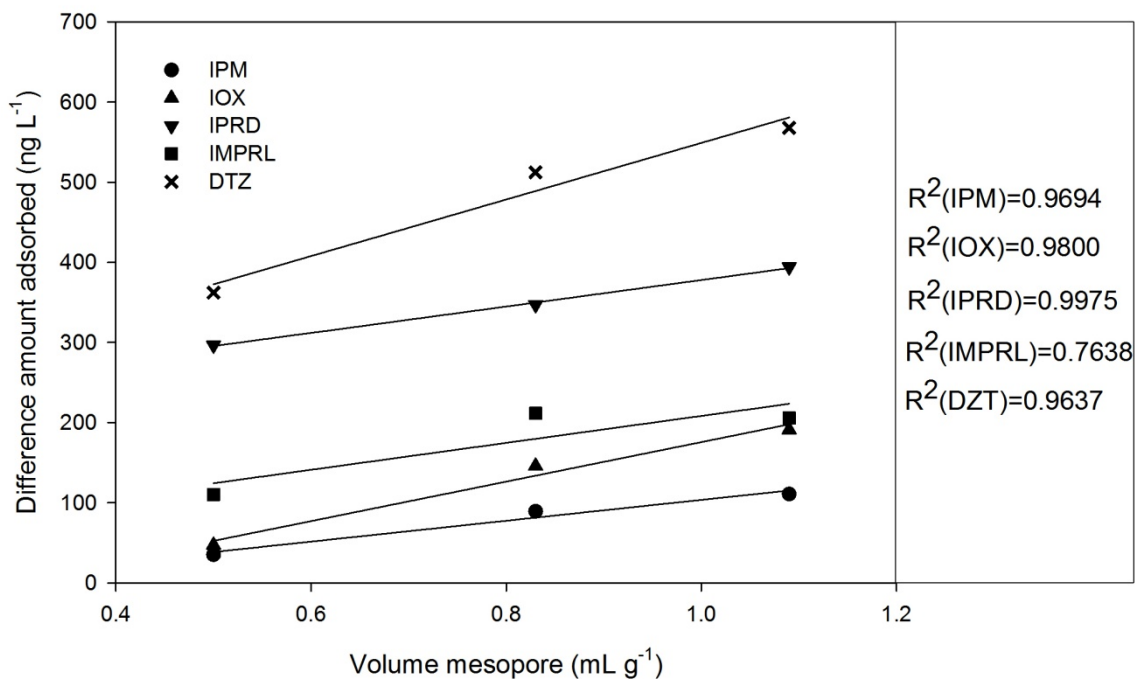
Figure 4.2.7 Different ICM adsorbed between Mil·li Q and surface water

At high concentration, the removal of ICM compounds were approximately a 15% on carbon xerogels (Fig SI 4f.), except iodixanol that the adsorption was higher than 70%. Moreover the presence of salicylic on the water was 50%, indicating electrostatic repulsions between high quantity of salicylates and negative charged NOM could be occurred. Moreover, the adsorption of the rest of pharmaceutical was higher than 65% indicating that carbon xerogels started to be exhausted.

4. Conclusions

The characterization of the three carbon xerogels (CX8, CX19 and CX45) showed a high mesoporous structure with a different mesopore diameter centered in 8, 19.5 and 45 nm respectively and a similar quantity of micropores (0.160 cm^3 g^{-1})They also present similar chemical composition around 97% of carbon content, 1% of oxygen, no ashes and a basic character. On the other hand, the commercial activated carbon, BAC, ROW and YAO, showed a high content of micropore while HYDC have mixture of micropore and mesopore and high ash content.

High correlation was observed on the adsorption of the different pharmaceutical, except diclofenac sodium with the ultramicropore and the total micropore volume of the

different carbon materials. In the case of phenol, salicylic acid and paracetamol similar volume of these molecules (approx. 0.105 cm^3 g^{-1}) were adsorbed onto the carbon xerogels suggested the similar micropore diameter.

The adsorption of the pharmaceuticals was related to their Dstokes values, the molecule dimensions and the hidrophobicity in the different adsorbents except onto HYDC which its high ash content made it a more hydrophilic activated carbon.

Different chemical interactions were observed between the adsorbates and the different adsorbents. Adsorption of salicylic acid was mainly due to electrostatic interactions and it was more adsorbed than phenol. Adsorption of phenol was affected by water which competed for the same adsorption sites. In reference the adsorption of caffeine and levodopa, it was expected that both molecules were adsorbed on the same sites, but the presence of acid groups can penalized the adsorption of levodopa onto the carbon xerogels and BAC and YAO which showed the less basic character. Diclofenac adsorption was produced on the wider micropore and on the mesopore.

The adsorption of ICM compounds was different on the carbon xerogels and on the commercial activated carbons. On carbon xerogels an increase of the ICM dimensions results in an increase on the adsorption while on commercial activated carbons were observed a decrease on the adsorption; suggesting the mesopore played an important role on the adsorption process.

Electrostatic interactions are responsible for the adsorption of DTZ due its acidic character. On the other hand the adsorption of IOX, IPM, IMPRL and IPRD can take place on the pore between 1.3-5 nm onto the different carbon materials, while the adsorption of IDXL can take place on pores between 2-10 nm in carbon xerogels.

The multi adsorption of ICM and pharmaceuticals on different solutions in ultrapure water and surface water showed different results. The pharmaceuticals were adsorbed on the total micropore, while ICM on the mesopore. At higher concentrations, the adsorption of ICM was drastically reduced onto the different carbon materials.

The presence of NOM on the multi solution compound affected the global adsorption of pharmaceuticals and ICM. In the case of ICM, both NOM and ICM compete for to be adsorbed onto the mesopores. Moreover, the adsorption of acidic compounds as

salicylic acid and DZT was affected by electrostatic interactions due to NOM can present negative charge.

Acknowledgements

References

[1] V. Osorio, R. Marcé, S. Pérez, A. Ginebreda, J.L. Cortina, D. Barceló, Occurrence and modeling of pharmaceuticals on a sewage-impacted Mediterranean river and their dynamics under different hydrological conditions., Sci. Total Environ. 440 (2012) 3–13.

[2] M. Gorga, S. Insa, M. Petrovic, D. Barceló, Occurrence and spatial distribution of EDCs and related compounds in waters and sediments of Iberian rivers., Sci. Total Environ. 503-504 (2015) 69–86.

[3] M. Kuster, M.J. López de Alda, M.D. Hernando, M. Petrovic, J. Martín-Alonso, D. Barceló, Analysis and occurrence of pharmaceuticals, estrogens, progestogens and polar pesticides in sewage treatment plant effluents, river water and drinking water in the Llobregat river basin (Barcelona, Spain), J. Hydrol. 358 (2008) 112–123.

[4] S. Pérez, D. Barceló, Fate and occurrence of X-ray contrast media in the environment., Anal. Bioanal. Chem. 387 (2007) 1235–46.

[5] B. Zonja, A. Delgado, S. Pérez, D. Barceló, LC-HRMS Suspect Screening for Detection-Based Prioritization of Iodinated Contrast Media Photodegradates in Surface Waters., Environ. Sci. Technol. 49 (2015) 3464–72.

[6] T. Ye, B. Xu, Z. Wang, T.-Y. Zhang, C.-Y. Hu, L. Lin, et al., Comparison of iodinated trihalomethanes formation during aqueous chlor(am)ination of different iodinated X-ray contrast media compounds in the presence of natural organic matter., Water Res. 66 (2014) 390–8.

[7] D.J. de Ridder, A.R.D. Verliefde, S.G.J. Heijman, J.Q.J.C. Verberk, L.C. Rietveld, L.T.J. van der Aa, et al., Influence of natural organic matter on equilibrium adsorption of neutral and charged pharmaceuticals onto activated carbon, Water Sci. Technol. 63 (2011) 416–423.

[8] M. Bjelopavlic, G. Newcombe, R. Hayes, Adsorption of NOM onto Activated Carbon: Effect of Surface Charge, Ionic Strength, and Pore Volume Distribution, J. Colloid Interface Sci. 210 (1999) 271–280.

[9] C. Pelekani, V.. Snoeyink, Competitive adsorption in natural water: role of activated carbon pore size, Water Res. 33 (1999) 1209–1219.

Section 4.1.2

[10] Q. Li, V.L. Snoeyink, C. Campos, B.J. Mariñas, Displacement Effect of NOM on Atrazine Adsorption by PACs with Different Pore Size Distributions, Environ. Sci. Technol. 36 (2002) 1510–1515.

[11] L. Kovalova, H. Siegrist, U. von Gunten, J. Eugster, M. Hagenbuch, A. Wittmer, et al., Elimination of Micropollutants during Post-Treatment of Hospital Wastewater with Powdered Activated Carbon, Ozone, and UV, Environ. Sci. Technol. 47 (2013) 7899–7908.

[12] S. Álvarez, R.S. Ribeiro, H.T. Gomes, J.L. Sotelo, J. García, Synthesis of carbon xerogels and their application in adsorption studies of caffeine and diclofenac as emerging contaminants, Chem. Eng. Res. Des. 95 (2015) 229–238.

[13] P.S. Fernández, A. Arenillas, E.G. Calvo, J.A. Menéndez, M.E. Martins, Carbon xerogels as electrochemical supercapacitors. Relation between impedance physicochemical parameters and electrochemical behaviour, Int. J. Hydrogen Energy. 37 (2012) 10249–10255.

[14] H.T. Gomes, P.V. Samant, P. Serp, P. Kalck, J.L. Figueiredo, J.L. Faria, Carbon nanotubes and xerogels as supports of well-dispersed Pt catalysts for environmental applications, Appl. Catal. B Environ. 54 (2004) 175–182.

[15] E.G. Calvo, J.A. Menéndez, A. Arenillas, Designing Nanostructured Carbon Xerogels, in: M. Rahman (Ed.), Nanomaterials, InTech, 2011.

[16] S.A.C. Carabineiro, T. Thavorn-Amornsri, M.F.R. Pereira, J.L. Figueiredo, Adsorption of ciprofloxacin on surface-modified carbon materials., Water Res. 45 (2011) 4583–91.

[17] S.A.C. Carabineiro, T. Thavorn-amornsri, M.F.R. Pereira, P. Serp, J.L. Figueiredo, Comparison between activated carbon, carbon xerogel and carbon nanotubes for the adsorption of the antibiotic ciprofloxacin, Catal. Today. 186 (2012) 29–34.

[18] N. Rey-Raap, J. Angel Menéndez, A. Arenillas, Simultaneous adjustment of the main chemical variables to fine-tune the porosity of carbon xerogels, Carbon N. Y. 78 (2014) 490–499.

[19] N. Rey-Raap, J. Angel Menéndez, A. Arenillas, RF xerogels with tailored porosity over the entire nanoscale, Microporous Mesoporous Mater. 195 (2014) 266–275.

[20] A.H. Moreno, A. Arenillas, E.G. Calvo, J.M. Bermúdez, J.A. Menéndez, Carbonisation of resorcinol–formaldehyde organic xerogels: Effect of temperature,

particle size and heating rate on the porosity of carbon xerogels, J. Anal. Appl. Pyrolysis. 100 (2013) 111–116.

[21] B.S. Bolton E, Wang Y, Thiessen PA, PubChem: Integrated Platform of Small Molecules and Biological Activities, in: American Chemical Society (Ed.), Annu. Reports Comput. Chem. V4, Elsevier B.V., Washington, DC, 2008.

[22] S.-W. Nam, D.-J. Choi, S.-K. Kim, N. Her, K.-D. Zoh, Adsorption characteristics of selected hydrophilic and hydrophobic micropollutants in water using activated carbon, J. Hazard. Mater. 270 (2014) 144–152.

[23] D.J. de Ridder, J.Q.J.C. Verberk, S.G.J. Heijman, G.L. Amy, J.C. van Dijk, Zeolites for nitrosamine and pharmaceutical removal from demineralised and surface water: Mechanisms and efficacy, Sep. Purif. Technol. 89 (2012) 71–77.

[24] J. Lladó, C. Lao-Luque, B. Ruiz, E. Fuente, M. Solé-Sardans, A.D. Dorado, Role of activated carbon properties in atrazine and paracetamol adsorption equilibrium and kinetics, Process Saf. Environ. Prot. (2015).

[25] A. Mendoza, J. Aceña, S. Pérez, M. López de Alda, D. Barceló, A. Gil, et al., Pharmaceuticals and iodinated contrast media in a hospital wastewater: A case study to analyse their presence and characterise their environmental risk and hazard., Environ. Res. 140 (2015) 225–41.

[26] M.A. Montes-Morán, D. Suárez, J. Angel Menéndez, E. Fuente, The Basicity of Carbons, in: J.M.. Tascón (Ed.), Nov. Carbon Adsorbents, Elsevier, 2012: pp. 173–203.

[27] J.A. Menendez-Diaz, I. Martín-Gullón, Types of carbon adsorbents and their production, in: T.J. Bandosz (Ed.), Act. Carbon Surfaces Environ. Remediat., first, Elsevier, New York, 2006: pp. 1–47.

[28] S. Brunauer, L.S. Deming, W.E. Deming, E. Teller, On a theory of the vander Waals adsorption of gases, J. Am. Chem. Soc. 62 (1940) 1723–1732.

[29] K.S.W. Sing, Reporting physisorption data for gas/solid systems with special reference to the determination of surface area and porosity (Provisional), Pure Appl. Chem. 54 (1982).

Section 4.1.2

[30] C. Namasivayam, S. Senthilkumar, Removal of Arsenic(V) from Aqueous Solution Using Industrial Solid Waste: Adsorption Rates and Equilibrium Studies, Ind. Eng. Chem. Res. 37 (1998) 4816–4822.

[31] E.L.K. Mui, W.H. Cheung, M. Valix, G. McKay, Dye adsorption onto activated carbons from tyre rubber waste using surface coverage analysis, J. Colloid Interface Sci. 347 (2010) 290–300.

[32] C. Moreno-Castilla, Adsorption of organic molecules from aqueous solutions on carbon materials, Carbon N. Y. 42 (2004) 83–94.

[33] D.J. de Ridder, L. Villacorte, a R.D. Verliefde, J.Q.J.C. Verberk, S.G.J. Heijman, G.L. Amy, et al., Modeling equilibrium adsorption of organic micropollutants onto activated carbon., Water Res. 44 (2010) 3077–86.

[34] L.M. Cotoruelo, M.D. Marqués, a. Leiva, J. Rodríguez-Mirasol, T. Cordero, Adsorption of oxygen-containing aromatics used in petrochemical, pharmaceutical and food industries by means of lignin based active carbons, Adsorption. 17 (2011) 539–550.

[35] E. Ayranci, O. Duman, Adsorption of aromatic organic acids onto high area activated carbon cloth in relation to wastewater purification., J. Hazard. Mater. 136 (2006) 542–52.

[36] E. Lorenc-Grabowska, G. Gryglewicz, M.A. Diez, Kinetics and equilibrium study of phenol adsorption on nitrogen-enriched activated carbons, Fuel. 114 (2013) 235–243.

[37] M. Franz, H.A. Arafat, N.G. Pinto, Effect of chemical surface heterogeneity on the adsorption mechanism of dissolved aromatics on activated carbon, Carbon N. Y. 38 (2000) 1807–1819.

[38] T.J. Bandosz, C.O. Ania, Surface chemistry of activated carbons and its characterization, in: T.J. Bandosz (Ed.), Act. Carbon Surfaces Environ. Remediat., Elsevier, New York, 2006: pp. 159–229.

[39] M. Galhetas, A.S. Mestre, M.L. Pinto, I. Gulyurtlu, H. Lopes, A.P. Carvalho, Chars from gasification of coal and pine activated with K2CO3: acetaminophen and caffeine adsorption from aqueous solutions., J. Colloid Interface Sci. 433 (2014) 94–103.

[40] M. Galhetas, A.S. Mestre, M.L. Pinto, I. Gulyurtlu, H. Lopes, A.P. Carvalho, Carbon-based materials prepared from pine gasification residues for acetaminophen adsorption, Chem. Eng. J. 240 (2014) 344–351.

[41] B. Ruiz, I. Cabrita, A.S. Mestre, J.B. Parra, J. Pires, A.P. Carvalho, et al., Surface heterogeneity effects of activated carbons on the kinetics of paracetamol removal from aqueous solution, Appl. Surf. Sci. 256 (2010) 5171–5175.

[42] A.P. Terzyk, Molecular properties and intermolecular forces--factors balancing the effect of carbon surface chemistry in adsorption of organics from dilute aqueous solutions., J. Colloid Interface Sci. 275 (2004) 9–29.

[43] I. Villaescusa, N. Fiol, J. Poch, A. Bianchi, C. Bazzicalupi, Mechanism of paracetamol removal by vegetable wastes: The contribution of pi-pi interactions, hydrogen bonding and hydrophobic effect, Desalination. 270 (2011) 135–142.

[44] E.F. Mohamed, C. Andriantsiferana, A.M. Wilhelm, H. Delmas, Competitive adsorption of phenolic compounds from aqueous solution using sludge-based activated carbon, Environ. Technol. 32 (2011) 1325–1336.

[45] I. Quesada-Penate, C. Julcour-Lebigue, U.-J. Jauregui-Haza, A.-M. Wilhelm, H. Delmas, Comparative adsorption of levodopa from aqueous solution on different activated carbons, Chem. Eng. J. 152 (2009).

[46] S.Á. Torrellas, R. García Lovera, N. Escalona, C. Sepúlveda, J.L. Sotelo, J. García, Chemical-activated carbons from peach stones for the adsorption of emerging contaminants in aqueous solutions, Chem. Eng. J. 279 (2015) 788–798.

[47] J.L. Sotelo, A. Rodriguez, S. Alvarez, J. Garcia, Removal of caffeine and diclofenac on activated carbon in fixed bed column, Chem. Eng. Res. Des. 90 (2012).

[48] E.-E. Chang, J.-C. Wan, H. Kim, C.-H. Liang, Y.-D. Dai, P.-C. Chiang, Adsorption of Selected Pharmaceutical Compounds onto Activated Carbon in Dilute Aqueous Solutions Exemplified by Acetaminophen, Diclofenac, and Sulfamethoxazole., ScientificWorldJournal. (2015) 186501.

Section 4.1.2

[49] A.S. Mestre, M. Machuqueiro, M. Silva, R. Freire, I.M. Fonseca, M.S.C.S. Santos, et al., Influence of activated carbons porous structure on iopamidol adsorption, Carbon N. Y. 77 (2014) 607–615.

[50] A.S. Mestre, R.A. Pires, I. Aroso, E.M. Fernandes, M.L. Pinto, R.L. Reis, et al., Activated carbons prepared from industrial pre-treated cork: Sustainable adsorbents for pharmaceutical compounds removal, Chem. Eng. J. 253 (2014) 408–417.

[51] G. Newcombe, M. Drikas, Adsorption of NOM onto activated carbon: Electrostatic and non-electrostatic effects, Carbon N. Y. 35 (1997) 1239–1250.

Supporting Information

Removal of pharmaceuticals and Iodinated Contrast Media (ICM) compounds on carbon xerogels and activated carbons. NOM and textural properties influences.

J. Lladó[1*], B. Ruiz[2],J. Aceña[3], C. Lao-Luque[1], M.Solé-Sardans[1], S. Pérez[3], D. Barceló[3], E. Fuente[2]

[1]*Department of Mining, Industrial and TIC Engineering (EMIT).* Universitat Politécnica de Catalunya. Bases de Manresa 61-73, 08242 Manresa, Spain.

[2]*"Biocarbon & Sustainability".* Instituto Nacional del Carbón (INCAR-CSIC), Francisco Pintado Fe, 26, 33011 Oviedo, Spain.

[3]*Department of Environmental Chemistry.* Instituto de Diagnóstico Ambiental y Estudios del Agua (IDAEA-CSIC), Barcelona, Spain

*Corresponding author/Email: jordi.llado@emrn.upc.edu

Figure SI 4.2.1 Nitrogen adsorption isotherms a) commercial activated carbon, b) Carbon Xerogels
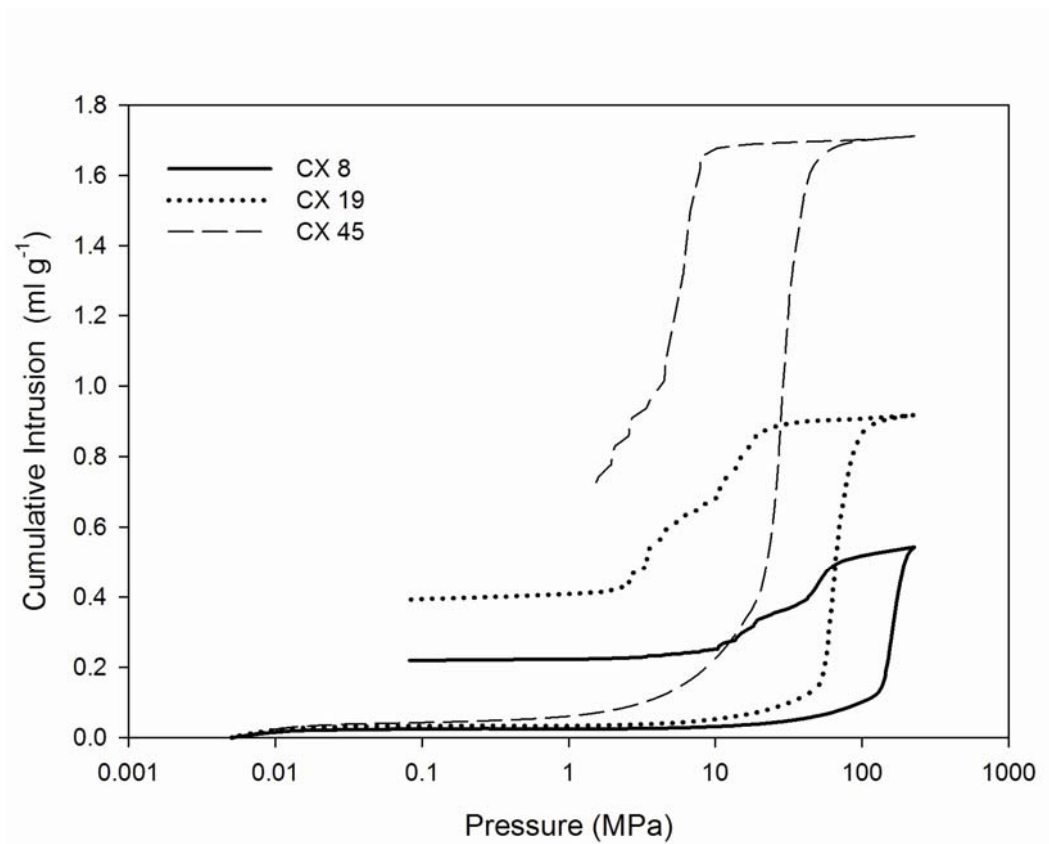
Figure SI 4.2.2 Cumulative intrusion on carbon xerogels

Table SI 4.2.1 Mercury porosimetry density, mesopore volume, macropore volume, total pore, average pore diameter

	Density (at 0.005 Mpa)	Density (at 0.1013 Mpa)	Density (at 228 Mpa)	Mesopores (5.5-50 nm) Vol intrus Hg (cm³ g⁻¹)	Macropore (50-250000 nm) Vol intrus Hg (cm³ g⁻¹)	Total pore (5.5-250000 nm) Vol intrus Hg (cm³ g⁻¹)	Porosity (%)	Average pore diameter (4V/A) (nm)
CX8	0.76	0.78	1.30	0.50	0.04	0.54	41.5	8.8
CX19	0.58	0.59	1.25	0.83	0.08	0.92	53.4	19.3
CX45	0.40	0.41	1.28	1.09	0.63	1.71	68.6	45.6
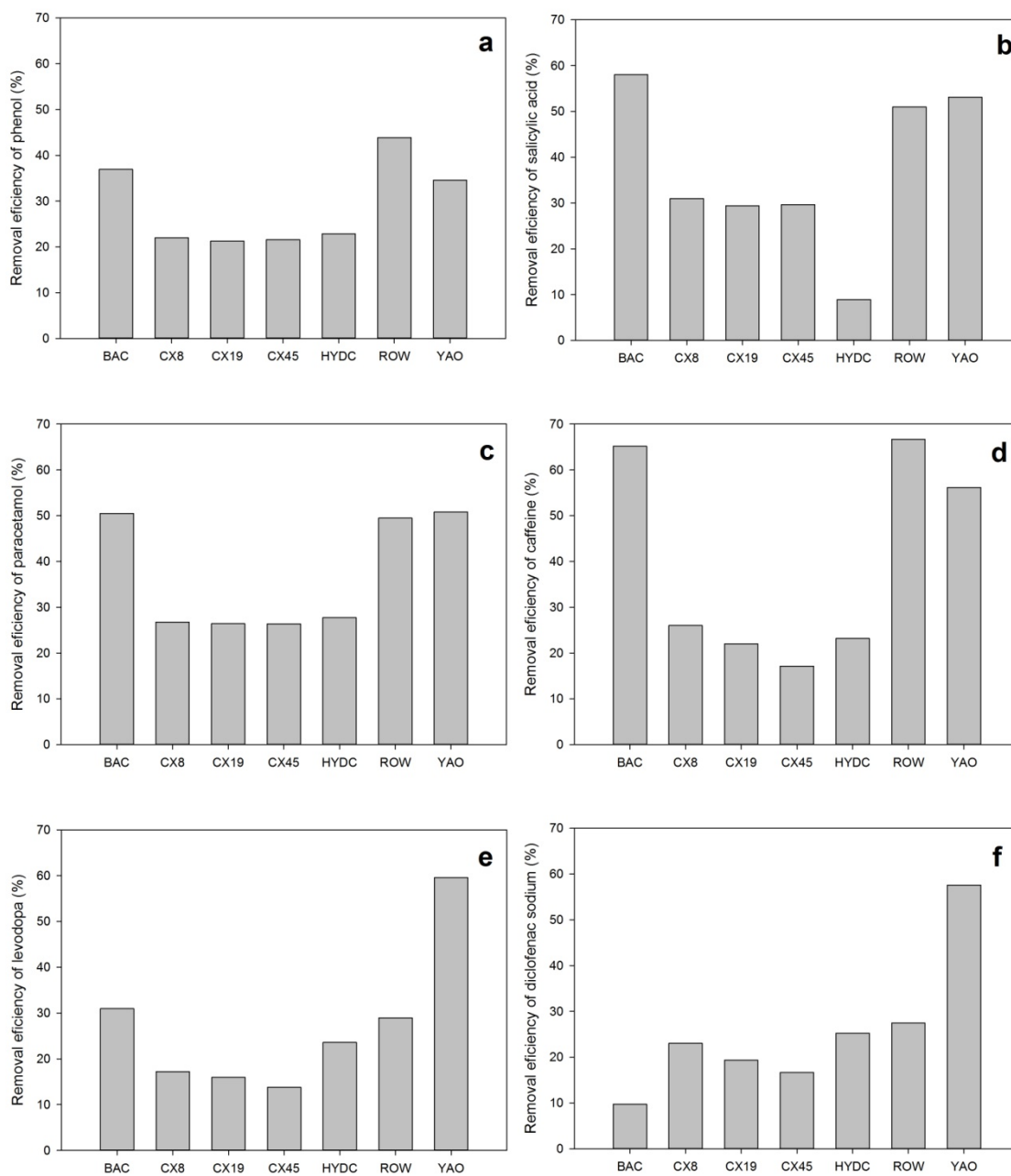
Figure SI 4.2.3 Removal efficiency for pharmaceuticals on the adsorbents assayed a)phenol, b) salicylic acid, c) paracetamol, d) caffeine, e) levodopa and f) doclofenac sodium
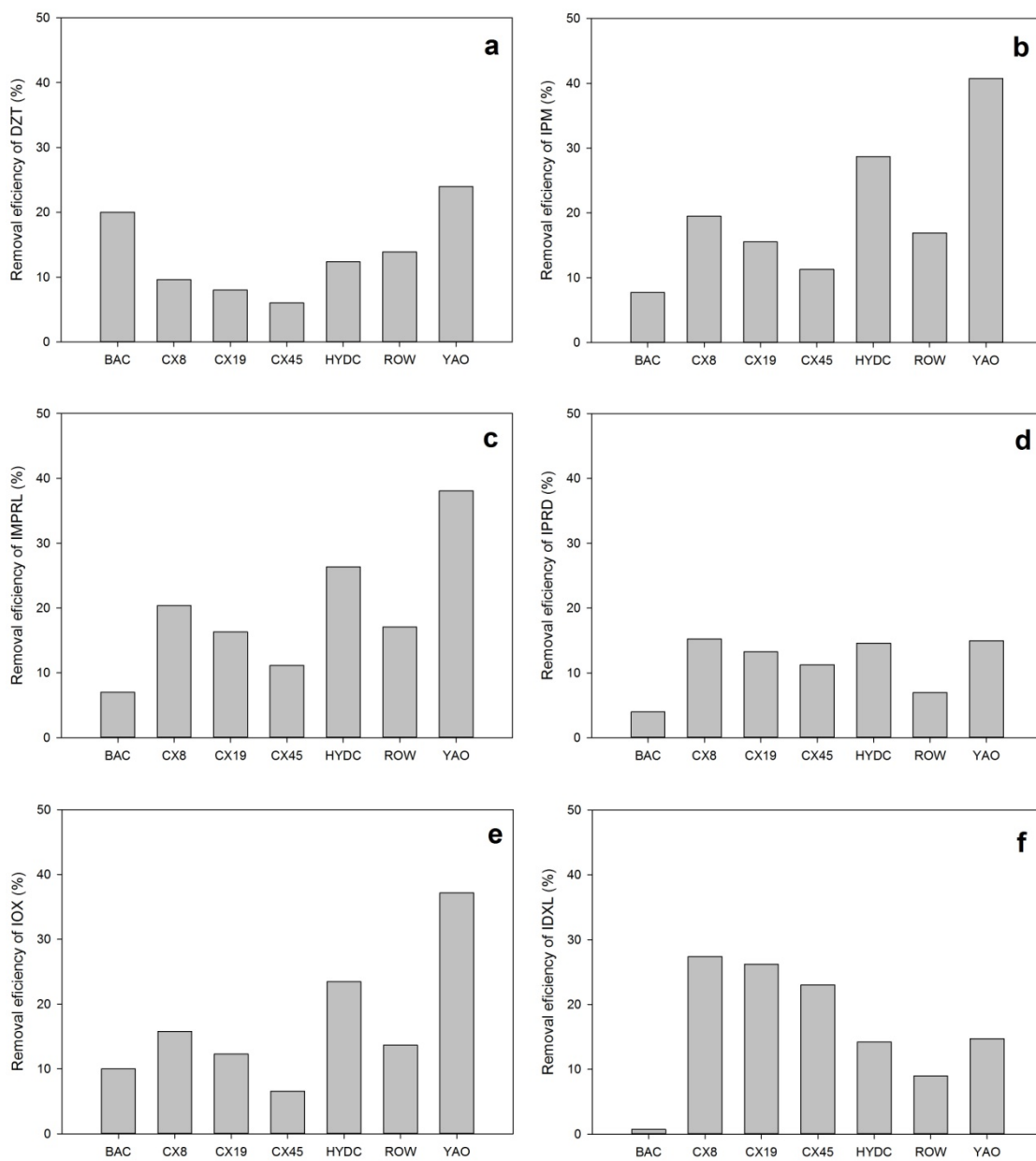
Figure SI 4.2.4 Removal efficiency for ICM on the adsorbents assayed a)DTZ, b) IPM, c) IMPRL, d) IPRD, e) IOX and f) IDXL
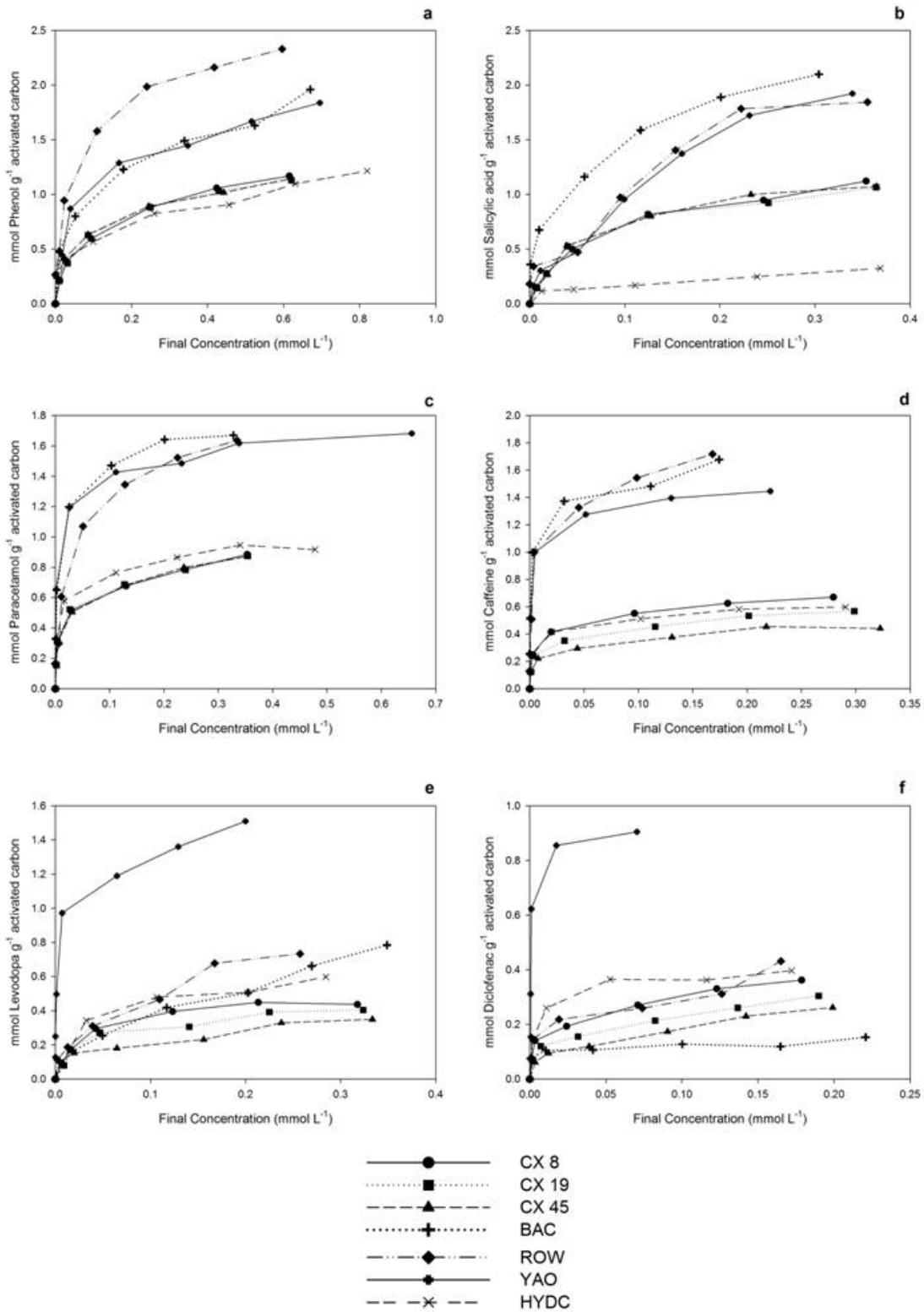
Figure SI 4.2.5 Pharmacautical adsorption isotherms a) Phenol, b) Salicylic acid, c) Paracetamol, d) Caffeine, e) Levodopa, f) Diclofenac onto the different adsorbents
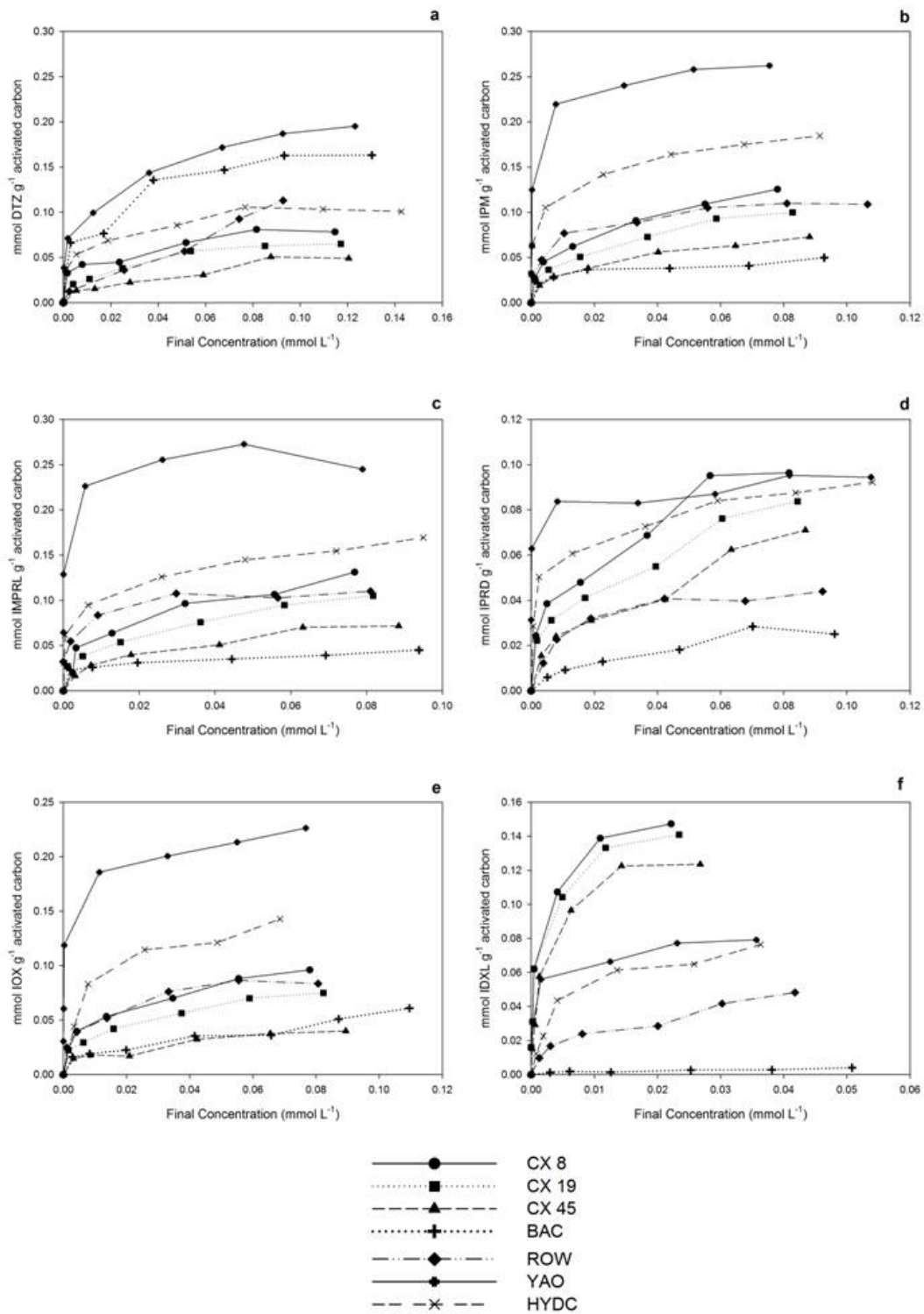
Figure SI 4.2.6 Pharmaceutical adsorption isotherms a) DTZ, b) IPML, c) IMPRL, d) IPRD, e) HSTZ, f) IDXL onto the different adsorbents

Table SI 4.2.2 Pharmaceutical and IDM isotherm parameters on BAC

		Langmuir			Freundlich		
		q_{max}*	K_L*	OF	K_F*	n	OF
BAC	Cafeine	1.5158	1084.2	0.3878	2.1757	6.6422	0.3529
	Diclofenac	0.1243	2236.3	0.037	0.1613	9.4794	0.0235
	DZT	0.1699	102.437	0.0446	0.3206	3.3298	0.0299
	HSTZ	0.0732	25.2487	0.0179	0.1532	2.1827	0.0118
	IDXL	0.0045	66.0389	0.0013	0.0138	2.2393	0.0009
	IMPRL	0.039	488.0968	0.0107	0.0647	5.5537	0.0042
	IMPL	0.0446	321.7309	0.0088	0.0749	5.0669	0.0059
	IPRD	0.0371	27.002	0.0055	0.0908	1.9825	0.0056
	Levodopa	1.1516	5.0622	0.1244	1.3856	1.7583	0.0634
	Paracetamol	1.5839	267.161	0.3105	2.2401	4.894	0.3009
	Phenol	1.9234	13.9373	0.383	2.1885	2.8073	0.1802
	Salicylic acid	2.5511	24.237	0.4871	3.1144	3.0893	0.2173

*q_{max} (mmol g^{-1}); K_L (L mg^{-1}); Kf (mmol g^{-1})(L mmol^{-1})$^{1/n}$

Table SI 4.2.3 Pharmaceutical and IDM isotherm parameters on CX8

		Langmuir			Freundlich		
		q_{max}*	K_L*	OF	K_F*	n	OF
CX8	Cafeine	0.6068	283.6648	0.1491	0.913	4.4869	0.0913
	Diclofenac	0.3316	135.4664	0.0936	0.59	3.5051	0.0299
	DZT	0.0763	181.3542	0.0257	0.013	4.0365	0.013
	HSTZ	0.0974	126.0774	0.0178	0.2268	2.9774	0.0057
	IDXL	0.1445	1351.4	0.0249	0.4278	3.7929	0.0271
	IMPRL	0.1382	83.6012	0.0241	0.3561	2.5224	0.0187
	IMPL	0.131	94.584	0.024	0.3134	2.7579	0.0047
	IPRD	0.1074	76.4415	0.0237	0.2502	2.7000	0.0124
	Levodopa	0.4908	34.9972	0.0216	0.6948	3.1690	0.0917
	Paracetamol	0.7988	123.4878	0.1879	1.1393	4.0449	0.0731
	Phenol	1.2776	11.2035	0.1396	1.4467	2.6179	0.072
	Salicylic acid	1.2769	14.6968	0.087	1.7808	2.3399	0.1185

*q_{max} (mmol g^{-1}); K_L (L mg^{-1}); Kf (mmol g^{-1})(L mmol^{-1})$^{1/n}$

Table SI 4.2.4 Pharmaceutical and IDM isotherm parameters on CX19

		Langmuir			Freundlich		
		q_{max}*	K_L*	OF	K_F*	n	OF
CX19	Cafeine	0.5064	237.8227	0.1325	0.7523	4.4440	0.0532
	Diclofenac	0.2859	67.7961	0.0759	0.4971	3.1422	0.0259
	DZT	0.0757	52.382	0.0089	0.15	2.7539	0.0073
	HSTZ	0.0807	88.3012	0.0152	0.1785	2.9086	0.0047
	IDXL	0.1361	1573.9	0.0274	0.3849	3.9522	0.027
	IMPRL	0.1134	78.9656	0.0235	0.2536	2.8172	0.0069
	IMPL	0.1116	70.1287	0.0219	0.2511	2.7281	0.0079
	IPRD	0.0937	58.4088	0.0198	0.219	2.5331	0.009
	Levodopa	0.4256	33.5907	0.0582	0.6089	3.0690	0.0768
	Paracetamol	0.7946	110.6908	0.1657	1.1432	3.9897	0.1234
	Phenol	1.219	13.0181	0.0972	1.3882	2.7682	0.1013
	Salicylic acid	1.1764	18.5207	0.0677	1.6456	2.5055	0.1678

*q_{max} (mmol g^{-1}); K_L (L mg^{-1}); Kf (mmol g^{-1})(L mmol^{-1})$^{1/n}$

Table SI 4.2.5 Pharmaceutical and IDM isotherm parameters on CX45

		Langmuir			Freundlich		
		q_{max}*	K_L*	OF	K_F*	n	OF
CX45	Cafeine	0.4207	143.9423	0.1214	0.5841	4.7731	0.039
	Diclofenac	0.2912	24.325	0.0628	0.4848	2.5187	0.0261
	DZT	0.0738	17.4211	0.0118	0.1558	1.9109	0.0096
	HSTZ	0.0457	58.1628	0.0115	0.0998	2.6717	0.0076
	IDXL	0.1332	529.4413	0.0115	0.4342	3.1254	0.0256
	IMPRL	0.0834	57.5981	0.0112	0.2005	2.4419	0.0076
	IMPL	0.0794	67.7967	0.0108	0.1822	2.6333	0.0032
	IPRD	0.0943	27.9344	0.0158	0.2374	1.9851	0.0097
	Levodopa	0.3417	31.1048	0.1057	0.4835	3.1247	0.0531
	Paracetamol	0.7983	109.4788	0.2164	1.1191	4.2265	0.0257
	Phenol	1.2615	17.9819	0.1527	1.3591	3.0241	0.0879
	Salicylic acid	1.2387	16.7301	0.0698	1.7325	2.4292	0.168

*q_{max} (mmol g^{-1}); K_L (L mg^{-1}); Kf (mmol g^{-1})(L mmol^{-1})$^{1/n}$

Table SI 4.2.6 Pharmaceutical and IDM isotherm parameters on HYDC

		Langmuir			Freundlich		
		q_{max}*	K_L*	OF	K_F*	N	OF
HYDC	Cafeine	0.559	312.3777	0.1605	0.7521	5.9876	0.1313
	Diclofenac	0.3866	252.9113	0.0381	0.6221	4.3984	0.083
	DZT	0.1018	223.1087	0.0266	0.1645	4.6803	0.0134
	HSTZ	0.1506	130.5217	0.0147	0.3796	2.7973	0.028
	IDXL	0.081	236.3704	0.0075	0.2578	2.7715	0.0141
	IMPRL	0.1451	1161.7	0.0479	0.2817	4.5422	0.016
	IMPL	0.1669	855.1358	0.059	0.2904	5.3336	0.0323
	IPRD	0.084	583.6246	0.0202	0.1433	5.0966	0.0085
	Levodopa	0.633	30.3402	0.0594	0.9581	2.7779	0.1107
	Paracetamol	0.8887	173.0516	0.1544	1.1556	4.8036	0.167
	Phenol	1.2264	10.4014	0.3394	1.2377	3.297	0.132
	Salicylic acid	0.696	2.9406	0.1262	0.5973	1.9082	0.0899

*q_{max} (mmol g^{-1}); K_L (L mg^{-1}); Kf (mmol g^{-1})(L mmol^{-1})$^{1/n}$

Table SI 4.2.7 Pharmaceutical and IDM isotherm parameters on ROW 0.8

		Langmuir			Freundlich		
		q_{max}*	K_L*	OF	K_F*	n	OF
ROW 0.8	Cafeine	1.5925	364.1662	0.3254	2.6012	4.5067	0.3406
	Diclofenac	0.3354	240.5708	0.138	0.6143	3.6553	0.0864
	DZT	0.1577	11.6298	0.0086	0.3429	1.6683	0.004
	HSTZ	0.0891	174.2544	0.0164	0.1836	3.5427	0.011
	IDXL	0.0538	103.5837	0.0104	0.1893	2.2674	0.0061
	IMPRL	0.1102	471.2005	0.0335	0.1722	6.078	0.0354
	IMPL	0.1097	254.4807	0.019	0.1948	4.3116	0.0147
	IPRD	0.0478	105.1414	0.0034	0.0944	3.3076	0.0084
	Levodopa	0.9413	12.6051	0.1369	1.3988	2.1863	0.081
	Paracetamol	1.6948	38.3985	0.2238	2.4385	3.1436	0.3059
	Phenol	2.3904	23.1436	0.3346	2.8571	3.2658	0.4139
	Salicylic acid	2.6244	5.3308	0.4264	3.4015	1.9368	0.4525

*q_{max} (mmol g^{-1}); K_L (L mg^{-1}); Kf (mmol g^{-1})(L mmol^{-1})$^{1/n}$

Table SI 4.2.8 Pharmaceutical and IDM isotherm parameters on YAO

		Langmuir			Freundlich		
		q_{max}*	K_L*	OF	K_F*	n	OF
YAO	Cafeine	1.3529	1134.7	0.3533	1.8465	7.2807	0.3349
	Diclofenac	0.9296	490.2541	0.1562	1.9427	4.0226	0.2651
	DZT	0.2491	57.7486	0.075	0.4552	3.1158	0.0436
	HSTZ	0.2077	6066.9	0.0418	0.3278	7.0935	0.0439
	IDXL	0.0765	1784.9	0.018	0.1426	5.9147	0.0195
	IMPRL	0.2627	1122	0.1488	0.2932	22.3205	0.1495
	IMPL	0.2511	2108.4	0.0581	0.4307	5.8477	0.0667
	IPRD	0.0889	1828.1	0.0333	0.1062	17.2397	0.0324
	Levodopa	1.3773	415.2745	0.3559	1.9817	5.7032	0.3337
	Paracetamol	1.5247	464.6646	0.3439	1.9208	5.9376	0.3517
	Phenol	1.8278	18.4526	0.3574	2.0642	3.2482	0.3457
	Salicylic acid	2.6810	4.1433	0.2412	3.8733	1.6623	0.2499

*q_{max} (mmol g^{-1}); K_L (L mg^{-1}); Kf (mmol g^{-1})(L mmol^{-1})$^{1/n}$

Table SI 4.2.9 Pore volume in different pore diameter sections

	Pore volume ($cm^3\ g^{-1}$)			
	1.3-5(nm)	2-5 (nm)	5-10 (nm)	2-10 (nm)
CX8	0.055	0.042	0.194	0.236
CX19	0.023	0.014	0.047	0.061
CX45	0.007	0.000	0.007	0.007
BAC	0.138	0.020	0.000	0.020
HYDC	0.046	0.030	0.034	0.064
ROW	0.136	0.023	0.002	0.025
YAO	0.068	0.009	0.004	0.013

Table SI 4.2.10 Initial and final concentration and % removal of pharmaceutical and ICM compounds onto the different adsorbents in surfare water

		Surface water						
		CX8	CX19	CX45	BAC	HYDC	ROW	YAO
Pharmaceuticals	Initial load (ng L^{-1})	152.6	152.6	152.6	152.6	152.6	152.6	152.6
	final load (ng L^{-1})	28.8	28.8	27.9	58.5	21.7	22.0	30.0
	% removal	81.1	81.1	81.7	61.7	85.8	85.6	80.4
ICM	Initial load (ng L^{-1})	439.5	439.5	439.5	439.5	439.5	439.5	439.5
	final load (ng L^{-1})	5.8	19.7	20.7	322.8	0.2	49.7	6.4
	% removal	98.7	95.5	95.3	26.5	100.0	88.7	98.5
Pharmaceuticals	Initial load (ng L^{-1})	1429.8	1429.8	1429.8	1429.8	1429.8	1429.8	1429.8
	final load (ng L^{-1})	31.2	40.2	37.0	477.4	30.1	90.5	30.9
	% removal	97.8	97.2	97.4	66.6	97.9	93.7	97.8
ICM	Initial load (ng L^{-1})	4395.6	4395.6	4395.6	4395.6	4395.6	4395.6	4395.6
	final load (ng L^{-1})	448.7	1063.4	1725.2	3373.2	51.8	1649.6	13.3
	% removal	89.8	75.8	60.8	23.3	98.8	62.5	99.7
Pharmaceuticals	Initial load (ng L^{-1})	13494.4	13494.4	13494.4				
	final load (ng L^{-1})	1825.6	2190.8	2931.8				
	% removal	86.5	83.8	78.3				
ICM	Initial load (ng L^{-1})	35098.9	35098.9	35098.9				
	final load (ng L^{-1})	27091.8	29170.3	29808.5				
	% removal	22.7	16.8	15.0				
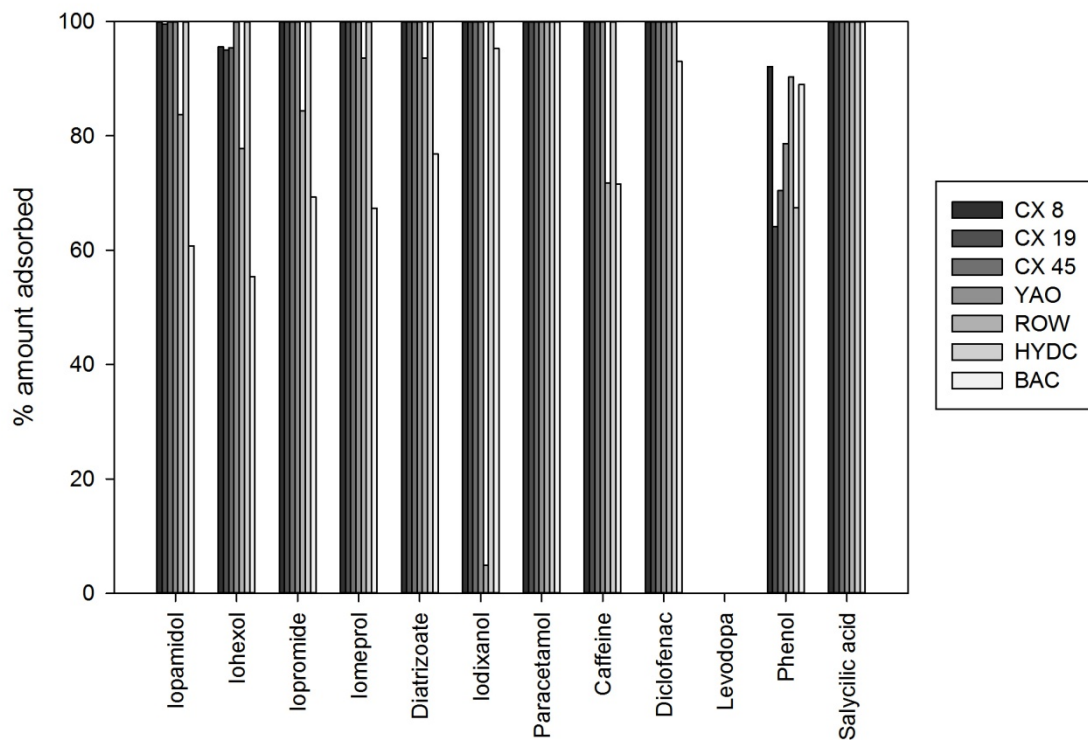
Figure SI 4.2.7 Multiadosrption of pharmaceuticals and ICM at 100 nmols mil·li Q water
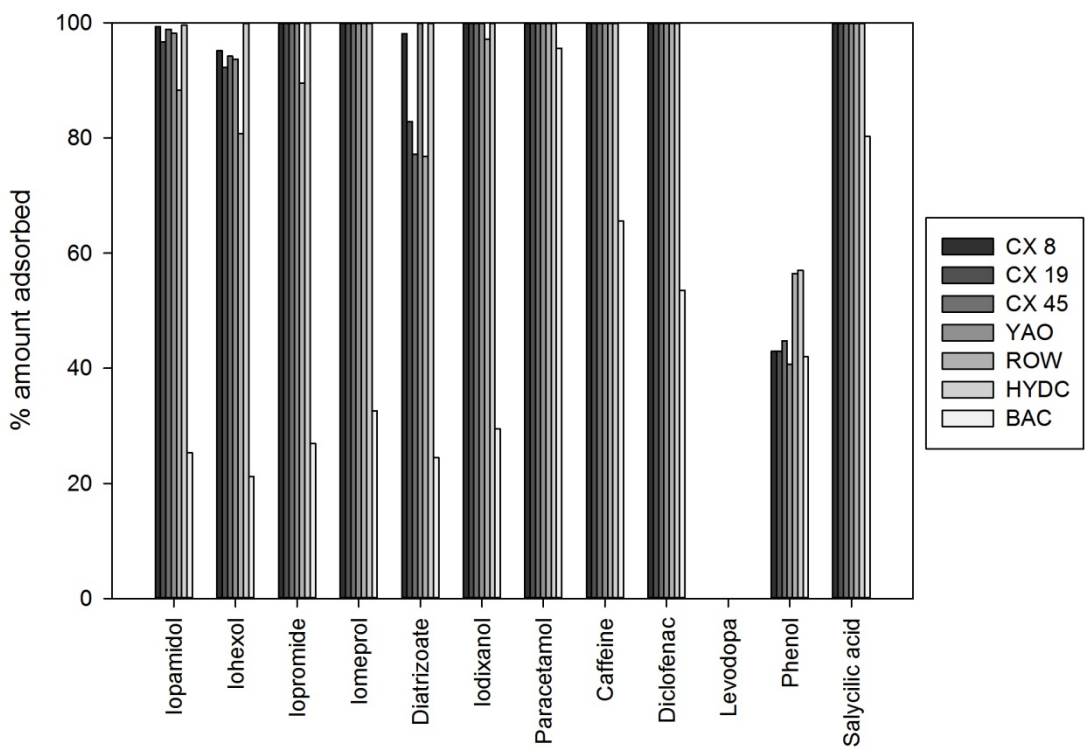
Figure SI 4.2.8 Multiadosrption of pharmaceuticals and ICM at 100 nmols surface water
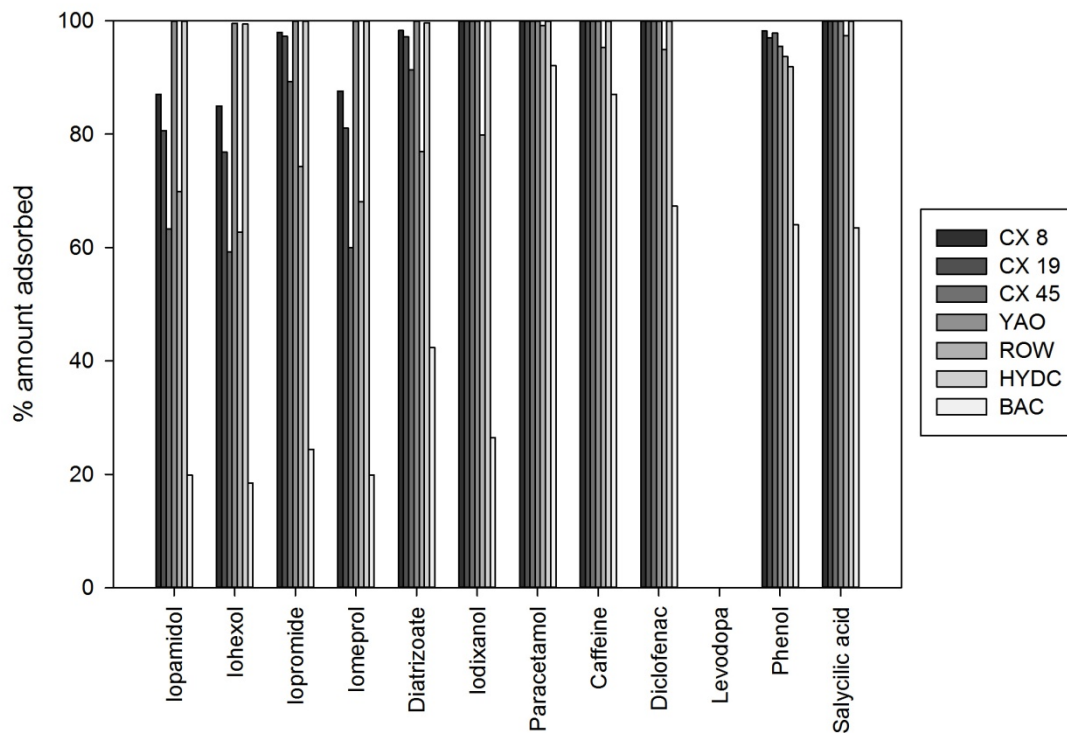
Figure SI 4.2.9 Multiadosrption of pharmaceuticals and ICM at 1 μmols mil·li Q water
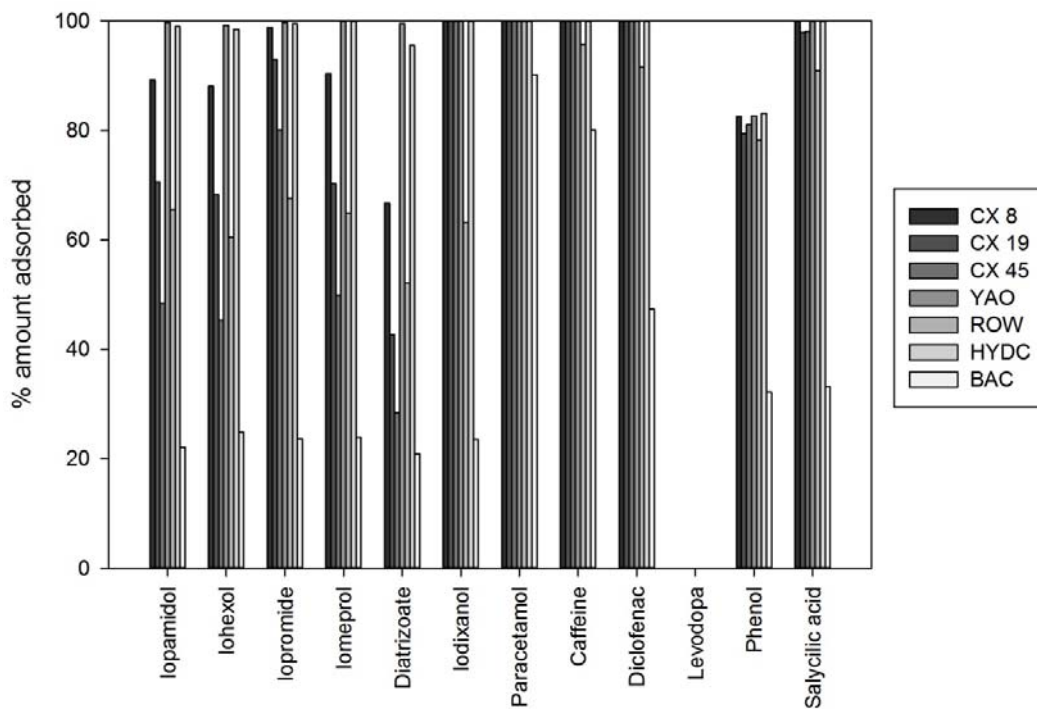
Figure SI 4.2.10 Multiadosrption of pharmaceuticals and ICM at 1 μmols surface water
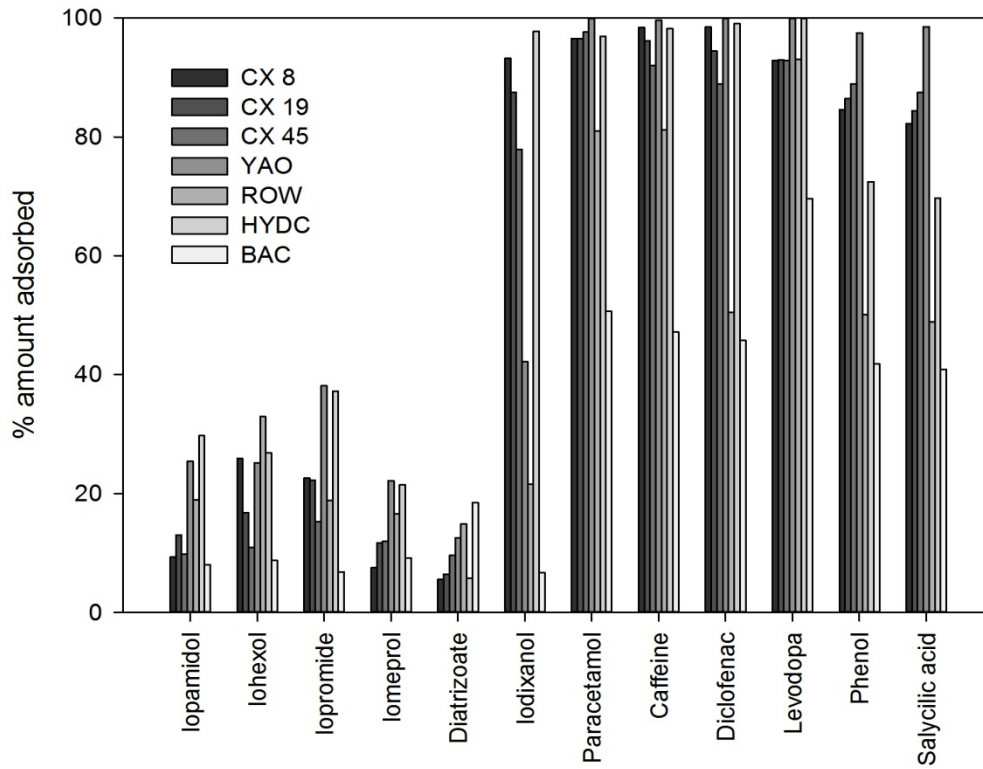
Figure SI 4.2.11 Multiadosrption of pharmaceuticals and ICM at 10 μmols mil·li Q water
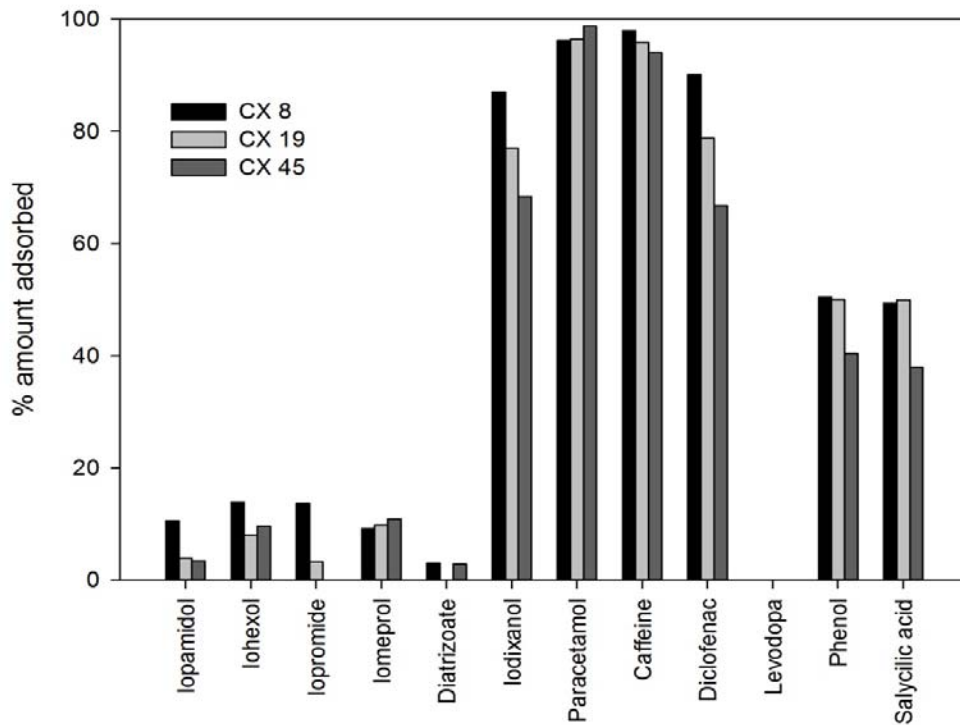
Figure SI 4.2.12 Multiadosrption of pharmaceuticals and ICM at 10 μmols surface water

Section 4.1.3

"Removal of pharmaceutical pollutants in water using coal-based activated carbons."

Removal of pharmaceutical pollutants in water using coal-based activated carbons

J. Lladó[1], B. Ruiz[2], E. Fuente[2*], M. Solé-Sardans[1], C. Lao-Luque[1]

[1]*Department of Mining, Industrial and TIC Engineering (EMIT).* Universitat Politécnica de Catalunya. Bases de Manresa 61-73, 08242 Manresa, Spain.

[2]*"Biocarbon & Sustainability".* Instituto Nacional del Carbón (CSIC), Francisco Pintado Fe, 26, 33011 Oviedo, Spain.

*Corresponding author/Email: enriquef@incar.csic.es

Graphical abstract
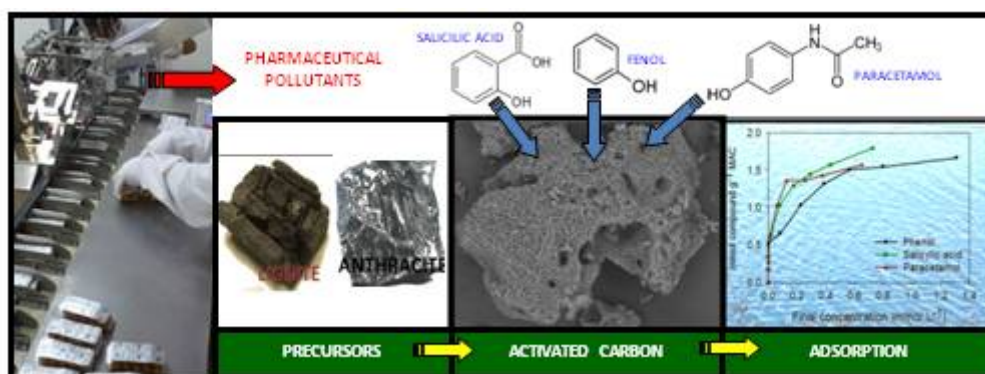
Highlights

- Lignite vs. anthracite: higher lignite revalorization
- Alkaline hydroxides activation produced good coal-based activated carbons
- High surface area (S_{BET} = 1839 m^2 g^{-1}) was obtained by the anthracite-based activated carbon
- The presence of sulphur functionalities (in MAC) improves the adsorption of salicylates
- The highest pharmaceutical pollutants uptake was achieved by anthracite-based activated carbon
- Adsorption of pharmaceutical pollutants depends on their hydrophobicity

Abstract

Several studies have demonstrated the presence of pharmaceutical compounds at trace levels in surface and groundwater. The main inputs of pharmaceuticals come from households and hospitals, and many of these compounds are not completely removed by wastewater treatment plants (WWTPs). An activated carbon is an adsorbent material that has been used successfully for the removal of pollutants from air, soil and liquids. The purpose of this dissertation is to study the modelling of the adsorption of three pharmaceutical compounds (paracetamol, phenol and salicylic acid) using new coal-based activated carbons. For this purpose, a lignite and an anthracite from Spain were chemically activated with alkaline agents (KOH and NaOH) obtaining two activated carbons (MAC and CNAC). Moreover, two commercial activated carbons widely used in water treatment (F400 and NPK) were selected for comparison purposes. The activated carbons were physical-chemical characterized with the purpose of study the influence of their properties on the adsorption of the three organic pollutants. The results showed a high surface BET (1839 m^2 g^{-1}) and total pore volume (0.83 cm^3 g^{-1}) on the anthracite-based activated carbon while lignite-based activated carbon was characterized by high sulphur content (6%). Vapour isotherms indicated a chemical interaction between the surface functional groups of the lignite based activated carbon, MAC, and the water molecules. The highest uptake of the three pharmaceutical compounds was achieved by anthracite-based activated carbon, CNAC. On the other hand, MAC showed a high affinity for anion salicylates (at pH 4-8). The maximum adsorption capacity (q_{max}) of the pollutants onto the different activated carbon followed the order salicylic acid > phenol > paracetamol which can be explained by hydrophobicity.

Keywords: Pharmaceutical-pollutants, modelling-adsorption, activated-carbon, lignite, anthracite

1. Introduction

In recent years, the emission of emerging contaminants (pharmaceuticals, pesticides, personal care products,…) has been causing serious environmental problems in aqueous media. These pollutants and their metabolites have been found in high concentrations in wastewater treatment plants (WWTP) due to their resistant biological degradation [1-3].

Among these emerging contaminants, pharmaceuticals are a cause of great concern [4,5], mainly due to their wide variety and high consumption over the past few years due to their use as means to combat diseases among the population. The discovery of a variety of pharmaceutical substances (such as antidepressants, antibiotics, antihistamines, analgesics and other medicines) in surface, ground, and drinking waters is raising concern about the potentially adverse environmental consequences of these contaminants [6-9].

Previous studies have demonstrated that the use of conventional treatment systems [10,11] is not sufficient to effectively remove this type of organic compounds. It is therefore necessary to investigate new technologically viable and economically feasible alternatives to effectively remove these pharmaceutical pollutants from water. Currently, the solutions under investigation are focused primarily on improving the purification process and use of activated carbon filters or the ultraviolet radiation. Activated carbon is an adsorbent material with a high adsorption capacity used in a wide range of liquid and gas phase applications, including water treatment, air purification, solvent vapour recovery, food and beverage processing and pharmaceuticals. In the future, apart from the traditional areas of application, several new focus spheres of activated carbons use are expected to emerge due to strict governmental regulations related with water quality.

More than 50% of the activated carbon manufactured in EEUU and China is based on coal [12]. Coal is a carbon-rich sedimentary rock that is formed from plants subjected to high pressure and heat over millions of years. During its formation and transformation, it incorporates different mineral matter including sulphur, heavy metals, etc. The degree of change undergone by a coal as it matures from peat to anthracite is known as coalification. Coalification has an important influence on physical and chemical properties of the coals and is referred to as the 'rank' of the coal (peat, lignite, sub-bituminous, bituminous, anthracite).

Coal has a direct role as an energy resource and plays a significant global role in sustainable development. It generates 41% of the total world electricity supply and is needed to produce 66% of the world's steel [13]. On the other hand, the combustion of the coal generates pollutant and greenhouse gas emissions (CO_2, SO_2, NO_x,...), making low rank coal (lignite), which can have a high sulphur content, a very hazardous

product. In this way, in Mequinenza, (Spain) power companies deny burn this kind of coal due to its high content in sulphur.

The aim of this work is the modelling of the adsorption of common pharmaceutical pollutant compounds present in aqueous solutions using coal-based activated carbons. With this purpose, two activated carbons from lignite (M), from the Mequinenza basin in Zaragoza (Spain), and from anthracite (CN), from Coto Minero Narcea in Asturias (Spain), will be developed for adsorption of emerging pollutants on waters. In addition, two commercial activated carbons, F400 and NPK obtained from bituminous coal and peat respectively and widely used in waste water treatment, were selected for comparison purposes. The four activated carbons were characterized on the basis of elemental composition, texture and water vapour isotherms for the purpose of establishing the factors involved in the adsorption of the three pharmaceutical pollutants selected (paracetamol, phenol and salicylic acid). Furthermore, of the pH upon the adsorption of the different organic compounds was investigated.

2. Materials and methods

2.1 Adsorbents

In this study, two activated carbons (CNAC and MAC) were prepared from different evolved coals (rank): an anthracite (CN) from Coto Minero Narcea, Asturias, Spain, and a lignite (M) from the Mequinenza basin in Zaragoza, Spain [14].

The precursors (CN and M) were activated by chemical activation using alkaline hydroxides (NaOH and KOH). The coals were mixed with the activated agent in solid state (physical mixture). Powdered alkaline hydroxides were selected as they would favour contact between the carbonaceous precursor and the activating agents [15]. The physical mixing method proposed is a very easy procedure that simplifies the first step in the preparation of activated carbons by chemical activation and it is widely used in the preparation of activated carbons from very different precursors such as coals and terrestrial and marine biomass [16-18]. After the physical mixing, the samples were chemically activated in a horizontal cylindrical furnace (Carbolite CTF 12/65/550) using NaOH (ratio 3:1) for anthracite (CN) and KOH (ratio 1:1) for lignite (M). The samples were heated up to 830 ºC in a 400 ml min^{-1} nitrogen flow in the case of the

anthracite and up to 750 ºC in a 150 ml min^{-1} nitrogen flow for the lignite, at a heating rate of 5 ºC min^{-1}. The maximum temperature was held for 1 hour in both cases. After chemical activation, in order to remove the activation products and any mineral matter blocking porosity, the adsorbent materials were washed with a 5M hydrochloric acid solution and subjected to a series of deionised water (Milli-Q) rinses. Finally the samples were dried at 105 ºC. The activated carbons obtained from the anthracite and lignite were named CNAC and MAC, respectively.

The anthracite was activated under more experimental drastic conditions (i.e., higher temperature and a higher activating agent/precursor ratio) in order to obtain a material with larger mesopore volume. The experimental conditions were selected from studies carried out by Perrin et al. on the activation of anthracites with NaOH [19]. From studies conducted by Girón et al. on the influence of the alkaline activating agent on the activation of forest biomass fly ash it was inferred that in the same experimental conditions the activating agent NaOH contributed to develop the mesopores more than the KOH agent [20].

Two commercial activated carbons commonly used for the treatment of water were also evaluated, Filtrasorb-400 (F400) and Norit PK 1-3 (NPK). F400 was developed by Chemviron (Feluy, Belgium) from a bituminous coal by physical activation (steam water). NPK was produced by Norit Americas Inc. (Marshall, USA) through steam-water activation of a peat.

2.2 Adsorbates
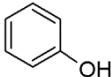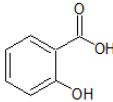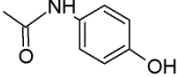
The organic pollutants evaluated were phenol (CAS 108-95-2, 98.5%, cod. 141322, Panreac, Spain), salicylic acid (CAS 69-72-7, 99.5%, Batch32347/2948, Scharlau, Spain) and paracetamol (CAS 103-90-2, 98%, lot L08100275, Fagron, Spain). Table 4.3.1 shows the physico-chemical properties of the three compounds [21]. The molecule dimensions (the close fitting "box" around the molecule), surface areas (grid and approximate) and volume were calculated using Hyperchem 8.0 [22].

Phenol, salicylic acid and paracetamol stock solutions (100 mg L^{-1}) were prepared with ultra-pure water from Milli-Q purification systems (Millipore academics). The samples

for calibration and for the sorption experiments were obtained from these solutions by dilution with ultra-pure water (Milli-Q).

Table 4.3.1 Physico-chemical properties of pharmaceutical compounds

Compound	Phenol	Salicylic acid	Paracetamol
Molecular structure			
Molecular formula	C_6H_6O	$C_7H_6O_3$	$C_8H_9NO_2$
Molecular weight (g mol^{-1})	94.11	138.12	151.16
Coefficient log octanol-water	1.46	2.26	0.46
pKa	9.99	2.97	9.38
Solubility (mg L^{-1})	82000	2240	14000
Dimensions (Å*Å*Å)	4.383*0.00031*5.767	5.391*2.426*6.077	4.781*1.740*9.184
Surface area grid (Å^2)	258.65	296.88	331.84
Surface area approx. (Å^2)	227.95	242.63	305.12
Volume (Å^3)	363.77	430.01	495.83

2.3 Characterization of the activated carbons

The activated carbons were characterized for their ultimate analysis using a LECO CHN-2000 and a LECO Sulphur Determination S-144-DR. Ash content and humidity were determined according to ISO 1171 and ISO 11722 procedures. The texture of the activated carbons was characterized by a N_2 adsorption isotherm at -196 ºC, in a conventional volumetric apparatus (ASAP 2420 from Micrometics). Before each experiment, the samples were outgassed under vacuum at 120 ºC overnight to remove any adsorbed moisture and/or gases. The isotherms were used to calculate the BET specific surface area (S_{BET}) and total pore volume (V_{TOT}) at a relative pressure of 0.95. The pore size distribution (PSD) was calculated on the basis of the density functional theory (DFT), assuming slit-shape pore geometry.

Water-Vapour sorption isotherms of the samples were determined at 25ºC for water activity (a_w) from 0 to 1. Water activity was evaluated by means of a Hydrosorb HS-12-HT model instrument (Quantachrome Instruments). The equilibrium moisture content was expressed as mmol per g of dry solid.

An SEM analysis (TM 1000 Tabletop microscope, Hitachi) was carried out to evaluate surface texture and porosity.

2.4 Adsorption assays

For equilibrium adsorption studies, 50 mg of adsorbent was added to 250 mL of organic compound solutions in different concentrations (1-150 mg dm^{-3}). The mixtures were stirred at 25ºC using a multipoint agitation plate. After 24 hours, the samples were taken out and filtered through a cellulose acetate filter (0.45 μm pore diameter) and the remaining concentration of adsorbate was analyzed in a UV/Vis-visible spectrophotometer (Lambda 25 PerkingElmer) at 242 nm for paracetamol, 269.9 nm for phenol and 295 nm for salicylic acid. The paracetamol, phenol and salicylic acid uptake, q, was determined by means of the formula:

$$q = \frac{(C_0 - C_f)\,V}{W} \qquad (1)$$

Where, q is the amount (mmol g^{-1}) of organic compounds adsorbed, C_0 and C_f are the initial and final concentration (mg L^{-1}), respectively, V is the volume (L) of adsorbate solution and W is the weight (g) of activated carbon used.

The effect of the pH upon the adsorption of the organic compounds was investigated over a pH range of 2-10, adjusting the pH by adding 0.1 M HCl or 0.1 M NaOH in 250 ml of 40 mg L^{-1} solutions.

2.5 Adsorption modelling

The experimental results were fitted by the models described in Table 4.3.2. The parameter estimation of the different isotherms was solved using MATLAB by minimizing the objective function (OF) in equation (4) [23]:

$$OF = \sqrt{\sum_{i=1}^{N} [q(P_1, P_2) - q^*]^2} \qquad (4)$$

where, N is the number of measurements taken, q* is the experimental solute uptake, q (P_1, P_2) is the predicted uptake by the model, P_1 and P_2 are the different estimated

parameters. In the case of Langmuir, the parameters used are q_{max} and K_L and for Freundlich K_f and n.

Table 4.3.2 Equilibrium adsorption models used in the study

Isotherms	Equations	Parameters	Definition
Langmuir	$q_e = \dfrac{q_{max} K_L C_e}{1 + K_L C_e}$ (2)	q_e (mmol g^{-1})	Amount of adsorbate in the adsorbent at equilibrium
		q_{max} (mmol g^{-1})	Maximum capacity
		K_L (L mmol^{-1})	Langmuir isotherm constant
		C_e (mmol L^{-1})	Equilibrium concentration
Freundlich	$q_e = K_f C_e^{1/n}$ (3)	K_f ((mmol g^{-1}) (L mmol^{-1})$^{1/n}$)	Freundlich isotherm constant
		n	Adsorption intensity

3. Results and discussion

3.1 Characterization of the activated carbons

The chemical composition of the precursors (M and CN) and the activated carbons are summarized in Table 4.3.3. As can be seen, the anthracite (CN) is characterized by a high carbon content (90.6 %) and a low ash content (4.4 %), whereas the lignite (M) has a low carbon content (56.6 %) and a high ash and sulphur content (16.2 % and 5.35% respectively), making this coal inappropriate for combustion applications.

The activated carbons, MAC and CNAC, obtained from the lignite and the anthracite respectively, have a higher carbon and lower ash content than their corresponding precursors (Table 4.3.3). It is noteworthy the reduction of ash content in the activated carbons obtained, especially in the lignite-based activated carbon (16.20% and 6.94% for M and MAC respectively). During the chemical activation process takes place the formation of new inorganic compounds that are soluble in hydrochloric acid and water and that can presumably be eliminated in the final step by means of a washing process.

Table 4.3.3 Humidity, ash and ultimate analysis of the precursors and activated carbons.

	Lignite	Lignite based AC	Anthracite	Anthracite based AC	Commercial ACs from Peat and Bituminous Coal	
	M	MAC	CN	CNAC	NPK	F400
Humidity (wt%)	12.30	2.40	3.1	1.37	5.58	2.17
Ash (wt%, dry basis)	16.20	6.94	4.4	0.72	8.57	6.92
Ultimate analysis (wt%, dry basis)						
Carbon	56.60	82.26	90.6	95.05	88.09	91.00
Hydrogen	3.42	0.26	2.1	0.15	0.54	0.34
Nitrogen	0.72	0.95	1.1	0.94	0.88	1.01
Sulphur	5.35	6.00	1.2	0.65	0.24	0.69
Oxygen*	17.71	3.59	0.6	2.49	1.68	0.04

AC: Activated carbon/ * Determined by difference

In the case of sulphur content, this increased in MAC by up to 6% and decreased in CNAC by 0.65 %. The high sulphur content on MAC could do very interesting this adsorbent for some environmental applications such as the mercury elimination in gas streams [24,25].

If the commercial carbons are compared with MAC and CNAC, their carbon content order is CNAC > F400 > NPK > MAC. It was expected that MAC would have higher carbon content than NPK because MAC is from lignite while NPK is from peat. However, the ash content of the activated carbons is NPK > MAC > F400 > CNAC in inverse proportional to their maturity.

Fig. 4.3.1 shows the nitrogen adsorption-desorption isotherms at -196 ºC of the four activated carbons. The textural properties (S_{BET}, V_{TOT} and PSD) of the four activated carbons as determined from the N_2 adsorption isotherms are summarized in Table 4.3.4.

All the isotherms are hybrid-shaped and belong to type I-IV according to the BDDT classification. Although the isotherms have a similar shape, some differences can be appreciated. The adsorption of N_2 took place fundamentally at low relative pressures (p/p0 <0.1), which is typical of microporous solids. The anthracite-based activated

carbon (CNAC) shows the highest nitrogen adsorption and the peat-based activated carbon (NPK) the lowest (Fig. 4.3.1). The knee of the isotherms is different for the coal-based activated carbons of different rank. The isotherms of CNAC and F400 present a broad knee at low relative pressures ($p/p^0<0.2$) which signifies the presence of wide micropores while the isotherms of MAC and NPK show a more pronounced knee which signifies that there is a narrower pore distribution (Fig. 4.3.1 and Table 4.3.4). The presence of a hysteresis loop (type H4 which is associated with narrow slit-shaped pores [26]) and an increase in the slope of the isotherm indicate a developed mesoporosity. These features are especially evident in NPK, which has the highest mesoporosity.
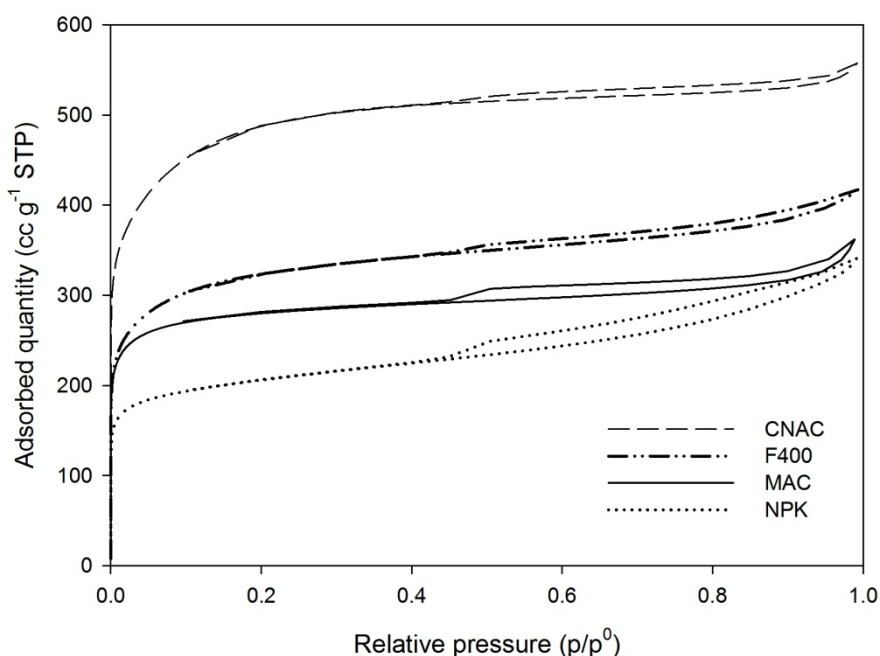
Figure 4.3.1 N_2 adsorption isotherms at -196ºC for CNAC, F400, MAC and NPK.

Table 4.3.4 Textural analysis of the activated carbons

AC	S_{BET} (m^2g^{-1})	V_{TOT} at $p/p^0= 0.95$ (cm^3g^{-1})	$*V_{ultramicro}$ (cm^3g^{-1})	$*V_{supermicro}$ (cm^3g^{-1})	$*V_{micro\ total}$ (cm^3g^{-1})	$*V_{meso}$ (cm^3g^{-1})	$*V_{micro-meso}$ (cm^3g^{-1})
MAC	1100	0.539	0.168	0.173	0.341	0.025	0.366
CNAC	1839	0.830	0.184	0.394	0.578	0.113	0.691
NPK	782	0.489	0.155	0.064	0.219	0.120	0.339
F400	1234	0.615	0.154	0.221	0.375	0.077	0.452

AC: Activated carbon / *Determined by DFT

Moreover, in Table 4.3.4, it can be observed that CNAC exhibits the highest total pore volume at $p/p^0=0.95$ ($V_{TOT} = 0.830$ cm^{3}g^{-1}) and specific surface area BET ($S_{BET} = 1839$ m^{2}g^{-1}) followed by F400, MAC and NPK. MAC presents a BET surface value of 1100 m^{2}g^{-1}, slightly higher than that obtained by T. Depci in the chemical activation with zinc chloride from Gölbaşi lignite (Turkey) [27].

The four activated carbons are basically microporous materials, although NPK has a high degree of mesoporosity ($\approx$36%). Regarding the pore volumes, the ultramicropore volume ($V_{ultramicro}$: <0.7 nm) is similar for all the activated carbons (between 0.154 and 0.184 cm^3 g^{-1}). With respect to supermicropore volume ($V_{supermicro}$: 0.7-2 nm), CNAC shows the highest value (0.394 cm^{3}g^{-1}) while NPK has the lowest (0.064 cm^{3}g^{-1}) and F400 and MAC have intermediate values (0.221 and 0.173 cm^{3}g^{-1}). Finally, the mesopore volume (V_{meso} : 2 - 50 nm) is similar for CNAC and NPK (0.113 and 0.120 cm^{3}g^{-1}) while for F400 and MAC this value is very low.

To gain a better understanding of the different pore volumes of the activated carbons, their pore size distribution was studied (Fig. 4.3.2). The main difference is in the mesopore region where CNAC shows mesopores of a small size (2-4 nm) while the NPK mesopores range between 2 and 20 nm.
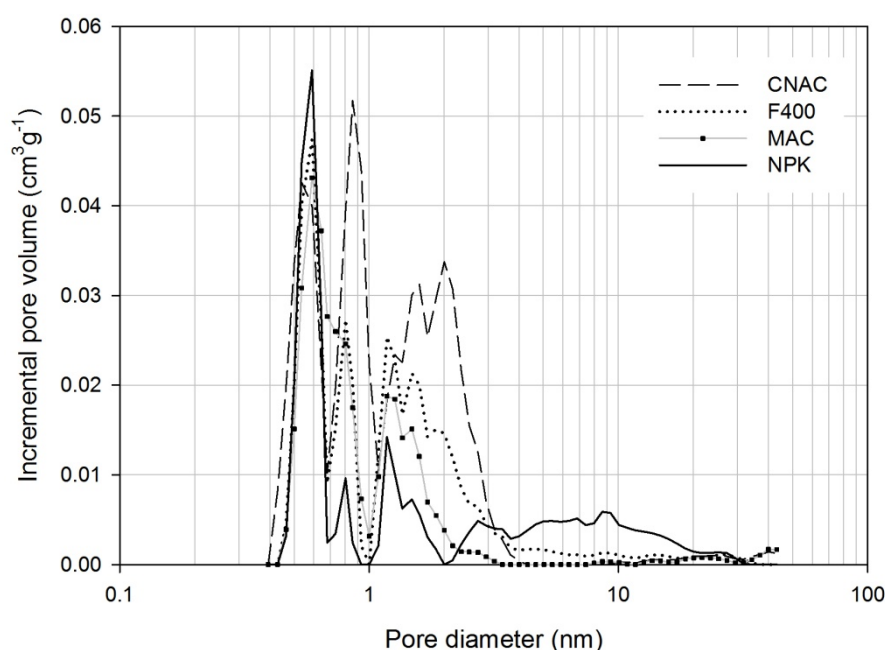
Figure 4.3.2 Pore size distribution (DFT) of the activated carbons

The effect of the thermochemical process on the texture of the coal-based (lignite and anthracite) activated carbons of different rank, MAC and CNAC, is clearly revealed by scanning electron microscopy, Figure 4.3.3. MAC (Fig. 4.3.3a) has a wide pore network structure resulting from chemical activation. The precursor of MAC is low-evolved coal (lignite, M) with a high volatile matter and ash content. Its chemical activation involves the thermal decomposition of the carbonaceous material, the elimination of volatile matter and as consequence the generation of a porous structure in the final material. On the other hand, CNAC (Fig. 4.3.3b) has a laminar structure and long pores according to the precursor which is a high rank coal (anthracite, CN), highly evolved and tidy and with a low volatile matter content.
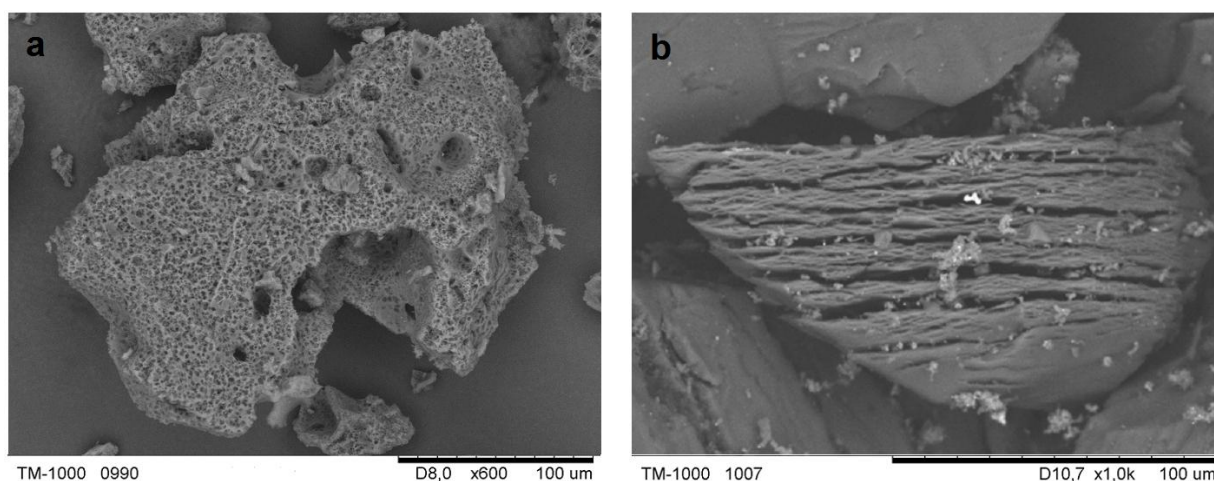
Figure 4.3.3 Scanning electron microscope (SEM) of the activated carbons obtained from: a) lignite (MAC) and b) anthracite (CNAC)

The water isotherms serve to clarify the chemical interactions with the surface groups and the physical adsorption between the water molecules and the material used [28,29], Figure 4.3.4.

Figure 4.3.4a shows the water vapour adsorption-desorption isotherms for the four activated carbons. The four isotherms are of type V, which is characteristic of weak adsorbate-adsorbent interactions. This type of isotherm is generally observed in microporous materials and often reported for activated carbons [24,25]. At low relatives pressures ($P/P^0 < 0.3$), the chemical interaction between the surface groups of the activated carbon and the water molecules are higher as can be seen in MAC (Fig. 4b), which suggests the presence of hydrophilic surface groups originating from sulphur and

oxygen groups (Table 4.3.3). Chemical interaction with the surface groups is lower in NPK and therefore the presence of functional groups is less apparent.
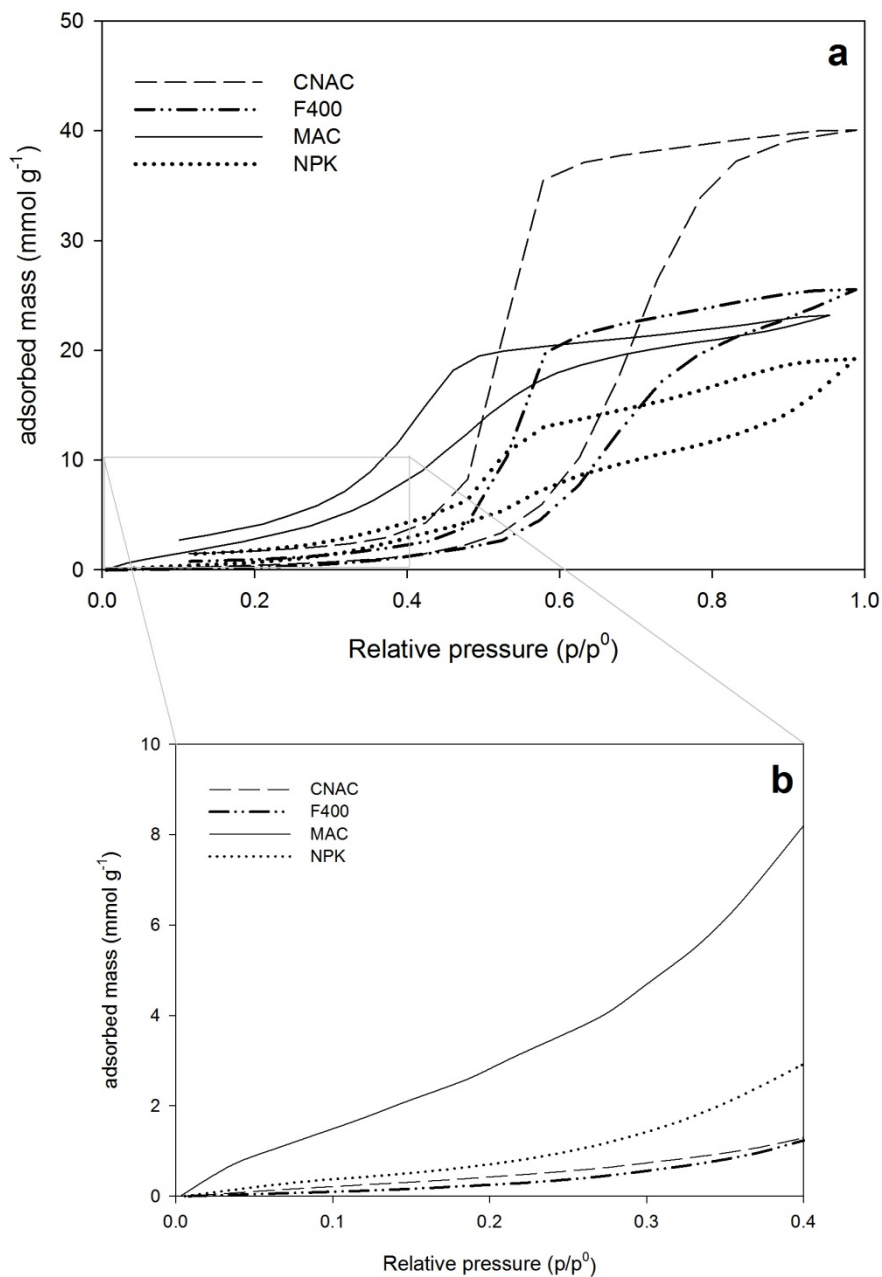
Figure 4.3.4 a) Water vapour adsorption-desorption (at 25ºC) of the materials b) detail of the adsorption at low pressures (0-0.4)

Finally, chemical interaction is negligible in CNAC and F400 suggesting the disappearance of surface groups due to maturity of the raw materials and the severe activation conditions (such as the high temperature and high ratio of the activating

agent). As the pressure increases (Fig. 4.3.4a) physical adsorption becomes more important due to the influence of the textural development. Therefore the CNAC isotherm presents the highest water adsorption (approx. 40.1 mmol/g), followed by F400 and MAC with NPK showing the lowest adsorption. These results are accord with the order of porosity obtained by nitrogen adsorption (CNAC > F400 > MAC > NPK).

3.2 Influence of pH

The influence of the pH of the solution on the adsorption of the three pollutants (paracetamol, phenol and salicylic acid) is shown in Figure 4.3.5.

As can be seen, there are no significant variations in the adsorption of paracetamol and phenol by the four activated carbons with respect to the pH (Fig. 4.3.5a and 4.3.5b). The molecules remain undissociated at a pH lower than pKa (9.99 or 9.38) and therefore the removal is constant. On the other hand, the adsorption of salicylic acid (Fig. 4.3.5c) shows a significant decrease with increasing pH. When the pH is lower than the salicylic pKa (2.97), the carboxylic groups are undissociated. This favours the adsorption of salicylic acid because, under acidic conditions, the chemical groups on the activated carbon cause a decrease in the total negative charge. The opposite effect occurs at a high pH. Salicylic acid is dissociated and the negative charged sites of the activated carbon increase. Therefore repulsion forces may arise between the salicylates and the negative charged surface, impeding the adsorption process.

It can also be seen in Figure 4.3.5c that between pH 4 and 8 the adsorption of salicylic acid by MAC is higher than in the others activated carbons. This behaviour can be explained by the presence of different functional groups on the surface of MAC as it can suggest the results on the chemical adsorption showed at low pressures in the water vapour isotherm (Fig. 4.3.4). Mui and Valix [30,31], suggested that depending on the acid-base nature of the carbon suspension, which is often affected by the elemental composition of carbon (particularly heteroatoms such as nitrogen, oxygen and sulphur), the adsorbent can be positively or negatively charged as shown below:

(Positive surface) $C=S^{\delta+}OH + H^+ \rightarrow C= S^{\delta+} + H_2O$

(Negative surface) $C=O^{\delta-}H^+ \rightarrow C=O^{\delta-} + H^+$
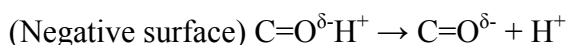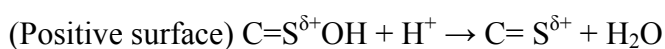
Here the salicylate can be expected to be adsorbed favourably onto the positively-charged carbon surface due to the presence of the high sulphur content. Therefore in the pH range of 4-8, the attraction of opposite charges between the surface and dissociated salicylic acid may contribute to the increase adsorption onto MAC
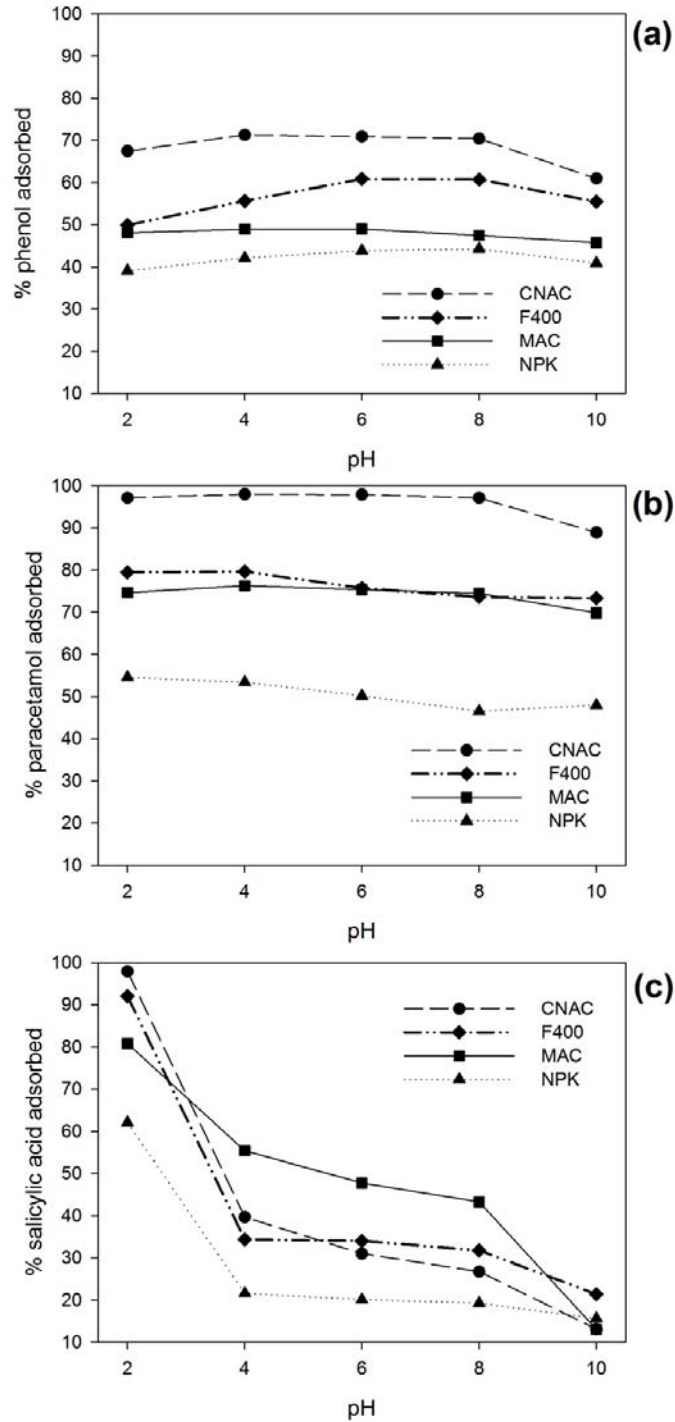
Figure 4.3.5 pH effect on the adsorption equilibrium a) phenol, b) paracetamol and c) salicylic acid

3.3 Adsorption isotherms and modelling

The experimental adsorption isotherms of the three pollutants on the four activated carbons are shown in Figure 4.3.6.
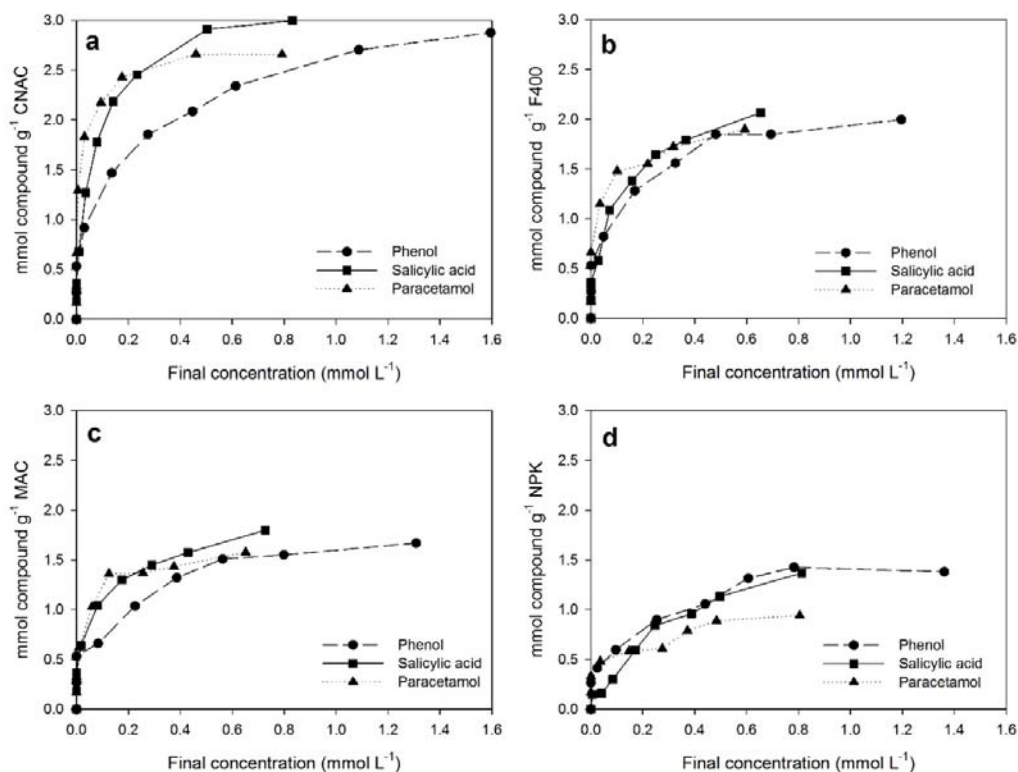
Figure 4.3.6 Pharmaceutical compounds adsorption onto the coal-based activated carbons: a) CNAC, b) F400, c) MAC and d) NPK

According to their initial slopes and Giles' classification [32,33], the NPK isotherm can be classified as of type L2, whereas the MAC, F400 and CNAC isotherms are of type H2. This suggests that the three carbons have a high affinity for paracetamol, phenol and salicylic.

The experimental data were fitted to two different two parameter isotherms (Langmuir, Freundlich). Table 4.3.5 shows the constants obtained and the objective function (OF) values for the two models. According to the OF values, paracetamol adsorption is best represented by the Freundlich model, whereas salicylic acid is best fitted by the Langmuir model. Phenol behaviour depends on the activated carbon used (F400 and MAC by Langmuir, CNAC and NPK by Freundlich). If the q_{max} from the Langmuir model for the four activated carbons are compared, the adsorption capacity follows the

order CNAC>F400>MAC>NPK which is the same order as some textural development characteristics (S_{BET} and total pore volume V_{TOT}) . The highest adsorption equilibrium constant values (K_L) are achieved for the adsorption for paracetamol onto the four activated carbons. This indicates that the four activated carbons have a high affinity for the adsorption of paracetamol.

Table 4.3.5 Adsorption parameters of paracetamol, phenol and salicylic acid on the activated carbons

Activated carbon	Compound	Isotherm of Langmuir			Isotherm of Freundlich		
		q_{max} (mmol g^{-1})	K_L (L mg^{-1})	OF	K_f (mmol g^{-1}) (L mmol^{-1})$^{1/n}$	n	OF
MAC	Paracetamol	1.7639	49.84	0.469	1.86	4.7619	0.4189
	Phenol	1.8639	6.45	0.6093	1.64	3.4258	0.6401
	Salicylic acid	2.0112	21.85	0.4823	1.98	3.8491	0.4107
CNAC	Paracetamol	2.5511	131.52	0.8524	2.91	7.3099	0.8052
	Phenol	2.9361	7.83	0.7647	2.63	3.5971	0.611
	Salicylic acid	3.0864	19.19	0.4897	3.79	3.1555	0.4997
NPK	Paracetamol	0.9291	17.95	0.4244	1.02	3.891	0.3836
	Phenol	1.6124	6.47	0.4167	1.43	3.1505	0.4112
	Salicylic acid	1.6476	3.29	0.1529	1.39	2.139	0.3592
F400	Paracetamol	1.8236	53.87	0.8028	1.96	6.9492	0.7682
	Phenol	2.1123	10.77	0.619	2.02	3.9277	0.6413
	Salicylic acid	2.2501	11.61	0.4269	2.48	2.9832	0.4618

With respect to the Freundlich model, the parameter 1/n is a measure of adsorption intensity or surface heterogeneity. According to Navasivayam [34], the value of n indicates favourable adsorption when 1<n<10. That is to say the lower its value within this range, the more favourable the adsorption. In this study, the value is between 2 and 7 indicating that the most favourable adsorption corresponded to phenol and salicylic acid (around 3, Table 4.3.5).

As can be seen in Figure 4.3.6, the highest pollutant adsorption capacities are obtained with CNAC. This high performance could be due to the high BET area and the development of the micropore and mesopore structure. A comparison of the different pore volumes and the compound sizes, would lead one to expect that molecules smaller than 0.7 nm (in the case of phenol and salicylic acid) would be adsorbed by

ultramicropores. In this case, MAC has a higher ultramicroporosity than F400, but the maximum capacity (q_{max}, Table 4.3.5) is achieved by F400. Therefore, the adsorption process must take place not only on the ultramicropores but also on the supermicropores. In other words, the supermicropores also have a pore filling role. Regarding the mesopores, CNAC and NPK show the same amount of mesoporosity but the mesopores differ in their diameter. Depending on the characteristics of the activated carbon, the mesopores allow the access of pollutants [35], or they make little contribution to the capture of molecules depending on the mechanism of adsorption on the active sites [36,37]. In this study, it was found that mesopores of NPK (with a large diameter of 2-20 nm) only make a small contribution adsorption due to the presence of surface groups (water vapour isotherm) and they allow the access. On the other hand, the small diameter mesopores of CNAC (2 - 4 nm) and the low chemical interactions with the surface groups can suggest a pore-filling adsorption mechanism.

Regarding the effect of the nature of the adsorbate, the single component isotherms (Figure 4.3.5) and the modelling results (Table 4.3.5) show that the highest adsorption capacity corresponded to salicylic acid followed by phenol and paracetamol. This order cannot be explained on the basis of the size of the compounds (Table 4.3.1) because the salicylic acid is larger than the phenol and smaller than the paracetamol. Another aspect to be considered is solubility. Moreno-Castilla et al [38] observed that their adsorption capacity increased with the decreasing water solubility of phenolic compounds. In our study, this parameter seems to be of secondary importance since paracetamol was less easily adsorbed than phenol.

Hydrophobicity might also explain the order of adsorption capacity of the different pollutants. According to Mohammed et al [39], activated carbons are mainly hydrophobic and display a strong affinity for organic molecules with a limited solubility in water. Hydrophobic compounds tend to be pushed to the adsorbent surface and hence they are more easily adsorbed than hydrophilic compounds. In this study, salicylic acid is the most hydrophobic pollutant followed by phenol and paracetamol.

4. Conclusions

Activated carbons obtained from anthracite (CNAC) and lignite (MAC) were successfully used as adsorbents for paracetamol, phenol and salicylic acid pollutant

removal in aqueous phase.

- A high decrease in the ash content was observed in the activation of the lignite (from 16.2% in M to 6.94% in MAC). On the other hand, CNAC had very low ash content making this activated suitable for water treatment.
- MAC was characterized by high sulphur content (6%), ten times more that the rest of the other activated carbon used in this study.
- CNAC was characterized by a high surface area (S_{BET} = 1839 m^2 g^{-1}), and a high total pore volume (0.83 cm^3 g^{-1}).
- At low relative pressures in the water vapour isotherms, MAC showed a higher vapour uptake than the rest of activated carbons due to the presence of sulphur functionalities. The adsorption of salicylic acid showed a strong dependence with the variations in the pH solutions. Maximum salicylic acid adsorption was observed at pH = 2 onto the different activated carbons. At the pH range 4-8, the adsorption of anion salicylates was favoured onto MAC suggesting that the presence of sulphur functionalities of the activated carbon favours the ionic interactions.
- The highest adsorption capacity of the three pharmaceutical pollutants was achieved by CNAC followed by F400, MAC and NPK. This order coincides with their BET surface, the total micropore volume and the total pore volume
- A study of pollutant adsorption on the different activated carbons showed that hydrophobicity was the main reason for the higher capacity of adsorption of salicylic acid.

Acknowledgements

Section 4.1.3

References

[1] C. Postigo, M.J. López de Alda, D. Barceló, Drugs of abuse and their metabolites in the Ebro River basin: occurrence in sewage and surface water treatment plants removal efficiency, and collective drug usage estimation, Environ. Int. 36 (2010) 75-84

[2] C. Alfonsín, A. Hospido, F. Omil, M.T. Moreira, G. Feijoo, PPCPs in wastewater – Update and calculation of characterization factors for their inclusion in LCA studies, J. Clean Prod. 83 (2014) 245-255

[3] V. Osorio, S. Pérez, A. Ginebreda, D. Barceló, Pharmaceuticals on a sewage impacted section of a Mediterranean River (Llobregat River, NE Spain) and their relationship with hydrological conditions, Environ. Sci. Pollut. Res. Int. 19 (2012) 1013-25

[4] S. Halling-Sørensen, P.F. Nors Nielsen, F. Lanzky, H.C. Ingerslev, S. Holten Lützhøft, S.E. Jørgensen, Occurrence, fate and effects of pharmaceutical substances in the environment – A review. Chemosphere 36 (1998) 357-393

[5] N.J. Ayscough, J. Fawell, G. Franklin, W. Young, Review of Human Pharmaceuticals in the Environment, UK Environment Agency, Bristol, 2000

[6] B. Petrie, R. Barden, B. Kasprzyk-Hordern, A review on emerging contaminants in wastewaters and the environment: Current knowledge, understudied areas and recommendations for future monitoring. Water Research 72 (2015) 3–27

[7] F.J. García-Mateos, R. Ruiz-Rosas, M.D. Marqués, L.M. Cotoruelo, J. Rodríguez-Mirasol, T. Cordero, Removal of paracetamol on biomass-derived activated carbon: Modeling the fixed bed breakthrough curves using batch adsorption experiments. Chem. Eng. J. 279 (2015) 18–30

[8] J.D. Méndez-Díaz, G. Prados-Joya, J. Rivera-Utrilla, R. Leyva-Ramos, M. Sánchez-Polo, M.A. Ferro-García, N.A. Medellín-Castillo, Kinetic study of the adsorption of nitroimidazole antibiotics on activated carbons in aqueous phase. J. of Colloid and Interface Science 345 (2010) 481–490

[9] K. Kümmener, Drugs in the environment: emission of drugs, diagnostic aids and disinfectants into wastewater by hospitals in relation to other sources--a review. Chemosphere 45 (2001) 957-969

[10] Emma Gracia-Lor, Juan V. Sancho, Roque Serrano, Félix Hernández, Occurrence and removal of pharmaceuticals in wastewater treatment plants at the Spanish Mediterranean area of Valencia. Chemosphere 87 (2012) 453–462

[11] M. Carballa, F. Omil, J.M. Lema, M. Llompart, C. Garcia-Jares, I. Rodriguez, M. Gomez, T. Ternes, Behavior of pharmaceuticals, cosmetics and hormones in a sewage treatment plant. Water Res. 38 (2004) 2918-2926

[12] The Economics of Activated Carbon, Sixth Edition, Roskill Information Services Ltd., London, 1998

[13] L. Schernikau Coal markets and products, in: A. Roncoroni, G. Fusai, M. Cummins Handbook of multy-commodity markets and products: Structuring, trading and risk management, Chichester: John Wiley & Sons, 2015, pp. 67-174

[14] L. Cabrera, M. Cabrera, R. Gorchs, F.X.C. de las Heras, Lacustrine basin dynamics and organosulphur compound origin in a carbonate-rich lacustrine system (Late Oligocene Mequinenza Formation, SE Ebro Basin, NE Spain), Sediment. Geol. 148 (2002) 289-317

[15] A. Ros, M.A. Lillo-Ródenas, E. Fuente, M.A. Montes-Moeán, M.J. Martín, A. Linares-Solano, High surface area materials prepared from sewage sludge-based precursors, Chemosphere. 65 (2006) 132-40

[16] M. Lillo-Ródenas, D. Lozano-Castelló, D. Cazorla-Amorós. A. Linares-Solano, Preparation of activated carbons from Spanush anthracite, Carbon. 39 (2001) 751-759

[17] R.R. Gil, B. Ruiz, M.S. Lozano, E. Fuente, Influence of the pyrolysis step and the tanning process on KOH-activated carbons from biocollagenic wastes. Prospects as adsorbent for CO_2 capture, J. Anal. Appl. Pyrolysis. 110 (2014) 194-204

Section 4.1.3

[18] N. Ferrera-Lorenzo, E.Fuente, I.Suárez-Ruiz, B. Ruiz, KOH activated carbon from conventional and microwave heating system of a macroalgae waste from the Agar-Agar industry, Fuel Process. Technol. 121 (2014) 25-31

[19] A. Perrin, A. Celzard, A. Albiniak, J. Kaczmarczyk, J.F. Marêché, G. Furdin, NaOH activation of anthracites: effect of temperature on pore textures and methane storage ability, Carbon 42 (2004) 2855-2866

[20] R.P. Girón, R.R. Gil, I.Suárez-Ruiz, E. Fuente, B. Ruiz, Adsorbents/catalysts from forest biomass fly ash. Influence of alkaline activating agent, Microporous Mesoporous Mater. 209 (2015) 45-53

[21] B.S. Bolton E, Y. Wang, P.A. Thiessen, OubChem: Integrated Platform of Small Molecules and Biological Activites, in: American Chemical Society (Ed.), Annu. Reports Comput. Chem. V4, Elsevier B.V., Washington, DC, 2008

[22] D.J. de Ridder, J.Q.J.C. Verberk, S.G.J. Heijman, G.L. Amy, J.C. van Dijk, Zeolites for nitrosamine and pharmaceutical removal from demineralised and surface water: Mechanisms and efficacy, Sep. Purif. Technol. 89 (2012) 71-77

[23] J. Lladó, C. Lao-Luque, B. Ruiz, E. Fuente, M. Solé-Sardans, A.D. Dorado, Role of activated carbon poperties in atrazine and paracetamol adsorption equilibrium and kinetics, Process. Saf. Environ. Prot. 95 (2015) 51-59

[24] M.A. Lopez-Anton, N. Ferrera-Lorenzo, E. Fuente, M. Díaz-Somoano, I. Suarez-Ruíz, M.R. Martínez-Tarazona, B. Ruiz, Impact of oxy-fuel combustion gases on mercury retention in activated carbons from a macroalgae waste: Effect of water, Chemosphere. 125 (2015) 191-197

[25] M.A. Lopez-Anton, R,R, Gil, E, Fuente, M. Díaz-Somoano, M.R: Martínez-Tarazona, B. Ruiz, Activated carbons from biocollagenic wastes of the leather industry for mercury capture in oxy-combustion, Fuel. 142 (2015) 227-234

[26] K.S.W. Sing, Reporting physisorption data for gas/solid systems with special reference to the determination of surface area and porosity, Pure Appl. Chem, 57 (1985) 603-619

[27] T. Depci, Comparison of activated carbon and iron impregnated activated carbon derived from Gölbaşi lignite to remove cyanide from water. Chem. Eng. J. 181-182 (2012) 467-478

[28] R.S: Vartenetyan, A.M. Voloshchuk, M.M. Dubinin, O.E. Babkin, Adsorption of water vapour and microporous structures of carbonaceous adsorbents. 10. The effect of preliminary preparation conditions and the modificaciton of activated charcoals on their adsorption properties, Bull. Acad. Sci. USSR Div. Chem. Sci (1986) 1763-1768

[29] J. Alcañiz-Monge, A. Linares-Solano, B. Rand, Mechanism of adsorption on water in carbon micropores as revealed by a study of activated carbon fibers, J. Phys. Chem. B. 196 (2002) 3209-3216

[30] E.L.K. Mui, W.H. Cheung, M. Valiz, G. McKay, Dye adsorption onto activated carbons from tyre rubber waste using surface coverage analysis, J. Colloid Interface Sci. 347 (2010) 290-300

[31] M. Valix, W.H. Cheung, G. McKay, Roles of the textural and surface chemical properties of activated carbon in the adsorption of acid blue dye, Langmuir. 22 (2006) 4574-4582

[32] C.H. Giles, D. Smith, A. Huitson, General treatment and classification of solute adsorption-isotherm. 1. Theoretical, J. Colloid Interface Sci. 47 (1974) 755-765

[33] C.H. Giles, D. Smith, A. Huitson, General treatment and classification of solute adsorption-isotherm. 2. Experimental interpretation, J. Colloid Interface Sci. 47 (1974) 766-778

[34] C. Namasivayam, S. Senthilkumar, Removal of Arsenic (V) from aqueous solution using industrial solid waste: adsorption rates and equilibrium studies, Ind. Eng. Chem. Res. 37 (1998) 4816-4822

[35] A. Dabrowski, P. Podkoscielny, Z. Hubicki, M. Barzak, Adsorption of phenolic compounds by activated carbon- a critical review, Chemosphere. 58 (2005) 1049-1070

Section 4.1.3

[36] J. Cai, S. Bennici, J. Shen, A. Auroux, Study of phenol and nicotine adsorption on nitrogen-modified mesoporous carbons, Water, Air, Soil Pollut. 225 (2014) 2088

[37] V. Fierro, V. Torné-Fernández, D. Montané, A. Celzard, Adsorption of phenol onto activated carbons having different textural and surface properties, Microporous Mesoporous Mater. 111 (2008) 276-284

[38] C. Moreno-Castilla, J. Rivera-Utrilla, M.V. López Ramón, F. Carrasco-Marín, Adsorption of some substituted phenols on activated carbons from bituminous coal, Carbon 33 (1995) 845-851

[39] E.F. Mohamed, C. Andriantsiferana, A.M. Wilhelm, H. Delmas, competitive adsorption of phenolic compounds from aqueous solution using sludge-based activated carbon, Environ. Technol. 32 (2011) 1325-1336

Section II

Analysis and adsorption process

Section 4.2.1

"Multicomponent adsorption on coal based activated carbons on aqueous media: new cross-correlation analysis method"

Multicomponent adsorption on coal-based activated carbons on aqueous media: new cross-correlation analysis method

J. Lladó[1*], Conxita Lao-Luque[1], B. Ruiz[2], E. Fuente[2], Montserrat Solé-Sardans[1], Jordi Bonet[1]

[1]*Department of Mining, Industrial and TIC Engineering (EMIT).* Universitat Politécnica de Catalunya. Bases de Manresa 61-73, 08242 Manresa, Spain.

[2]*"Biocarbon & Sustainability"*. Instituto Nacional del Carbón (CSIC), Francisco Pintado Fe, 26, 33011 Oviedo, Spain.

*Corresponding author/Email: jordi.llado@emrn.upc.edu

Graphical abstract
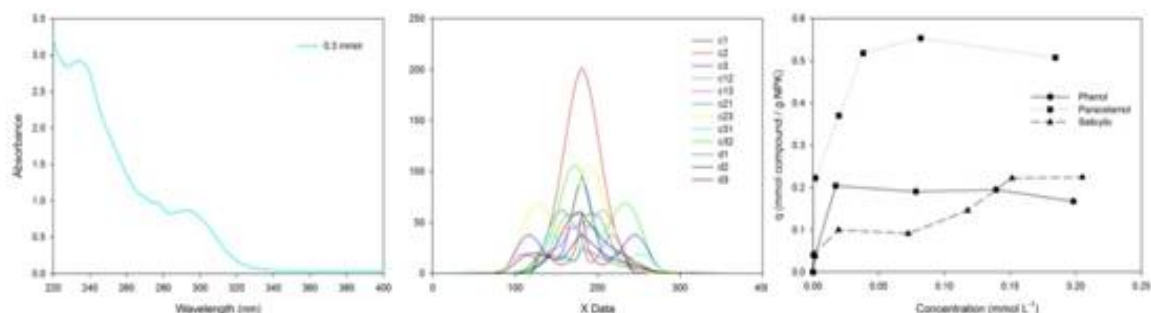
1. Summary

The aim of this section is to study the adsorption competition in binary and ternary mixtures of phenol, paracetamol and salicylic acid onto four different coal based activated carbons (CNAC, F400, MAC and NPK) used in the section 4.1.3. The different mixtures were analysed by UV-vis because it is a quicker and cheaper technique than HPLC, although UV-vis can show some shortage as lower detection limits and difficulty to analyse mixtures containing several compounds.

A general method to analyze mixtures by UV-vis is the Vierordt's method, which it is based on the Lambert Beer Law. The literature shows that this method can give some

errors due to the overlap of different signals that come from the presence of two or more compounds in a mixture. For this reason, the present works attempts to develop a new method (cross-correlation method) to solve the Vierordt's method constraints because of it is based on the analysis of individual compounds signals in the mixture. Results showed that our new method exhibit fewer errors and more accurate values than Vierordt's one. The cross-correlation method was used to analyse adsorbates in binary and ternary solutions before and after the adsorption onto the four activated carbons: CNAC, F400, MAC and NPK.

Adsorption results showed that the presence of sulphur groups on MAC enhances the adsorption of salicilates in presence of paracetamol. On the other hand, oxygen groups in NPK favour phenol adsorption against salicylic acid at low concentrations. In the binary system phenol-paracetamol, phenol was significantly less adsorbed onto CNAC than F400; suggesting that the high quantity of water adsorbed onto CNAC disfavour the adsorption of phenol. In the ternary mixtures, the presence of a third compound on the solution reduced the total amount of the compounds adsorbed, but similar effects than in binary mixtures were observed during the adsorption process.

Keywords: Paracetamol; Phenol; Salicylic Acid; Cross_correlation, activated carbon, adsorbate-competition, adsorption

2. Material and Methods

2.1 Adsorbents

The four adsorbent used (CNAC, F400, MAC and NPK) were characterized in the section 4.1.3.

2.2 Adsorbates

Phenol (F) (CAS 108-95-2, 98.5%, cod. 141322, Panreac, Spain), salicylic acid (SA) (CAS 69-72-7, 99.5%, Batch32347/2948, Scharlau, Spain) and paracetamol (P) (CAS 103-90-2, 98%, lot L08100275, Fagron, Spain).were used on the single and multicomponent solutions experiments.

2.3 Preparation of standard solutions

Single component stock solutions (100 mg L^{-1}) were prepared with ultra-pure water (Mil:li Q). From stock solution of each compound, different concentration solutions (1-40 mg L^{-1}) were prepared.

Four different mixtures were prepared with ultra-pure water (Mil·li Q) of 1 mmol L^{-1} concentration. The mixtures were phenol-paracetamol (FP), phenol-salicylic acid (FSA), paracetamol-salicylic acid (PSA) and phenol-paracetamol-salicylic acid (ternary). From each mixture, different solutions were made (0.01, 0.05, 0.1, 0.15, 0.2 and 0.3 mmol L^{-1}).

2.4 Apparatus

A Lambda 25 PerkinElmer UV/Vis spectrophotometer was used for all the absorbance measurements. The individual spectra of the three evaluated compounds and the different mixtures were determined 5 times; the linearity range, wavelength and correlation coefficient on single and multiple systems are shown in Table 4.4.1 and Table 4.4.2.

Table 4.4.1 Single UV-vis analysis, linearity and correlation coefficient of phenol, paracetamol and salicylic acid

Analysis	λ (nm)	Linearity range (mg /L)	Correlation coefficient
Individual compound			
Phenol (F)	270	1.0 - 80	0.9999
Paracetamol (P)	242	1.0 – 40	0.9997
Salycilic acid (SA)	295	1.0 – 40	0.9997

Table 4.4. 2 Multiple analysis linearity range of binary and ternary solutions

Multiple compound	λ (nm)	Linearity range (mmol L^{-1})
FP	200 – 400	0.05-0.25
FSA	200 – 400	0.05-0.30
PSA	200 – 400	0.05-0.20
Ternary	200 – 400	0.05-0.20

2.5 Spectrophotometric methods

2.5.1 Method A: Single (or simple) Vierordt's method

This method is based on solving a equation system with *n* unknowns (applying Lambert Beer Law) using absorbance values (A) obtained from absorbances measured *N* suitable wavelengths *N* compounds in the mixture [1,2]. The unknown concentrations of the different compounds on the mixture preparation are then calculated from *N* simultaneous equations, that, for *N=3*, take the following form:

$$A_1 = \alpha\, C_1 + \beta\, C_2 + \gamma\, C_3 \text{ for } \lambda_1 = 270 \text{ nm}$$

$$A_2 = \alpha\, C_1 + \beta\, C_2 + \gamma\, C_3 \text{ for } \lambda_2 = 242 \text{ nm}$$

$$A_3 = \alpha\, C_1 + \beta\, C_2 + \gamma\, C_3 \text{ for } \lambda_3 = 295 \text{ nm}$$

Where A_1, A_2 and A_3 are the total absorbances of a mixture solutions at λ_1, λ_2 and λ_3 wavelengths. C_1, C_2 and C_3 are the concentrations of phenol, paracetamol and salicylic acid, respectively, and α, β and γ are their respective molar absortivites constants. α, β and γ can be solved by means of the program 'Matlab' in the computer and the concentrations of each compound in the mixture were determined.

2.5.2 Method B Cross-correlation method

The cross-correlation method proposed consists on the measure of similarity of two signals to try to find relevant features in an unknown signal by comparing it with one that is known.

$$(f \star g)(n) \stackrel{\text{def}}{=} \sum_m f(m) g(m - n) \qquad (1)$$

Where f(m) and g(m) are the respective samples at different wavelengths of the signals that we compare.

Two parts of the spectra with poor quality information were eliminated, before to proceed with the cross-correlation method: wavelengths lower than 220 nm (190 – 220nm) and wavelengths higher than 340 nm (Fig. SI 4.1). The first range of

wavelengths (λ<220) can be affected by the absorbance of different substances present on the solution media, while the second range (λ>340) has zero absorbance.

The resulting individual spectres Si (S_1, S_2 and S_3, on Fig. SI 4.1, subscript 1 for phenol, 2 for paracetamol and 3 for salicylic acid) were autocorrelated obtaining the different Cii (as example c11, c22 and c33 on Fig 4.4.1).

$$S_1 \star S_1 = c11; \ S_2 \star S_2 = c22; \ S_3 \star S_3 = c33 \qquad (2)$$
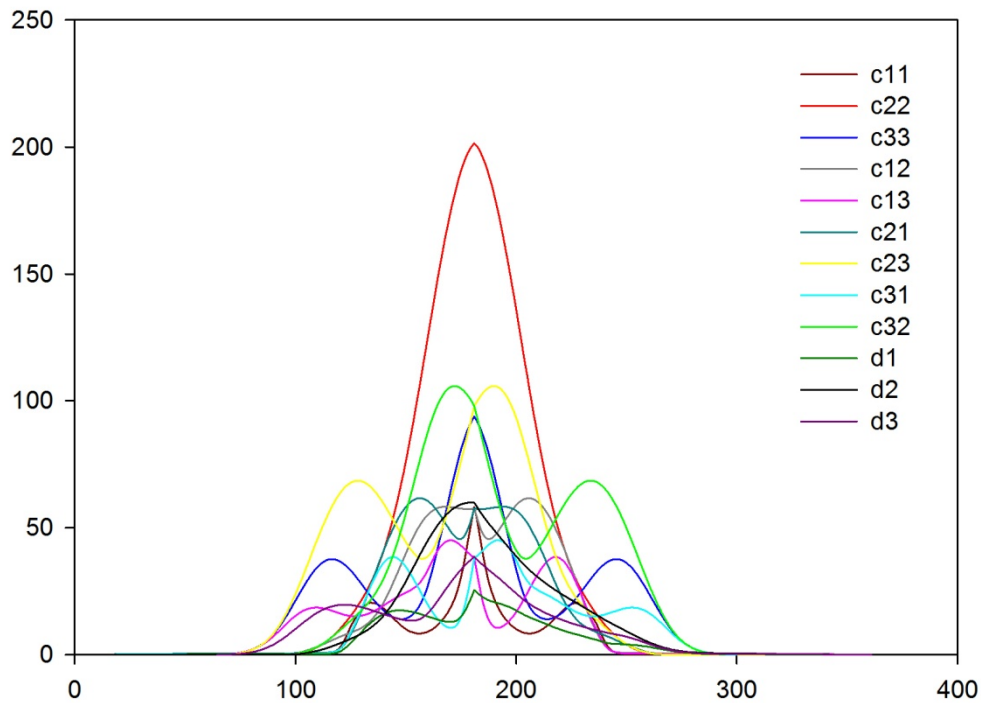
Figure 4.4.1 Cross correlation of individual spectra, combination on a ternary mixture

Each individual spectra i was cross-correlated with the other individual spectra, j different from i to obtain the cross-correlations cij (as example c12, c13, c21, c23, c31 and c32 on ternary mixture on Fig. 4.4.1).

$$S_1 \star S_2 = c12; \ S_1 \star S_3 = c13 \qquad (3)$$

$$S_2 \star S_1 = c21; \ S_2 \star S_3 = c23 \qquad (4)$$

$$S_3 \star S_1 = c31; \ S_3 \star S_2 = c32 \qquad (5)$$

Finally, each individual spectra was cross-correlated with the binary or ternary compound spectra b_{ijk} (b12, b13, b23, b123, Fig. SI 4.2); obtaining the cross-correlations d1, d2 and d3 of Fig. 4.4.1 (on the ternary solution). The different cross-correlations obtained of the three different binary solutions are on Fig SI 4.3.

$$S_1 \star b_{123} = d1; \quad S_2 \star b_{123} = d2; \quad S_3 \star b_{123} = d3 \qquad (6)$$

$$b_{123} = \alpha\, S_1 + \beta\, S_2 + \gamma\, S_3 \qquad (7)$$

The points di(n) of each cross-correlations d1, d2 and d3 that are low in comparison the maximum value of its cross-correlation are eliminated. Each of the remaining points leads to an equation:

$$d_i(n) = \alpha\, ci1 + \beta\, ci2 + \gamma\, ci3 \qquad i = \{1,2,3\} \qquad (8)$$

$$\begin{aligned}
d_1(n) &= \alpha C_{11}(n) + \beta C_{12}(n) + \gamma C_{13}(n) \\
d_2(n) &= \alpha C_{12}(n) + \beta C_{22}(n) + \gamma C_{23}(n) \qquad (9) \\
d_3(n) &= \alpha C_{13}(n) + \beta C_{23}(n) + \gamma C_{33}(n)
\end{aligned}$$

So, it is resolved the equations (9) for all the points (n=-199:199) that they have been given for the criteria, obtaining the different values of α, β and γ. Due the high possible accepted values of α, β and γ that can be generated (dot points in Fig. 4.4.2, Fig SI 4.5, Fig SI 4.6 and Fig. SI 4.7), it was observed that the set of three equations at some points were ill-conditioned.
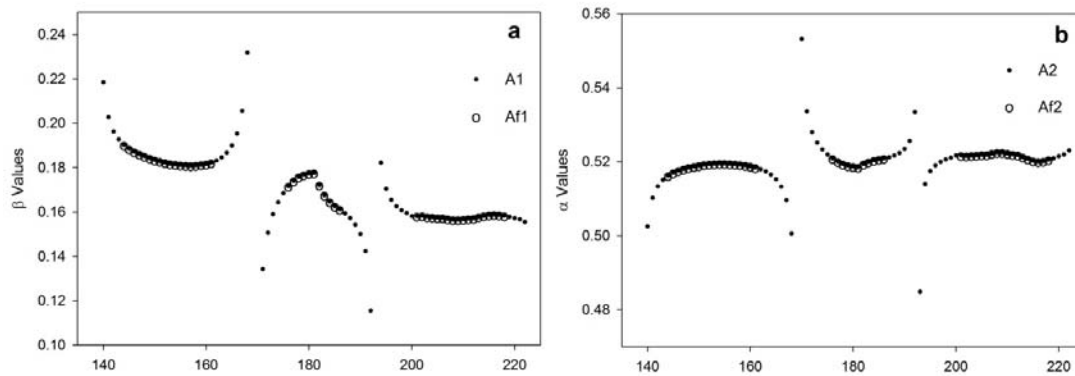
Figure 4.4.2 β and α values obtained before (A1, A2) and after (Af1, Af2) applying the conditional number threshold in the binary mixture (FP) at 0.15 mmol L^{-1}.

By this sense, it was applied a threshold parameter to the condition number, that measures the sensibility of a system of equations to changes or errors with a condition number which do not accomplish (achieve) this criteria. As can be seen in Fig. 4.4.2, "o" points are the accepted final values after applying the threshold parameter.

In this work, it was checked two different thresholds (10% and 100%) where the set of three equations with conditional number greater than 10% or 100% were rejected than minimum condition number of all sets of three equations.

Finally the accepted values were averaged to obtain α, β and γ values and then determine the different final concentrations of each compound in the mixtures. Moreover, it was calculated the expected error of the analysis or the experiment.

2.6 Batch multi adsorption studies

For equilibrium adsorption studies, 10 mg of adsorbent was added to 50 mL of organic compound solutions in different concentrations (0.01-0.3 mmol L^{-1}). The mixtures were stirred at 25ºC using a multipoint agitation plate. After 24 hours, the samples were taken out and filtered through a cellulose acetate filter (0.45 μm pore diameter) and the spectrum of the remaining mixture was obtained by the UV/Vis-visible spectrophotometer (Lambda 25 PerkingElmer) and analysed. The compound uptake (q) of each mixture solution, was determined by means of the formula:

$$q = \frac{(C_0 - C_f) V}{W} \qquad (10)$$

where q is the amount (mmol g^{-1}) of organic compounds adsorbed, C_0 and C_f are the initial and final concentration (mg dm^{-3}), respectively, V is the volume (dm^3) of adsorbate solution and W is the weight (g) of activated carbon used.

3. Results and discussion

3.1 Vierordt's and cross-correlation method

As can be seen in table 4.4.3, the determination of two or three compounds were possible though direct absorbance measurements using the Vierordt's method at the

maximum wavelengths. However, high differences between the values of the parameters α, β and γ obtained from the different solutions at 0.15 mmol L^{-1} are observed. The parameter β shows values between 0.1399 and 0.1830. Furthermore, incongruent results were obtained on the α, β and γ on the ternary solution, which γ was negative. These results can suggest that the resolution of the Vierordt's equations on the maximum wavelength is not the optimum solution due to the equations system can give multiple solutions.

Table 4.4.3 Comparison of α, β and γ between Vierordt's and Cross-correlation methods on the different solutions studied

	Vierordt's			Cross-correlation		
	A	**β**	**γ**	**α**	**β**	**γ**
FP	0.5555	0.1399	-	0.5201	0.1707	-
FSA	-	0.1830	0.5160	-	0.1884	0.5058
PSA	0.5175	-	0.5043	0.5382	-	0.5043
Ternary (100%)	0.1106	0.5580	-0.1587	0.5249	0.1994	0.5248
Ternary (10%)	-	-	-	0.5365	0.2065	0.5060

Cross-correlation method shows better results than Vierordt's method. In the cross-correlation method, similar α, β and γ values were obtained from the different solutions. For example, α values are between 0.5201 and 0.5382 that are a extremely narrow range.

The application of different threshold values on the ternary solution show that the lower threshold (10%) can show better results for α and γ values due to the higher similarities of the rest of binary values than the threshold of 100%. Moreover, it can be show that determination of phenol could be a little distort because its spectra is overlapped with the other two (paracetamol and salicylic acid).

Table 4.4.4 shows the error obtained between the analysed and the expected theoretical values. As can be seen, Vierordt's method exhibits higher error on the determination of phenol and paracetamol than cross-correlation method in most the analysed samples. Moreover, the higher errors observed in ternary solution with Vierordt's were due to the discordances of solving of this method using only three points for the equations. On the other hand, the higher error values observed on cross-correlation method were due at the high concentrations used (0.25 or 0.30) caused by the saturation of the apparatus signal.

Table 4.4.4 Error obtained used Vierordt's and cross-correlation method with the expected theoretical values

	Method A			Method B		
	Error P (|%|)	Error F (|%|)	Error SA (|%|)	Error P (|%|)	Error F (|%|)	Error SA (|%|)
FP	0.5-5.0	<20.0	-	2.0-5.0	1.0-6.0	-
FSA	-	2.5-5.0	0.5-4.0	-	3-0-8.0	0.5-7.0
PSA	<20.0	-	1.5-8.0	3.0-10.0	-	3.5-9.5
Ternary	<65.0	>70.0	>90.0	<11.0	<8.0	<5.0

3.2 Binary and ternary batch adsorption studies

The experimental isotherms of the binary and ternary adsorption system studied are shown in the Fig 4.4.3, Fig. 4.4.4, Fig. 4.4.5 and Fig. 4.4.6. These isotherms were compared with the single isotherms in the section 4.1.3. As can be seen, lower adsorption capacities for all the compounds are attained in complex system respect to single ones. This suggests competitive effects between the molecules for the available sites on the activated carbon surface. In general, competitive effects can be attributed to several factors that can be observed on the following binary and ternary adsorption studies (FP, FSA, PSA and ternary); they can be the molecular structure of the competing adsorbates, the initial concentration of the pollutants [3], interactions between the different molecules in solution, change of the adsorbent surface as a consequence of adsorption and displacement effects due competition between the organic molecules for the active site on the carbon surface.

3.2.1 FP adsorption

The shapes of the different isotherms are all type H2 (Fig. 4.4.3) according to the initial slopes and Giles' classification [4,5].

The higher adsorption of paracetamol respect phenol onto the four activated carbons can be due to the high affinity (K_L) of paracetamol for the activated carbon observed in the individual isotherms (Table 4.3.5, section 4.1.3). This feature can be observed at low adsorption concentrations in the individual isotherms, but no at high concentrations. Moreover, similar phenol adsorption is observed on CNAC and F400. F400 shows a high affinity value for phenol than CNAC suggesting that some interactions can be

produced in F400 or in CNAC. The presence of higher adsorption of water on CNAC (Fig. 4.3.4 section 4.1.3) can suggest that adsorption of phenol can be disfavoured. According to Franz et al [6], the effect of hydrogen bonding was not observed on the adsorption of phenol on oxygenated surfaces due to the adsorption of water was dominant.

The adsorption of phenol is higher on NPK than MAC. Both activated carbons show a chemical interaction on the water adsorption isotherms (Fig 4.3.4, section 4.1.3) suggesting that different interactions can be produced between both adsorbates and the activated carbons.
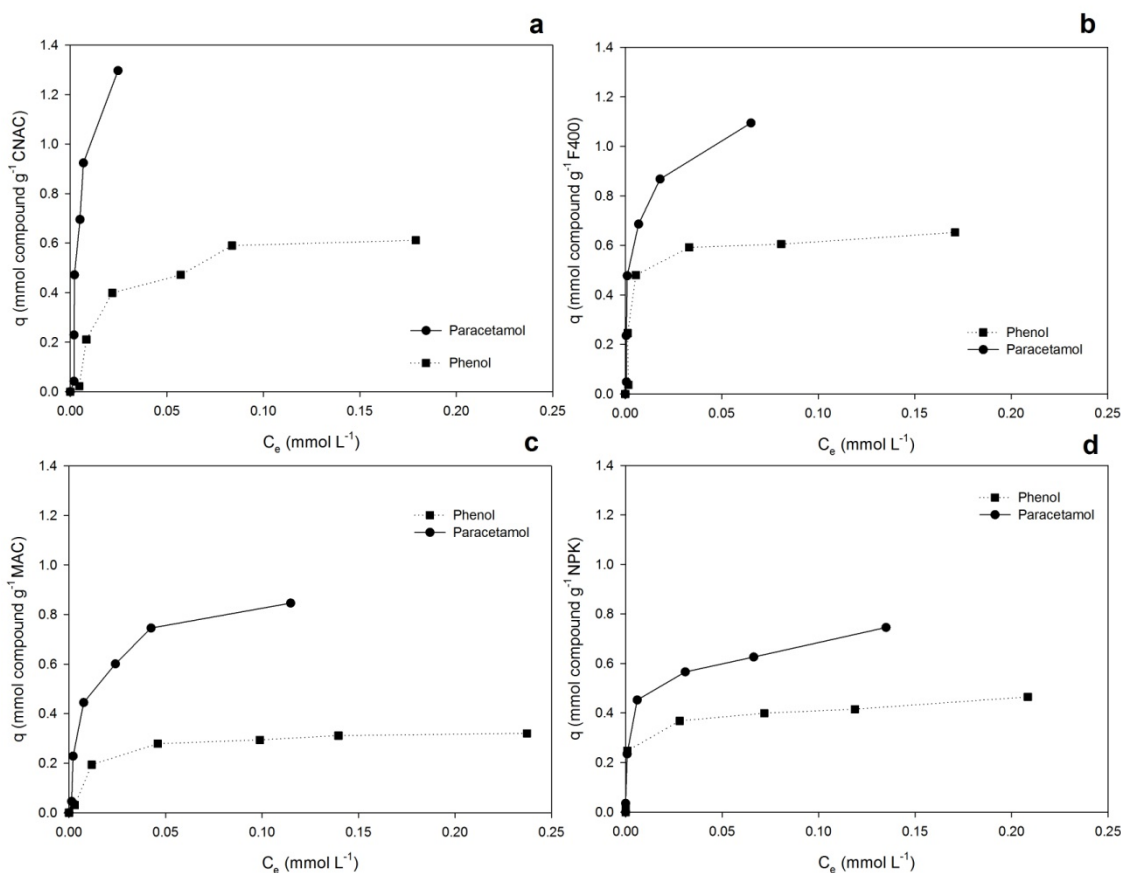
Figure 4.4.3 FP binary adsorption onto the different activated carbons a) CNAC, b) F400, c)MAC, d) NPK

Lorenc-Grabowska et al [7] proposed the formation of a donor-acceptor complex on the wider micropores and mesopores between the surface donor groups and the phenol if it acts as the acceptor [8]; It can be suggested that the higher volume of mesopore on NPK respect of F400 (Table 4.3.4, section 4.1.3) could act as active sites of adsorption of phenol in front of the presence of paracetamol. In this way, Terzik et al. [9] suggested

that phenol can do strong interactions with the surface and the polymerization of phenol can be initiated via the free radical mechanism with oxygen at neutral pH solutions; in the case of paracetamol, its polymerization or creation of chemical bonds can be produced at acidic solutions by interactions via Lewis centers on the carbon surface.

Regarding MAC, the high adsorption of water at low relative pressures (Fig 4.3.4b, section 4.1.3) suggests the lower adsorption of phenol and paracetamol due to the heterogeneity content. The increase of water on the surface of the activated carbon can reduce the π-π interactions of the aromatic ring of phenol and those of MAC, producing the named solvent effect [10].

3.2.2 FSA adsorption

As can be seen in Fig. 4.4.4, the shape of phenol isotherm onto CNAC, F400 and NPK are type S group 2, more pronounced in NPK. The S isotherm can indicate a strong competition between water and phenol molecule due to hydrogen bond formation [7]. In the case of MAC, the shape of the phenol isotherm is type L group 2 suggesting a different affinity of MAC towards to phenol.

On the other hand, the shape of the isotherm for salicylic acid is type L group 2 onto CNAC, F400 and MAC while onto NPK is type L group 3. Moreover, at higher concentrations on CNAC, F400 and MAC it can be observed the 2c subgroup [4,5]; suggesting that some adsorption could be produced on the microporosity in the substrate[4].

The different behaviours showed on Fig. 4.4.4 can be explained by different ways:

As can be seen on Table 4.3.5 section 4.1.3, CNAC, F400 and MAC show a higher affinity (K_L) for salicylic acid than phenol. The S type isotherm suggests that phenol can be adsorbed by hydrogen mechanism and compete with water for the same sites; salicylic acid is favoured in front of this competition because electrostatic interactions can be harder than hydrogen bond.

On the contrary, the affinity of NPK for phenol is higher than for salicylic acid. As can be seen in Fig 4d, the process of adsorption was different respect than the rest of the

adsorbents. It can be suggested that the competition of both molecules for the active sites on the carbon surface could produce a displacement effect on the surface.
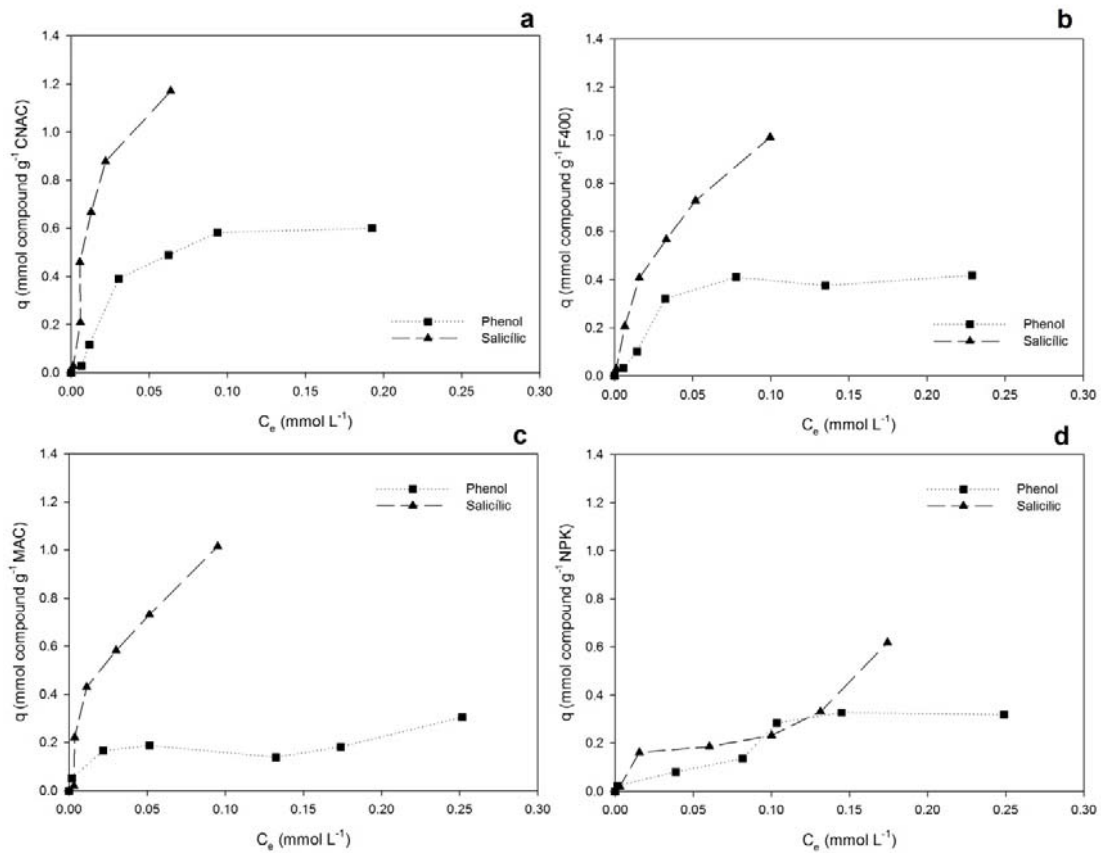
Figure 4.4.4 FSA binary adsorption onto the different activated carbons a) CNAC, b) F400, c) MAC, d) NPK

NPK is a basic activated carbon (pH=11.7), thus at neutral solutions, the surface can be positive charged due to the presence of oxygen groups [11].

$C=O^{\delta-}H^{+} \rightarrow C=O^{\delta-} + H^{+}$ [12] (Negative or positive surface depending on water pH)
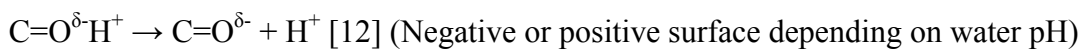
It can be suggested that during the adsorption the pH solution can change due to the different pKa of the compounds, and the surface can be more positive or negative charged favouring the adsorption of phenol or salicylic acid.

3.2.3 Adsorption of PSA

As can be seen in Fig. 4.4.5, the paracetamol isotherm for all the activated carbons is type H2, while for salicylic acid is type L2 onto CNAC, F400 and NPK and type H2 for MAC.

In all the four cases, the K_L values (Table 4.3.5, section 4.1.3) from individual isotherms of paracetamol are higher than salicylic acid. As it is expected, the adsorption of paracetamol is higher than salicylic acid onto activated carbons CNAC, F400 and NPK. On the other hand, a different behaviour is observed onto MAC (Fig. 4.4.5c) which the same adsorption is produced of both compounds. Sulphur groups on the surface can enhance the adsorption of salicylic acid; as it can be suggested the highest K_L value observed on MAC respect the rest of carbons. At neutral solution salicilates interact with the S^+ of the surface increasing the adsorption and blocking the adsorption of paracetamol.

(Positive surface) $C=S^{\delta+}OH + H^+ \rightarrow C= S^{\delta+} + H_2O$ [12,13]
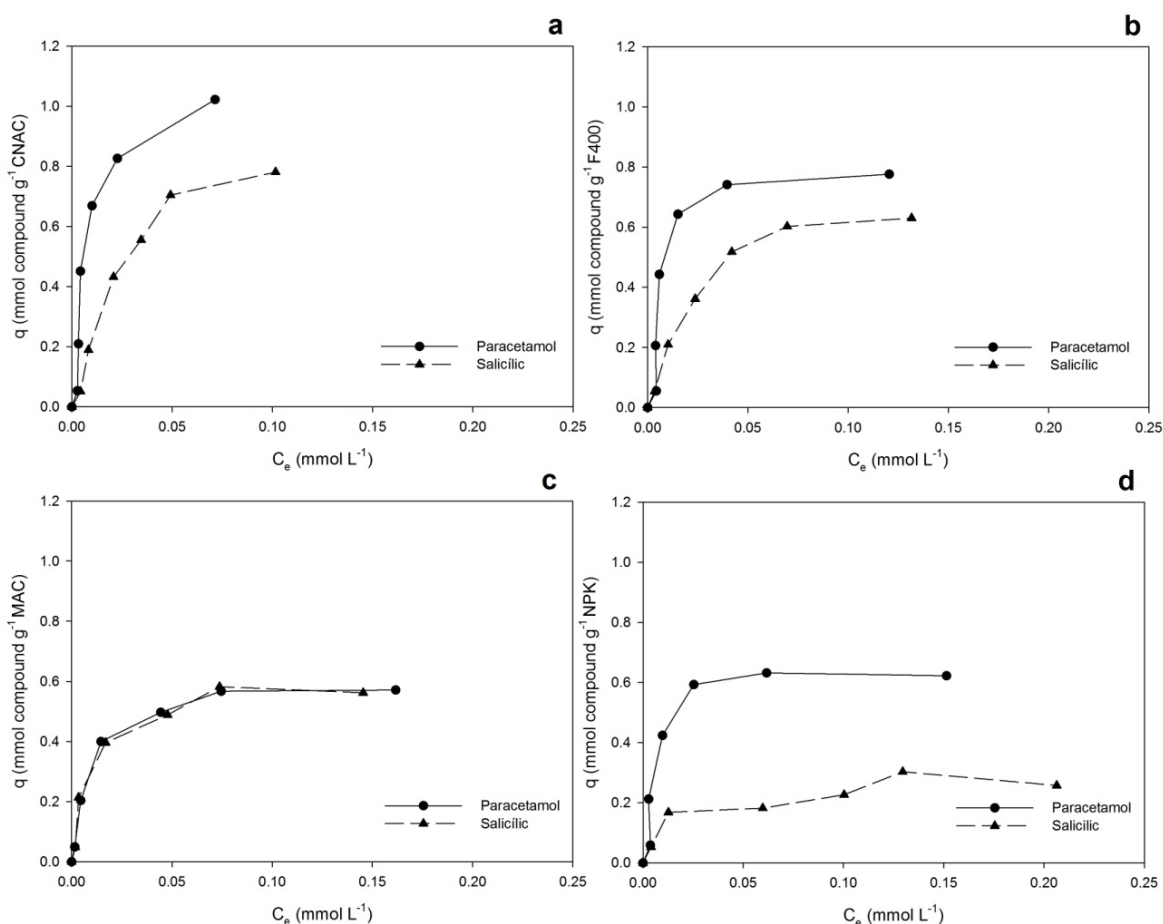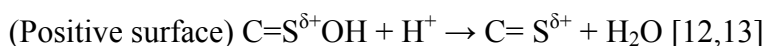
Figure 4.4.5 PSA binary adsorption onto the different activated carbons a) CNAC, b) F400, c)MAC, d) NPK

3.2.4 Adsorption of ternary mixture

In this case (Fig. 4.4.6), similar behaviours are observed between the adsorption on tertiary and binary mixtures. The most significant different is the L max curve observed on phenol isotherm which it can means that an increase in solution concentration decrease the quantity adsorbed of phenol; it can suggest that different interactions can be occurred with phenol and the substrate.

Moreover, the adsorption of salicylic acid is also affected at high concentration onto F400, which the amount adsorbed started to be reduced.

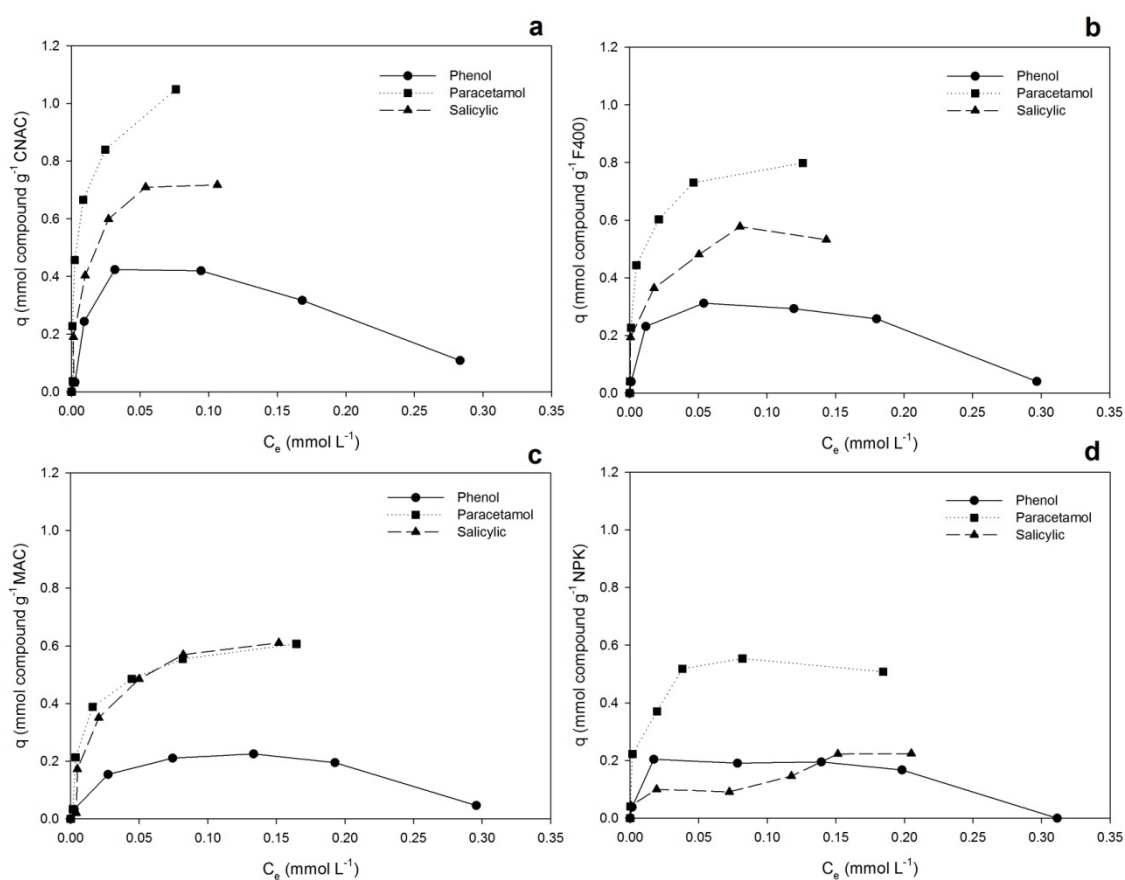**Figure 4.4.6** Ternary adsorption onto the different activated carbons a) CNAC, b) F400, c)MAC, d) NPK

4. Conclusions

This work formulates a new approach to the simultaneous analysis of binary and ternary mixtures of paracetamol, phenol and salicylic acid which have overlapping spectra. The new developed method called cross-correlation was compared with a used traditional

214

method (Vierordt's method). Although Vierordt's method seems to be suitable for the analysis of binary mixtures, it presented some differences on the obtained parameter values α, β and γ. On the other hand, the cross-correlation method developed showed to be a good tool to determine two or three compounds in a mixture at moderate high concentrations. Moreover, high errors can be shown on the analysis of phenol on the Vierordt's method, it can be due for two facts: the overlapped spectra of the different compounds in binary systems, or that Vierordt's equation system, only two or three points, can not give the best answer to the solution.

The different results obtained from the binary and ternary adsorption showed that phenol has a strong competition with salicylic acid for the adsorption onto NPK. It can be due to the different oxygen groups that are in the surface of the activated carbon. These groups can disfavour the hydrogen bonding with phenol adsorbing water as can show the S type isotherm. Moreover salicylic acid adsorption is highly influenced onto MAC due to the presence of sulphur groups can enhance the adsorption of anionic salicylates with the presence of paracetamol. In the case of paracetamol onto the other combinations (binary or ternary), it is the highest compound adsorbed due to the high affinity to the activated carbons. Moreover, the adsorption of the binary solution FP onto CNAC seems to disfavour the adsorption of phenol due to the high quantity of water that CNAC can adsorb.

The new method presented (cross-correlation) has great promise for the routine determination of two or more compounds in mixtures and for the analysis of different pharmaceutical compounds in water and their competition in the adsorption onto different activated carbons.

Agreements

References

[1] E. Dinç, A comparative study of the ratio spectra derivative spectrophotometry, Vierordt's method and high-performance liquid chromatography applied to the simultaneous analysis of caffeine and paracetamol in tablets, J. Pharm. Biomed. Anal. 21 (1999) 723–730.

[2] E. Dinç, F. Onur, Application of a new spectrophotometric method for the analysis of a ternary mixture containing metamizol, paracetamol and caffeine in tablets, Anal. Chim. Acta. 359 (1998) 93–106.

[3] C. Pelekani, V.. Snoeyink, Competitive adsorption in natural water: role of activated carbon pore size, Water Res. 33 (1999) 1209–1219.

[4] C.H. Giles, D. Smith, A. Huitson, General treatment and classification of solute adsorption-isotherms. 1. Theoretical, J. Colloid Interface Sci. 47 (1974) 755-765.

[5] C.H. Giles, A.P. Dsilva, I.A. Easton, General treatment and classification of solute adsorption-isotherms. 2. Experimental interpretation, J. Colloid Interface Sci. 47 (1974) 766-778.

[6] M. Franz, H. a. Arafat, N.G. Pinto, Effect of chemical surface heterogeneity on the adsorption mechanism of dissolved aromatics on activated carbon, Carbon N. Y. 38 (2000) 1807–1819.

[7] E. Lorenc-Grabowska, G. Gryglewicz, M.A. Diez, Kinetics and equilibrium study of phenol adsorption on nitrogen-enriched activated carbons, Fuel. 114 (2013) 235–243.

[8] J.A. Mattson, H.B. Mark, M.D. Malbin, W.J. Weber, J.C. Crittenden, Surface chemistry of active carbon: Specific adsorption of phenols, J. Colloid Interface Sci. 31 (1969) 116–130.

[9] A.P. Terzyk, Molecular properties and intermolecular forces--factors balancing the effect of carbon surface chemistry in adsorption of organics from dilute aqueous solutions., J. Colloid Interface Sci. 275 (2004) 9–29.

[10] A. Dabrowski, P. Podkoscielny, Z. Hubicki, M. Barczak, Adsorption of phenolic compounds by activated carbon - a critical review, Chemosphere. 58 (2005).

[11] J.A. Menendez-Diaz, I. Martín-Gullón, Types of carbon adsorbents and their production, in: T.J. Bandosz (Ed.), Act. Carbon Surfaces Environ. Remediat., first, Elsevier, New York, 2006: pp. 1–47.

[12] E.L.K. Mui, W.H. Cheung, M. Valix, G. McKay, Dye adsorption onto activated carbons from tyre rubber waste using surface coverage analysis, J. Colloid Interface Sci. 347 (2010) 290–300.

[13] M. Valix, W.H. Cheung, G. McKay, Roles of the textural and surface chemical properties of activated carbon in the adsorption of acid blue dye., Langmuir. 22 (2006) 4574–82.

Supporting information

Multicomponent adsorption on coal-based activated carbons on aqueous media: new cross-correlation analysis method

J. Lladó[1]*, Conxita Lao-Luque[1], B. Ruiz[2], E. Fuente[2], Montserrat Solé-Sardans[1], Jordi Bonet[1]

[1]Department of Mining, Industrial and TIC Engineering (EMIT). Universitat Politécnica de Catalunya. Bases de Manresa 61-73, 08242 Manresa, Spain.

[2]"Biocarbon & Sustainability". Instituto Nacional del Carbón (CSIC), Francisco Pintado Fe, 26, 33011 Oviedo, Spain.

*Corresponding author/Email: jordi.llado@emrn.upc.edu
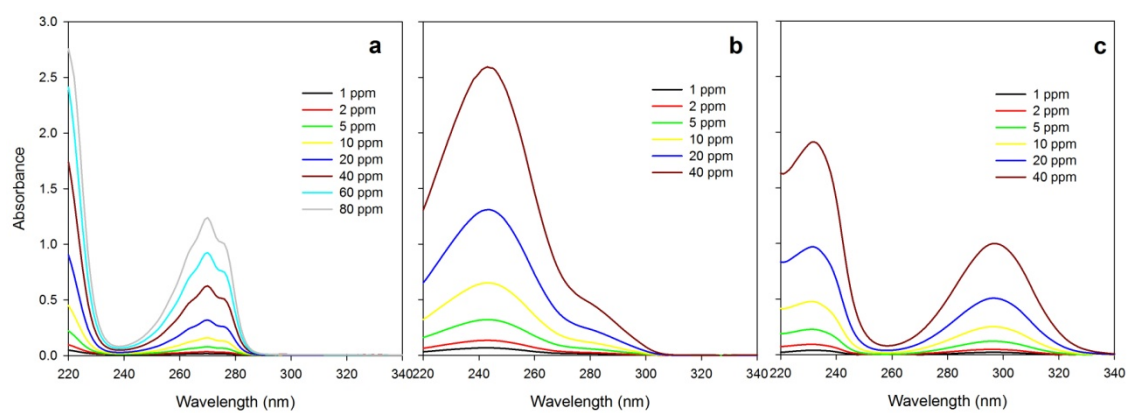
Figure SI 4.4.1 Individual spectra a) S_1 = Phenol b) S_2 =Paracetamol c) S_3 =Salicylic acid
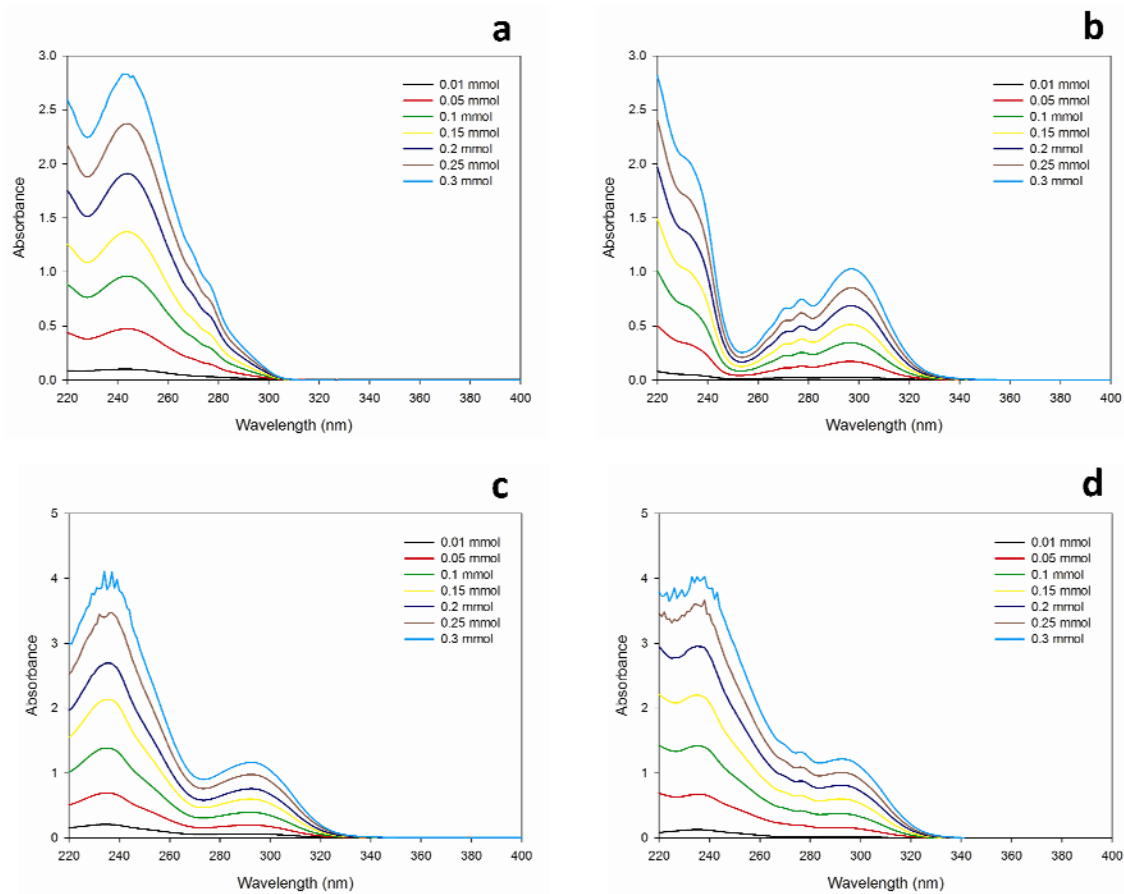
Figure SI 4.4.2 Initial binary and ternary spectra of the different solutions at different concentrations a)b_{12} = FP b) b_{13} = FSA c) b_{23} = PSA d) b_{123} = Ternary
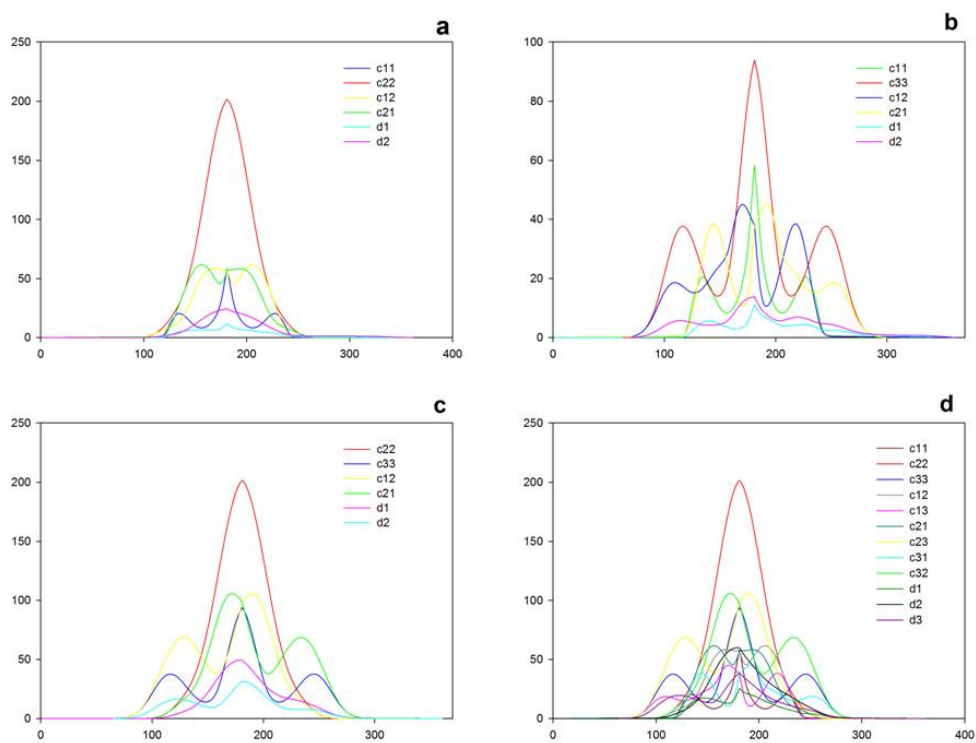
Figure SI 4.4.3 Cross correlation of the different solutions a) FP b)FSA c)PSA d) ternary
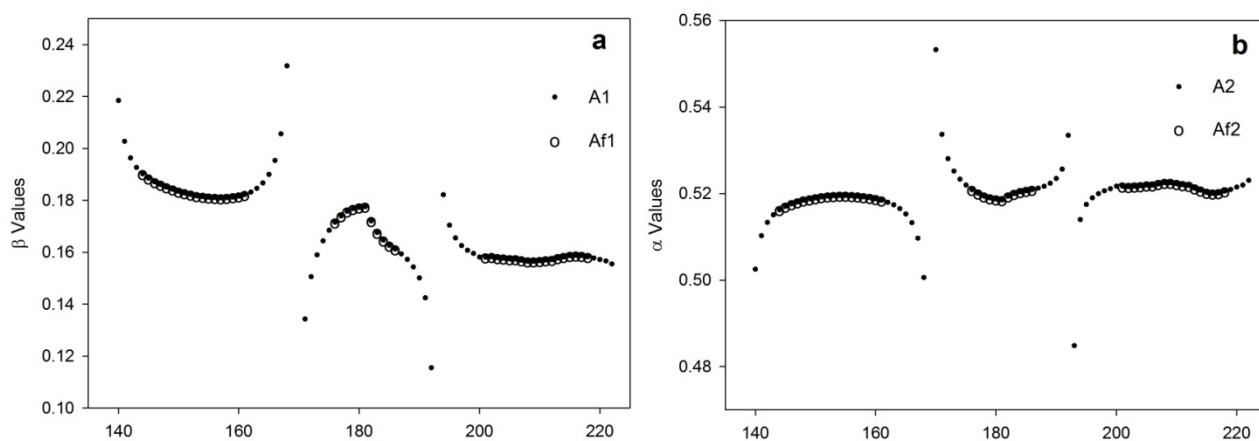
Figure SI 4.4.4 β and α values obtained before (A1, A2) and after (Af1, Af2) applying the conditional number threshold in the binary mixture (FP) at 0.15 mmol L^{-1}
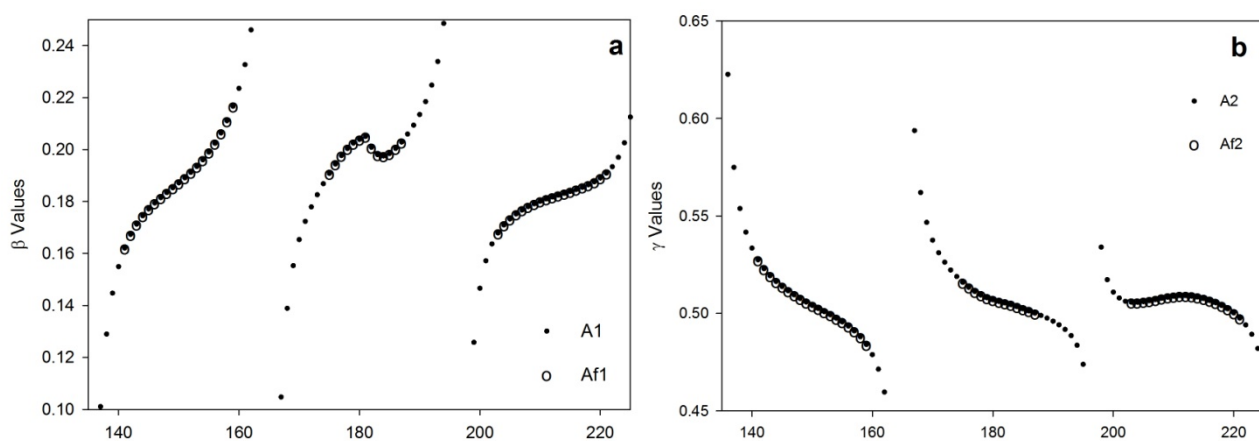
Figure SI 4.4.5 β and γ values obtained before (A1, A2) and after (Af1, Af2) applying the conditional number threshold in the binary mixture (FSA) at 0.15 mmol L^{-1}
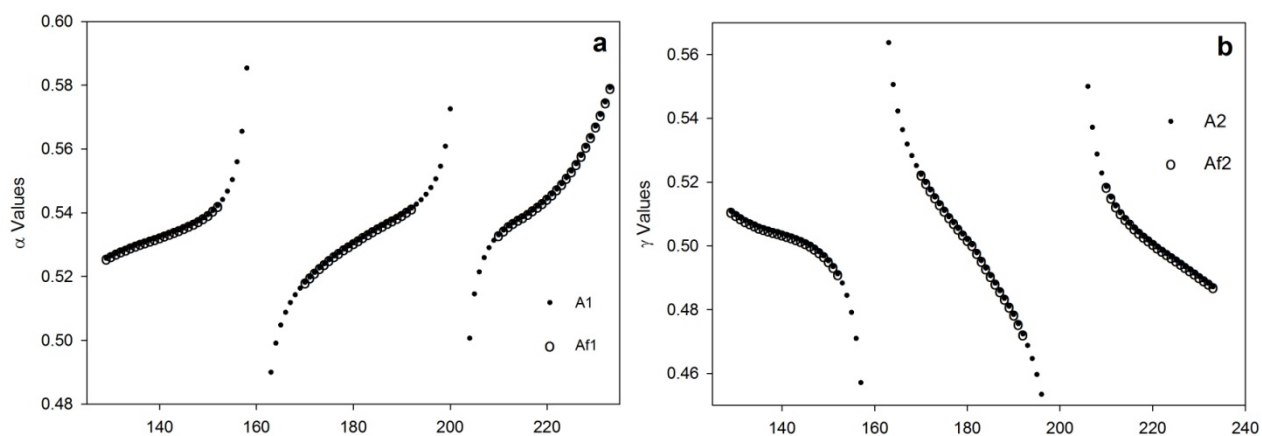
Figure SI 4.4.6 α and γ values obtained before (A1, A2) and after (Af1, Af2) applying the conditional number threshold in the binary mixture (PSA) at 0.15 mmol L^{-1}
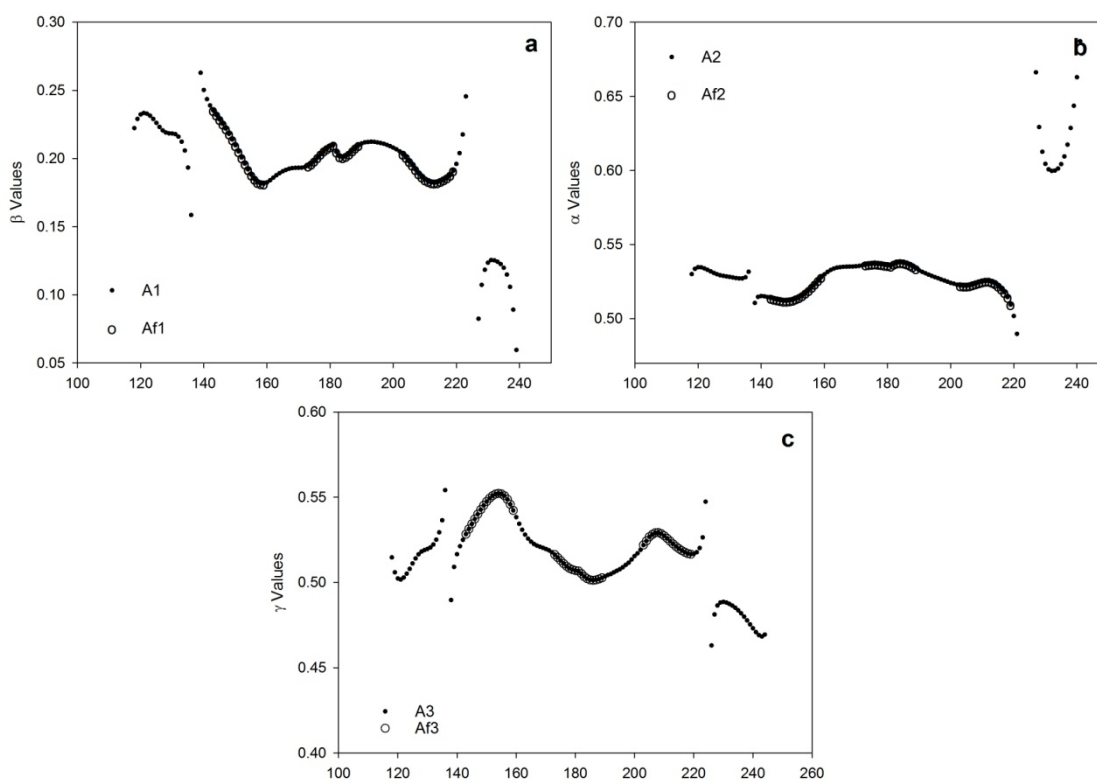
Figure SI 4.4.7 α, β and γ values obtained before (A1, A2) and after (Af1, Af2) applying the conditional number threshold in the ternary mixture at 0.15 mmol L^{-1}
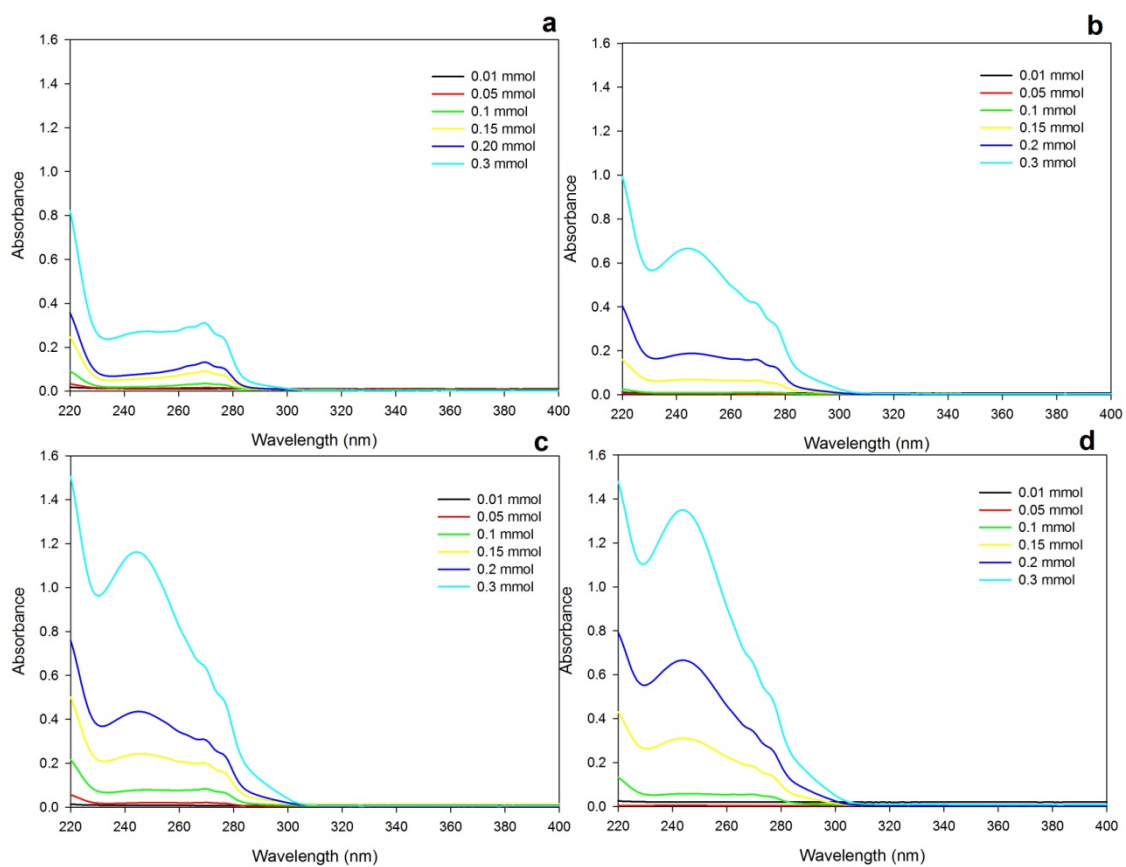
Figure SI 4.4.8 FP adsorption onto a) CNAC b) F400 c) MAC d) NPK
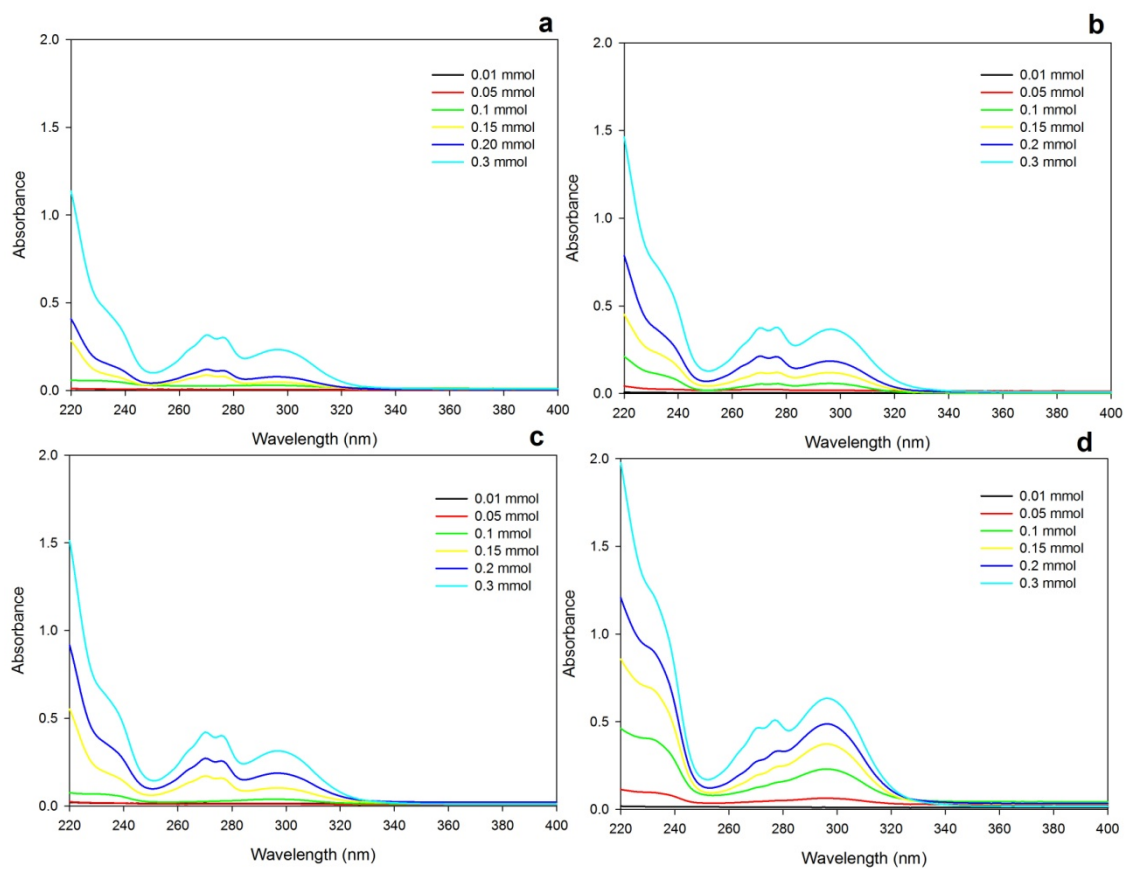
Figure SI 4.4.9 FSA adsorption onto a) CNAC b) F400 c) MAC d) NPK

Figure SI 4.4.10 PSA adsorption onto a) CNAC b) F400 c) MAC d) NPK
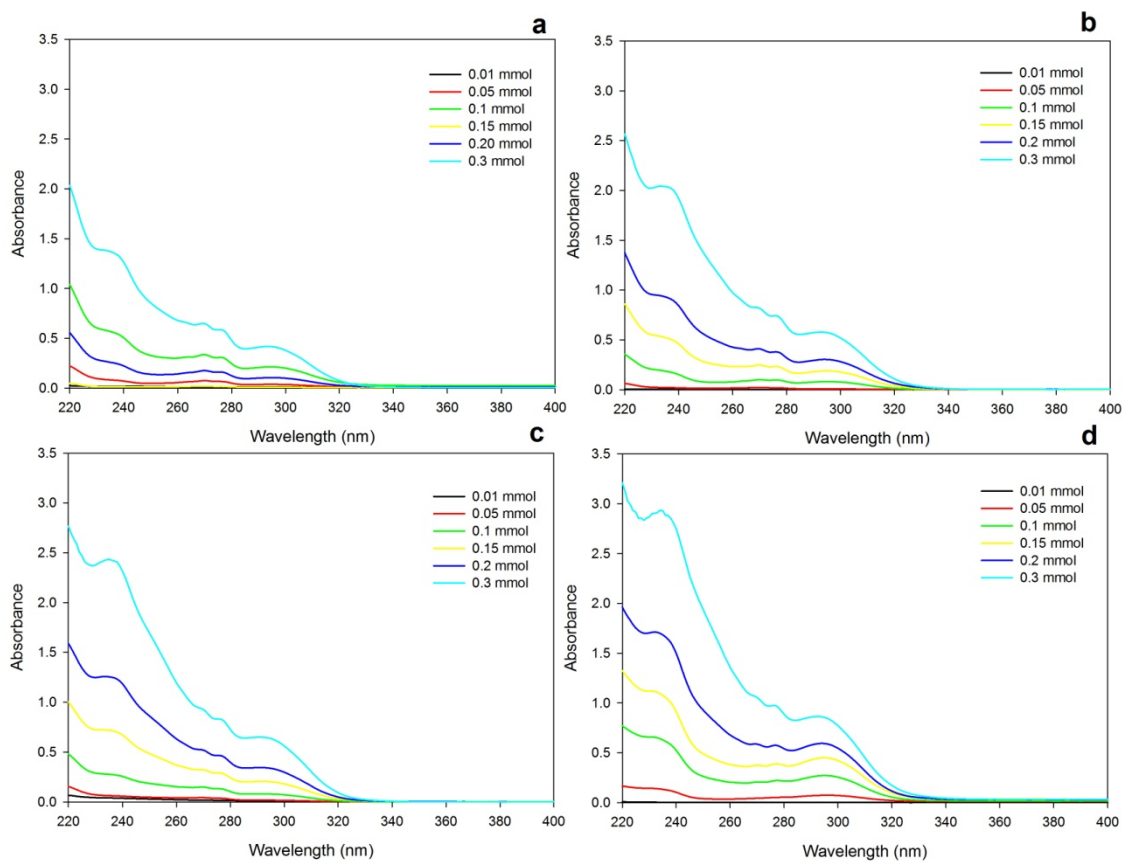
Figure SI 4.4.11 Ternary adsorption onto a) CNAC b) F400 c) MAC d) NPK

Section 4.2.2

"Role of activated carbon properties in atrazine and paracetamol adsorption equilibrium and kinetics."

Role of activated carbon properties in atrazine and paracetamol adsorption equilibrium and kinetics.

J. Lladó[1*], Conxita Lao-Luque[1], B. Ruiz[2], E. Fuente[2], Montserrat Solé-Sardans[1], Antonio David Dorado[1]

[1]Department of Mining Engineering and Natural Resources. Universitat Politècnica de Catalunya, Bases de Manresa, 61-73, 08240

[2]Department of Chemical Processes in Energy and Environment. Instituto Nacional del Carbón (INCAR), CSIC. Francisco Pintado Fe, 26, 33011 Oviedo, Spain

*Corresponding author/Email: jordi.llado@emrn.upc.edu

Abstract

Adsorption of two widespread emerging water contaminants (atrazine and paracetamol) onto three different activated carbons was investigated. The carbons were characterized and the influence of their physicochemical properties on the adsorption performance of atrazine and paracetamol was evaluated. The adsorption equilibrium data were fitted to different adsorption isotherm models (Langmuir, Freundlich, and Dubinin-Radushkevich) while the adsorption rates were described using three different kinetic models (pseudo second order, intraparticle diffusion and a new approach based on diffusion-reaction models). The results indicated that hydrophobic character of the compounds does not affect the sorption capacity of the tested carbons but does influence the uptake rate. The model proposed, based on mass balances, lead to interpret and compare the kinetic of different adsorbents in contrast to classical empirical models. The model is a simple and powerful tool able to satisfactorily estimate the sorption capacities and kinetics of the carbons under different operation conditions by means of only two parameters with physical meaning. All the carbons studied adsorbed paracetamol more effectively than atrazine, possibly due to the fact that sorption takes place by H-bonding interactions.

1. Introduction

The emission of so-called "emerging contaminants" has arisen recently as an environmental problem. This group is mainly composed of compounds used in large quantities in everyday life, such as human and veterinary pharmaceuticals, personal care products, surfactants, pesticides and different industrial additives. Removal of some emerging contaminants in wastewater treatment plants (WWTP) was found to be rather low due to the fact that most of them are resistant to biological degradation. Consequently sewage effluents are one of the main sources of these compounds and their metabolites, which can potentially end up in finished drinking water [1,2].

One effective way to eliminate these recalcitrant compounds could be to introduce an adsorption step before dumping WWTP effluents. Activated carbons are widely used to adsorb organic substances from gases or liquids. They are commonly obtained from various organic precursors such as bituminous coal, peat, wood, coconut shell [3]. In recent years, there has been a growing interest in converting organic waste materials with high carbon content into activated carbon [4]. Sludge is waste material produced in large volumes in the sewage treatment plants. It can be recycled by composting and used in agricultural land, incinerated or used in landfills. Nowadays, new environmentally benign alternatives for this residue are being sought. In this sense, sewage sludge has been investigated as an attractive precursor for activated carbon production [5].

The adsorption capacity of an activated carbon depends on its physic-chemical characteristics (e.g. surface area, pore size, functional groups,..) and the nature of the adsorbate (e.g. molecular weight and size, hydrophobicity, polarity, functional groups [6]. In the literature, several solute properties that influence organic solute adsorption onto activated carbon have been discussed. Some authors have tried to directly relate octanol–water coefficient (Kow) to adsorption capacity [2]. A good relation between this property and adsorption was found for most of the hydrophobic contaminants onto activated carbons. However, a poor correlation was shown when the solutes were small and hydrophilic [7] or when they were aromatic compounds [8]. In the case of aromatic compounds several authors have suggested that they can be adsorbed on activated carbons by dispersion interactions between the π-electrons of the aromatic ring and those of the graphene layers [9]. Functionalization of either the adsorbent or the

adsorbate profoundly affects these dispersion interactions. On the other hand, if the aromatic compounds have hydrogen-bonding functional groups, hydrogen bonding can contribute to the compound adsorption [10,11]. However, the specific mechanisms, through which adsorption of aromatic compounds occur are still not well established.
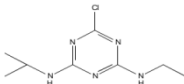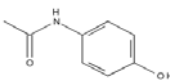
In this work, we study the adsorption of two widespread water emerging contaminants, atrazine (1,3,5-Triazine-2,4-diamine, 6-chloro-N-ethyl-N'-(1-methylethyl)) and paracetamol (N-acetyl-p-aminophenol) onto different activated carbons prepared from various raw materials: a bituminous coal, a lignite and sewage sludge. To understand interactions between the sorbents and the target contaminants, the texture and chemical properties of active carbons were characterized. This research aims to provide new information for a better understanding of the factors and the mechanism involved in the adsorption process. Moreover, a new kinetic model, based on mass balances and description of transfer processes, has been proposed to describe with physical interpretation the sorption kinetic, overcoming the limitation of classic kinetic empirical models.

2. Material and Methods

2.1 Adsorbates

The adsorbates used were a pesticide, atrazine (Sigma-Aldrich, Germany) and a pharmaceutical, paracetamol (Fagron, Spain). Table 4.5.1 shows physico-chemical properties of these two compounds.

Table 4.5.1 Physico-chemical properties of atrazine and paracetamol.

Compound	Atrazine	Paracetamol
Molecular structure		
Molecular formula	$C_8H_{14}ClN_5$	$C_8H_9NO_2$
Molecular weight (g mol^{-1})	215.69	151.16
Log K_{ow}	2.43	0.46-0.49
pK$_a$	2.27	9.86
Molar volume (cm^3 mol^{-1})	169.8	120.9

Paracetamol stock solution (200 mg L^{-1}) was prepared with ultra-pure water (Milli-Q). Atrazine stock solution (1000 mg L^{-1}) was prepared with acetone (Scharlau, Spain). From these solutions, samples for calibration and sorption experiments were obtained by dilution.

2.2 Adsorbents

Three activated carbons were evaluated. Two of them were commercial activated carbons. Filtrasorb-400 (F-400) was supplied by Chemviron (Belgium) and obtained from a bituminous coal. Norit PK 1-3 (NPK) was produced from peat by Norit Americas Inc. (USA). The third carbon was a sludge-based activated carbon-like material (SBC) prepared from sludge from WWTP through the methodology described by Smith and Fowler [12].

2.3 Textural and chemical carbons characterization methods

The texture of the three carbons was characterized by N$_2$ adsorption isotherm at -196 ºC, in a conventional volumetric apparatus (ASAP 2420 from Micrometics). Before each experiment, the samples were outgassed under vacuum at 120ºC overnight to remove any adsorbed moisture and/or gases. The N$_2$ isotherms were used to calculate the specific surface area (S$_{BET}$), total pore volume, (V$_{TOT}$), at a relative pressure of 0.95, and pore size distribution. The pore size distribution (PSD) was evaluated using the density functional theory (DFT), assuming slit-shape pore geometry.

The carbons were further characterized for their elemental analysis using a LECO CHN-2000 and a LECO Sulphur Determination S-144-DR. The ash content and humidity were determined according to the methods described in ISO 1171 and ISO 5068.

FTIR technique was applied in order to determine the main functional groups on the surface carbons. For this purpose spectra were determined between 4000 and 400 cm^{-1} using an FTIR spectroscope (Spectrum 65 FT-IR, PerkinElmer).

2.4 Adsorption assays

For kinetics studies, 50 mg of adsorbent were added to 250 mL of 40 mg L^{-1} atrazine or

paracetamol solutions. Mixtures were stirred at 25°C in a multipoint agitation plate. At different times (from 1 to 48 hours), samples were taken and filtered through a cellulose acetate filter (0.2 μm diameter pore) and the remaining concentrations were analyzed in a UV/Vis spectrophotometer (Lambda 25 PerkinElmer) at 242 nm for paracetamol and 224.9 nm for atrazine. The detection limit for paracetamol was 144 ppb and for atrazine 220 ppb. The paracetamol and atrazine uptake (q_t) was calculated by:

$$q_t = \frac{(C_0 - C_t)\,V}{W} \qquad (1)$$

Where q_t is the amount (mg g^{-1}) of atrazine or paracetamol adsorbed at time t, C_0 is the initial concentration (mg L^{-1}), C_t is the concentration at time t (mg L^{-1}), V is the volume (L) of the adsorbate solution and W is the weight (g) of carbon used.

Equilibrium adsorption studies were made at 25°C varying the atrazine or paracetamol concentration (1-150 mg L^{-1}). The remaining atrazine and paracetamol concentrations after equilibrium time were determined as described above and the uptake was calculated using Eq. (1).

2.5 Adsorption modeling

Isotherms experimental data were fitted to two-parameter isotherm models: Langmuir (Eq.2), Freundlich (Eq.3) and Dubinin-Radushkevich (DR) (Eq. 4,5 and 6)

$$q_e = \frac{q_{max}K_L C_e}{1 + K_L C_e} \qquad (2)$$

$$q_e = K_f C_e^{\,1/n} \qquad (3)$$

$$\ln q_e = \ln q_{max} - \beta \mathcal{E}^2 \qquad (4)$$

$$\mathcal{E} = RT \ln\left(1 + 1/C_e\right) \qquad (5)$$

$$E = \frac{1}{\sqrt{2\beta}} \qquad (6)$$

Where q_e (mg g^{-1}) is the amount of compound adsorbed per mass unit of activated carbon, C_e (mg L^{-1}) is the organic compound concentration at equilibrium, q_{max} (mg g^{-1})

is the maximum adsorption capacity, K_L (L mg^{-1}) is a constant related to the affinity between the pollutant and the adsorbent, K_f ((mg g^{-1}) (L mg^{-1}) $^{1/n}$) is the Freundlich sorption constant and "n" is a constant related to adsorption intensity. $\mathcal{E}$ is the Polanyi potential, R is the gas universal constant (J (molK)$^{-1}$), T is temperature (K) and β is a constant related to free energy (E) of adsorption (Jmol^{-1}) of the adsorbate.

Kinetic modeling in sorption processes has been described for different approaches [13-16]. In the present work, the different kinetic models such as pseudo-second order (Eq. 7), intraparticle diffusion (Eq. 8), and the diffusion-adsorption model were used to describe the non-equilibrium stage of adsorption.

$$\frac{\partial q_t}{\partial t} = k_2 \, (q_e - q_t)^2 \qquad\qquad (7)$$

$$q_t = k_p t^{0.5} + A \qquad\qquad (8)$$

Where k_2 (L (mg min)$^{-1}$) is the rate constant, k_p is the intraparticle rate constant (mg (L·min$^{0.5}$)$^{-1}$) and A is the intercept (mg L^{-1}).

The diffusion-adsorption model is based on the well-known diffusion-reaction mathematical model [17] which has been successfully used in a wide range of chemical engineering related systems [18]. The model proposed is based on the following assumptions:

1.-Isothermal conditions across the batch system and over time.

2.-Planar geometry and perpendicular diffusion through the solid are used to derive to the model equations.

3.-The aqueous-solid interface resistance is negligible.

4.-Aqueous-solid interface equilibrium is described by Langmuir's isotherm, according to previous results (Table 4.5.4).

5.-There is a maximum penetration depth for the pollutant into the solid phase.

Isothermal conditions are needed to define the isotherm equilibrium and they are ensured by means of controlled room temperature. Planar geometry only influences in the coordinate system used for solving the differential equations. The assumption that

interface resistance is negligible is consistent with the operation conditions used in the experimental work since an optimal stirring was ensured. Finally, the concept of maximum penetration is employed for comparing the behavior of the system under different conditions and the boundary set is in concordance with the size of the particles.

According to the above specifications, the mass balance in the liquid phase can be formulated as:

$$\frac{\partial C_t}{\partial t} = -\frac{D * a_s}{\mathcal{E}_D}\left(\frac{\partial C_s}{\partial x}\right)\Big|_{x=0} \qquad (9)$$

for the initial conditions: t=0, $C_t = C_0$

Where D is the diffusion coefficient (m^2 min^{-1}), a_s is the effective specific surface area (m^2 m^{-3}), $\mathcal{E}_D$ is the fraction of liquid in the total volume, C_s and C_t (mg L^{-1}) are organic compound concentrations in the solid and liquid phases, respectively and x is the depth from the sorbent material surface (m).

The mass balance in the solid phase is described by the following equation (10)

$$\frac{\partial C_s}{\partial t} = -D\left(\frac{\partial^2 C_s}{\partial x^2}\right) \qquad (10)$$

With the following boundary conditions:

$$at\ x = 0, \qquad C_s = \frac{q_{max}k_L C_e}{1 + k_L C_e} \qquad (11)$$

$$at\ x = \delta, \qquad \frac{\partial C_s}{\partial x} = 0 \qquad (12)$$

Where δ is the maximum penetration depth for the pollutant into the solid phase (m), q_{max} and k_L are the Langmuir constants shown in Table 4.5.4. The set of partial differential equations was discretized in space in eight nodes along the sorbent thickness [18].

The parameter estimation of the different isotherm and kinetic models were solved using MATLAB, minimizing the objective function (OF) given in the equation (13).

$$OF = \sqrt{\sum_{i=1}^{N} [q(P_1, P_2) - q^*]^2} \qquad (13)$$

Where N is the number of measurements realized, q* is the experimental solute uptake, q (P₁, P₂) is the predicted uptake by the model, P_1 and P_2 are the different estimated parameters. In the case of Langmuir, the parameters are q_{max} and K_L, for Freundlich K_f and n, for DR q_{max} and β, for second order k_2 and q_e, for intraparticle K_p and A and for the adsorption diffusion model D and a_s.

3. Results and discussion

3.1 Activated carbons characterization

The results of elemental analysis, ash and humidity of the three carbons (F-400, NPK and SBC) are listed in Table 4.5.2. Data shows that the elemental composition is similar for F-400 and NPK which have high carbon content (about 90%) and differs significantly from those of SBC, which has a carbon content of only 41%. On the other hand, SBC has the highest ash content. High ash content is a common feature of materials prepared from sewage sludge due to the chemical composition and mineral content of this precursor material [19].

Table 4.5.2 Elemental analysis, ash and humidity of the activated carbons.

	F-400	NPK	SBC
Elemental analysis (Dry basis, wt%)			
Carbon	91.00	88.09	41.62
Hydrogen	0.34	0.54	0.62
Nitrogen	1.01	0.88	1.57
Sulfur	0.69	0.24	0.47
Ash	6.92	8.57	55.37
Humidity (wt%)	2.17	5.58	3.97

Carbons textural properties determined from N_2 adsorption isotherms data are summarized in Table 4.5.3. It can be seen that F-400 has the maximum S_{BET} (1234 m^2g^{-1}), approximately twice as high as those of NPK (782 $m^2\ g^{-1}$), whereas the BET surface area of SBC was, by far, the lowest (260 $m^2\ g^{-1}$). This low BET value of

sludge based activated carbon could be attributed to the low carbon content and the high ashes content of their sludge precursor [5,20].

Table 4.5.3 BET area, total pore volume and of ultamicropore, micropore and mesopore of F-400, NPK and SBC activated carbons.

	S_{BET} $(m^2 g^{-1})$	V_{TOT} $(cm^3 g^{-1})$	V_{umi} $(cm^3 g^{-1})$	V_{mi-umi} $(cm^3 g^{-1})$	V_{mi} $(cm^3 g^{-1})$	V_{meso} $(cm^3 g^{-1})$
F-400	1234	0.615	0.154	0.221	0.375	0.077
NPK	782	0.489	0.155	0.064	0.219	0.12
SBC	260	0.161	0.049	0.023	0.073	0.049

With regards to the adsorption isotherm results (Fig. 4.5.1), the F-400 carbon presents the largest nitrogen adsorption followed by the NPK carbon. The N_2 adsorption onto NPK and F-400 takes place, fundamentally, at low relative pressures which is typical of microporous materials.
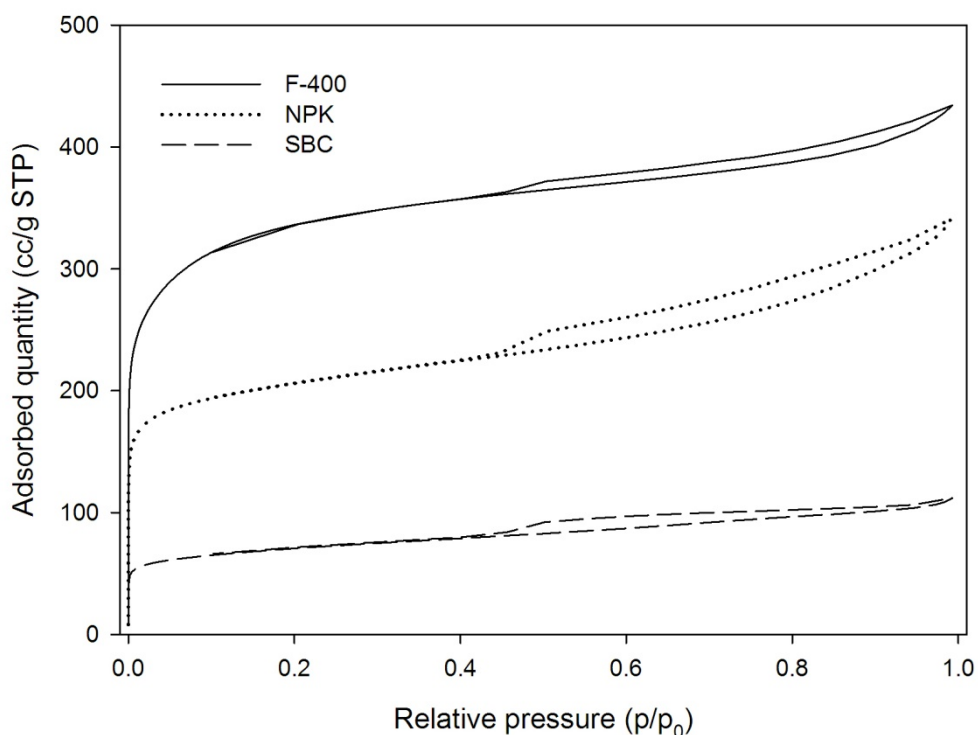
Figure 4.5.1 N_2 adsorption isotherms at -196 ºC for F-400, NPK and SBC carbons.

Their isotherms show a gradually upward increase from relative pressures above 0.2, indicating the presence of well-developed mesoporosity. Moreover these isotherms

show a hysteresis loop, more important for NPK sample, which is associated to capillary condensation inside the mesopores. The adsorption isotherms present a type I-IV hybrid shape according to the BDDT classification, with a sharp knee at low relative pressures for NPK material suggesting that the microporosity of this sample is mainly composed of pores of a small diameter. The broad knee present in the F-400 isotherm indicates that this carbon has micropore sizes greater than those assigned to NPK. The shapes of hysteresis loops have often been related to specific pore structures. In this respect, the shape of the loop in the nitrogen isotherms of the activated carbons is Type H4, according to the IUPAC nomenclature, which is often associated with narrow slit-like pores. On the other hand, the SBC material shows a small N_2 adsorption capacity with an incipient hysteresis loops. The isotherm belongs to Type I in the BDDT classification, with a clear sharp knee at low relative pressures indicating that the microporosity of this sample is mainly composed of pores of small diameter.
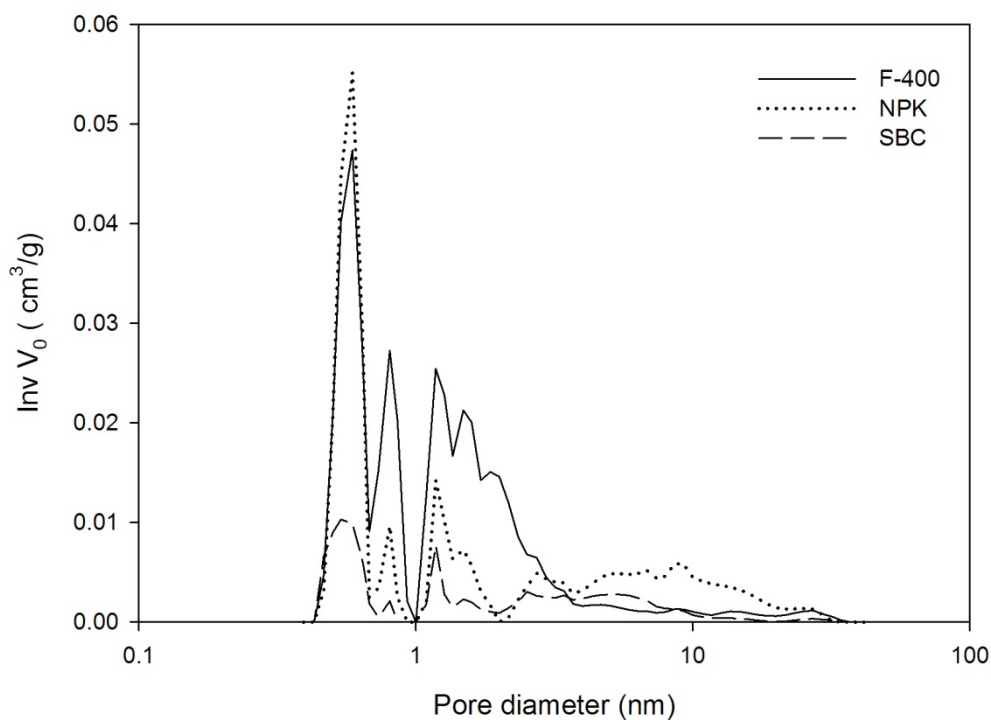
Figure 4.5.2 Pore size distribution of the activated carbons, obtained by application of the DFT model to the N_2 adsorption data at −196 °C.

The total pore volume values (V_{TOT}) are shown in Table 4.5.3. The F-400 exhibits the highest V_{TOT} (0.615 cm^3 g^{-1}) whereas the lowest was obtained for SBC (0.161 cm^3 g^{-1}).

The pore size distribution was calculated by means of the DFT method and the results are presented in Table 4.5.3 and the corresponding plots in Fig. 4.5.2. An intensive peak at the pore diameter range between 0.6 nm and 0.8 nm can be observed for F-400 and NPK carbons (Fig. 4.5.2) indicating the presence of narrow micropores or ultramicropores. This is confirmed by the value of ultramicropore volume obtained for these two carbons, $\approx$ 0.155 cm^3 g^{-1}, (Table 4.5.3). Nevertheless, the contribution of medium-sized microporosity (0.7 nm-2 nm) is much more important in the F-400 activated carbon (0.221 cm^3 g^{-1}) than in NPK carbon (0,064 cm^3 g^{-1}). In contrast, the activated carbon obtained from sewage sludge presents a low value of both, ultramicropore volume (0.049 cm^3 g^{-1}) and medium-size microporosity (0,023 cm^3 g^{-1}).

Regarding mesoporosity, NPK presents the highest mesopore volume (0.120 cm^3 g^{-1}) which is significantly higher than those of F-400 (0.077 cm^3 g^{-1}) and SBC (0.049 cm^{3}g^{-1}) carbons.

The carbons were also characterized by infrared spectroscopy in order to get information about the main functional groups on the carbons surface. The three IR spectra exhibit a similar profile as can be seen in Fig. 4.5.3.
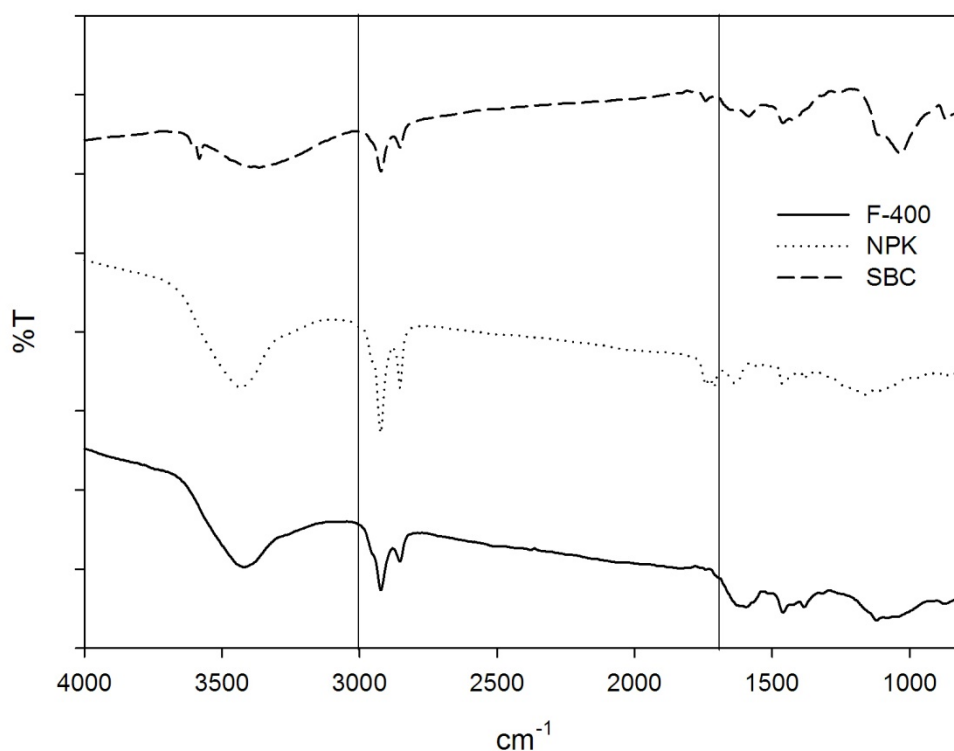
Figure 4.5.3 IR spectra of SBC, NPK and F-400 carbons.

However, there are some significant differences among them. In regards to the common bands, the broad band in the 3500-3200 cm^{-1} region due to O-H stretching vibration can be seen. This band appears in all three recorded spectra, but it is considerably more intense in F-400 and NPK than in SBC. This hydroxyl function could belong to an alcohol, phenol or carboxylic group. However, for F-400 spectra, the absence of a peak at approximately 1750-1680 cm^{-1} characteristic of C=O stretching vibrations rules out the presence of carboxylic group. In contrast, NPK and SBC spectra show a weak band at 1741 cm^{-1} that indicates the presence of carbonyl function.

The two closest and acute bands at 2925 and 2853 cm^{-1} also appear in the three spectra and correspond to asymmetric and symmetric C-H stretching vibrations of aliphatic groups, -CH$_3$ and –CH$_2$-. These bands are more intense in the two commercial activated carbons than in the SBC. Their corresponding bending vibrations are observed between 1470 and 1380 cm^{-1}. The overlapped bands at the 1585-1650 cm^{-1} region, also common for the three carbons, are due to C=C stretching vibrations in sp^2 hybridized carbons in polyaromatics rings. This band is substantially stronger in F-400 activated carbon than in NPK and exhibits a very low intensity in SBC. An important point of difference between the two commercial activated carbons and SBC appears at 1000-1111 cm^{-1} region cm^{-1}. This strong band, only present in SCB activated carbon spectra, could be attributed to Si-O stretching vibration of mineral matter contained in the carbon (silicates). This result is in agreement with the high ash content found in SCB activated carbon.

3.2 Adsorption isotherms

Adsorption isotherms for atrazine and paracetamol sorption on F-400, NPK and SBC activated carbons are shown in Fig. 4.5.4. According to their initial slopes, the NPK and SBC isotherms can be classified as L-type, whereas the F-400 isotherm is H-type according to Giles' classification [21,22]. This suggests that F-400 has a high affinity for atrazine and paracetamol.

The experimental data were fitted to two-parameter isotherms (Langmuir, Freundlich and Dubinin-Radushkevich). The constants obtained from these three models and the objective function (OF) values are listed in Table 4.5.4.
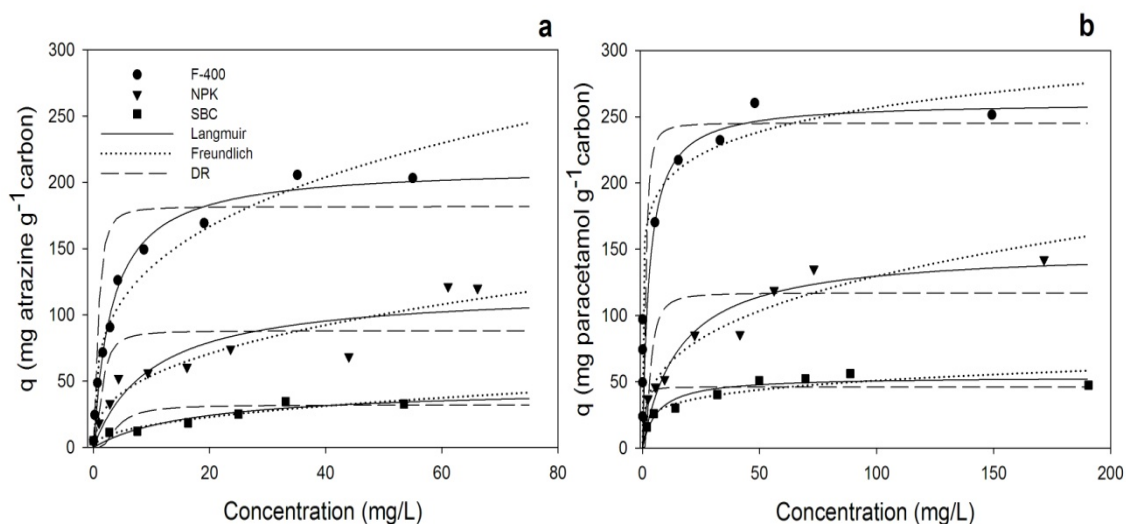
Figure 4.5.4 Experimental data and model predictions for a) atrazine and b) paracetamol adsorption onto the different activated carbons.

Table 4.5.4 Isotherm parameters for atrazine and paracetamol sorption on F-400, NPK and SBC.

		Atrazine			Paracetamol		
		F 400	**NPK**	**SBC**	**F 400**	**NPK**	**SBC**
Langmuir	q_{max}	212.26	119.45	45.49	261.04	150.08	53.75
	K_L	0.31	0.09	0.05	0.35	0.06	0.15
	OF	26.79	45.80	9.65	135.10	37.14	12.89
Freundlich	Kt	69.57	22.28	5.99	157.07	28.79	19.04
	n	3.42	2.59	2.23	9.35	3.06	4.69
	OF	44.45	38.65	9.09	138.29	29.57	16.82
DR	β	0.01	0.02	0.13	0.02	0.09	0.02
	q_{max}	181.76	87.96	32.02	245.18	116.97	45.97
	OF	74.43	63.58	15.09	136.52	68.78	22.54
	E	7.45	4.77	1.93	4.90	2.34	5.87

According to the OF values, the Langmuir equation provides a better description of the atrazine and paracetamol adsorption onto F-400 and SBC activated carbons, while the Freundlich model explains better the adsorption of these compounds on NPK. DR isotherm shows a lower fitting (higher values of OF) for all the studied cases, indicating this model does not offer a satisfactory description of the experimental behavior. As can be seen from Fig. 4.5.4, the NPK experimental isotherm presents two steps: a first step with a short plateau, followed by an increase in the amount of the micropollutant adsorbed and then, a second plateau. This profile, which is more pronounced for

243

atrazine sorption, could be related to the higher mesoporosity of NPK carbon. Konda et al. [23] showed that the sorption behavior of some organic pesticides on soil could be described by a two-step isotherm and they pointed out that this shape might represent the occurrence of a different type of adsorption mechanism.

F-400 exhibits the highest adsorption capacities (q_{max}) for the two adsorbates (Table 4.5.4). Moreover, the higher value of K_L for F-400 compared to those of NPK and SBC indicates that F-400 has a greater affinity for the two contaminants. The different behaviors of the three carbons can be attributed not only to their different surface area but also to their different size pore distribution, functional groups and mineral matter content [10,24].

To assess the influence of pore size distribution on atrazine and paracetamol adsorption, the maximum adsorption capacities (q_{max}) were correlated with the meso, micro and ultramicroporous volumes of the three activated carbons (Table 4.5.5).

Table 4.5.5 Correlation of determination (r^2) for atrazine and paracetamol sorption capacity (q_{max}) with pore volume.

	Correlation coefficient (r^2)	
	atrazine	Paracetamol
Ultramicropores (< 0.7 nm)	0.680	0.707
Supermicropores (0.7-2 nm)	0.934	0.920
Mesopores (2-50 nm)	0.109	0.125

As it can be seen, the maximum adsorption capacity (q_{max}) shows a good linear correlation with the micropore volume values in the 0.7-2 nm width range, suggesting that sorption occurs predominantly in this kind of pores. These results agree with those obtained by other authors studying similar micropollutants sorption on different activated carbons [9,10,25]. In this sense, the high adsorption of the F-400 carbon could be ascribed to its higher microporous content compared to the other two carbons. The low adsorption capacity of SBC is due to its lower surface area. In addition, the high amount of SBC mineral matter might have a negative effect on the sorption process because mineral matter is able to block the pores of the carbon matrix by adsorbing water due to its hydrophilic character [10]. In this sense, Dorado et al. [26] observed for the same material (SBC) a decrease of around 60% in the sorption capacity for the organic compounds due to the competition with water for the active sites. However,

when comparing the sorption capacity for the same specific surface area, the amount of paracetamol adsorbed per square meter of adsorbent material (0.207 mg m^{-2}) is higher than that of NPK (0.192 mg m^{-2}) and even similar to that of F-400 in the case of atrazine (0.175 and 0.172 mg m^{-2} respectively).

When the two compounds adsorptions are compared, it can be seen that paracetamol is more adsorbed than atrazine onto the three activated carbons (Table 4.5.4). The adsorption of organic compounds is influenced by different molecular features such as the size, the hydrophobicity and the nature of the functional groups which determine the interaction between the adsorbent and adsorbates (π-π interactions, Hydrogen bounds) [10].

Although paracetamol is slightly smaller than atrazine, its molecular dimensions are very similar (0.65 nm for paracetamol and 0.72 nm for atrazine) [27]. Thus, the two molecules are small enough to access the micropores with widths in the 0.7 to 2 nm range. Consequently, the differences found in sorption capacities cannot be attributed to size exclusion effects.

It is well known that the nonpolar surface of activated carbons preferably adsorbs hydrophobic compounds with a high octanol/water coefficient (K_{ow}). The K_{ow} may be regarded as an initial indicator of the sorption onto activated carbon [7]. Mohamed et al. [6] studied the adsorption of four substituted phenols and concluded that the compound's hydrophobicity is the main factor determining a higher adsorption capacity. The same behavior was observed by Li et al. [9] for simple aromatic compounds. According to these studies, as atrazine has a higher K_{ow} coefficient than paracetamol (Table 4.5.1), a higher adsorption might be expected for atrazine if hydrophobic interactions were the main sorption mechanism. However, in our study paracetamol was more adsorbed than atrazine onto the three carbons. These results are in accordance with the findings of other authors. Pan and Xing [28] reported no explicit relationship between the sorption constants on carbon nanotubes and K_{ow} for different organic compounds. De Ridder et al.[2] developed a model to predict equilibrium carbon loading on a specific activated carbon for different solutes that refleted a wide range of solute properties. They concluded that hydrophobic partitioning was the dominant removal mechanism for solutes with log $K_{ow} > 3.7$. However, solutes with a relative low log K_{ow} and with groups which are capable of forming H-bonds (such as the compounds

tested in the present study) showed higher carbon loading at similar log K_{ow} values than the solutes without these groups. This means that K_{ow} is not always a determinant factor in adsorption.

Several works indicate that the π-stacking interaction between aromatic π-systems in organic compounds and in sorbents is a key mechanism in adsorption processes [10,29,30]. Atrazine and paracetamol have different aromatic rings in their structure. Inductive and resonance effects of the substituents affect the charge distribution within aromatic molecules. The –NHR and –OH groups in paracetamol causes an electron density addition to the aromatic ring so that it can act as a π-donor. Conversely, atrazine is a π-deficient N-heterocyclic compound and has a –Cl substituent which is electron-withdrawing. These two features make atrazine a π-acceptor compound. On the other hand, the IR analyses showed that the F-400 and NPK carbons have -OH aromatic groups which increase the electron density of the activated carbon graphitic planes. This makes activated carbon a surface π-donor. It was therefore expected that atrazine (π-electron acceptor) would have more affinity for these activated carbons than paracetamol. However, our experimental results do not support this theory.

Another possible mechanism proposed for organic compounds sorption is that based on H-bonding interactions [2,10,11,31,32]. O-H groups present on the surface of the activated carbons can form H-bonds with N-H in Atrazine and O-H in paracetamol. Because OH-OH interactions are more intense than OH-NH interactions, this adsorption mechanism could explain the fact that paracetamol was more adsorbed than atrazine. Furthermore, *in* the case of atrazine, the steric effect of side-chains might hinder the formation of hydrogen bonds between the molecule and the functional groups of the activated carbons. This proposed mechanism is in agreement with Terzyk [33] which proposed different adsorption mechanisms for different organic molecules (paracetamol, aniline, phenol and acetanilide) depending on pH conditions. At neutral pH paracetamol was adsorbed via OH group in carbon and carbon modified with NH_3, and via amide group on modified carbons with acid (H_2SO_4 and HNO_3). On the other hand, the interaction of aniline with surface groups was via weak hydrogen bonds (NH) as suggested by the small value of enthalpy adsorption.

3.3 Adsorption kinetics

A series of kinetic studies was performed to compare the rates of sorption of both organic compounds on the activated carbons F-400, NPK and SBC. The kinetics describes the pollutant uptake, which in turn controls the residence time. This is the key to designing further appropriate sorption treatment processes. Concentration profiles over time are shown in Fig. 4.5.5 together with the kinetic models tested.
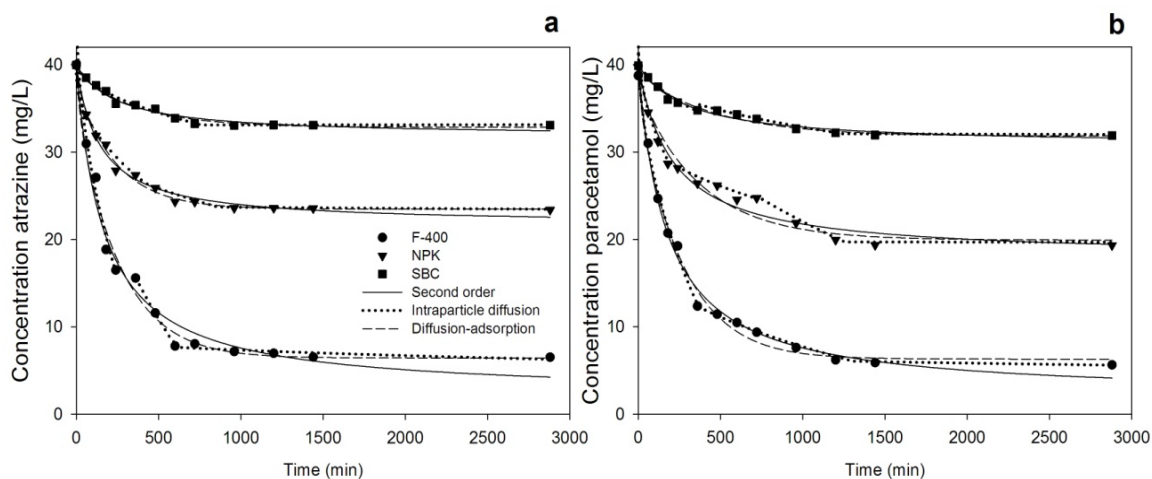
Figure 4.5.5 Kinetic experimental data and models of a) atrazine, b) paracetamol adsorption onto different activated carbons.

The sorption capacity of the carbons influences the abatement rate since the concentration gradient is the driving force of the process. In this sense, the initial removal rate of both compounds on F-400 is significantly higher than on NPK and much superior to that on SBC. In order to compare the kinetic characteristics of each carbon, the parameters that define the three models tested (pseudo second order, intraparticle diffusion and diffusion-adsorption model) were determined by fitting them to the experimental concentrations measured (Table 4.5.6). The OF values indicate the degree of agreement between the model predictions and experimental data. According to the results, the best fitting (the lower OF value) was achieved for the pseudo second order and the diffusion-adsorption models.

In the case of the pseudo second order model, the k_2 value is proportional to the sorption rate on the materials. An analysis of this parameter shows that, although F-400 and NPK have a higher sorption capacity, the kinetic constant is significantly higher in SBC than in the two other carbons (up to 2.8 and 2.3 times higher than F-400 for atrazine and

paracetamol, respectively). These results indicate that with its similar sorption capacity, SBC could become an interesting economic alternative by reducing the time required to achieve equilibrium by more than half.

Table 4.5.6 Kinetic parameters for atrazine and paracetamol sorption on F-400, NPK and SBC.

		Atrazine			Paracetamol		
		F-400	**NPK**	**SBC**	**F-400**	**NPK**	**SBC**
Second order	k_2 x 10^{-4}	1.41	3.5	3.94	1.52	2.16	3.7
	qe (calc) (mg/g)	195.2	93.55	43.7	190.1	110.3	46.2
	OF	4.69	1.69	1.04	3.31	3.52	1.16
Intraparticle	k_{p1}	1.99	0,61	0,27	1,51	1,03	0,35
	A_1	-7.13	1.06	-0.44	-2.86	-2.86	-1.21
	k_{p2}	1.41	0.31	-48	0.37	0.32	0.21
	A_2	-2.36	7.28	7.05	20.69	6.74	0.54
	k_{p3}	0.13	$4.2*10^{-3}$	-	0.03	0.61	$3.8*10^{-3}$
	A_3	28.6	16.19	-	32.99	-1.42	7.79
	k_{p4}	-	-	-	-	$1.3*10^{-3}$	-
	A_4	-	-	-	-	20.24	-
	OF	7.45	4.83	4.63	8.26	3.84	3.16
Adsortion_difusion	**D x 10^{-10}**	7.86	9.29	5.64	7.48	5.9	4.72
	a_s	135.15	112.77	131.34	110.95	109.29	124.75
	OF	4.43	1.48	1.02	3.23	4.15	1.2

An analysis of the results from the intraparticle model, although the model predictions diverge slightly from those of the other models, helps to explain the number of stages that occur in the sorption of each compound (Fig. 4.5.6). Whereas three stages were detected in the sorption of atrazine on F-400 and NPK, only two were observed for SBC. Similarly, SBC was one of the carbons with fewest stages in the sorption of paracetamol (three as against the four stages for NPK). It is thought that when there are three stages, the first one corresponds to the external mass transfer, followed by intraparticle diffusion and finally the equilibrium achievement [34]. The higher number of stages observed in the NPK carbon illustrate the different behavior of the sorption process through mesoporous and microporous according to the previous characterization of the material.
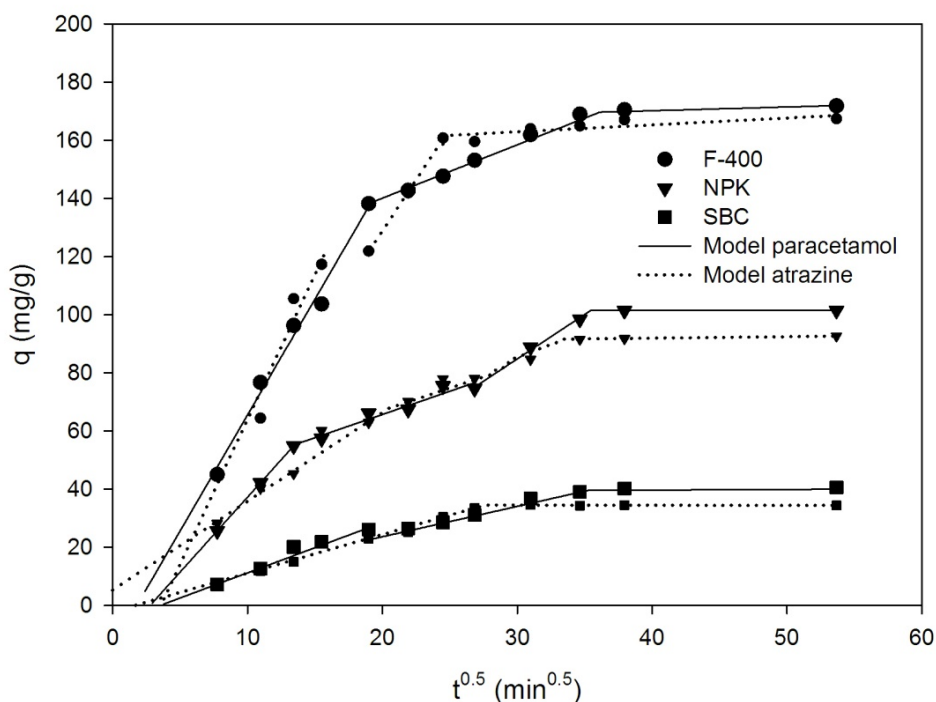
Figure 4.5.6 Intraparticle-diffusion plots adsorption of atrazine and paracetamol on the different activated carbons.

The model developed in the present work, based on the classic diffusion-adsorption reaction models, allows a quantitative comparison of the behavior of different materials by means of only two parameters with physical meaning, in contrast to the previous empirical models. The coefficient diffusion (D) value denotes the relative rate of transfer through the material (i.e. sorption rate) and the effective area (a_S) is the relative amount of area involved in the process. Thus, the most relevant information obtained from this model is that SBC, although it shows the lowest specific surface area, in terms of kinetic behavior has an effective area of the same order of magnitude as F-400 and NPK. In view of the specific surface area of the three materials (Table 6) the percentage of effectiveness was found to be between 11% for F-400 and 50% for SBC.

In comparison, for the same carbon and without any exception, the diffusion coefficient of atrazine is always higher than for paracetamol. Although the sorption capacity for atrazine (more hydrophobic) is lower than paracetamol (Table 4.5.4), atrazine is adsorbed onto the carbons at a higher rate (and, thus, in a shorter contact time).

4. Conclusions

The characterization of the three activated carbons revealed that F-400 has the highest total microporous volume, containing mainly medium-sized micropores (0.7 nm-2 nm). NPK was found to have the highest mesopore volume whereas its microporosity consists fundamentally of ultramicropores (<0.7 nm). SBC shows low micro and mesoporosity, probably due to its precursor characteristics. F-400 has the highest aromaticity. In contrast, NPK and SBC are richer in carboxylic groups.

The Langmuir equation describes the atrazine and paracetamol adsorption onto the F-400 and SBC activated carbons whereas the Freundlich model explains the adsorption of these compounds onto NPK carbon better. The NPK isotherm present two steps and this behavior seems to be related with its higher mesoporosity. F-400 exhibits the highest adsorption capacities and a great affinity for the two adsorbates.

Several kinetic models have been used for predicting the uptake rate of emergent contaminants by carbons. The new approach model, presented here, based on diffusion-reaction equations provides the best description of the experimental data. The good agreement with model predictions confirms the feasibility of representing the complex phenomena occurring during sorption by means of relatively simple models. This model provides a powerful predictive tool together with relevant process parameter values (effective area and diffusion coefficient), which allow the characterization and comparison of different materials by means of fitting parameters with physical meaning (e.g. relation between diffusion coefficient and size of pores). Similarly, different surface coatings, carbon activation processes and carbon origins, among others, could be assessed, focusing not only on sorption capacities but also on kinetic limitations. For instance, these kinetic studies have shown SBC to be a promising sorbent material if the specific surface area can be enhanced. The hydrophobic character of the compounds does not show any correlation with the sorption capacities of carbons but it directly relates with the uptake rate, which is a decisive parameter if contact time is a critical factor.

Irrespective of the pore structure and surface chemistry, the three activated carbons showed a higher adsorption capacity for paracetamol than for atrazine. Taking into

account the characteristics of these compounds, hydrogen bonding is likely to be the main mechanism governing the sorption of the two contaminants.

Acknowledgements

Section 4.2.2

References

[1] Petrovic, M., Gonzalez, S., Barcelo, D., 2003. Analysis and removal of emerging contaminants in wastewater and drinking water. Trends. Anal. Chem. 22, 685-696.

[2] De Ridder, D.J., Villacorte, L., Verliefde, A.R.D., Verberk, J.Q.J.C., Heijman, S.G.J., Amy, G.L., Van Dijk, J.C., 2010. Modeling equilibrium adsorption of organic micropollutants onto activated carbon. Water Res. 44, 3077-3086.

[3] Marsh, H., Rodriguez-Reinoso, F., 2006. Activated carbon. Elsevier Science Ltd.

[4] Schröder, E., Thomauske, K., Oechsler, B., Herberger, S., 2011. Progress in biomass and bioenergy production. Ed Dr. Shahid Shaukat, InTech, 18, 333-356.

[5] Smith, K.M., Fowler, G.D., Pullket, S., Graham, N.J.D., 2009. Sewage sludge-based adsorbents: A review of their production, properties and use in water treatment applications. Water Res. 43, 2569-2594.

[6] Mohamed, E.F., Andriantsiferana, C., Wilhelm, A.M., Delmas, H., 2011. Competitive adsorption of phenolic compounds from aqueous solution using sludge-based activated carbon. Environ. Technol. 32, 1325-1336.

[7] Westerhoff, P., Yoon, Y., Snyder, S., Wert, E., 2005. Fate of endocrine-disruptor, pharmaceutical, and personal care product chemicals during simulated drinking water treatment processes. Environ. Sci. Technol. 39, 6649-6663.

[8] Chen, W., Duan, L., Zhu, D., 2007. Adsorption of polar andnonpolar organic chemicals to carbon nanotubes. Environ.Sci. Technol. 41, 8295–8300.

[9] Li, B., Lei, Z., Huang, Z., 2009. Surface-treated activated carbon for removal of aromatic compounds from water. Chem. Eng. Technol. 32, 763-770.

[10] Moreno-Castilla, C., 2004. Adsorption of organic molecules from aqueous solutions on carbon materials. Carbon 42, 83-94.

[11] Terzik, A. P., 2000. The impact of carbon surface composition on the diffusion and adsorption of paracetamol at different temperatures and at the neutral pH. J. Coll. Interf. Sci. 230, 219-222.

[12] Smith, K.M., Fowler, G.D., 2011. Production of activated carbon from sludge, in Fabregat, A., Bengoa, C., Font, J., Stueber, F. Reduction, modification and valorization on sludge, 1st ed. IWA Publishing London, UK, 141-154.

[13] Clark, R.M., 1987. Evaluating the cost and performance of field-scale granular activated carbon systems. Environ. Sci. Technol. 21, 573–580.

[14] Wolborska, A., 1989. Adsorption on activated carbon of p-nitrophenol from aqueous solution. Water Res. 23, 85–91

[15] Yan, G.Y., Viraraghavan, T., Chem, M., 2001. A new model for heavy metal removal in a biosorption column. Adsorpt. Sci. Technol. 19, 25–43.

[16] Ho, Y.S., McKay, G., 1998. A comparison chemisorption kinetic models applied to pollutant removal on various sorbents. Process Saf. Environ. 76,332-340.

[17] Cutlip, M.B., Shacham, M., 2008. Problem Solving in Chemical and Biochemical Engineering with POLYMATH, EXCEL and MATLAB. Prentice Hall: New York.

[18] Dorado, A.D., Gamisans, X., Valderrama, C., Solé, M., Lao, C., 2014. Cr (III) removal from aqueous solutions: A straightforward model approaching of the adsorption in a fixed-bed column. J. Environ. Sci. Health Part A-Toxic/Hazard Subst. Environ. Eng. 49, 179–186.

[19] Lillo-Rodenas, M.A., Ros, A., Fuente, E., Montes-Moreno, M.A., Martin, M.J., Linares-Solano, A., 2008. Further insights into the activation process of sewage sludge-based precursors by alkaline hydroxides. Chem. Eng. J. 142, 168-174.

[20] Anfruns, A., Martin, M.J., Montes-Moran, M.A., 2011. Removal of odourous VOCs using sludge-based adsorbents. Chem. Eng. J. 166, 1022-1031.

[21] Giles, C.H., Smith, D., Huitson, A., 1974a. General treatment and classification of solute adsorption-isotherm 1. Theoretical. J. Colloid Interface Sci. 47,755-765.

[22] Giles, C.H., Smith, D., Huitson, A., 1974b. General treatment and classification of solute adsorption-isotherm. 2. Experimental interpretation. J. Colloid Interface Sci. 47, 766-778.

Section 4.2.2

[23] Konda, L.N., Czinkota, I., Fuleky, G., Morovjan, G., 2002. Modeling of single-step and multistep adsorption isotherms of organic pesticides on soil. J. Agric. Food Chem. 50, 7326-7331.

[24] Haydar, S., Ferro-Garcia, M.A., Rivera-Utrilla, J., Joly, J.P., 2003. Adsorption of p-nitrophenol on an activated carbon with different oxidations. Carbon 41, 387-395.

[25] Pelekani, C., Snoeyink, V.L., 2000. Competitive adsorption between atrazine and methylene blue on activated carbon: the importance of pore size distribution. Carbon 38, 1423-1436.

[26] Dorado, A.D., Lafuente, F.J., Gabriel, D., Gamisans, X., 2010. The role of water in the performance of biofilters: Parameterization of pressure drop and sorption capacities for common packing materials. J. Hazard. Mater. 180, 693-702.

[27] Rossner, A., Snyder, S.A., Knappe, D.R.U., 2009. Removal of emerging contaminants of concern by alternative adsorbents. Water Res. 43, 3787-3796.

[28] Pan, B., Xing, B., 2008. Adsorption Mechanisms of Organic Chemicals on Carbon Nanotubes. Environ. Sci. Technol. 42, 9005-9013.

[29] Cotoruelo, L.M., Marques, M.D., Leiva, A., Rodriguez-Mirasol, J., Cordero, T. 2011. Adsorption of oxygen-containing aromatics used in petrochemical, pharmaceutical and food industries by means of lignin based active carbons. Adsorpt.-J Int. Adsorpt. Soc. 17, 539-550.

[30] Keiluweit, M., Kleber, M., 2009. Molecular-level interactions in soils and sediments: the role of aromatic pi-systems. Environ. Sci. Technol. 43, 3421-3429.

[31] Villaescusa, I., Fiol, N., Poch, J., Bianchi, A., Bazzicalupi, C., 2011. Mechanism of paracetamol removal by vegetable wastes: The contribution of pi-pi interactions, hydrogen bonding and hydrophobic effect. Desalination 270, 135-142.

[32] Welhouse, G.J., Bleam, W.F., 1993. Cooperative hydrogen bonding of atrazine. Environ. Sci. Technol. 27, 500-505.

[33] Terzik, A.P., 2004. Molecular properties and intermolecular forces – factors balancing the effect of the carbon surface chemistry in adsorption of organic from dilute aqueous solutions. J. Coll. Interf. Sci. 275, 9-29.

[34] Ruiz, B., Cabrita, I., Mestre, A.S., Parra, J.B., Pires, J., Carvalho, A.P., Ania, C.O., 2010. Surface heterogeneity effects of activated carbons on the kinetics of paracetamol removal from aqueous solution. Appl. Surf. Sci. 256, 5171-5175.

Chapter 5

Conclusions

1. Conclusions

This Thesis is focused on the study of the adsorption process for the elimination of different microorganic pollutants (pharmaceuticals, pesticides, industrials,...) in aqueous media by means of different carbon materials. The results of this Thesis are divided in two different sections, which the first one was focused on the adsorption of different polluntants on new carbon materials, the production and characterization of these carbon materials, and the study of the influences involved on the adsorption of organic and emerging pollutants. In the second one was proposed a new method of analysis for a multiadsorption solution and a new kinetic adsorption process, both were also focused on the adsorption of emerging pollutants. The main conclusions of this Thesis are divided into the different works from the chapter 4 (sections I and II):

1.1 Highly microporous activated carbons from biocollagenic wastes as adsorbents of organic pollutants in water from industrial activities

Eight activated carbons were prepared from different biocollagenic precursor materials (biocollagenic wastes (BCT) and pyrolysed biocollagenic wastes (BCTP)) by means of chemical activation with alkaline agents (KOH and K_2CO_3) at different temperatures (750 and 900ºC).

The eight biocollagenic activated carbons were chemically characterized showing a high heterogeneity composition (high carbon nitrogen (from 82 to 93%), high nitrogen content (up to 3%) and different oxygen content (from 2.5 to 10%)). Good textural properties were developed on the different activated carbons S_{BET} from 838 $m^2\ g^{-1}$ up to 1664 $m^2\ g^{-1}$.

All these materials were characterized by a high microporosity and a low grade of mesoporosity. The BCT activated carbons showed a higher development of supermicropores while BCTP materials contain a high volume of ultramicropores.

Textural development were higher using KOH as a chemical agent than using K_2CO_3, although the high temperatures (900 ºC) applied on BCT materials with KOH had a deleterious effect producing lower textural development respect the other materials. In general, the higher activating temperature the higher development of porosity on the activated carbon.

Dispersion/repulsive interactions between activated carbons surface and aromatic compounds with different functional groups (acetanilide, aniline, benzaldehyde, benzoic acid, methyl benzoate and phenol) were proposed as the main adsorption mechanism in the biocollagenic wastes activated carbons. Moreover, high nitrogen content (around 3%) on the biocollagenic activated carbons influenced negatively on the adsorption of acetanilide, aniline and benzoic acid, possibly due to the adsorption of water by hydrogen bonding, that it results in a decrease of adsorption of monosubstitued aromatic compounds. Acidity and basicity of the activated carbons also influenced on the adsorption of benzoic acid due to its electrostatic interactions with the surface.

1.2. Removal of pharmaceuticals and Iodinated Contrast Media (ICM) compounds on carbon xerogels and activated carbons. NOM and textural properties influences.

Three carbon xerogels (CX8, CX19 and CX45) were selected by the different development of mesoporosity and macroporosity and very similar microporosity. They all had approximately a similar of carbon content (97%) and basic character. They do not present humidity and ashes due to their synthetic origin.

The three carbon xerogels were compared with four commercial activated carbons (BAC, HYDC, ROW and YAO) which showed a microporosity structure for BAC, ROW and YAO and a mixture of micro and mesopore structure in the case of HYDC.

The adsorption of six pharmaceuticals and six Iodinated Contrast Media (ICM) compounds was influenced by different factors as microporosity and mesoporosity of the carbon materials, the dimensions and hydrophobicity-hydrophilicity of the molecules. An increase in size of the pharmaceuticals results in a decrease in the adsorption onto the carbon xerogels and commercials activated carbons. On the other hand, the presence of mesopore on carbon xerogels enhance the adsorption of voluminous ICM molecules in contrast the decrease of adsorption of ICM onto microporous commercial activated carbon. The character hydropobic and hydrophilic also affected the adsorption as it can be seen through the high correlation between the different parameters of the Langmuir and Freundlich models.

Multiple adsorption of the different pharmaceutical and ICM compounds showed that ICM compounds were less adsorbed than pharmaceticals at high concentrations onto the

carbon materials at higher concentrations. It was suggest that ICM compounds competed for the mesopore allowing pharmaceutical (lower dimensions) access to the micropore

The presence of NOM in surface water sensibly reduced the quantity of ICM adsorbed due to competition for mesopores since NOM was also adsorbed in mesopores. The adsorption of diatrizoate acid (DTZ) and salicylic acid was highly affected by the presence of NOM due electrostatic repulsion between the acids and NOM.

1.3 Removal of pharmaceutical pollutants in water using coal-based activated carbons.

Two coal-based activated carbons come from anthracite and from lignite were successfully used as adsorbents for paracetamol, phenol and salicylic acid pollutant removal in aqueous phase. Different experimental activation conditions were applied on the anthracite and the lignite due to their different composition. In the case, of the anthracite higher activating temperature (850ºC) and chemical agent (NaOH)/precursor material ratio (3:1) were used in order to develop a higher mesoporosity of small diameter. The obtained activated carbon (CNAC) had a S_{BET} of 1839 m^2 g^{-1} , high volume of mesopore of 0.113 cm^3 g^{-1} and a high carbon content (95.05%). On the other hand, the activation of the lignite was carried out with KOH (1:1 agent/raw material ratio) at 750 ºC. The obtained activated carbon MAC was characterized by a high sulphur content (6%) and a S_{BET} of 1100 m^2 g^{-1}. Water adsorption isotherm showed that functional groups on MAC interact with water enhancing chemicals interactions; otherwise a higher water amount was physically adsorbed onto CNAC.

The adsorption of three compounds (paracetamol, phenol and salicylic acid) related to the pharmaceutical industries onto different coal-based activated carbons (CNAC, F400, MAC and NPK) was studied. Paracetamol showed the higher affinity for all these activated carbons although it was the less adsorbed than salycilic acid and phenol. The higher adsorption of salicylic acid respect phenol was due to electrostatic interactions between the activated carbons and acidic molecules. Moreover, adsorption of salicylates onto MAC was higher than on the rest of activated carbon between pH 4-8 due to the presence of sulphur groups; it can suggest that MAC could be a good material for the adsorption of anionic species or even also for adsorption of mercury. The highest

adsorption of the three compounds was produced onto CNAC which showed the highest pore volume and mesopore diameter between 2-4 nm.

1.4 Multicomponent adsorption on coal based activated carbons on aqueous media: new cross-correlation analysis method

A new cross-correlation spectrographic method was developed and compared with the traditional Vierord's method; to study the adsorption interactions between adsorbates in binary solutions (paracetamol-phenol, paracetamol-salicylic acid and phenol-salicylic acid) and ternary solutions (paracetamol, phenol and salicylic acid) onto the coal-based activated carbons (CNAC, F400, MAC and NPK).

The cross correlation model developed in this work showed better results than Vierordt's method due to Vierordt's method only measures absorbance at the wavelengths which showed the maximum absorbance, whereas our method analyses the absorbance in the whole absorption spectrum The Vierordt's method showed errors up to 20% in some of the binary solutions analysis and higher than 50% on the ternary solution. In the case of cross-correlation method the errors were lower than 10% in binary and ternary solutions.

The results from binary and ternary solutions showed that the adsorption of the compounds depended on their affinities (K_L) which were obtained from the individual compound isotherm. A higher affinity implied a higher adsorption of the compound. Moreover the higher amount of water adsorbed on CNAC the less adsorption of phenol in the presence of paracetamol respect to F400. In the adsorption of phenol and salicylic acid onto NPK was observed a strong competition between phenol, water and salicylic acid. In the case of binary and ternary adsorption of paracetamol and salicylic acid onto MAC, the adsorption of salicylic acid was clearly favoured by the presence of sulphur on the activated carbon.

1.5 Role of activated carbon properties in atrazine and paracetamol adsorption equilibrium and kinetics.

The sludge activated carbon (SBC) was selected for its origin and the physical activation with steam. It was characterized by a low carbon content and a high mineral matter content due to the origin of the raw material. The porosity developed was poor

with a $S_{BET} = 260$ m^2 g^{-1} and the total volume of 0.161 cm^3 g^{-1}.

Paracetamol and atrazine were adsorbed onto SBC and compared with the activated carbons F400 and NPK. The presence of high quantity of ashes in SBC activated carbon complicates the adsorption of both compounds due to mineral matter can block the pore entrances and its hydrophilic character can allow the adsorption of water. The higher adsorption of paracetamol in front of atrazine could not be explained by the different physic-chemical characteristics as hydrophobicity, dimensions and electron-donor interactions between molecules and activated carbon. It was concluded that a possible mechanism of the adsorption of both molecules was the hydrogen bond interactions between OH groups present in the activated carbons; considering that OH-OH interactions are more intense than OH-NH interactions. The adsorption of atrazine onto NPK showed a two step isotherm typical on the adsorption of pesticides; and it could be due to the presence a high volume of mesopore.

A new kinetic model (adsorption-diffusion model) based on mass balances was developed to interpret and compare the kinetics of paracetamol and atrazine adsorption SBC, F400 and NPK. The model was proved to be a powerful tool, able to estimate the adsorption capacities and kinetics of these two compounds onto the activated carbons used by means of only two parameters with physical meaning. The obtained results showed that the coefficient diffusion (D) denoted the relative rate of transfer through to the material, this value was higher on F400 than SBC suggesting that the presence of ashes could block the pores. The second parameter modelized in the adsorption-diffusion model was the effective area (area involved on the process) which showed (good) great results for the SBC activated carbon. In this case the effectiveness on the adsorption process of the SBC was 50% compared with the 11% of F400 suggesting that SBC was a good adsorbent although it had the lowest S_{BET}.

Chapter 6

Future work

1. Future work

This Thesis is focused on the use of new activated carbons for the adsorption of emerging pollutants on water. Different aspects have been evaluated on the adsorbents, the adsorption, analysis, engineering models and statistical analysis; but further research is needed to improve these parts.

1.1 Adsorbents

As can be seen in section 4.1.1 the chemical composition of biocollagenic wastes played an important role on the adsorption of the different monosubstitued pollutants. It can be considered the analysis of the chemical surface by means vapour isotherms, TPD and XPS, to know how affected more properly the adsorption of water, acidity or basicity of the different groups and the nature of these groups.

Develop different activated carbon from the lignite of Mequinenza, studying different variables as activation temperature, different chemical agents, change the ratio agent/precursor; with the objective to study how the sulphur composition of the materials is affected.

1.2 Adsorption

Use MAC and CNAC for adsorption of different emerging pollutants to observe the influence the sulphur groups in the case of MAC and the mesopore in CNAC.

Study the adsorption kinetics of IDXL onto the different carbon xerogels (in different kinds of water) to observe the diffusion of this molecule through the different mesopore and its adsorption.

1.3 Analysis

Cross-correlation spectrophotometric method enhanced the analysis of binary and ternary solutions. By this sense, it can be improved to analysis more than 3 compounds and use this method as alternative tool to other expensive analysis as GC/MS, HPLC, ...

Propose other new spectrophotometric methods using the derivate spectra.

1.4 Engineering

Development a new kinetic model on the adsorption of emerging pollutant, based on the textural and chemical characteristics of the activated carbons.

1.5 Modelling and statistical analysis data

With the aim to study the influence of the pore diameter onto the adsorption of the different molecules (phenol, salicylic acid, paracetamol, diclofenac and IDXL) and create a multiple linear regression model, it was carried out the study of principal component analysis, textural dendrogram and best subsets regression and Mallows' Cp. 26 activated carbons from different origin were analysed their chemical and textural properties. Moreover, phenol, salicylic acid, paracetamol, diclofenac and IXDL were selected according to their different dimensions. The adsorption process was taken onto the different adsorbents and adsorbates and isotherms experimental data were fitted to two-parameter isotherm model Langmuir.

The different results obtained are partially shown and described bellow:

Fig. 6.1 shows the similarities between the different carbon materials. As can be seen, four different groups are shown according to the total Surface area (S_{BET}) and the different pore volumes. The first group (Blue lines) is composed by carbon materials with S_{BET} higher than 1600. The second one (red lines) are formed by carbons materials with S_{BET} 1000 to 1400 m^2 g^{-1}, the third one (green lines) S_{BET} compressed between 600 and 1000 m^2 g^{-1}, and the last one is formed by SBC which shows the lower textural properties.

The eigenvalues obtained and the cumulative variance from the PCA are shown in Table 6.1 and Fig. 6.2. Eigenvalues higher than 1 were selected to choose principal components. As can be seen, most of the variation in the data set can be explained by the first six principal components. The first component represents the 40.6 % of the total variance and the cumulative variance on the six principal component is 88%
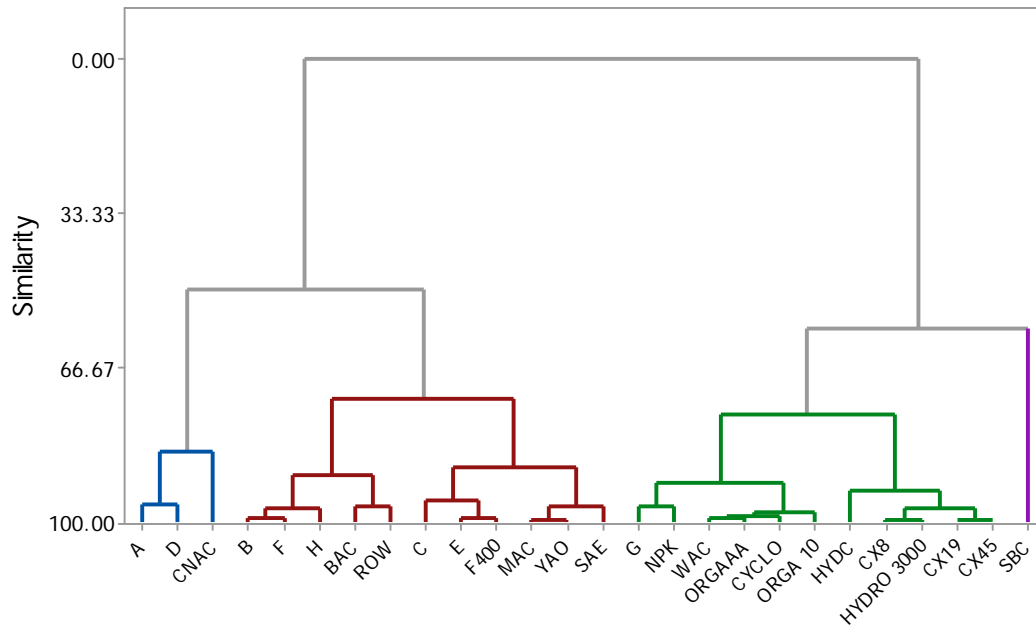
Figure 6.1 Dendrogram of the textural properties of the carbon materials

Table 6. 1 Variance, cumulative variance and eigenvalues obtained by means of PCA

	CP1	CP2	CP3	CP4	CP5	CP6	CP7
Eigenvalue	10.568	4.82	3.539	1.477	1.372	1.095	0.807
Variance	0.406	0.185	0.136	0.057	0.053	0.042	0.031
Cumulative	0.406	0.592	0.728	0.785	0.837	0.880	0.911

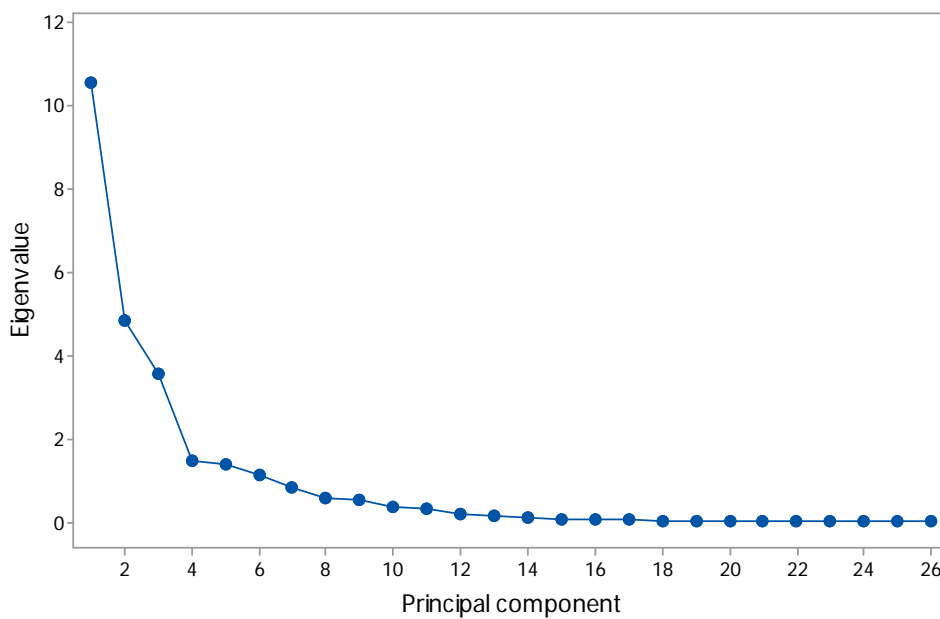**Figure 6.2** Eigenvalues of the different principal component

Fig. 6.3 shows the different activated carbons (scores) and variables (loadings) used on the space of the first and second principal component. As can be seen, the first component was related to the S_{BET}, Vmicro, q_{max} of phenol and paracetamol. It can suggest that the adsorption of both compounds can be produced onto the total micropore. On the other hand, the second principal component was related to the higher mesopore diameter 10-50 nm) and the total pore volume.
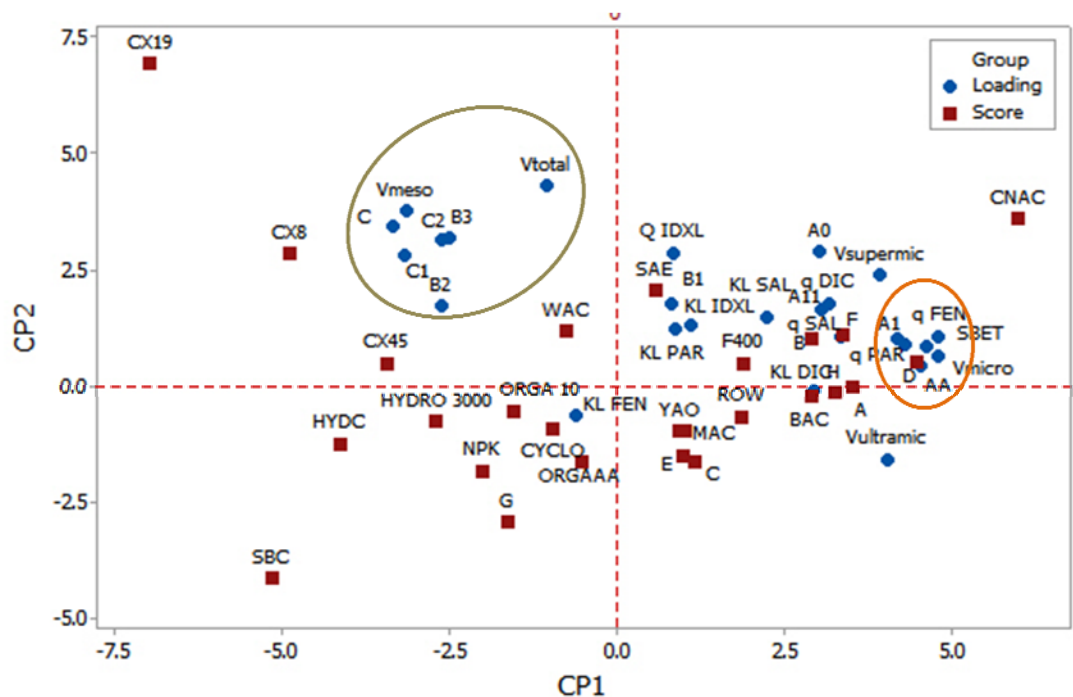

Figure 6.3 Scores (activated carbons) and loadings (variables) on the space of the first and the second principal components

The different multiple lineal regression model proposed are shown on table 6.3. As can be seen, phenol, paracetamol and IDXL models were explained with only two variables obtaining a coefficient correlation higher than 70%. On the other hand, salicylic acid and diclofenac models showed a lower correlation ($r^2 < 60\%$) suggesting the need to introduce other parameters (as example chemical) on the equation.

The different models obtained were tested and compared with other studies from mestres and Galhetas [1,2] (Table 6.4).

Table 6.2 Multiple lineal regression models proposed for every studied molecule

Compound	Proposed model	r^2	Cp Mallows
FEN	qFEN = 0.675 + 0.64 V_{umic} + 3.455 V_{micro}	76.21%	
SAL	qSAL = 0.768 + 1.84 V_{umic} + 3.41 V_{micro}	40.26%	
SAL (2)	qSAL = -0.442 + 9.07 V_{umic} + 5.25 A11 + 6.37 B2 + 1.056 V_{total}	57.78%	2.5
PAR	qPAR = 0.293 + 0.309 V_{umic} + 3.328 V_{micro}	83.18%	
DIC	qDIC = 0.241 + 3.697 A11	43.00%	4.5
DIC (2)	qDIC = -0.034 + 1.409 V_{micro} + 5.17 B1 - 0.53 B2	55.98%	2.5
IDXL	qIDXL= -0.0379 + 2.138 B1 + 0.1343 V_{total}	69.92%	0.0
IDXL (2)	qIDXL = -0.0554 + 2.194 B1 - 0.0661 V_{meso} + 0.1827 V_{total}	70.64%	1.5

Table 6. 3 Comparison between obtained and calculated results with materials of this study and other studies [1,2]

	qm obtained	V_{ultra}	V_{micro}	qm calculated	% error
A	1.719	0.250	0.513	2.078	20.86
BAC	1.584	0.177	0.453	1.855	17.13
CNAC	2.551	0.170	0.544	2.156	15.49
CX19	0.795	0.000	0.159	0.822	3.42
D	2.199	0.243	0.535	2.149	2.29
MAC	1.764	0.141	0.337	1.458	17.34
ORGANO 10	0.979	0.115	0.261	1.197	22.28
ROW	1.695	0.179	0.426	1.766	4.19
SAE	1.493	0.130	0.282	1.272	14.82
SBC	0.394	0.042	0.066	0.526	33.41
Pi-fa/800 @ 20 ℃	1.539	0.190	0.410	1.716	11.53
Pi-fa/900 @ 20 ℃	1.438	0.020	0.450	1.797	24.93
S/700 @ 20 ℃	2.281	0.180	0.360	1.547	32.19
CP @ 20 ℃	1.539	0.160	0.400	1.674	8.77
SH800	3.397	0.000	1.080	3.887	14.43
SC800	3.121	0.350	0.620	2.465	21.03
NS	1.771	0.020	0.400	1.630	7.94

References

[1] M. Galhetas, M.A. Andrade, A.S. Mestre, E. Kangni-foli, M.J. Villa de Brito, M.L. Pinto, The influence of the textural properties of activated carbons on acetaminophen adsorption at different temperatures., Phys. Chem. Chem. Phys. 17 (2015) 12340–9.

[2] A.S. Mestre, E. Tyszko, M.A. Andrade, M. Galhetas, C. Freire, A.P. Carvalho, Sustainable activated carbons prepared from a sucrose-derived hydrochar: remarkable adsorbents for pharmaceutical compounds, RSC Adv. 5 (2015) 19696–19707.